Geology of the Sugarloaf and Delamar Mountain areas, San Bernardino Mountains, California

by

Christopher Scott Cameron

A.B., Brown University
(1975)

M.A., Rice University
(1978)

SUBMITTED IN PARTIAL FULFILLMENT
OF THE REQUIREMENTS OF THE
DEGREE OF

DOCTOR OF PHILOSOPHY IN
GEOLOGY

at the

MASSACHUSETTS INSTITUTE OF TECHNOLOGY

June 1981

Signature of Author_____
Department of Earth and Planetary Sciences

Certified by_____
B. C. Burchfiel
Thesis Supervisor

Accepted by_____
Theodore R. Madden
Chairman, Departmental Graduate Committee

GEOLOGY OF THE SUGARLOAF AND DELAMAR MOUNTAIN AREAS, SAN BERNARDINO MOUNTAINS, CALIFORNIA

by

CHRISTOPHER SCOTT CAMERON

Submitted to the Department of Earth and Planetary Sciences
on March 2, 1981 in partial fulfillment of the
requirements for the degree of Doctor of Philosophy in
Geology

ABSTRACT

The San Bernardino Mountains lie within the Mesozoic batholithic belt of the Cordilleran orogen. Roof pendants at Big Bear include: 1) older Precambrian gneisses, unconformably overlain by 2) the Upper Precambrian Big Bear Group, conformably overlain by 3) rocks correlative with uppermost Precambrian-Cambrian formations known from the eastern Mojave Desert, which tie this area to the Cordilleran miogeocline. The Big Bear Group is lithologically distinct from Upper Precambrian miogeoclinal rocks to the east, indicating there were significant facies variations across the Mojave Desert during the initial stages of miogeoclinal deposition. In view of such variability, it is likely that other enigmatic metasedimentary sequences in southern California include unrecognized Upper Precambrian rocks of the Cordilleran miogeocline. The Precambrian-Cambrian sequence is thrust over marbles correlative with Devonian-Permian(?) marginal miogeoclinal-cratonal formations known further east. This section is distinct from Upper Paleozoic rocks of the nearby western Mojave terrane, which may be tectonically displaced. Recurrent epeirogenic tectonism greatly influenced Precambrian-Paleozoic deposition in the Mojave Desert.

During the Mesozoic, the Big Bear area was the site of recurring arc-related orogenesis (deformational episodes D_{1-4}). D_1 polyphase deformation and low P-intermediate T metamorphism and D_2 plutonism are interpreted as a progressive sequence, related to the initiation of arc activity. D_{1a} included zonal isoclinal folding of the miogeoclinal rocks and superposed, generally NE-directed folding and thrusting involving Precambrian gneisses. The D_{1a} metamorphic peak was locally prekinematic, with $P \leq 3.76$ kb, T_{max}= 475-540°. Miogeoclinal cover rocks were recrystallized during D_{1a} but Precambrian gneisses were affected only in the vicinity of fault zones, where fluids may have been available. Superposed D_{1b} folds are NE to E trending, generally upright and post-metamorphic. D_2 events include low-angle normal faulting and emplacement of the Fawnskin Monzonite. D_3 low-angle normal faulting occurred, in part, contemporaneously with emplacement of the Sugarloaf Intrusive Complex and effected significant east-west extension (60%+) of roof rocks at Sugarloaf Mountain. Roof extension occurred during D_3 emplacement of the Bertha Diorite and related units at Delamar Mountain. Pre-Mesozoic rocks and earlier Mesozoic plutonic rocks are preserved in the roof of a Late Cretaceous granitic batholith; its emplacement during D_4 was probably attended by roof extension, but the magnitude is uncertain. Contact metamorphism and penetrative deformation related to D_{2-4} plutonism are limited. Pre-existing metamorphic assemblages

generally remained stable except adjacent to intrusive contacts or along faults and fractures where access to fluids was presumably greater.

$^{40}Ar/^{39}Ar$ and K/Ar geochronologic data indicate the Mesozoic batholith complex includes Permo-Triassic (D_2), Late Jurassic (D_3) and Late Cretaceous (D_4) rocks. Pre-Cretaceous plutons yield Late Cretaceous (70.2-83.5 m.y.) biotite K/Ar ages, indicating nearly complete outgassing during D_4 plutonism. Hornblendes from these rocks yield disturbed $^{40}Ar/^{39}Ar$ age spectra; intermediate to high temperature steps resemble model spectra for diffusive loss of ^{40}Ar during Late Cretaceous reheating. The Fawnskin Monzonite (minimum age 214.1±2.9 m.y.) may be a Permo-Triassic pluton. Diorite of the Sugarloaf Intrusive Complex (minimum age 148.2±3.1 m.y.) and the Bertha Diorite (minimum age 126.7±3.6 m.y.) are probably of Late Jurassic age. Anomalously old ages obtained for the lowest temperature steps from hornblendes of the Fawnskin Monzonite and Sugarloaf Quartz Diorite are attributed to anomalously high concentrations of ^{40}Ar in non-crystallographic sites. This may have resulted from diffusive redistribution of radiogenically derived ^{40}Ar during reheating, or more likely, indicates that excess ^{40}Ar was assimilated during or after diffusive Ar loss. Evidence of excess Ar contamination at Big Bear indicates caution must be taken in evaluating the significance of K/Ar hornblende ages from complex plutonic terranes.

Regional considerations are suggestive that D_{1-2} are related to the inception of an Andean-type arc in the western and central Mojave region during the Permo-Triassic following arc-continent collision, tectonic truncation of the Paleozoic margin, and arc polarity reversal. The progression of events may record the area's transition from a back-arc (D_1) to intra-arc setting (D_2). Renewed magmatism and associated extensional tectonism of Late Jurassic age (D_3) indicates the Jurassic arc extends further west than was previously recognized. This area lay along the axis of the Late Cretaceous batholith, whose emplacement (D_4) was accompanied by regional reheating but only limited metamorphism of the moderately buried roof terrane. Rapid regional uplift and cooling of the arc terrane during the Late Cretaceous may have been a consequence of shallow-dipping subduction, when thrusting of upper crustal rocks of the arc terrane over Pelona Schist rocks (≃ Franciscan complex) apparently terminated Mesozoic arc magmatism in the western Mojave Desert.

Evidence from the Big Bear area suggests that arc-related heating need not be accompanied by widespread metamorphism or ductile deformation. Permo-Triassic metamorphism was "thin-skinned", with thorough recrystallization confined to the "wet" miogeoclinal cover, while underlying "dry" gneisses record only zonal development of D_1 fabrics. Following D_1 metamorphic devolatilization of the cover rocks, only zonal metamorphism and ductile deformation is recognized in association with later plutonism. These observations suggest that access to fluids (particularly water) was important in limiting the extent of metamorphism and penetrative ductile deformation associated with arc magmatism and tectonism.

Roof rock extension, accommodated primarily by low-angle normal faulting, accompanied emplacement of Late Jurassic (and perhaps Permo-Triassic and Cretaceous) plutons. This observation supports the hypothesis that batholith emplacement may be accommodated by upper crustal extension, involving roof stretching and/or wall rock spreading. Late Jurassic roof

extension at Big Bear and back-arc thrusting to the east were contemporaneous, so it is likely some component of thrust belt telescoping represents the combined effects of crustal shortening and batholithic wedging. At the least, it appears that extension in roof terranes and compression in back-arc regions and at deeper crustal levels beneath the arc may occur simultaneously.

Thesis Supervisor: B. C. Burchfiel

Title: Professor of Geology

TABLE OF CONTENTS

ILLUSTRATIONS

Figures

Tables

Plates (in pocket at back)

ACKNOWLEDGMENTS

A great many people have contributed to my graduate education and to the completion of this thesis. To all I owe a great debt and I extend my heartfelt thanks. Clark Burchfiel supervised my graduate work and introduced me to the geology of the southern Cordillera. His instruction, advice, cooperation and friendship have been and are greatly appreciated. Thanks are due to faculty members John Southard, Frank Spear, and Stan Hart, who reviewed various sections of the thesis. John waded through snow drifts to examine sections in the study area with me and his enthusiasm stimulated my interest in the sedimentology of the metasedimentary rocks there. Frank helped me in developing my ideas concerning the metamorphic history of the Big Bear area. Stan provided reassuring criticism of my geochronologic interpretations. John Sutter (now at U.S.G.S., Reston, Virginia) criticized an early draft of the geochronology chapter and made many valuable suggestions which were incorporated in the present version. Several discussions with John helped me to formulate my interpretations of the geochronologic data presented here.

I have learned and hopefully grown a great deal in the company of my fellow students at M.I.T. I thank them all. A special thanks is due the Cordilleran and Caledonian clones: Gary Axen, John Bartley, General Peter Guth, Kip Vernon Hodges, John Sharry, Jon Spencer, Brian Wernicke and James Igor Willemin. Discussions with Noah Bartley, Kip and Brian were especially valuable in assisting me in formulating the ideas concerning intra-arc metamorphism and extensional tectonism presented here. I salute the clones. In addition, honorary clones Doug Walker and Peter Vrolijk and guest clone Tim Byrne contributed significantly to the 10th floor intellectual ambiance. Julie Morris and Kevin Bohacs provided much needed input from the geochemical and sedimentological perspectives.

Much of the geochronologic data presented here was obtained while I was a guest scientist at the Branch of Isotope Geology, U.S.G.S., Menlo Park, California. Special thanks are due Bob Fleck, who supervised my work there, and Marv Lanphere, Project Chief during my stay. "Hands-on" instruction, supervision, and sympathy with the laboratory aspects of my data collection were provided by James Sabarumaru, Elliot Sims and Jerry Von Essen. Irradiations for U.S.G.S samples were made

at the Survey's TRIGA reactor in Denver, and appreciation is extended to G. P. Kraker and his staff. Some mass spectrometry was completed at the Branch's Denver facility, and the hospitality and help of Harald Mehnert are greatly appreciated. Additional $^{40}Ar/^{39}Ar$ geochronologic studies were undertaken in conjunction with John Sutter, at the Dept. of Geology and Mineralogy, The Ohio State University, Columbus, Ohio. John performed the incremental heating experiments and mass spectrometry on two of the age spectra reported here. Irradiations for the O.S.U. samples were made at the Phoenix Memorial Lab, Univ. of Michigan, and thanks are due to Gary Cook.

During my stay at Menlo Park I benefited from discussions with several geologists, in particular John Stewart, Keith Howard, Don Ross, Gordon Haxel, Doug Morton, Jon Matti and Bret Cox. Fred Miller and Janet Morton provided me access to their unpublished K/Ar data for the San Bernardino Mountains and western Mojave Desert, as well as other valuable insights from the results of their studies in progress. Jon Matti lent me color air photos of the Big Bear area. While in California, access to various pieces of research equipment was kindly afforded me by Greg Davis at the University of Southern California and by Othmar Tobisch and Rob Coe at the University of California, Santa Cruz.

Several geologists visited me in the field and shared their expertise with me for which I am grateful. These include: Cliff Ando, Bob Powell, Lee Silver and Chuck Weisenberg. Bob Powell and Elizabeth Miller took me on field trips to areas they were studying which proved extremely valuable. In addition, these two geologists have shared their insights concerning the regional geology of southern California during many stimulating discussions.

Conversations with my fellow geologists working in the Big Bear area have proved extremely valuable. Martin Stout and Perry Ehlig (California State University at Los Angeles) provided me with unpublished data and useful advice. Special thanks are due to Peter Sadler (University of California, Riverside) who passed on to me the advice of Doug Morton that the Sugarloaf area might hold the key to the stratigraphy of the Big Bear area, which indeed it does. Pete's careful work remapping the Chicopee Canyon area convinced me that detailed mapping

was a must at Big Bear, and that the apparently simple geology there is in reality quite complex.

Assistance and friendship in the field was ably given me by John Pinkston and Steve Richards. Penelope Bowen assisted with collection of geochronology samples and managed all aspects of field camp during my final season. Abner Bowen proved a tireless, though somewhat distracted field assistant. Doony and Zucchini Bowen were vigilant camp guards. Numerous residents of Fawnskin are thanked for their kindness during my work at Big Bear. In particular, I thank Hal Zirin of the Big Bear Solar Observatory (California Institute of Technology) for permission to use freely the facilities of the Observatory as a home away from home. Thanks are also due to the Observatory staff, especially Allen Patterson, Gene Longbrake and Alberta Altman for their hospitality and friendship. They made my stay a very pleasant memory. Chuck Weisenberg provided a welcome way station for weary geologists in Redlands, California, for which I am grateful. My sister Robin Sweeney and her family provided us with a resting spot during the final field season, and displayed enviable patience with her geologist brother.

Financial support during my tenure at M.I.T. was provided by a fellowship granted by the Fannie and John Hertz Foundation. Research was supported by N.S.F. grant EAR-77-13637 awarded to B. C. Burchfiel, a G.S.A. grant and Sigma Xi grant awarded to me, and by a grant from the U. S. Geological Survey. Numerous miscellaneous expenses were paid for by Student Research grants from the Department of Earth and Planetary Sciences at M.I.T.

Drafting assistance was provided by Carolyn Mosher and Larky Hodges. Carolyn also enlarged and printed the photographs, a gift of great kindness. Barbara Davis and Sandy Williams typed most of the final manuscript. Penelope Bowen typed several earlier drafts and performed numerous missions which facilitated the more speedy completion of this thesis (what a long strange trip it's been).

During sojourns in the San Francisco Bay area, I was kept sane by my housemates at Barton Place, including Mike Amylon, Rick Stead, Liz Ryll, Jill Miller and Greg Shaw. Bill Bagby and Alec and Emily Skolnick opened their homes to us during later stays there. During the long, final frenzy to the finish line, Kip and Larky Hodges and Rick Stead

and Liz Ryll insanely offered us places to stay in the Boston area, which we exploited to the limit. My family has given me loyal support during all aspects of my education. I particularly acknowledge my mother, Betty Cameron. I gratefully acknowledge the patience of Penelope for enduring my stumbling progress well beyond the limits of good taste. One thesis down, one to go...

CHAPTER I: INTRODUCTION

Purpose of Study

This study focuses on the evolution of an intra-arc orogenic terrane which developed within continental crust (an Andean-type arc, Hamilton, 1969). Detailed geologic and geochronologic studies were undertaken in the Big Bear area, San Bernardino Mountains, southern California. During the Mesozoic this area was the site of protracted arc-related orogenic activity, including events related to the inception of an Andean-type margin in the southern Cordillera of the western United States. In addition, the structural basement for this arc includes previously unrecognized Upper Precambrian metasedimentary rocks that are among the earliest deposits along the ancient continental shelf.

Major objectives of this study included: 1) establish the stratigraphic framework of the pre-batholithic rocks and their depositional and tectonic setting in the early history of the southern Cordilleran margin; 2) reconstruct the chronology and characterize the structural style of Mesozoic intra-arc orogenic events in this area; 3) investigate the temporal and spatial relationships between magmatism, metamorphism and deformation in a continental arc terrane.

The San Bernardino Mountains are located approximately 75 miles east of Los Angeles, California (Fig. 1), and comprise the highest range in southern California. Physiographically, the San Bernardino Mountains are part of the Transverse Ranges. Although the late Cenozoic history of this area reflects uplift related to regional strike-slip tectonism, the Big Bear area lies northeast of the San Andreas fault zone. Hence the Mesozoic and earlier geologic history of this area is tied to the adjacent Mojave Desert region.

The San Bernardino Mountains lie within the Mesozoic batholithic terrane of the southern Cordillera (Mesozoic as used here includes Late Permian). The batholith belt is believed to represent the roots of a continental (Andean-type) volcano-plutonic arc which developed along the

Figure 1: Index map of the southern Cordilleran orogen.

Tectonic elements
- Craton: unshaded
- Miogeocline: dots
- Oceanic terrane accreted in mid-Paleozoic: diagonal rule
- Oceanic terrane accreted in Permo-Triassic: horizontal rule
- Arc terrane accreted in Permo-Triassic: vertical rule
- Terranes accreted during Mesozoic-Cenozoic: horizontal dashes
- Mesozoic batholith belt: crosses
- Cenozoic cover: v's

Localities and specific features
- B: Baker
- EK: Eastern Klamath Mountains
- GA: Golconda allochthon
- LA: Los Angeles
- NS: Northern Sierra Nevada
- NWN: Northwestern Nevada
- RMA: Roberts Mountain Allochthon
- SAFZ: San Andreas Fault Zone
- SB: San Bernardino Mountains
- SF: San Francisco
- V: Victorville
- WMT: Western Mojave Terrane

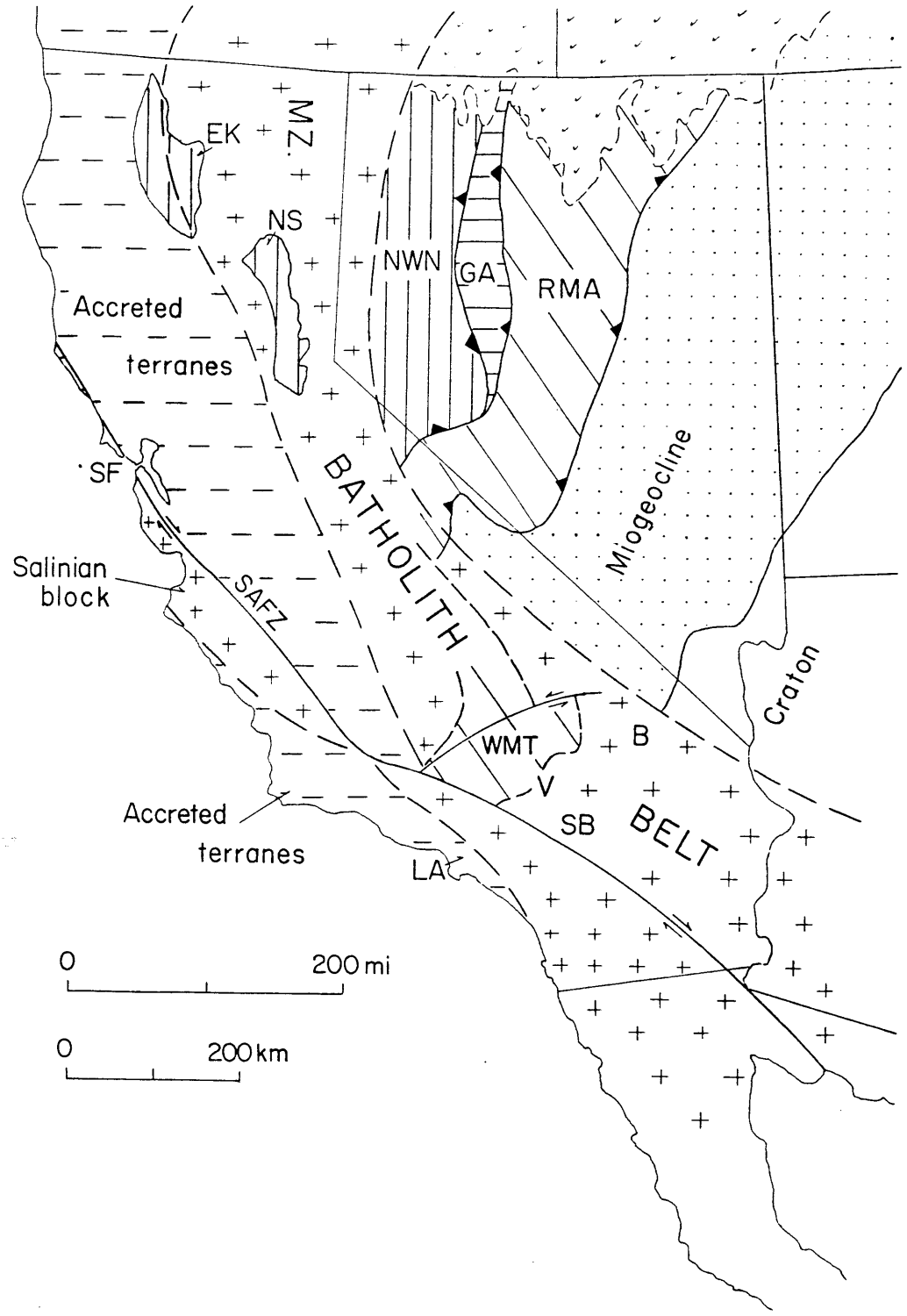
EK
MZ
NS
NWN
GA
RMA
Accreted
terranes
SF
BATHOLITH
Miogeocline
Salinian
block
SAFZ
Craton
WMT
B
V
SB
BELT
Accreted
terranes
LA
0
200 mi
0
200 km

Cordilleran continental margin during Mesozoic plate convergence (Hamilton, 1969; Burchfiel and Davis, 1972). This arc crosscut pre-Mesozoic paleogeographic and tectonic trends, thus its basement varied along strike (Fig. 1). In southern California, Arizona and Sonora, Mexico, the arc developed atop rocks of the Paleozoic platform (craton) and continental shelf (miogeocline). Further north in California and Nevada, the arc's basement consists of eugeoclinal rocks, and includes Paleozoic island arc and oceanic or marginal basin terranes (Roberts Mountain and Golconda allochthons) accreted to the Cordilleran margin during Paleozoic plate convergence.

Pre-Mesozoic rocks in the western Mojave Desert region are preserved as roof pendants within the Mesozoic batholith. The paleogeographic setting of these metamorphic rocks has long been an enigma. Recent geologic studies (Stewart and Poole, 1975; Tyler, 1975; E. Miller, 1977) have suggested that quartzite, marble and metapelite sequences in the Victorville-San Bernardino Mountains region (Fig. 2) are correlative with areally extensive Upper Precambrian-Paleozoic formations of the Cordilleran miogeocline and craton which are exposed in eastern portions of the batholith terrane, in the eastern Mojave Desert. These miogeoclinal rocks are distinct from eugeoclinal metamorphic rocks of Paleozoic age found in the northwestern Mojave Desert (here called the western Mojave terrane; see Fig. 1), which may be regionally out of place and perhaps offset from accreted Paleozoic terranes to the north (Davis and others, 1978; E. Miller and others, 1979). Because the fossil record is largely obliterated in these metamorphic rocks, the rock stratigraphic correlations are based on rock types, sequence, and preserved (or inferred) sedimentary structures. A lithologically distinctive rock sequence correlative with uppermost Precambrian-Cambrian (miogeoclinal) formations known further east has provided the key to regional correlations; these rocks have been recognized in the Big Bear and Victorville areas. Their presence in this region indicates rocks of the Cordilleran miogeocline extend into the western Mojave Desert. However, the relationship of these suspected uppermost Precambrian-Cambrian rocks to older Precambrian gneisses and other enigmatic metasedimentary terranes exposed nearby was not resolved during earlier studies.

Figure 2: Geologic index map of the San Bernardino Mountains-Victorville region.

Rock units
(known and inferred age assignments)
Cenozoic rocks and surficial deposits: unshaded
Mesozoic plutonic rocks: dots
Mesozoic volcanic and sedimentary rocks: v's
Upper Precambrian-Paleozoic metasedimentary rocks: vertical rule
Older Precambrian metamorphic rocks: diagonal waves

Localities
BBL: Big Bear Lake
BL: Baldwin Lake
BM: Black Mountain
BV: Bear Valley
CC: Chicopee Canyon
DM: Delamar Mountain
GM: Granite Mountains
HV: Holcomb Valley
JF: Juniper Flats
QM: Quartzite Mountain
RM: Rodman Mountains
RoM: Rose Mine
SiM: Sidewinder Mountain
SM: Sugarloaf Mountain
V: Victorville

Structures
safz: San Andreas Fault Zone
sat: Santa Ana Thrust
dt: Doble Thrust
hf: Helendale Fault

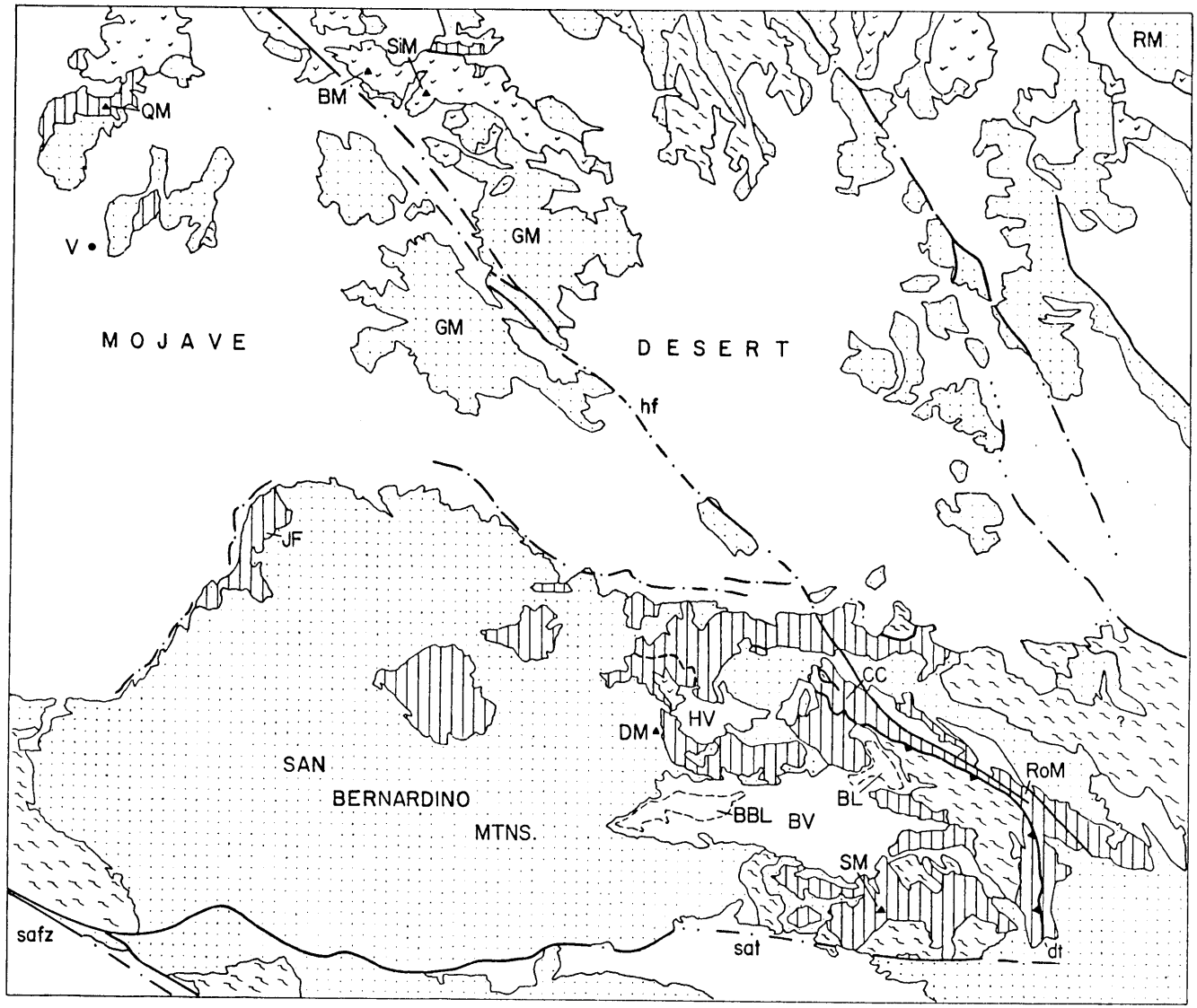
SiM
BM
RM
QM
V
GM
GM
MOJAVE
DESERT
hf
JF
CC
DM
HV
SAN
BERNARDINO
MTNS.
RoM
BL
BBL
BV
SM
safz
sat
dt
10mi
10km

Silver (1971) reported Precambrian ages from gneisses in the Big Bear area that were similar to ages of basement rocks underlying miogeoclinical strata in the eastern Mojave Desert-Death Valley region. However, Silver and Anderson (1974) have suggested that Precambrian gneisses in the western Mojave Desert are some 700 km out of place, and were displaced to their present position along a left-lateral strike-slip fault zone (the Mojave-Sonora megashear, Anderson and Silver, 1979) during mid-Mesozoic time. If true, a major tectonic dislocation would be inferred between the Precambrian gneisses and Big Bear and nearby uppermost Precambrian-Cambrian miogeoclinal rocks. Alternatively, Stewart and Poole (1975) and Tyler (1975) suggested these gneisses constitute the stratigraphic basement for the miogeoclinal terrane. Study of metasedimentary rocks of possible Late Precambrian age which unconformably overlie the Precambrian gneisses and are inferred to underlie uppermost Precambrian-Cambrian rocks in the Big Bear area was undertaken to resolve this issue. The detailed stratigraphy, contact relations, and depositional setting of these rocks had not been described previously. Based on paleogeographic inferences of earlier workers, it appeared that the Big Bear area might contain the most complete section of Upper Precambrian-Cambrian miogeoclinal rocks in the western Mojave Desert. Since Upper Precambrian miogeoclinal rocks are almost unknown south and west of Baker, California (Fig. 1), it was anticipated that reconstructing the stratigraphic and depositional framework of this terrane would provide important new insights concerning the early history of the Cordilleran continental margin, and a reference point from which to evaluate the paleogeographic position of other possible miogeoclinal sequences in this region.

The Mojave Desert region records a complex Mesozoic history of arc-related magmatism, metamorphism and deformation (Burchfiel and Davis, 1981). Recent studies indicate the western Mojave Desert contains the earliest record of arc activity known in the southern Cordillera. Geologic and geochronologic studies in the Victorville area indicate that arc plutonism began in earliest Mesozoic or Permo-Triassic time. A pluton of this generation intrudes metamorphosed and poly-deformed miogeoclinal rocks there. E. Miller (1977) suggested all these events are related to the initiation of arc activity.

The Permo-Triassic orogenic episode was followed by a complex sequence of events including extensive erosion, deposition of intra-arc sediments and multiple episodes of volcanism (undated), folding, faulting, and emplacement of a regionally extensive Late Cretaceous batholith.

It seems likely that a similarly complex Mesozoic history may be recorded in the Big Bear area. Early workers (Richmond, 1960, for example) considered all Mesozoic plutonic rocks in the range to be related to a late Mesozoic batholith. More recent geochronologic studies suggest that although the bulk of the batholithic rocks may be of Late Cretaceous age, older plutons, perhaps of earliest Mesozoic age, may be present (Armstrong and Suppe, 1973; C. Miller, 1977). Earlier geologic maps suggest that folding of pre-Mesozoic rocks at least locally predates one of these early plutons (Richmond, 1960; Dibblee, 1964b). Thus a deformational event correlative with that at Victorville may be present at Big Bear. Earlier workers reached no consensus concerning the relationship between deformation and metamorphism here. Some recognized only contact metamorphism related to the batholithic rocks (Richmond, 1960; McJunkin, 1976); Guillou (1953) and Tyler (1975) suggested that metamorphism accompanied folding and thrusting in the areas they studied and predated the emplacement of the Cretaceous batholith. The areal extent of this dynamothermal metamorphism had not been evaluated, nor were P, T conditions constrained. Of particular importance, it was uncertain if metamorphism occurred in an intra-arc setting, or was wholly unrelated to plutonism. Structural and geochronologic studies were undertaken to attempt to resolve these questions. By reconstructing the sequence of deformational, magmatic and metamorphic events it was hoped that the regional Mesozoic history might be better understood, and that the style of intra-arc orogenesis here might be better characterized. Important questions included: What is the extent of Permo-Triassic deformation here (if any) and is there evidence that this event occurred in an intra-arc setting? Are there other pre-Cretaceous magmatic events here? If so, how are they characterized and what is their regional setting? What style of tectonism is associated with the emplacement of plutons? How did the structural response of the

miogeoclinal cover sequence compare with that of underlying older Precambrian gneisses? These questions in turn bear on the more fundamental relationships between arc magmatism and regional metamorphism and deformation. Are back-arc fold and thrust belts an expression of intraplate crustal shortening (Burchfiel and Davis, 1972), or is back-arc shortening at upper crustal levels the result of wedging due to spreading batholiths beneath the volcanic arc (Hamilton, 1978)?

Two areas in the Big Bear region were selected for detailed geologic mapping. In the Sugarloaf area, the most complete sequence of suspected Upper Precambrian miogeoclinal rocks is exposed. Although these rocks are highly disrupted by Mesozoic structural events, they nevertheless afford the best available opportunity to reconstruct the stratigraphy and depositional setting of the Upper Precambrian section, and to evaluate its contact relations with the better known uppermost Precambrian-Cambrian section. In addition, Precambrian gneisses are widely exposed here and are involved in Mesozoic deformational events. This proved an excellent locale to compare the structural response of basement and cover rocks during intra-arc orogenesis. The Delamar Mountain area was selected for study primarily because Mesozoic igneous rocks present here were thought to be among the oldest in the range. Reconstructing the sequence of magmatic events and their relationships to deformation and metamorphism of the pre-Mesozoic country rocks was a major objective. It was of particular interest to constrain the timing of the earlier Mesozoic events. Geochronologic studies of suspected pre-Cretaceous igneous units here and at Sugarloaf were undertaken in hopes of dating these events, and of providing information concerning the thermal effects of later Mesozoic magmatism.

Previous Work

The presence of pre-batholithic metamorphic rocks in the Big Bear vicinity had been known since the pioneering studies of Vaughan (1922) and Woodford and Harris (1928). They recognized these rocks were preserved as roof pendants in the batholithic terrane. Woodford and

Harris reported the local occurrence of Carboniferous fossils from marbles on the north slope of the range.

Guillou (1953) differentiated the Baldwin Gneiss from other metasedimentary rocks in the Baldwin Lake area (Plate I), noting their more complex deformational history. He speculated these gneisses might be of Precambrian age, which Silver (1971) later confirmed. Dibblee (1964a, 1964b) reported a major unconformity separated these gneisses and the overlying Saragossa Quartzite in several localities. Dibblee mapped much of the range (and much of the Mojave Desert as well!) at a scale of 1:62500 (also see Dibblee, 1967a,b). His mapping and compilations proved invaluable as references during this study.

The stratigraphic nomenclature suggested by Dibblee (1964a) is that most frequently used in discussions of the areal geology. Metasedimentary rocks were grouped into two formations. Quartzites and metapelitic rocks were assigned to the Saragossa Quartzite and included quartzites unconformably overlying Precambrian gneisses. All marbles and calc-silicate rocks were assigned to the Furnace Limestone, and were interpreted to conformably overlie the Saragossa Quartzite, based on local contact relations described by Guillou (1953) and Richmond (1960). Because marbles on the north slope of the range had yielded Carboniferous fossils (Woodford and Harris, 1928; Richmond, 1960; Hollenbaugh, 1968) it was assumed that <u>all</u> marbles were of late Paleozoic age and overlay the Saragossa Quartzite. These conclusions were not based on detailed stratigraphic reconstructions, nor on a continuous stratigraphic section. As a result of stratigraphic oversimplifications, several important geologic structures, including the Doble Thrust between Rose Mine and Onyx Summit and most faults bounding Mesozoic younger-over-older allochthons, were not recognized.

Stewart and Poole (1975) and Tyler (1975) were the first to recognize that rocks at Chicopee Canyon, which were previously included in the uppermost Saragossa Quartzite and lowermost Furnace Limestone (Dibblee, 1964b), were lithologically correlative with uppermost Precambrian-Cambrian miogeoclinal formations known from the southern Great Basin. Tyler's (1975) detailed mapping here supported Guillou's

(1953) observation that folding and faulting of the pre-Mesozoic rocks also involved Precambrian gneisses and was contemporaneous with greenschist facies metamorphism.

All or parts of the Delamar Mountain and Sugarloaf study areas were included in areas described by Richmond (1960) and McJunkin (1976) respectively, and were encompassed by Dibblee's (1964a,b; 1967a,b) 15' quadrangle maps. Richmond (1960) examined Mesozoic igneous rocks north of Big Bear Lake in some detail. He recognized a complex sequence of magmatic events here which he believed were related to the evolution of a late Mesozoic batholith. He first identified many of the igneous units described here, including the areally extensive pluton I have referred to as the Fawnskin Monzonite. Richmond's (1960) interpretation of some contact relationships differs significantly from that presented here. In addition C. Miller (1977) studied the petrology, trace element and U/Pb, Rb/Sr geochemistry of the Fawnskin Monzonite. McJunkin (1976) mapped a large area in the vicinity of Sugarloaf Mountain. He did not significantly modify the stratigraphic framework of Dibblee (1964a) though he noted rocks of Upper Precambrian-Paleozoic age might be present (following Stewart and Poole, 1975). Like Richmond (1960) he interpreted folding of the pre-Mesozoic rocks to have occurred prior to contact metamorphism associated with late Mesozoic plutonism. Neither McJunkin (1976) nor Richmond (1960) recognized evidence of dynamothermal metamorphism, such as that described by Guillou (1953) and Tyler (1975). A major focus of McJunkin's study was late Cenozoic tectonism, including the geology in the vicinity of the Santa Ana thrust fault and the distribution of Quaternary landslides. Some of the latter structures recognized by McJunkin (1976) may be younger-over-older allochthons of Mesozoic age.

Reconnaissance K/Ar geochronologic studies of Mesozoic plutons in the San Bernardino Mountains were included in a regional study by Armstrong and Suppe (1973). Their data suggested both Late Cretaceous and perhaps early Mesozoic plutons are present in the Big Bear area. Other geochronologic data was reported by C. Miller (1977). More extensive K/Ar studies of Mesozoic plutons in the range are in progress

by F. Miller, D. Morton and J. Morton of the U.S. Geological Survey, Menlo Park, California.

Physical Setting and Access

The San Bernardino Mountains are a high arid range located adjacent to the Mojave Desert but with a summer climate moderated by elevation and proximity to the Pacific Ocean. The study areas range from about 6800-10,000' (2100-3050 m) in elevation. Summer field days are warm and dry (with occasional thunderstorms). Elevation and winter snowfall have provided for locally extensive forest cover of Jeffrey Pine, pinyon and juniper. Desert vegetation is widespread on the lower, northeastern slopes.

Exposures range from poor to good. Forest cover often makes locating outcrops a tedious proposition. Surficial deposits, including older alluvium (often occurring as erosional remnants on ridge crests), talus and ever present colluvium are troublesome for the bedrock geologist, and all too often conceal vital contact relations (of course!).

Access to and within the range is generally excellent. Several well-maintained highways lead to the Big Bear Lake area (a major vacation resort), and traverse or pass near the study areas. Interior access along U.S. Forest Service gravel roads is also excellent. Numerous trails and abandoned jeep and logging roads are also available (many are now closed in portions of the Sugarloaf area slated for Wilderness status). Although portions of the range are impressively precipitous, the terrain near Big Bear, although locally steep, provides no major obstacles to mapping.

Wildlife is abundant, including deer, coyotes, rabbits, rare bobcats, bear, and the ever present rattlesnake. The most dangerous creature in the forest is man (particularly during hunting season, in the Autumn). The major hazard is driving to and from the field during any weekend when tourists are in season.

Procedure of Study

This study involved detailed geologic mapping completed during the 1978 and 1979 field seasons. In addition, the results of reconnaissance mapping during a portion of the summer of 1977 are described briefly. The areas described in detail here include approximately 38 mi^2, and were mapped at a scale of about 4" = mile (1:15840). The maps used for compilation were photographically enlarged from the U.S. Geological Survey's Big Bear City, Moonridge, Rattlesnake Canyon and Onyx Summit 7.5' quadrangles (Plate II: Sugarloaf area) and the Fawnskin 7.5' quadrangle (Plate III: Delamar Mountain area). Thicknesses of stratigraphic sections described here were measured with a Jacob's Staff or from cross sections (note these are structural thicknesses). Sedimentologic observations described herein were made during the course of regular field work. Geometric structural analysis (following techniques of Turner and Weiss, 1963) was used to supplement field observations where appropriate. Petrographic studies were undertaken to supplement general rock descriptions, and to assist in interpretations of the structural geology and metamorphic petrology of the area. Geochronologic studies were completed by the author at the Branch of Isotope Geology, U.S. Geological Survey, Menlo Park, California, and Denver, Colorado; additional studies reported here were completed in cooperation with J. Sutter at the Ohio State University. The $^{40}Ar/^{39}Ar$ and K/Ar techniques were used in hopes of recovering both geologically meaningful emplacement ages for plutonic rocks in the study areas and additional information concerning their later thermal history.

CHAPTER II: STRATIGRAPHIC FRAMEWORK OF PRE-MESOZOIC ROCKS

General Statement

The roof pendants in the San Bernardino Mountains comprise the southwesternmost known exposures of the Cordilleran miogeocline-craton terrane. It had long been suspected that the quartzites and marbles here were tied in some way to Upper Precambrian-Paleozoic miogeoclinal sequences in the southern Great Basin-Death Valley region (Hamilton, 1969, Burchfiel and Davis, 1972). Stewart and Poole (1975) were the first to suggest that Great Basin stratigraphic units were present in the Big Bear-Victorville region (later confirmed by Tyler (1975) and E. Miller (1977)).

The Big Bear area contains the most complete (although disrupted) sequence of Upper Precambrian-Cambrian miogeoclinal rocks known in the western Mojave Desert (Fig. 3). This is the only locality where a relatively complete Upper Precambrian succession is present overlying older Precambrian basement. This Upper Precambrian sequence (here named the Big Bear Group) is quite distinct from coeval units in the southern Great Basin, although overlying Cambrian rocks are virtually identical in both areas. On the north slope of the range, Upper Paleozoic marbles are exposed which are believed to correlate with marginal miogeoclinal or cratonal formations in the southern Nevada-eastern Mojave Desert region. The Upper Paleozoic rocks are discussed only briefly. Pre-Mesozoic rocks form the roof for the extensive Mesozoic batholith complex in the Big Bear area.

It is understood that the reader will refer to the appropriate plates (I: Generalized Geologic Map of the Big Bear Area; II: Geologic Map of the Sugarloaf Area; III: Geologic Map of the Delamar Mountain Area) as necessary. The locations of structures in the Sugarloaf area cited here are given in Plate VI (Tectonic map of the Sugarloaf area). Repeated references to these plates are omitted in this and subsequent chapters.

Figure 3: Stratigraphic columns of Upper Precambrian-Cambrian rocks in the Big Bear area, San Bernardino Mountains, California. Lithologic symbols are standard; thicknesses shown are structural thicknesses.

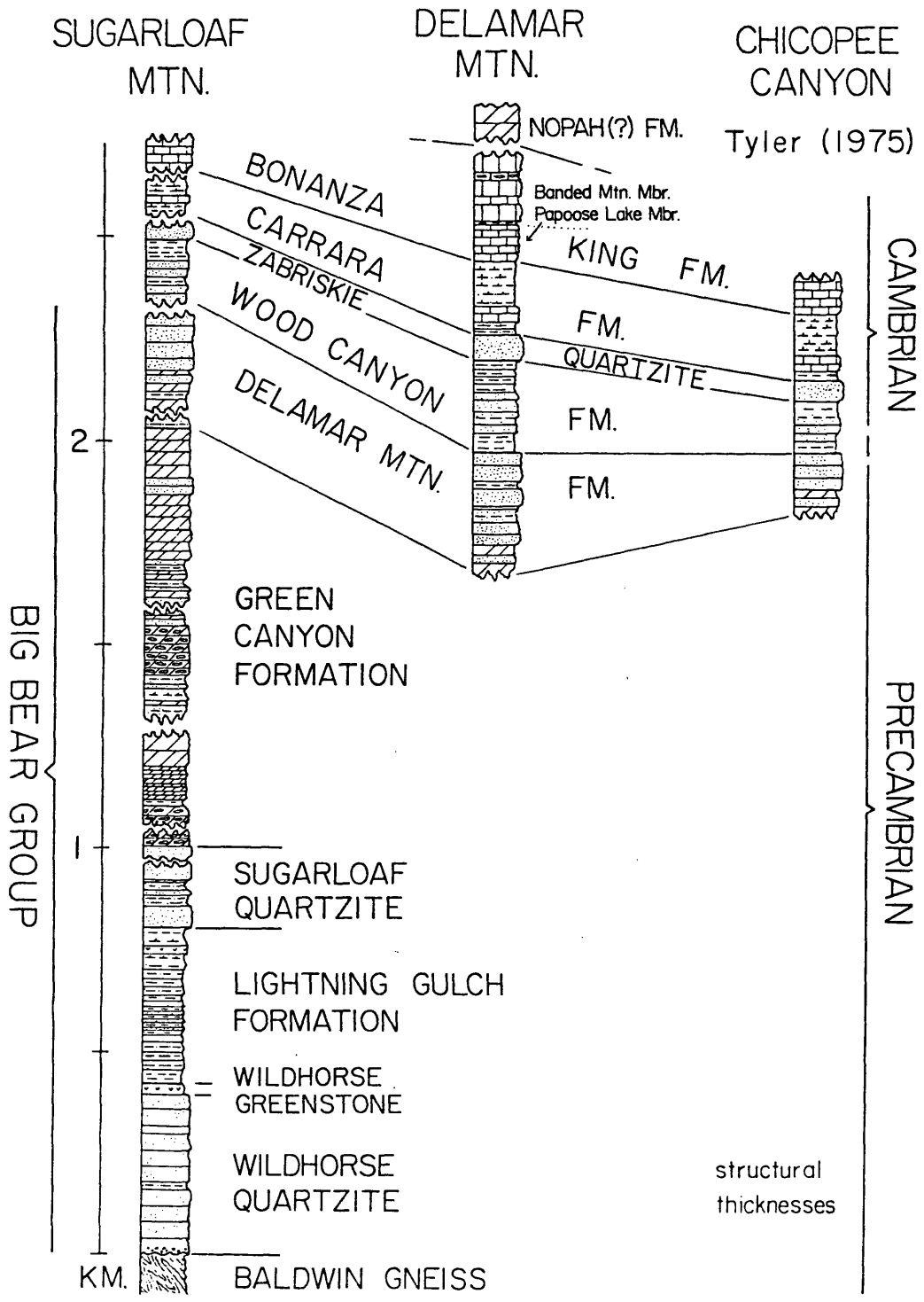

Precambrian Gneiss Complex

The oldest rocks in the study area and the stratigraphic basement for Upper Precambrian-Cambrian metasedimentary rocks at Big Bear are part of a Precambrian gneiss complex. The gneiss complex includes an older sequence of paragneisses, schists and quartzites, and a younger suite of orthogneisses (primarily granitic augen gneiss) and pegmatites which intrude them. This metamorphic complex, the Baldwin Gneiss of Guillou (1953), is widely exposed in the Sugarloaf area where it is overlain uncomformably by the Wildhorse Quartzite, the basal unit of the Big Bear Group. Since detailed study of the basement rocks was not an objective of this investigation, these rocks were generally mapped as a single unit (p€gn). However, several distinct lithologies are present. Unfortunately, the gneiss complex is often poorly exposed and southwest of Route 38 it forms recessive slopes, commonly overlain by talus of the Wildhorse Quartzite. The best exposures occur northeast of the highway.

Schists, banded paragneisses, and rare quartzites are the oldest rocks in the gneiss complex. Original sedimentary features were not recognized in these rocks. The compositional layering is parallel to a tectonic foliation (s_1), formed by early isoclinal folding and shearing (f_1). Schists consist predominantly of biotite (up to 90 percent) with subordinate muscovite, quartz, and feldspar. One to five meter thick lenses of white or green-grey quartzite are sometimes interlayered with other metasedimentary lithologies. Feldspathic quartzite, micaceous quartzite, and orthoquartzite are recognized. Thick sections of quartzite may be present in the gneiss complex northeast of the study area (mapped as gneissic quartzite in the Old Woman Springs 15' quadrangle, Dibblee, 1967b) and in the west center of the Morongo Valley 15' quadrangle (previously mapped as Saragossa Quartzite, J. Matti and B. Cox, personal comm., 1979).

These lithologies are interlayered with grey, thin to medium banded paragneisses. Coarse-grained quartzo-feldspathic layers containing microline and plagioclase alternate with medium to fine-grained quartz-muscovite-biotite-rich layers. The banding appears to

be the result of metamorphic differentiation. The relative proportions of quartzo-feldspathic and micaceous lithologies varies considerably. These are typically quartz-rich rocks, usually containing 50-60% quartz, while biotite and muscovite often reach 30-40%. The predominance of quartz and mica suggests the protoliths were compositionally immature sedimentary rocks for the most part, perhaps greywacke. However, some of the more feldspathic banded gneisses may have had igneous protoliths, perhaps volcanic flows or tuffs, or hypabyssal rocks of intermediate composition.

Foliated, coarse-grained biotite-K-feldspar-quartz pegmatites are widespread in the schists, quartzites and paragneisses. Their emplacement was pre- or early syntectonic with respect to the early isoclinal folding event because they too record this deformation.

Granitic augen gneiss intrudes the paragneisses, schists and quartzites. These orthogneisses locally comprise much of the basement complex. They typically contain 80% or more feldspar (mostly microcline) and quartz, with 10-25% biotite and muscovite. Plagioclase is subordinate or absent. Augen (up to 5 cm in length) consist of K-feldspar and quartz.

Original intrusive contact relationships are recognized locally (Fig. 4). This may be observed in Sections 23 and 26 (T2N, R2E) where the augen gneisses are locally differentiated on Plate II (pCgrgn), particularly in the SW1/4 of Section 23, immediately below the base of the Wildhorse Quartzite northwest of Arrastre Creek. Here, foliated, coarse-grained augen gneiss grades over a few meters into a "porphyritic" border facies (the K-feldspar augen persist here). Lensoidal xenoliths, with long dimensions parallel to the predominant foliation, increase in abundance in these finer-grained gneisses. The xenoliths are of biotite-plagioclase-quartz-rich rock and are similar to country rock gneisses seen nearby. However, they preserve an earlier foliation, not seen in the augen gneiss or the country rocks. Near the base of the Wildhorse Quartzite, the augen gneiss is interlayered with banded gneisses. The augen gneisses may be relict dikes injected into the country rocks.

This intrusive contact zone has been transposed into parallelism with the predominant foliation, which is recognized in both the intrusive augen gneiss and country rocks. Intrusion of the augen gneiss

Figure 4: Precambrian gneiss complex: augen gneiss intrudes older metamorphic rocks. Contacts are concordant with s_1 foliation. Non-foliated granitic dike is present in lower right corner. Hammerhead in upper center is 20 cm long.

Figure 4.

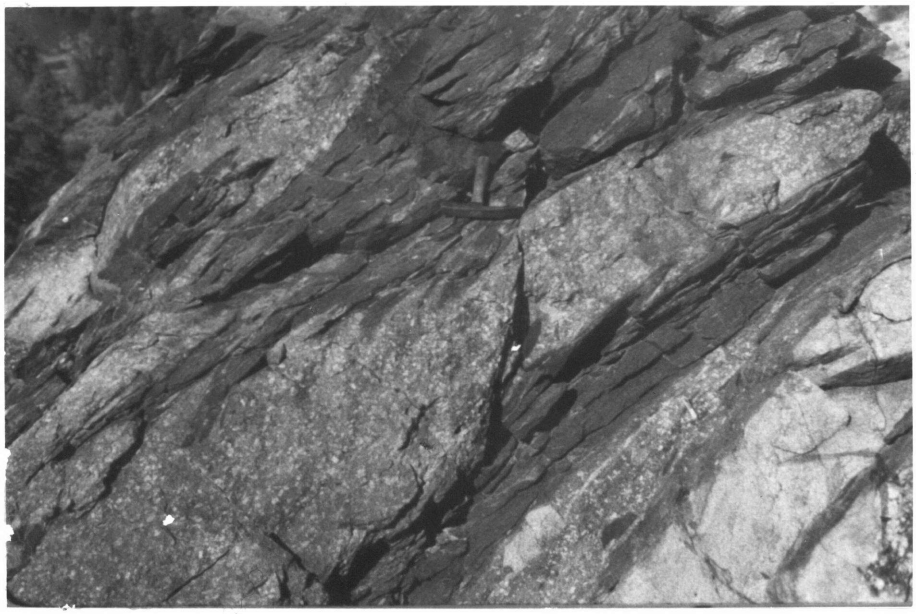

occurred prior to or during an early phase of the isoclinal folding and shearing event which produced the principal foliation and compositional banding (s_1) recognized in the basement complex. The pre- to syntectonic pegmatites recognized in the paragneisses, schists and quartzites may be dikes of this intrusive complex. A variety of post- or late syntectonic pegmatitic dikes and quartz veins cut all rocks of the basement complex but not the overlying Upper Precambrian metasedimentary rocks.

Silver (1971) has reported a minimum U/Pb zircon age of 1750 $\pm$ 15 m.y. on "plutons, intrusive into still older gneisses" in the San Bernardino Mountains. The dates were obtained from augen gneiss in the Baldwin Lake area (Silver, personal comm., 1978). These rocks are probably equivalent to the granitic augen gneisses described herein. Whether the 1750 m.y. minimum age reported by Silver relates to time of crystallization or deformation and metamorphism is uncertain. Silver (1971) indicated similar ages are obtained from Precambrian gneisses nearby in the Mojave Desert.

Upper Precambrian Big Bear Group

Introduction

Metasedimentary rocks of presumed Late Precambrian age are widespread in the Big Bear area, particularly east of Big Bear Lake. These strata are here referred to as the Big Bear Group. The complete stratigraphic succession had not been described previously and it's reconstruction was a major objective of this study. Six new stratigraphic units of formational rank are described (Fig. 3). Reconstruction of the upper part of the Upper Precambrian section is inhibited by structural complexity in the Sugarloaf area.

Previous workers included Upper Precambrian rocks in the Sugarloaf area with the Saragossa Quartzite and Furnace Limestone (Dibblee, 1964a; McJunkin, 1976). Upper Precambrian rocks in the Delamar Mountain and Chicopee Canyon areas were included in the Chicopee or Chicopee Canyon Formations (Guillou, 1953; Richmond, 1960). It is suggested that the previous nomenclature be abandoned.

The basal unit of the Upper Precambrian sequence unconformably overlies

the older Precambrian gneiss complex in the Sugarloaf area and elsewhere east of Big Bear Lake. The uppermost rocks of this section are overlain with conformity by the Uppermost Precambrian-Lower Cambrian Wood Canyon Formation at Delamar Mountain and at Chicopee Canyon. In the Sugarloaf area Upper Precambrian strata are not in normal sequence with the Cambrian rocks; the contact is always a fault or an intrusive contact.

Each of the Upper Precambrian units is described below. Sections were measured for the lower units (Fig. 5, thickness refers to structural thickness), however not for the upper units because they are so dismembered by faults and intrusions as to make section measurement unreliable. For these, structural thicknesses were measured from cross sections.

Wildhorse Quartzite

Distribution. A sequence of conglomerate and quartzite unconformably overlying older Precambrian gneisses and overlain by either the Wildhorse Greenstone or Lightning Gulch Formation is referred to as the Wildhorse Quartzite. This formation has its type section northwest of Wildhorse Meadow (SW1/4 of Section 4, T1N, R2E). The Wildhorse Quartzite is widely exposed within and adjacent to the Sugarloaf map area. These quartzites were included in Dibblee's (1964a,b; 1967a,b) lowermost Saragossa Quartzite.

Description. The Wildhorse Quartzite consists predominantly of well-bedded quartzite, with conglomerate lenses at the base. Other subordinate lithologies include micaceous quartzite, quartz phyllite, laminated calc-silicate rock and quartz-plagioclase-epidote-actinolite schist. Throughout much of the Sugarloaf area, the Wildhorse is divided into two members (W1 and W2), which are in gradational contact; in areas of poor exposure, however, the Wildhorse Quartzite is mapped as undifferentiated (W).

The lower member (W1) overlies the basement complex with spectacular angular unconformity which is well exposed in several places. Notable examples include exposures in: SW1/4 of Section 4 (T1N, R2E), along Wildhorse Road; SE1/4 of Section 6 and SW1/4 of Section 5 (T1N,

Figure 5: Stratigraphic column of the lower Big Bear Group

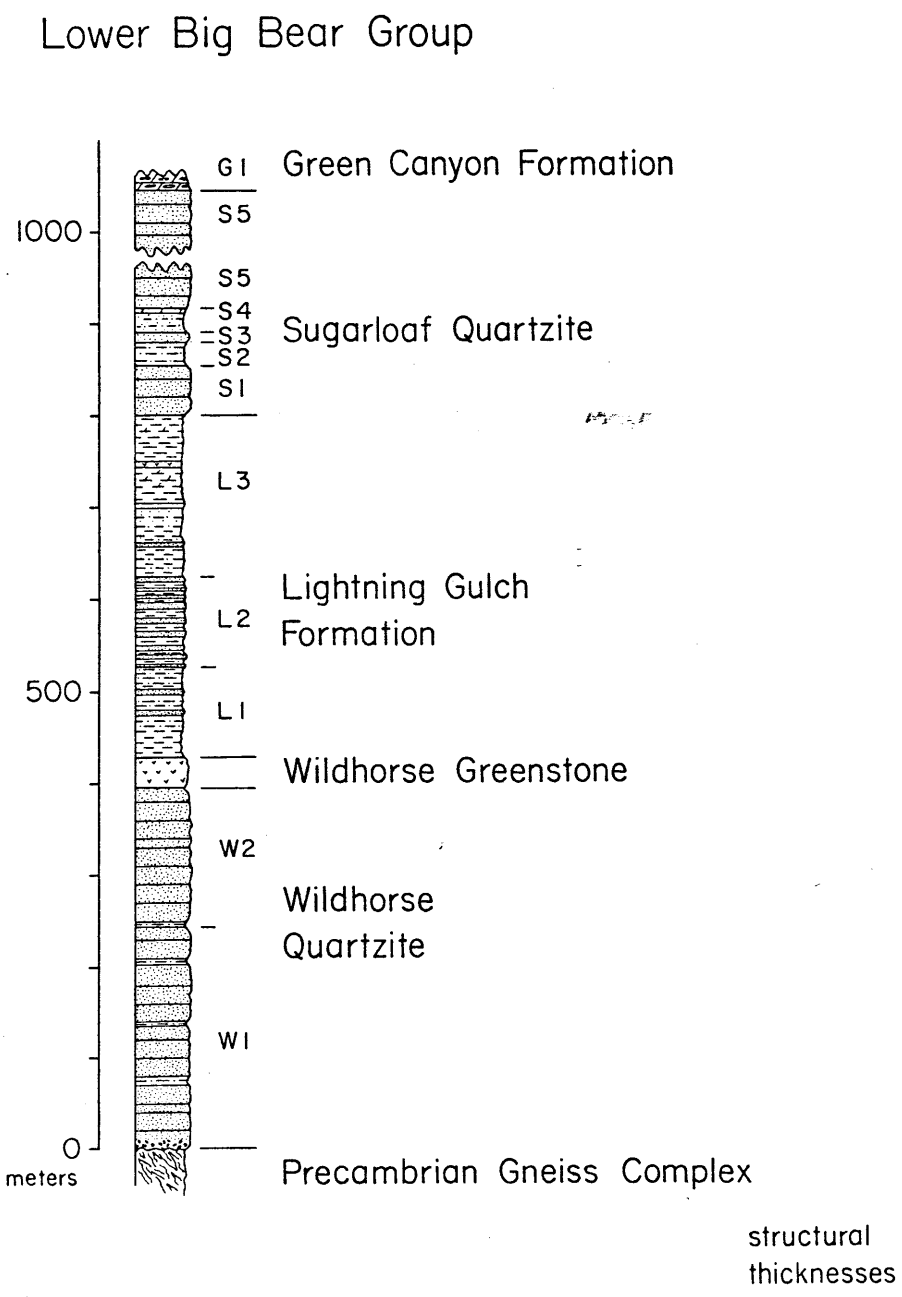

R2E); E Center of Section 33 (T2N, R2E); SW1/4 of Section 22 and SW1/4 of Section 23 (T2N, R2E). A basal conglomerate or conglomeratic quartzite is found at the unconformity at most localities (Fig. 6). A notable exception is the section northwest of Arrastre Creek above the Arrastre Fault, where clasts are rare in the basal quartzites. The basal conglomerate varies in thickness, from two to ten meters, and grades rapidly upward into clast-free quartzite. Clasts include vein quartz, quartzite, granitic pegmatite and plagioclase and K-feldspar. Sorting is poor and clast size variable. Coarse clasts (five to 30 cm diameter) are usually very angular. These clasts were probably derived locally from the underlying gneiss complex. The conglomerate is usually matrix-supported by recrystallized coarse sand to granule-sized quartz and K-feldspar grains in varying proportions. Grain size and feldspar content decrease rapidly upsection as does the abundance of larger clasts. Clasts and detrital feldspar are rare more than ten meters above the unconformity. In only one locality was a channel recognized, cutting one to two meters deep into the basement (SW1/4 of Section 22, T2N, R2E). Elsewhere the basal surface is subplanar. A paleoweathered zone is recognized at the top of the underlying basement rocks below and northwest of Wildhorse Road in the SW1/4 of Section 4 and below the Wildhorse Fault in the NW1/4 of Section 3 (T1N, R2E). Here original metamorphic micas were weathered out in zones locally extending ten meters below the conglomerate. Relict gneissic layering is crudely preserved, but the rock has the appearance of a poorly sorted sandstone. Many clasts were probably derived from these paleoweathered zones.

Low-angle cross stratification, tabular trough cross sets, flaser-lenticular ripple cross laminated bedding and mudcracks are present in the basal parts of member W1. Conglomeratic beds sometimes occur at the base of fining upward sequences, overlain by lenticular bedded quartzites, often grading into laminated micaceous quartzite with mudcracks.

Above the basal conglomerate member W1 is comprised mainly of blue-grey but more typically green-grey, fine-grained quartzite. Orthoquartzite predominates; these rocks usually contain 90% or more quartz and little feldspar. Minor white mica, biotite, and chlorite

Figure 6a: Wildhorse Quartzite (member W1): basal contact with underlying Precambrian gneisses. Quartzite with rare angular vein quartz and K-feldspar clasts overlaps interlayered paragneiss and granitic pegmatite of the gneiss complex. Hammerhead at upper left is 20 cm long. Photo taken in SW1/4 of Section 5 (T1N, R2E).

Figure 6b: Wildhorse Quartzite (member W1): well-developed basal conglomerate overlying Precambrian granite gneiss. Angular, locally derived clasts are more abundant here than at locality pictured in Figure 6a. Some clasts were likely derived from paleoweathered zones which are recognized in underlying gneisses exposed nearby. Hammerhead in lower center is 18 cm long. Photo taken along Wildhorse Road in SW1/4 of Section 4 (T1N, R2E).

Figure 6a.

Figure 6b.

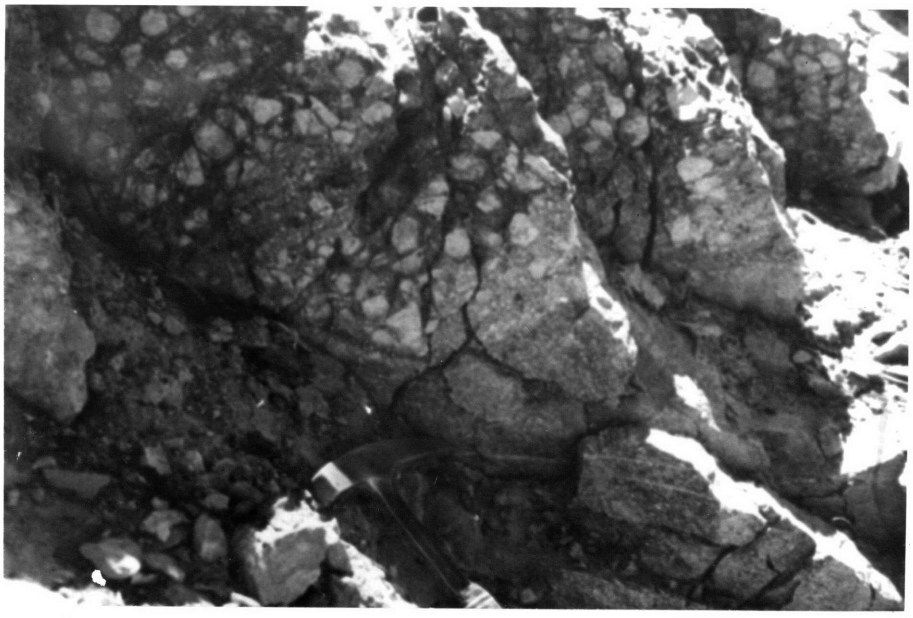

(up to 10%) are generally present. The greenish color of much of member W1 is due to traces of chlorite and biotite. Quartzites are sometimes interbedded with poorly exposed micaceous quartzites and quartz phyllites or schists.

The sedimentary structures of member W1 are a distinctive feature of the unit. Thick bedding is often defined by large scale (one half to two meters thick) tabular sets of tangential cross strata. Tangential sets occur singly or in groups, often with minor variations in foreset dip directions. Occasional 180 degree reversals are present. Individual or multiple sets are commonly overlain by thick beds of plane or flaser-lenticular bedded quartzite. At the base of these beds asymmetric ripples or more rarely oscillation ripples typically truncate the tangential sets (Fig. 7). Where measured, the asymmetric ripples commonly indicate reversed paleocurrent direction from that of underlying, large-scale bedforms. The plane and flaser beds sometimes grade up into laminated micaceous quartzite or phyllite. Rarely, these fine-grained rocks exhibit mudcracks. Ledges of well-bedded quartzite are often discontinuous and separated by slopes underlain by float of micaceous quartzite, phyllite and schists. These micaceous lithologies are doubtlessly more important than indicated here, but are rarely exposed.

Quartz-plagioclase-epidote-actinolite schists, often thinly laminated, are present in several areas in member W1. Plagioclase-epidote-actinolite layers are often interlayered with quartz-rich laminae suggesting that these beds were metatuffaceous rocks of mafic to intermediate composition. A 244 m thick section of member W1 was measured northwest of the Balky Horse Fault and Wildhorse Meadows, in Section 4 (T1N, R2E).

The upper member of the Wildhorse Quartzite (W2) is primarily exposed south of Route 38, and on the west end of Gold Hill. Its lower contact with member W1 is gradational, and its upper contact with the Lightning Gulch Formation and Wildhorse Greenstone is discussed below. The upper member consists of fine to medium-grained quartzites that are dominantly light grey or white to blue-grey. Sedimentary structures are distinctive for differentiating members W2 and W1. Unlike member W1,

Figure 7a: Wildhorse Quartzite (member W1): large-scale, tangentially cross-stratified quartzite overlain by flaser-lenticular bedded quartzite. Outcrop is approximately 10 m high. Note falling rock in center. Photo taken in the SE1/4 of Section 22 (T2N, R2E).

Figure 7b: Wildhorse Quartzite (member W1): large-scale cross-set truncated at top by lenticular or flaser beds. Hammer-head is 20 cm long. Photo taken in the NW1/4 of Section 26 (T2N, R2E).

Figure 7a.

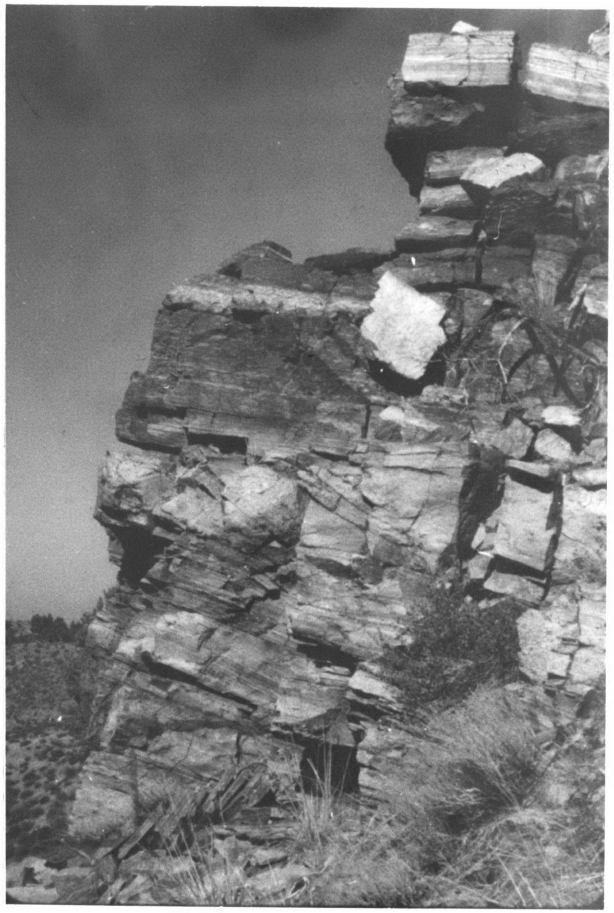

Figure 7b.

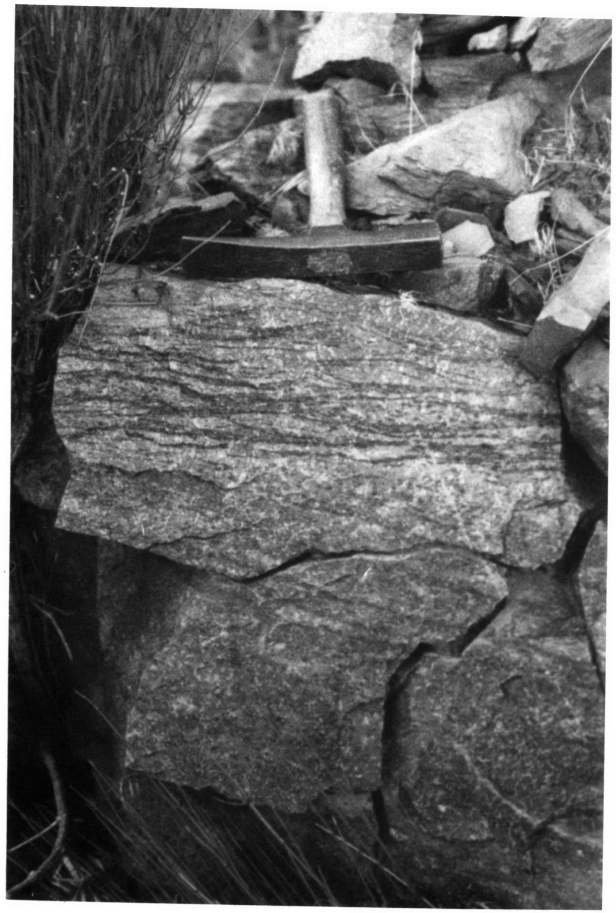

tabular sets of medium to small scale trough cross strata are common in member W2. Heavy mineral laminations define bedforms. These trough cross-stratified quartzites are often interbedded with tabular sets of tangentially cross-stratified quartzites. However, thick beds of the latter are not common in member W2, nor are flaser-lenticular bedded quartzites.

In lower Green Canyon and the north slope of Hill 8055' the lower contact of member W2 is placed at the base of a massive white quartzite bed overlying a thick section of green-grey to grey tangentially cross-stratified quartzite. Laminated dark grey or hematite-stained micaceous quartzite and quartz phyllite, with local interbeds of laminated calc-silicate rock and rare actinolite schist overlie this white quartzite and underlie trough cross-stratified quartzites. Where exposures are poor the base of member W2 is defined by the lowest predominant occurrence of light grey trough cross-stratified quartzite. Member W2 has a structural thickness of 151 m northwest of Wildhorse Meadow.

Feldspar is rare in member W2 (typically 5% or less), and these quartzites typically contain 90% quartz. However, in the uppermost few meters, quartzite, quartz and K-feldspar pebble-granule conglomerate is often found, directly underlying the Lightning Gulch Formation or Wildhorse Greenstone. This marks the principal influx of detrital feldspar between the basal conglomerate and member G8 of the Green Canyon Formation.

Wildhorse Greenstone

Distribution. A greenstone (flow?) unit that overlies the Wildhorse Quartzite and underlies or interfingers with the Lightning Gulch Formation is designated as the Wildhorse Greenstone. This unit is best exposed along Sugarloaf Ridge, northwest of Wildhorse Meadow (type area: W Center of Section 4, T1N, R2E). It is also exposed southeast of Wildhorse Meadow, above Lightning Gulch, and in float on the north slope of Gold Hill. Contact relations between the greenstone and adjacent formations are discussed below. The greenstone was apparently not recognized by Dibblee (1964a).

Description. The Wildhorse Greenstone consists primarily of fine-grained plagioclase-chlorite-actinolite schist. Chlorite and actinolite constitute 50-60% of the rock and are randomly oriented, showing typical granoblastic textures. Although actinolite greenschist predominates, biotite-epidote-hornblende-bearing greenstones are also present and coexisting hornblende and actinolite are locally recognized. The protolith of the Wildhorse Greenstone was probably basalt or basaltic andesite. Although evidence presented below is not conclusive, the unit is interpreted to have been a flow rather than a sill. The greenstone is 30 m thick northwest of Wildhorse Meadow in its type area.

A conspicuous feature of the greenstone at all localities is the presence of spherical to ellipsoidal polycrystalline quartz aggregates, averaging 5 mm in diameter, which are interpreted as quartz-filled amygdules subsequently recrystallized during metamorphism (Fig. 8). In thin section, contacts between the quartz-filled amygdules and the greenstone matrix are sharp and no relict reaction rims are preserved. These amygdules are primarily concentrated near the top of the unit but can be seen throughout the formation. Larger (up to 15 cm long), irregularly shaped pegmatite and quartzite xenoliths are widespread in the greenstone as well, particularly near its top. The xenoliths display a preferred orientation, with their long dimensions parallel to the Wildhorse Greenstone's upper and lower contacts, and parallel to beds in adjacent formations. Many of the elliptical amygdules are oriented similarly. Although this dimension-preferred orientation is, in part, tectonic (as evidenced by features indicative of intra- and inter-crystalline strain observed in thin section), this flattening appears to be superposed on a primary igneous flow foliation. In many cases the oriented xenoliths have retained highly angular or irregular shapes that appear to be primary. Unfortunately, because of thorough recrystallization the amygdules and flow(?) foliation are the only vestiges of igneous texture recognizable in the greenstone.

The upper and lower contacts of the greenstone are not exposed. However, evidence of flow top or bottom structures, relict chill or baked zones or other volcanic features are conspicuously absent within one meter of these contacts. Recrystallization may have been so complete

Figure 8: Wildhorse Greenstone with quartz-filled amygdules. Hammerhead is 20 cm long. Photo taken in W center of Section 4 (T1N, R2E).

Figure 9: Lightning Gulch Formation (member L1): lenticular-bedded quartzite and quartz phyllite. Note cleavage (S_1) is essentially parallel to bedding. Hammer is 28 cm long. Photo taken in W center of Section 4 (T1N, R2E).

Figure 8.

Figure 9.

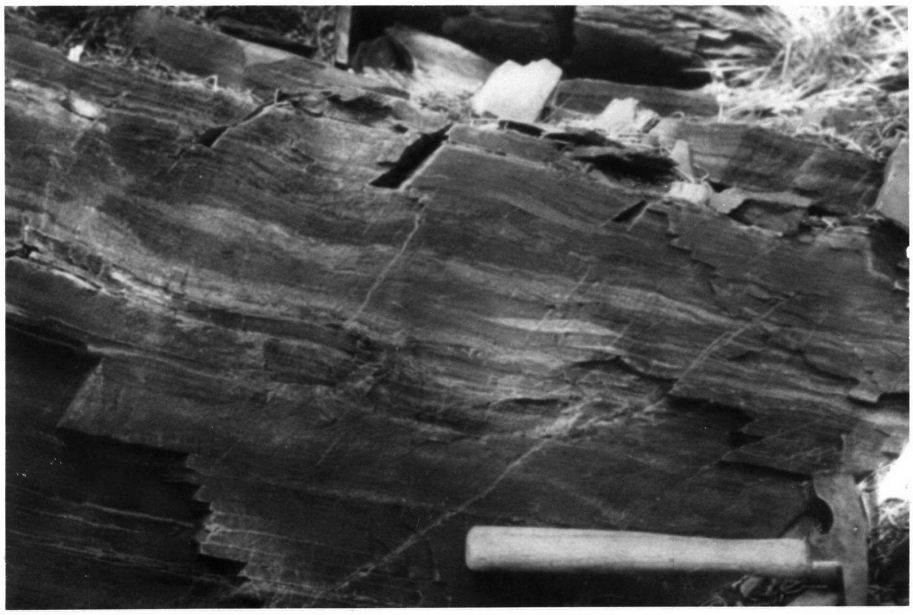

as to obliterate these primary features, or alternatively, the greenstone may be a sill. Flow fabrics and amygdules have been reported from shallow sills and this interpretation would account for the absence of subaerial or subaqueous volcanic structures. The uniformity of grain size in the unit, even near the contacts, is not conclusive for origin as either a sill or flow. Indirect evidence, however, supports the latter interpretation. Metatuffaceous rocks (laminated plagioclase-epidote-actinolite schists) are present in the overlying Lightning Gulch Formation. Thus, there were active volcanic centers in the region near this time. In the Sugarloaf area the greenstone is always present at approximately the same stratigraphic level. The lower contact of the greenstone is of particular interest. Along Sugarloaf Ridge the Wildhorse greenstone overlies the top of the Wildhorse Quartzite (here a quartz-feldspar granule-bearing quartzite). Locally, thin phyllite lenses intervene. These lenses are identical to rock types in the overlying Lightning Gulch Formation. Southeast of Wildhorse Meadow, the lower contact of the greenstone transgresses upsection so that it overlies and underlies the lowest member (L1) of the Lightning Gulch Formation. In this area, the lower Lightning Gulch Formation interfingers with the upper Wildhorse Quartzite. Lenses of granule quartzite similar to those at the top of the Wildhorse Quartzite are found in the lower Lightning Gulch, just below the greenstone.

The Wildhorse Quartzite-Lightning Gulch Formation contact is a time transgressive surface. The lower contact of the greenstone may represent a time line cutting across a facies boundary represented by the contact between these formations. If the greenstone were a sill, it is curious it would abandon the structural control of a sandstone-shale contact and cut up section.

Wildhorse Greenstone outcrops are not continuous southeast of Wildhorse Meadow. This may be a result of poor exposure, or the greenstone may be lensing out in this direction. In the latter case, the discontinuous exposures may be erosional remnants. An erosional upper contact of the greenstone, at least locally, is supported by the presence in float of quartz-white mica-biotite-chlorite-actinolite schists near the top of the greenstone in a fault block east of Sugarloaf

Mountain (E Center of Section 6, T1N, R2E). The protolith of these greenschists, present above typical amygdaloidal greenstone and below Lightning Gulch Formation, may have been volcaniclastic sedimentary deposits atop the greenstone, in part locally derived from the underlying flow.

Lightning Gulch Formation

Distribution. Phyllites and quartzites overlying the Wildhorse Quartzite and/or Wildhorse Greenstone and overlain by the Sugarloaf Quartzite are here included in the Lightning Gulch Formation. In the study area, this unit is only known from the Sugarloaf area, and is best exposed along Sugarloaf Ridge. Its type area is in the NW1/4 of Section 4 (T1N, R2E). An incomplete section of Lightning Gulch Formation is also exposed southeast of Wildhorse Meadow (above Lightning Gulch), in the lower Green Canyon area, and at the west end of Deadman's Ridge. The Lightning Gulch includes rocks mapped as the Phyllite Member of the Saragossa Quartzite (Dibblee, 1964a). The contacts with the Wildhorse Quartzite and Sugarloaf Quartzite are conformable; the contact relations with the Wildhorse Greenstone were discussed above.

Description. On Sugarloaf Ridge, the Lightning Gulch Formation can be divided into three members. Although the sections elsewhere are incomplete or tectonically disrupted, this three-fold subdivision is still recognizable. The lower phyllite member (Ll) conformably overlies and interfingers with the top of the Wildhorse Quartzite. The Wildhorse Greenstone occurs at or just above this contact (see above). The lower third of member Ll consists primarily of phyllite (often graphitic) while the upper two thirds is comprised of quartz phyllite, with interbeds of quartzite. The phyllites are generally laminated with layer parallel slaty cleavage but become more massive where quartz-rich. Porphyroblasts of biotite (often retrograded to chlorite) and andalusite (sometimes retrograded to form pseudoporphyroblasts of fine-grained white mica and quartz) are common. The matrix consists of very fine-grained

white mica (muscovite), biotite, chlorite and variable amounts of quartz. Fine-grained quartzite interbeds one to three cm thick frequently display lenticular or wavy bedding (Fig. 9). The quartzites often display ripple cross lamination, defined by micas and other heavy minerals. Pinstripe tidal bedding (Wunderlich, 1970) is also recognized. Soft sediment deformation features occur including small scale (two to four cm amplitude) rootless folds, load structures, and dewatering and escape structures. A structural thickness of 99 m was measured on Sugarloaf Ridge.

The middle quartzite member (L2) of the Lightning Gulch Formation overlies the lower phyllite member with gradational contact. It consists of red-brown (hematite-bearing) quartzites and interbedded quartz phyllites characterized by flaser-wavy bedding and pinstripe tidal bedding (Fig. 10). These quartzites interfinger with laminated phyllites vertically and laterally. Graded bedding is commonly observed in thin section (often metamorphically reversed); quartzite layers grade upward into quartz phyllite and phyllite, overlain sharply by succeeding quartzites. Biotite and andalusite porphyroblasts are often terminated abruptly at the top of graded sequences. Quartzites show small scale ripple cross-stratification. Other sedimentary structures include mudcracks, dewatering and escape structures, soft sediment folds, and spectacular load structures. A 98 m thick section of the middle quartzite member was measured on Sugarloaf Ridge.

The upper phyllite member (L3) of the Lightning Gulch is quite similar to member L1 and has a structural thickness of 176 m on Sugarloaf Ridge. Laminated quartz phyllite and graphitic phyllite are the predominant lithologies. Graphitic phyllite is particularly conspicuous near the top of the Lightning Gulch, where porphyroblasts of tourmaline as well as biotite and andalusite are common. The upper half of member L3 consists of 78 m of phyllite interbedded with laminated calc-silicate rock and plagioclase-actinolite schist. Protoliths of the latter were probably interbedded marls and mafic tuffs. In the lower part of member L3 lenticular interbeds of ripple cross-laminated quartzite are common. Spectacular large scale mudcracks are common in the uppermost Lightning Gulch (Fig. 11).

Figure 10: Lightning Gulch Formation (member L2): pinstripe tidal bedding in quartzite and quartz phyllite. Graded bedding is present here. Much of the contortion of bedding at this locality is due to soft sediment deformation related to loading and (?)bioturbation. Hammerhead is present in lower right. Photo taken in the W center of Section 4 (T1N, R2E).

Figure 11: Lightning Gulch Formation (member L_3): large-scale mudcracks in phyllite. Hammer in lower left is 28 cm long. Photo taken in the NW1/4 of Section 4 (T1N, R2E).

Figure 10.

Figure 11.

The lower and upper phyllite members of the Lightning Gulch contain very similar lithologies and sedimentary structures. The intervening middle quartzite member is differentiated by a predominance of quartzite although sedimentary structures are similar to those in members L1 and L3. The middle member marks a significant influx of fine grained quartz sand within a formation dominated by finer-grained pelitic rocks.

Sugarloaf Quartzite

Distribution. A sequence of quartzite and quartz phyllite which conformably overlies the Lightning Gulch Formation and underlies the Green Canyon Formation is assigned to the Sugarloaf Quartzite. This unit is only known presently in the Sugarloaf area. Its type area is at Peak 9433', 1.5 km northeast of Sugarloaf Mountain. These rocks were previously included in the Saragossa Quartzite (Dibblee, 1964a).

Description. The Sugarloaf Quartzite is generally found in complexly faulted tectonic slivers in the southwest portion of the Sugarloaf map area. A complete section is not exposed at any single locality. Fortunately, individual members of this formation are distinctive enough that a composite section can be reconstructed. A nearly intact section occurs at Peak 9433' and constitutes the type locality for the five members discussed below. In spite of structural complexities, this five-fold division is recognizable throughout the map area.

The lowest member of the Sugarloaf Quartzite (S1) consists of massive white vitreous quartzite. Member S1 forms bold angular outcrops which are distinctive even from a distance. Original bedding is almost indistinguishable. Various joint sets are easily mistaken for bedding but faint heavy mineral laminae are the only reliable indicators. Where laminations are present however, medium to large scale low-angle cross-stratification can sometimes be recognized. Mineralogically, member S1 is an orthoquartzite, with only trace amounts of biotite and

white mica. The protolith was a mature quartz sandstone. These rocks are medium-grained.

The lower contact of S1 is poorly exposed in the Sugarloaf area. At Peak 9433' for example, this contact is covered by talus shed across slopes underlain by recessive member L3 phyllites. Southeast from 9433' and just west of the Trail Fault, member S1 quartzite overlies poorly exposed graphitic phyllites, calc-silicate rocks and plagioclase-actinolite schists of member L3. Two to three meters of well-bedded grey quartzite is present at the top of member L3, immediately below the white quartzites. East of the Trail Fault, member S1 quartzites crop out above member L3 phyllite, calc-silicate hornfels and plagioclase-actinolite schists. The latter are poorly exposed here as colluvium covers much of the outcrop, however, float of the grey quartzite is again present between typical member L3 and S1 lithologies. West of the Trail Fault and south of the Wildhorse Fault, member S1 quartzite crops out above member L3 phyllites. Here, blocks of white quartzite at the base of member S1 contain casts of mudcracks. This is interpreted as evidence that member S1 was deposited conformably above member L3 phyllites, which were at least locally subaerially exposed.

Other possibly conformable contacts between member L3 phyllite and member S1 quartzite occur on Hill 8055' (between Green Canyon and the Wildhorse Road) and at the west end of Deadman's Ridge. In many cases, however, this contact is sheared or faulted, and section is missing. Locally, this was a zone of structural decoupling during Mesozoic deformations.

Member S2 consists of recessive, laminated quartz phyllite with lenses of lenticular-wavy bedded quartzite that overlie the white quartzites of member S1 with apparent conformity. The contact is best exposed on the south slope of Hill 8055' and south of the Wildhorse Fault in Green Canyon. The lithology and sedimentary structures of member S2 (and most of member S4) are virtually indistinguishable from those of the Lightning Gulch Formation. The phyllites consist of fine-grained white mica, biotite and minor chlorite with varying amounts of fine-grained quartz. Porphyroblasts of biotite and

pseudoporphyroblasts of white mica and quartz are common. Locally abundant hematite gives these rocks a red-brown color, although dark grey is their more characteristic color. As in the Lightning Gulch Formation, lenticular-wavy bedded quartzite lenses, sometimes with ripple cross-lamination, are common. Mudcracks, load structures and dewatering and escape structures are also present. Protoliths were thinly interbedded shales, siltstones and sandstones. A 26 m thick section was measured at Peak 9433'.

Member S2 is conformably overlain by well-bedded light grey to tan quartzite of member S3. These resistant quartzites are exposed at 9433' and at Hill 8055'. Mineralogically, member S3 quartzites consist of approximately 94% quartz grains with 2% biotite and white mica, and about 4% feldspar. Like member S1, member S3 was derived from a mature quartz sandstone.

Member S3 quartzites contain large and medium scale low-angle cross-stratification. At Peak 9433', massive basal quartzite of member S3 contains elongate rip-up clasts of member S2 phyllites (Fig. 12). Also, blocks of member S3 quartzite with casts of mudcracks are present near the member's base at various localities, and indicate a conformable contact between members S2 and S3. The presence of a one meter thick bed of member S3-like quartzite near the top of member S2 on the southwest slope of Hill 8055' suggests these lithologies interfinger. Member S3 is 12 m thick at Peak 9433'.

Member S4 is similar in lithology to S2, and overlies member S3 with apparent conformity. It is best exposed at Peak 9433' and in the synform to the northeast. Other incomplete sections occur on Hill 8055', at the west end of Deadman's Ridge, and on the north slope of Sugarloaf Mountain.

The lower 20 m of member S4 consists primarily of dark grey to red-brown laminated quartz phyllite and micaceous quartzite, with lenticular interbeds of fine grained quartzite. Protoliths were siltstone and interbeds of fine-grained sandstone. In meta- pelitic rocks the matrix consists of very fine-grained white mica and minor amounts of chlorite. Quartz is present in the matrix and in lenticular quartzite interbeds, and may account for more than 50 percent of the

Figure 12: Sugarloaf Quartzite (member S3): rip-up clasts of member S2 phyllite at base. Member S3 quartzite is massive here, but well bedded a few m up-section. Hammerhead in upper center is 20 cm long. Photo taken at Peak 9433', in the NW1/4 of Section 5 (T1N, R2E).

Figure 13: Sugarloaf Quartzite (member S5): large-scale, low-angle cross stratification. These quartzites are near the base of member S5. Hammer in right center is 28 cm long. Photo taken at Peak 9433', in the NW1/4 of Section 5 (T1N, R2E).

Figure 12.

Figure 13.

rock in many cases. Biotite porphyroblasts, sometimes altered to chlorite, are common as is accessory Fe tourmaline. Interstitial hematite accounts for local red-brown coloration. Member S4 phyllites are generally laminated, as are the micaceous quartzites. Quartzites exhibit lenticular-wavy bedding and pinstripe tidal bedding typical of the Lightning Gulch Formation and member S2. Graded beds are common. Mudcracks, load structures, and soft sediment dewatering and escape structures are also present. Microscopic deformed rip-up clasts or burrow tubes of micaceous quartzite were present in one specimen of otherwise laminated phyllite.

At Peak 9433', the top five meters of member S4 consists of light grey laminated calc-silicate marble. Similar marble is present in tectonic slivers on the north slope of Sugarloaf Mountain and in the section on Deadman's Ridge. The protolith was siliceous dolomitic limestone.

The uppermost member of the Sugarloaf Quartzite, S5, overlies member S4 marble with apparent conformity at Peak 9433'. Only the lower part of member S5 is exposed near the peak and on the slopes below. Rocks correlated with these and assigned to the upper part of member S5 are exposed in tectonic slivers on the north slope of Sugarloaf Mountain, and are overlain with apparent conformity by the Green Canyon Formation (member G1). Quartzite overlying calc-silicate marble (assigned to member S4?) in a fault sliver on Deadman's Ridge is also tentatively assigned to member S5. Member S5 consists of generally well-bedded (but locally massive) light blue-grey to white quartzite, which forms bold, angular outcrops. At Peak 9433', this quartzite contains about 95% fine grained quartz, 5% metamorphic plagioclase and traces of white mica. The quartzite immediately below the Green Canyon Formation marbles north of Sugarloaf Mountain consists of 95% quartz with about 5% tremolite. These accessory phases may have been derived from original calcareous cement in the protolith quartz sandstones. At both localities, large scale low-angle tabular cross-stratification is present (Fig. 13). Smaller scale planar tabular cross-stratification can also be recognized. In isolated

exposures of quartzite assigned to member S5 north of Sugarloaf Mountain, bedding laminations are difficult to recognize. On the slope northeast of Peak 9433', float blocks of member S5 found near its base contain mudcrack casts (Fig. 14). Member S4 is present only in float here, but mudcracks are observed in some float blocks. These relations are interpreted as evidence of a conformable contact. The thin marble in the upper part of member S4 is not present here, although it may be covered.

At Peak 9433', 61 m of member S5 quartzite were measured above member S4. On the north slope of Sugarloaf Mountain, at least 64 m of member S5 are present below member G1 of the Green Canyon Formation. Thus, member S5 has a minimum thickness of 64 m.

Green Canyon Formation

General Statement. The name Green Canyon Formation is applied to a complexly imbricated and intruded sequence of dolomitic marble, calc-silicate rock, phyllite and quartzite which is exposed primarily southwest of lower Green Canyon. This sequence, as well as overlying units in the Sugarloaf area, is exceptionally disrupted by low- and moderate-angle normal faults. Nowhere is a complete, intact section of the Green Canyon Formation present. Thus, no type section is defined. However, detailed mapping has permitted reconstruction of a tentative composite stratigraphic section of the Green Canyon Formation, which includes nine members (G1 through G9). This composite unit, the Green Canyon Formation, overlies the Sugarloaf Quartzite and underlies the Delamar Mountain Formation and is presently known only from the Sugarloaf area. It includes rocks previously correlated with the Upper Paleozoic Furnace Limestone (Dibblee, 1964a). In this section, the distribution and lithology of each member is discussed separately. Members G1-G3 constitute a composite sequence overlying the Sugarloaf Quartzite. Members G4-G9 form a composite sequence underlying the Delamar Mountain Formation. The only break without a clear overlap of section occurs between members G3 and G4, as discussed below. The various parts of the composite section are depicted in Fig. 15.

Figure 14: Sugarloaf Quartzite (member S5): Casts of mudcracks in quartzite blocks from base of unit. Member S5 is inferred to have conformably overlain metapelitic rocks of member S4 which contain mudcracks. Hammer is 28 cm long. Photo taken in the SE1/4 of Section 32 (T2N, R2E).

Figure 16: Green Canyon Formation (member G5): deformed stromatolites in dolomitic marble. Pencil is for scale. Photo taken in SE1/4 of Section 31 (T2N, R2E).

Figure 14.

Figure 16.

Figure 15: Stratigraphic columns of the Green Canyon Formation

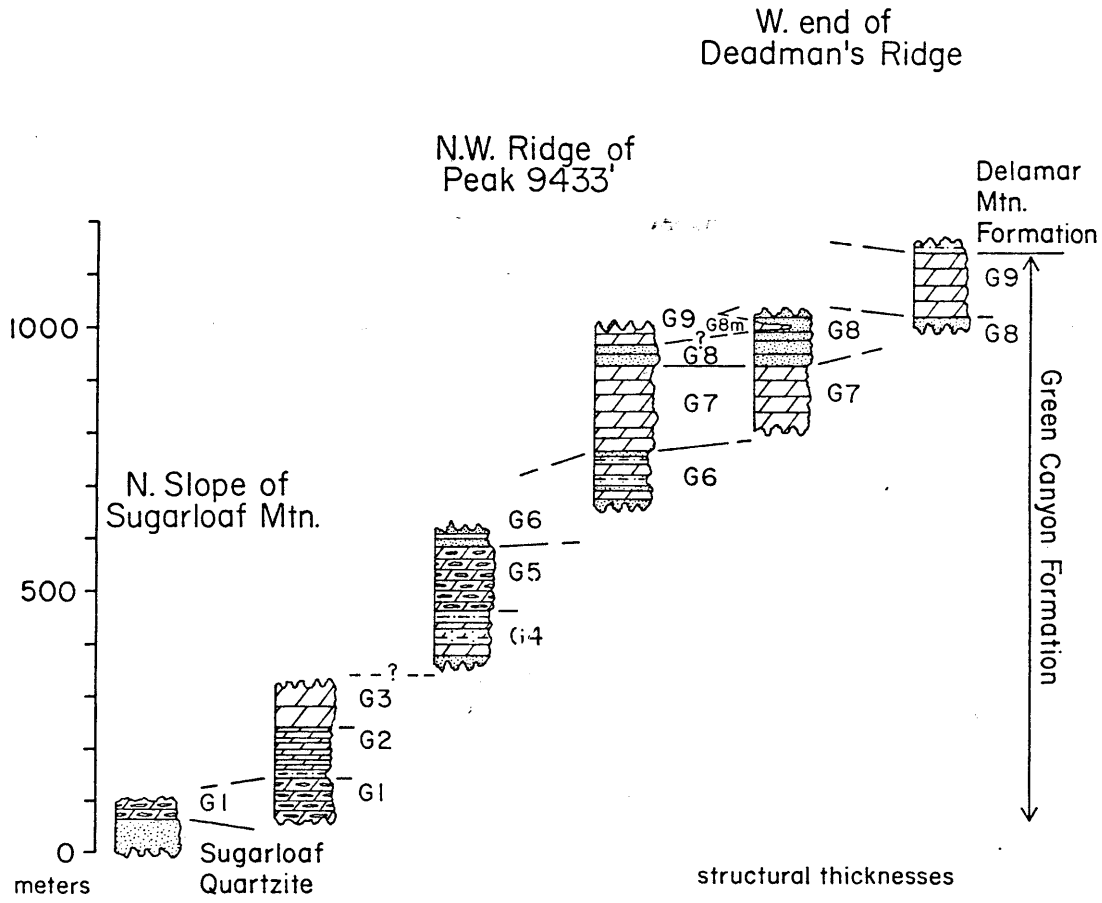

Thickness of units must be considered with caution. Estimates given represent structural thicknesses, and in several cases the members in question, particularly marble units, are internally isoclinally folded, and original bedding is transposed. Furthermore, this is a composite section, reconstructed into a vertical sequence from laterally exposed outcrops. Depositional and tectonic interfingering of members is present, thus the "minimum" thickness calculated for the composite section may overestimate its true structural thickness. Wherever possible, thickness estimates are presented for the least deformed sections of a given member.

Description of Members G1-G3. The lowest member of the Green Canyon Formation (G1) consists of calc-silicate marble whose protolith was a cherty dolomitic limestone. On the north ridge of Sugarloaf Mountain (9200' elevation), 16 m of marble included in this unit overlie quartzite correlated with member S5 of the Sugarloaf Quartzite with apparent conformity. A similar relationship is inferred at outcrops a short distance to the south, but surrounded by talus. In the NE1/4 of Section 6 (T1N, R2E), 80 m of calc-silicate marble assigned to member G1 are overlain conformably by quartzite of member G2. A similar relationship is present northwest of Peak 9433', immediately above the intruded Green Canyon Fault, which cuts out the base of member G1. Based on these exposures, member G1 has a minimum structural thickness of 80 m.

The distinctive feature of these light grey marbles is the presence of "chert" nodules, lenses, layers and laminations, now composed of quartz and calc-silicate minerals. These weather red-brown and define original and transposed bedding in member G1. Chert layers and nodules range from 1 cm to 0.3 m in thickness and are usually discontinuous. Many of the elliptical chert nodules resemble silicified algal heads and display intricate concentric internal structure. Locally, chertified stromatolites are outlined by calc-silicate laminations. Laminated marbles may be recrystallized algal mat dolomitic limestones. Mineralogically, the marbles consist of calcite and dolomite with cherty horizons represented by varying

proportions and combinations of quartz, tremolite, diopside, and epidote. Numerous small pendants of cherty marble on the north flank of Sugarloaf Mountain are assigned to member G1, as are the larger blocks of cherty marble within the chaos in a gravity slide block in the SE1/4 of Section 32 (T2N, R2E).

The cherty marbles of member G1 are overlain conformably by member G2 quartzite and marble in the NE1/4 of Section 6, and in the NW1/4 of Section 5 (T1N, R2E). At its base, member G2 consists of 16 m of dark grey to red-brown weathering, fine grained, laminated tremolite-bearing quartzite which is locally interbedded with laminated calc-silicate marble. Above the quartzites, laminated calc-silicate marble is present, locally interbedded with massive light grey marble. Resistant calc-silicate laminae (primarily tremolite), 0.5 to 2 cm thick, are interbedded with thin recessive layers of marble. The calc-silicate marbles in the upper part of member G2 have an approximate structural thickness of 80 m in the NW1/4 of Section 5 (T1N, R2E). Calc-silicate layers often constitute more than 50 percent of the rock. The protoliths of member G2 included silty limestone and dolomite and calcareous sandstone. Unfortunately, no diagnostic facing indicators were recognized in member G2, in either the basal quartzites or the marbles that overlie them. These rocks are assigned a stratigraphic position above member G1 because nearby member G1 cherty marbles are underlain by the thick and distinctive Sugarloaf Quartzite.

The laminated calc-silicate marbles of member G2 are overlain gradationally by white to light grey weathering, massive dolomitic marbles of member G3. This contact is exposed in the NE1/4 of Section 6 (T1N, R2E), where member G3 forms resistant cliffs above the calc-silicate marbles of member G2. The same contact is also recognized above the Green Canyon Fault, in the NW1/4 of Section 5 (T1N, R2E) where the contact is isoclinally folded on a mesoscopic scale. Here too, massive marbles of member G3 overlie the laminated calc-silicate marbles of member G2. The upper contact of member G3 is a fault, intruded or covered in both areas. A minimum structural thickness for member G3 of 80 m is estimated from these exposures. The protolith of this coarse grained dolomitic marble was a dolomitic limestone. Compositional

layering is difficult to recognize in these massive marbles, and is defined by rare, thin calc-silicate layers which are the transposed remnants of thin beds or laminations.

Members G1-G3 constitute the lower part of the composite section of Green Canyon Formation. There is sufficient stratigraphic overlap between the disrupted sections of these rocks to justify a stratigraphic reconstruction in which members G1 through G3 overlie the Sugarloaf Quartzite. The upper members of the Green Canyon Formation constitute a separate composite section, which does not appear to overlap stratigraphically with members G1-G3, but probably originally lay above them.

Description of Members G4-G9. The lowest exposed member of the upper composite section of the Green Canyon Formation is member G4 and is only present below marbles of member G5 at one locality in the SE1/4 of Section 31 (T2N, R2E). Member G4 is poorly exposed, and consists of a few low outcrops of grey to red-weathering, laminated fine-grained micaceous quartzite and quartz phyllite with thin interbeds of grey marble. Areas between rare outcrops are underlain by float of red-brown weathering, fine-grained, laminated quartzite and grey phyllite, laminated calc-silicate rock and marble. Hematite gives the quartz-rich rocks their red color. The quartzites were derived from impure sandstones judging by the abundance of interstitial white mica. Sandstones and interbedded laminated siltstones, shales, marls and limestones formed the protoliths for rocks assigned to member G4. This member has a minimum structural thickness of approximately 105 m.

The calc-silicate marbles of member G5 overlie member G4 with apparent conformity in the SE1/4 of Section 31 (T2N, R2E) and are overlain by member G6 in adjacent parts of Sections 5 and 6 (T1N, R2E). Member G5 consists predominantly of marbles derived from cherty dolomitic limestones. In SE1/4 of Section 31, member G5 has a structural thickness of 121 m. The lower contact is placed immediately below a resistant 10 m thick ledge of blue-grey laminated tremolite-calcite rock. These calc-silicate rocks contain white, elliptical calc-silicate (originally

chert) nodules or concretions, ranging from 0.5 cm to more than 5 cm in diameter. These nodules appear to be diagenetic because in several cases primary laminations can be traced into and through the concretions, and are deflected outwards about a core of coarse calcite marble. These cores weather out to produce a cratered bedding surface, and may represent relict diagenetic features. Many of these concretions are nearly spherical, indicating they have not been highly strained. Overlying the calc-silicate rocks is a 4 m thick section of tan-weathering laminated quartzite and phyllite. Rare cross-stratification indicates the sequence is upright. Above these rocks is a 10 m thick transition zone of laminated calc-silicate rock and cherty marble, overlain by more resistant outcrops of light grey cherty marble. These marbles are the most distinctive rocks of member G5 and contain algal stromatolites, outlined by the thin calc-silicate laminations (Fig. 16). Locally, small colonies of vertically aggrading stromatolites are recognized. These are best preserved near the base of member G5, as higher up-section the marbles are tightly folded and stromatolitic structures are transposed on attenuated fold limbs. Primary parallel laminations in these marbles may represent algal mat laminae, and these too are often transposed by folding. Cherty marbles belonging to member G5 are also exposed in several pendants in the SW1/4 of Section 32 (T2N, R2E).

The principal exposures of members G4 and G5 occur in the core of a refolded and faulted anticline in the SE1/4 of Section 31 (T2N, R2E). Along the south limb of this fold, rocks of member G6 overlie member G5. This poorly exposed section consists of thin-bedded calc-silicate rock and red-weathering laminated quartzite. No facing indicators were found in these outcrops, but mesoscopic structural data and occasional facing directions from underlying rocks of member G5 suggest tops are to the south. Thus these rocks represent a stratigraphically higher member, and do not represent a north facing section of member G4. Rocks correlated with members G5 and G6 and interpreted to represent the down-faulted and intruded, north limb of this anticline occur in Sections 31 and 32 (T2N, R2E). The anticline is refolded by the northwest plunging Green Canyon Synform.

On the southwest limb of this synform, member G6 is conformably overlain by the marbles of member G7.

Along this locally overturned fold limb member G6 includes laminated graphitic phyllite and schist, red-weathering, fine-grained, laminated quartzite, thin bedded calc-silicate rock, marble, and locally, medium-grained green-grey quartzite. Laminated phyllite and fine-grained quartzite are the most abundant lithologies; the other rock types occur as interbeds generally 1-5 m thick. Thin-layered dolomitic marble and calc-silicate rock are most prevalent near the top of the member, marking a transition into the overlying marble unit, member G7. Ledge-forming green-grey vitreous quartzite occurs in nearly all sections of member G6. This relatively pure, medium-grained quartzite exhibits small scale cross-stratification which provides facing control. Phyllite of member G6 consists of white mica and graphite, variable amounts of quartz, minor plagioclase, porphyroblasts of biotite (or retrograde chlorite) and Mg-tourmaline. Hematite is abundant in quartz-rich rocks. The exposed minimum thickness of member G6 varies from 77 to 193 m along the southwest limb of the Green Canyon Synform. In the SW1/4 of Section 32, quartzite, phyllite and marble of member G6 are exposed on the ridge due north of Peak 9433'. These structurally overlie cherty marbles of member G5 although the original contact has been intruded.

Rocks assigned to member G6 are present in several fault blocks above and west of the Green Canyon Fault in lower Green Canyon. They are best exposed in the northern fault block. The lowest exposed rocks are 48 m of red-weathering laminated to thin-bedded impure quartzite, graphitic phyllite and calc-silicate rock. Above these rocks are 48 m of light grey vitreous quartzite with large scale, low-angle cross-beds. Overlying the quartzite is 19 m of dark grey, laminated graphitic phyllite, with euhedral porphyroblasts of Mg-tourmaline. The phyllite interfingers with overlying, thin-layered dolomitic marble which has a minimum exposed thickness of 28 m. In fault blocks to the south, the marble is overlain by more graphitic phyllite.

The graphitic phyllites resemble those seen nearby in the Lightning Gulch Formation. However, these phyllites include thick interbeds of pure quartzite and marble which are not recognized in the Lightning Gulch

Formation. For this reason, this sequence is correlated with lithologically similar rocks of member G6.

In the SE1/4 of Section 31 and the SW1/4 of Section 32 (T2N, R2E), the predominantly metaclastic rocks of member G6 are overlain with gradational contact by massive marble of member G7. The contact is placed immediately above the highest outcrops of red-brown to grey-weathering laminated quartz phyllite and micaceous quartzite. Interbeds of grey marble are present at the top of member G6 and suggest a transitional upper contact. The overlying marbles of member G7 are exposed in the core of the Green Canyon Synform and are overlain by quartzite of member G8. In this area, member G7 consists of boldly outcropping, light grey to white-weathering dolomitic marble. The marble is massive, coarse-grained, with compositional layering defined by rare calc-silicate layers. This layering represents original bedding only near the upper and lower contacts of member G7. Here, faint (algal mat?) laminations can be recognized. Internally, the marbles of member G7 are complexly folded; bedding is transposed on the limbs of tight to isoclinal folds. Because of the structural transposition, few sedimentary structures are preserved. Lenticular interbeds (1-2 m thick) of pebbly, trough cross-stratified quartzite near the top of member G7 are also tightly folded. Thin-layered cherty marble locally occurs at the top of member G7 in the core of the Green Canyon Synform. The protoliths of member G7 included dolomitic limestones (locally cherty) with local interbeds of quartz pebble-bearing sandstone near the top. A structural thickness of 161 m of member G7 is present on the southwest limb of the synform in the east half of Section 31 (T2N, R2E).

West of the Green Canyon Synform, rocks correlated with member G7 crop out in the center of Section 31 (T2N, R2E). These rocks underlie the distinctive quartzite of member G8 and include grey dolomitic marble with thin calc-silicate (chert) interbeds which locally is interbedded with trough cross-stratified quartzite. These rocks are similar to those present near the top of member G7 in the syncline in Section 31. Other sections of massive marble correlated with member G7 on the basis of lithologic similarity and stratigraphic or structural position below rocks of member G8 include marbles at the west end of

Deadman's Ridge (NW1/4 of Section 29, T2N, R2E) and in the E1/2 SW1/4 of Section 32 (T2N, R2E). Marbles tentatively included with member G7 in the center of Section 31 (T2N, R2E) are not in contact with any other unit but are surrounded by intrusive rocks. These generally massive marbles are most akin to member G7, which is exposed nearby to the south.

Member G7 is overlain conformably by the distinctive feldspathic quartzite of member G8. This contact is exposed in the core of the Green Canyon Synform in the east half of Section 31, in the SE1/4 of Section 31, and on the west end of Deadman's Ridge in the NW1/4 of Section 29 (all in T2N, R2E). Quartzite of member G8 is conformably overlain by the massive marbles of member G9.

Member G8 consists of boldly outcropping coarse-grained white to light grey K-feldspar-bearing quartzite. The presence of coarse grey K-feldspar in these quartzites is their most distinctive feature. These rocks commonly contain up to 20-30% K-feldspar, along with up to 5% muscovite, and abundant quartz. Both microcline and orthoclase are present. In less recrystallized rocks these grains are rounded and clearly of detrital origin. Rarely, relict granules of granitic rock (microcline-quartz) are present in thin section. Beds of quartzite pebble and feldspar granule conglomerate (0.5-1m thick) and rare quartzite cobble conglomerate are locally present at the west end of Deadman's Ridge. The protolith of member G8 was an arkosic sandstone. Member G8 is significant not only as a distinctive stratigraphic horizon, but it also marks the transition from predominantly orthoquartzite and subarkosic protoliths in underlying units (with rarely more than five percent feldspar) to the predominantly subarkosic to arkosic protoliths at the top of the Big Bear Group.

Interbeds of thin-layered calc-silicate (cherty) dolomitic marble (G8m) occur within member G8 in exposures underlying member G9 (NE1/4 of Section 31, T2N, R2E) and may indicate an interfingering of members G8 and G9. Marbles assigned to member G8m interfinger with quartzites of member G8 on the west end of Deadman's Ridge. These quartzites and the marbles are folded in a tight east vergent synform. A distinctive conglomerate bed occurs above the member G8m marbles on both limbs of the synform, and the marbles appear to thicken on the west limb. At this

locality, marbles of member G8m may actually represent tongues of member G9.

Small scale trough cross-bedding and medium to large scale tabular tangential cross sets are quite common in member G8. Heavy mineral concentrations define bedding laminations. Member G8 varies in thickness: 40 m of quartzite are present above member G7 in the core of the Green Canyon Synform in the east half of Section 31, and a minimum of 100 m of quartzite is exposed at the west end of Deadman's Ridge.

The grey K-feldspar-bearing quartzites of member G8 are also exposed in the S center of Section 32 (T2N, R2E). Light grey-weathering feldspathic quartzites exposed on Green Spot Hill in the SE1/4 of Section 30 (T2N, R2E) are similarly cross-bedded, underlie marbles assigned to member G9, but only locally contain grey K-feldspar. They are assigned to member G8. Fault-bound outcrops of similar feldspathic quartzite in the SW1/4 of Section 29 are also tentatively assigned to member G8.

The massive dolomitic marbles of member G9 constitute the uppermost unit of the Green Canyon Formation. These marbles conformably overlie quartzites of member G8 at the west end of Deadman's Ridge, at the east side of Green Spot Hill, in the NE1/4 and SE1/4 of Section 31, and in the SW1/4 of Section 32 (T2N, R2E). Member G9 is overlain with gradational contact by the Delamar Mountain Formation at the west end of Deadman's Ridge.

Member G9 consists almost exclusively of grey to white weathering coarse-grained dolomitic marble. These marbles form resistant outcrops, and are generally massive. Bedding is defined by occasional calc-silicate (chert) lenses and thin interbeds. The lower contact of member G9 is placed just above the highest feldspathic quartzites of member G8, at the beginning of a thick sequence of massive marble. A few meters of thin-bedded calc-silicate rocks are present at the base of exposures in the SE1/4 of Section 32 (above the Green Canyon Fault).

Member G9 is widely exposed in the Green Canyon area and is usually present in sequence with member G8. The top of member G9 is only exposed at the west end of Deadman's Ridge. The presence of thin (0.5 m thick) lenses of interbedded quartzite near the top suggests a gradational contact. At Deadman's Ridge, 121 m of member G9 marble were

measured. Member G9 appears to be thicker elsewhere in the Sugarloaf area where member G8 is thinner. These variations may be due to tectonic thickening, stratigraphic interfingering with member G8, or both.

Discussion of Correlations. The Green Canyon Formation composite section consists of three parts. At the base, 16 m of cherty algal marble (here assigned to member G1) are exposed, overlying upright beds of uppermost Sugarloaf Quartzite (member S5). The top of these marbles is an intrusive contact. The middle part of the composite section (members G1 through G3) is exposed in two relatively coherent blocks, but its stratigraphic facing is uncertain, and its upper and lower contacts are intruded. The upper part of the Green Canyon Formation is relatively intact and consists of members G4 through G9. Stratigraphic facing is determined by sedimentary structures in members G5, G6, and G8. The upper part of the section is overlain by the Delamar Mountain Formation, however, its base is an intrusive contact.

The interpretation favored here is that members G1 through G9 are successive members of a single section. The marbles above the Sugarloaf Quartzite are correlated with those underlying members G2 and G3, and thus define the facing for members G1-G3 in the middle part of the section. In this interpretation, the only gap in the Green Canyon Formation occurs between members G3 and G4. Section is missing here, but how much is uncertain. According to this interpretation, the Green Canyon Formation has a minimum thickness of approximately 881 m (calculated using minimum thickness estimates for each member cited above).

An alternative interpretation for members G1-G3 is possible. The rocks of the "middle" part of the sequence are quite similar to members G5-G7. The cherty algal marbles of G1 may be equivalent to those of member G5. Likewise, the massive marbles of G3 may correlate with those of member G7. Such correlations reduce the total minimum thickness of the Green Canyon Formation to 641 m.

Two factors argue against this interpretation. Members G2 and

G6 do not match easily. Member G2 consists primarily of laminated calc-silicate marble, with quartzite only near the base. Member G6 is composed predominantly of metaclastic rocks. Graphitic phyllites and relatively pure quartzites present in member G6 have no correlatives in member G2. The base of member G5 is exposed, and it overlies member G4 and not rocks similar to the uppermost Sugarloaf Quartzite. It seems unlikely that the quartzites at the top of member S5 would grade laterally into rocks like those of member G4 (micaceous quartzite, phyllite, calc-silicate rocks and marble) within such a short distance. The marbles overlying member S5 are similar to those of member G1, not rocks of member G4. This correlation scheme requires that the cherty algal marbles overlying the Sugarloaf Quartzite must eventually pass upwards into lithologies like those of member G4, then back into cherty algal marbles of member G5. While this is a possibility, it still leaves a gap in the section.

While the correlation of members G1-G3 with members G5-G6 is potentially attractive, the dissimilarity of members G2 and G6 makes the overall match suspect. For this reason, a nine-fold division of the Green Canyon Formation is suggested here.

Delamar Mountain Formation

Distribution. The name Delamar Mountain Formation is applied to rocks which underlie strata of the Uppermost Precambrian-Lower Cambrian Wood Canyon Formation near Fawnskin. These rocks are exposed in the core of the major antiform southeast of Delamar Mountain. This locality is designated as the type section. The lower contact of this formation is intrusive at Delamar Mountain. However, a correlative sequence occurs in the Sugarloaf area and overlies the uppermost member (G9) of the Green Canyon Formation. Based on these relationships, the Delamar Mountain Formation is considered the highest unit of the Big Bear Group.

The rocks of the Delamar Mountain Formation exposed near Fawnskin were previously included in the lower member of the Chicopee Canyon Formation of Richmond (1960) and in the Saragossa Quartzite (Dibblee,

1964). In the Sugarloaf area they were included in both the Saragossa Quartzite and the Furnace Limestone by Dibblee (1964a).

Rocks correlative with the Delamar Mountain Formation are also present in the Chicopee Canyon area, northwest of Baldwin Lake (this area is called Jacoby Canyon on the Big Bear City 7.5' quadrangle). Correlative rocks here were previously assigned to the Chicopee Formation (Guillou, 1953), the Saragossa Quartzite (Dibblee, 1964b), the Upper Precambrian Johnnie Formation and Stirling Quartzite (Stewart and Poole, 1975), and the D and E members of the Stirling Quartzite(?) equivalent by Tyler (1975). Reassignment of correlative rocks in Chicopee Canyon is discussed below (Age and Local Correlation of the Big Bear Group).

Description. In both the Delamar Mountain and Sugarloaf areas, the Delamar Mountain Formation is divided into two members. These are member D1, a lower fine-grained clastic and marble unit, and member D2, an upper feldspathic quartzite unit (Fig. 17). In the Delamar Mountain area, member D1 is exposed in the SE1/4 of Section 1 (T2N, R1W) and the SW1/4 of Section 6 (T2N, R1E). Member D1 consists of a heterogeneous sequence of interbedded calc-silicate rock, flaser-lenticular bedded quartzite and quartz biotite schist (or phyllite), marble, and feldspathic quartzite. Protoliths include marl, siltstone and shale, siliceous dolomitic limestone and arkosic sandstone. These rocks are best exposed on the east limb of the Delamar Mountain Antiform. The upper contact of member D1 can be traced near roadcut exposures here, where resistant outcrops of well-bedded, light grey feldspathic quartzite of member D2 conformably overlie well-bedded micaceous quartzite, thinly bedded to laminated calc-silicate rock, and flaser-lenticular bedded quartzite and schist of member D1. The latter lithologies contain graded beds (often metamorphically reversed) and ripple cross-laminations. Thin layered cherty marble and interbedded feldspathic quartzite occur structurally below these rocks in outcrops surrounded by the Bertha Diorite and faulted against Zabriskie Quartzite. These rocks are the lowest parts of member D1 exposed at Delamar Mountain. A minimum thickness of 68 m

Figure 17: Stratigraphic columns of the Delamar Mountain Formation

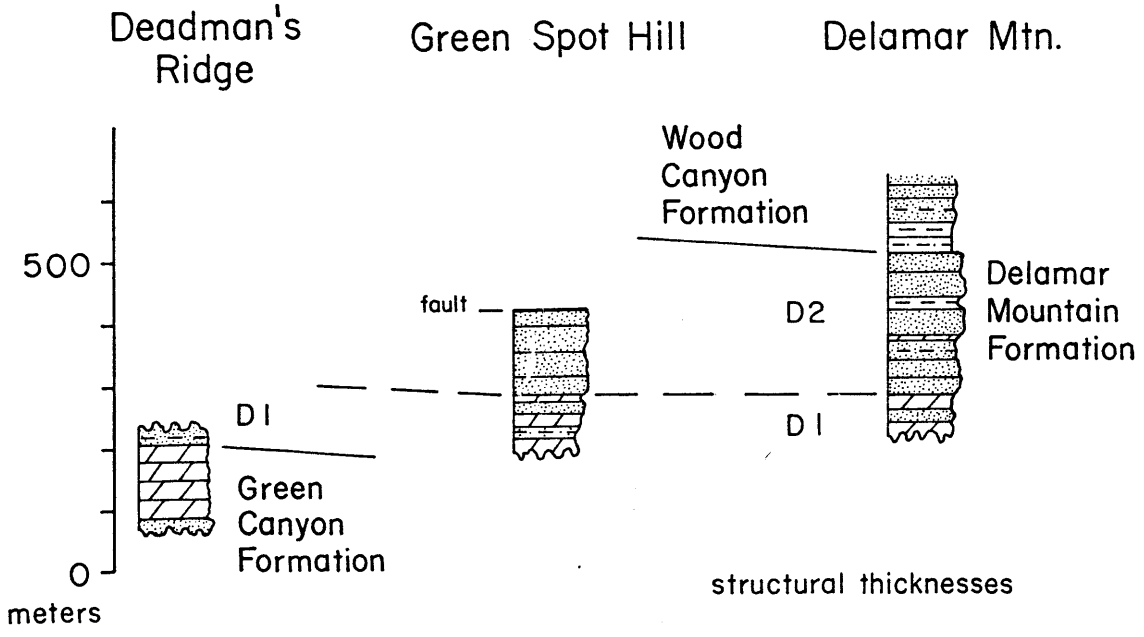

of member D1 is present here.

The overlying quartzites of member D2 are well exposed locally in the roadcuts and above on adjacent ridges. They are overlain with apparent conformity by phyllite and quartzite of the Wood Canyon Formation. Well-bedded light grey quartzite is the principal rock type, but occasional interbeds of thin-layered cherty marble, micaceous quartzite and phyllite are present. The quartzites display large, medium and small scale tabular tangential cross-stratification. They are usually medium-to coarse-grained, contain 10-20% feldspar and traces of muscovite. The feldspar is primarily albite and (?) plagioclase; K-feldspar is not conspicuous (in contrast to member G8). Some of the feldspar occurs in coarse rounded grains, and is probably of detrital origin. The uppermost quartzites locally contain discontinuous laminae of calc-silicate minerals, which weather out as spots on bedding surfaces. The protolith of member D2 consisted of arkosic sandstone with interbeds of siliceous limestone and siltstone and calcareous sandstone. On the ridge between Peak 7856' and the SW corner of Section 6 (T2N, R1E), 217 m of member D2 is present. Member D2 thickens tectonically to the northwest in the nose of the Delamar Mountain antiform.

In the Sugarloaf area, the Delamar Mountain Formation occurs in several fault blocks or slivers. Quartzites assigned to member D2 locally overlie a heterogeneous section of rocks here assigned to member D1. In a nearby section, lithologically similar strata, also correlated with member D1, overlie the upper member of the Green Canyon Formation.

In the Sugarloaf area rocks assigned to the lower part of member D1 overlie marbles of the uppermost Green Canyon Formation (member G9) in a tight synform at the west end of Deadman's Ridge (NW1/4 of Section 29). Here member D1 consists of recessive, thin-bedded fine-grained micaceous quartzite (red-brown weathering with abundant hematite), laminated calc-silicate rock, phyllite and rare interbeds of pale purple vitreous quartzite. The lower contact of member D1 appears gradational into rocks of the Green Canyon Formation. At this locality, the uppermost beds of member G9 of the Green Canyon Formation consist of laminated cherty marble with interbeds of fine grained quartzite. Downsection

these grade quickly into massive dolomitic marble, typical of member G9. The contact between the Delamar Mountain Formation (member D1) and the Green Canyon Formation (member G9) is placed at the top of the laminated cherty marbles, which separate the predominantly fine-grained metaclastic rocks of member D1 above from the massive marbles of member G9 below. Member D1 has a minimum thickness of 20 m here.

Rocks assigned to the upper part of member D1 are exposed on the southeast side of Green Spot Hill, where they are overlain gradationally by quartzite of member D2. They are interpreted to be downfaulted against member G9 marble on the east and west. The exposed member D1 section here is 121 m thick and includes interbedded laminated calc-silicate rock, massive and cherty marble, quartz phyllite, thin-bedded micaceous quartzite (hematite-bearing) and massive ledges up to five meters thick of white feldspathic quartzite. These quartzites often are cross-bedded, and the finer grained clastic rocks sometimes contain rip-up clasts and soft sediment folds. Individual beds cannot be traced very far along strike; this may be in part due to interfingering of lithologies.

At Green Spot Hill the upper contact of member D1 is located near the ridge crest, where the proportion of marble and calc-silicate rock in the section decreases and light grey feldspathic quartzite predominates. Quartzite outcrops at the ridge crest are assigned to member D2. The rocks of member D2 crop out poorly, although float is abundant. Coarse-grained feldspathic quartzite is the principal lithology, with some interbeds of marble and calc-silicate rock recognized just above member D1. The quartzites here are similar to those of member D2 at Delamar Mountain. They contain 15-20% feldspar, about 5% muscovite, biotite and chlorite, and 75-80% quartz. The feldspar is primarily albite and (?) plagioclase. K-feldspar is not conspicuous. At least some feldspar (coarse, rounded grains) is detrital in origin. Relict quartzite pebbles and granules are common. An east trending high-angle fault bounds this section of member D2, which has a structural thickness of 137 m.

North of this fault, rocks of member D2 may be tightly folded on

the north slope of Green Spot Hill. Interbedded feldspathic quartzite and flaser bedded quartzite face south, at least locally. These lithologies are similar to those at the contact between members D1 and D2 at Delamar Mountain. These rocks may constitute the north limb of a faulted, east trending synform with member D2 in its core. Massive white vitreous quartzite is faulted against these rocks at the north edge of the hill. The faults appear to dip northward and the coarse grained quartzites are tentatively included with member D2.

Another fault-bounded section assigned to member D2 occurs in the NE1/4 of Section 31 (T2N, R2E), above the Green Canyon Fault. These light grey, locally cross-bedded, coarse-grained quartzites contain 20% or more feldspar. The feldspar is predominantly albite and (?) plagioclase, but microcline is also present. Relict detrital feldspar can be recognized. One grain has inclusions of fine-grained muscovite, and may be a detrital porphyroblast from an older metamorphic terrane (such textures are locally present in nearby Precambrian gneisses). A continuous marble bed (about five meters thick) was recognized in this section. Again, lithologic similarity with the type section of member D2 is the basis for this correlation.

Age and Local Correlation of the Big Bear Group

Age. The formations described above constitute the Big Bear Group. This sequence unconformably overlies a previously deformed basement complex which has yielded a 1.75 b.y. minimum age (U/Pb zircon, Silver, 1971) on granitic augen gneiss. The uppermost unit of the Big Bear Group is overlain with conformity by rocks lithologically correlated with the uppermost Precambrian-Lower Cambrian rocks of the Wood Canyon Formation. Although the Wood Canyon Formation has not yielded fossils in the Big Bear area, the typical Early Cambrian trace fossil Scolithus has been recognized in the upper Wood Canyon and overlying Zabriskie Quartzite at Chicopee Canyon (Stewart and Poole, 1975; Tyler, 1975) and at Delamar Mountain (this study). These data indicate a Late Precambrian age for the Big Bear Group.

Correlation with Rocks at Chicopee Canyon. Upper Precambrian and Cambrian rocks are also present at Chicopee Canyon northwest of Baldwin Lake (Fig. 3). It was here that the Wood Canyon Formation and overlying Cambrian units were first recognized in the San Bernardino Mountains, by Stewart and Poole (1975). They suggested that a section of metasedimentary rocks previously mapped by Guillou (1953) and Dibblee (1964b) were correlative with the Wood Canyon Formation, Zabriskie Quartzite, Carrara Formation and Bonanza King Formation, which are widely exposed in the miogeoclinal belt of the southern Great Basin. Tyler (1975) reached a similar conclusion based on his detailed mapping at Chicopee Canyon.

In the southern Nevada-Death Valley region, the Wood Canyon Formation is underlain by an Upper Precambrian stratigraphic succession which is lithologically uniform over a wide region. This sequence locally includes the Noonday Dolomite at its base, but more typically the lowest strata are fine grained clastics of the Johnnie Formation, overlain by massive sandstones of the Stirling Quartzite, and the Wood Canyon Formation (Stewart, 1970).

At Chicopee Canyon, phyllite and quartzite of the Wood Canyon Formation conformably overlies 91 m of well-bedded, coarse-grained (locally conglomeratic) light grey feldspathic quartzite (Tyler, 1975; this study). These quartzites gradationally overlie a lower unit (exposed thickness: 61 m) of interbedded coarse feldspathic quartzite, massive and (locally) laminated cherty marble, and red-brown weathering fine-grained quartzite. Stewart and Poole (1975) interpreted a contact between the lower unit and nearby Precambrian gneisses as an unconformity. Based on general lithologic similarity, but in particular on apparent stratigraphic position, they correlated the lower unit with the Johnnie Formation, and the overlying quartzite with the Stirling Quartzite section. They suggested these rocks are similar to the thin Johnnie-Stirling in the Providence Mountains (eastern Mojave Desert, California).

Tyler (1975) accepted Stewart and Poole's correlations for the Wood Canyon Formation and younger units, but differed on correlation of the underlying strata. He concluded that the "basal contact" cited by Stewart

and Poole was a fault contact. Further, he recognized a 450 m thick section of quartzite at Gold Mountain which he concluded must underlie the pre-Wood Canyon strata at Chicopee Canyon. Based on the predominance of quartzite in these two areas, he tentatively correlated the pre-Wood Canyon section in the Big Bear area with the Stirling Quartzite. He assigned the upper quartzite and lower marble and quartzite units in Chicopee Canyon to the E and D members respectively of the Stirling Quartzite (see Stewart, 1970). Although the quartzites at Gold Mountain are not in sequence with the section at Chicopee Canyon, he assigned them to the lower part of his "Stirling Quartzite equivalent", which he believed was the lowest unit in the Upper Precambrian-Cambrian sequence exposed at Big Bear.

Neither Tyler nor Stewart and Poole were aware of the thick Upper Precambrian succession present nearby in the Sugarloaf area. The pre-Wood Canyon strata exposed in Chicopee Canyon are correlative with the uppermost rocks of the Big Bear Group. During the course of this study the Chicopee Canyon section was reexamined. Based on lithologic similarity and equivalent stratigraphic position it is suggested that Tyler's E and D members correlate with members D2 and D1 respectively of the Delamar Mountain Formation.

The upper quartzite member (D2) is thinner (91 m, Tyler, 1975) than Member D2 at Delamar Mountain (217 m) or at Sugarloaf (minimum 137 m; see Fig. 3). However, thickness variations should be expected as 1) member D2 interfingers with member D1-like lithologies in the Delamar Mountain and Sugarloaf sections; and 2) the Chicopee Canyon section lies in the lower plate of the Doble thrust, across which some tectonic telescoping occurred. The general similarity of these three sections however suggests that this displacement was not extreme.

The quartzites at Gold Mountain were not examined in detail during this study. Based on cursory examination of roadcuts they are believed to correlate with rocks of the lower Big Bear Group.

Uppermost Precambrian-Cambrian Rocks

Introduction

Metasedimentary rocks correlative with Uppermost Precambrian-Cambrian miogeoclinal formations of the southern Great Basin are present at Delamar Mountain, Sugarloaf, and Chicopee Canyon (where first recognized by Stewart and Poole, 1975). Stratigraphic columns from these three areas are shown in Fig. 3. At Chicopee Canyon and Delamar Mountain these strata conformably overlie rocks of the Upper Precambrian Big Bear Group. Reconnaissance mapping undertaken during this study indicates that Uppermost Precambrian-Cambrian rocks are widely exposed elsewhere in the Big Bear area (see Plate I): below the Doble Thrust, west of Sugarloaf Mountain, and north and east of Delamar Mountain. Cambrian (?) marbles are thrust over Upper Paleozoic marbles on the north slope of the range.

The lower portion of this Uppermost Precambrian-Cambrian sequence consists of readily distinguished units and has provided the key for pre-Mesozoic stratigraphic correlations across the Mojave Desert. These distinctive formations overlie regionally heterogeneous Upper Precambrian strata and underlie monotonous, usually strongly deformed sections of Upper Paleozoic marble.

Correlation with fossiliferous sections in the eastern Mojave Desert and southern Death Valley region is based primarily on rock types and lithologic sequence. No fossils (aside from trace fossils) have been collected from these metamorphic rocks. The correlations of Stewart and Poole (1975) are followed here with only slight modification.

Wood Canyon Formation

Distribution and Description. Rocks assigned to the Wood Canyon Formation (original reference: Nolan, 1929; type area: Spring Mountains, Nevada) are exposed in the Sugarloaf area, below the Doble Thrust near Rose Mine, and at Delamar Mountain. Only the Delamar Mountain section is complete, where rocks of the Wood Canyon Formation conformably

overlie the Delamar Mountain Formation and are overlain conformably by the Zabriskie Quartzite. The upper and lower contacts are best exposed in roadcuts SE of Delamar Mountain. Similar conformable contact relationships are present at Chicopee Canyon (Stewart and Poole, 1975). North of Sugarloaf Mountain, Zabriskie Quartzite overlies the Wood Canyon Formation, but its lower contact is intrusive. An incomplete, overturned Wood Canyon section occurs below the Doble Thrust near Rose Mine and its upper and lower contacts here are faulted. Rocks here assigned to the Wood Canyon Formation were previously included in the lower member of the Chicopee Canyon Formation (Richmond, 1960) and the Saragossa Quartzite (Dibblee, 1964b; 1967a,b). Portions of the Wood Canyon Formation were included in Dibblee's phyllite member of the Saragossa Quartzite.

The Wood Canyon Formation consists primarily of micaceous (biotite-muscovite) feldspathic quartzite and quartzo-feldspathic biotite schist and phyllite, with lesser conglomeratic quartzite. A lithologic sequence generally correlative with Stewart's (1970) three-fold division of the Wood Canyon (lower siltstone member, middle arkosic quartzite member, upper siltstone member) can generally be recognized. Because of poor outcrop however, the Wood Canyon was mapped as a single formation.

At Delamar Mountain, the lower contact is placed above the uppermost thick quartzite ledge of the more resistant Delamar Mountain Formation. Recessive outcrops of laminated phyllite and schist with occasional thin lenticular interbeds of cross-stratified quartzite occur at the base. Some thicker interbeds of light grey (member D2-like) feldspathic quartzite locally occur.

These rocks are overlain by a thick sequence of trough cross-stratified impure quartzite (locally conglomeratic, with granules of feldspar and quartz). Laminated phyllite and micaceous quartzite often truncate the top of cross sets (a fining upward sequence). Interbeds of flaser-lenticular bedded quartzite are also present.

The upper portion of the Wood Canyon Formation is composed mainly of quartz-albite-biotite schist and phyllite with some flaser-lenticular bedded quartzite. The former often contain elongate quartz-feldspar filled tubes, up to 5 cm in length and 1 cm in diameter (Fig. 18). The

Figure 18: Wood Canyon Formation: deformed burrow tubes (Scolithus?) near top of unit. Tubes are rotated toward parallelism with S1a cleavage (hammer handle parallels trace of S1a on outcrop surface) which intersects bedding (seen at lower left) at an acute angle. Hammerhead is 20 cm long. Photo taken at roadcut SE of Delamar Mountain in the center of Section 1(T2N, R1W).

Figure 18.

tubes, believed to be sand filled burrows, are sometimes oriented at a high angle to layering. More often, original bedding is not recognized, and the tubes are sheared and rotated parallel to cleavage, which in turn parallels or is inclined at a low angle to bedding in nearby outcrops. These burrow tubes may be deformed Scolithus tubes. Scolithus (typically vertical worm burrows) is a common Early Cambrian trace fossil and is characteristic of the upper Wood Canyon Formation (Stewart, 1970). Deformed Scolithus tubes are present in the upper Wood Canyon Formation at Chicopee Canyon (Stewart and Poole, 1975).

Above the Scolithus-bearing beds, thin bedded to laminated phyllite and quartzite of the uppermost Wood Canyon Formation grade into the vitreous Zabriskie Quartzite over a few meters. A one meter thick lense of Zabriskie-like quartzite often occurs near the top. The Wood Canyon Formation at Delamar Mountain has a structural thickness of 225 m, measured on the southwest ridge of Peak 7856'.

Phyllite and micaceous feldspathic quartzite assigned to the Wood Canyon Formation are present in several roof pendants north of Sugarloaf Mountain. Roof pendants of Uppermost Precambrian-Cambrian rocks here are the remnants of younger-over-older allochthons which were extensively intruded by Mesozoic plutonic rocks. Wood Canyon strata are recognized either by their stratigraphic position below the distinctive Zabriskie Quartzite, or where they occur as isolated outcrops, by their lithology and distinctive sedimentary structures. Lenticular trough cross-stratified feldspathic quartzites and conglomerates here are identical to the trough cross-bedded quartzites at Delamar Mountain. A minimum thickness of 153 m of Wood Canyon Formation is present at Sugarloaf.

Correlative trough cross-stratified quartzite and interbedded phyllite and quartz pebble conglomerate are present beneath the Doble Thrust in Section 19 (T2N, R3E). These rocks are isoclinally folded, and although the general stratigraphic sequence in this east-facing overturned limb matches a Wood Canyon, Zabriskie, Carrara, and Bonanza King sequence, the formational contacts are all faults. Exposure of rock units becomes poorer along strike to the northwest. In Section 13 (T2N, R3E), rocks below the Zabriskie Quartzite are tentatively assigned to the Wood Canyon Formation and include well bedded quartzite, impure

quartzite, schist, calc-silicate rock and marble. The possibility exists that an unrecognized fault separates these rocks from more typical Wood Canyon rocks further south.

Age and Correlation. In the southern Great Basin, the Cambrian to Late Precambrian boundary occurs within the Wood Canyon Formation (Stewart, 1970). Trilobites and archeocyathids from its upper member date the top of the Wood Canyon Formation as Early Cambrian. No fossils are reported below the upper member, but evidence of metazoan life is present (burrows, tracks, etc.) in the lower Wood Canyon Formation and these rocks are assigned a Latest Precambrian age (Stewart, 1970). Scolithus is a characteristic Early Cambrian trace fossil and common in the upper Wood Canyon Formation and overlying Zabriskie Quartzite. Eastward, the upper Wood Canyon Formation correlates with the lower Tapeats Sandstone (Stewart, 1970).

In the San Bernardino Mountains, strata are assigned to the Wood Canyon Formation because of their stratigraphic position beneath the distinctive Zabriskie Quartzite, the presence of possible Scolithus tubes, and lithologic similarities to the three members of the Wood Canyon Formation described by Stewart (1970). Additional evidence for a Cambrian age for the uppermost Wood Canyon Formation is the presence of possible trilobite tracks and trails identified by J. Mount (personal comm., 1979) in samples collected at Chicopee Canyon by the author.

Stewart and Poole (1975) suggested the lower member of the Wood Canyon is missing at Chicopee Canyon, as it is in some sections along the eastern margin of the miogeocline in the eastern Mojave Desert. However, it is suggested here that laminated phyllite and lenticular bedded quartzite conformably overlying the Delamar Mountain Formation at Chicopee Canyon and Delamar Mountain correlate with the lower member of the Wood Canyon. These lithologies are similar to strata of the lower member described by Diehl (1974) from southern Death Valley.

The Wood Canyon Formation in the San Bernardino Mountains contrasts with correlative strata at Quartzite Mountain near Victorville. There, the upper Wood Canyon Formation includes thick beds of dolomitic marble

(Stewart and Poole, 1975; E. Miller, 1977). Carbonate and calcareous rocks are rare or absent in the Wood Canyon Formation at Big Bear. This may indicate a more basinward setting for the Quartzite Mountain section (Stewart and Poole, 1975; E. Miller, 1977), based on analogy with facies trends in southern Death Valley (Diehl, 1974).

Zabriskie Quartzite

Distribution and Description. Rocks assigned to the Zabriskie Quartzite (original reference: Hazzard, 1937; type area: Resting Spring Range, California) crop out at Delamar Mountain, Sugarloaf, and below the Doble Thrust. Conformable upper and lower contacts, with the Carrara Formation and Wood Canyon Formation respectively, are present at Chicopee Canyon (as recognized by Stewart and Poole, 1975), Delamar Mountain, and Sugarloaf. The Zabriskie is usually fault bound below the Doble Thrust. Here as elsewhere regionally, the Zabriskie Quartzite is a key stratigraphic marker.

The Zabriskie Quartzite includes strata previously mapped as the upper member of the Chicopee Canyon Formation (Richmond, 1960) and uppermost Saragossa Quartzite (Dibblee, 1964b; 1967a,b). Throughout the Big Bear area the Zabriskie Quartzite consists of massive, white or red-stained cliff-forming orthoquartzite. Its protolith was a silica-cemented quartz-arenite, which was recrystallized to form a coarse, dense vitreous orthoquartzite in which relict detrital grains can rarely be distinguished. Quartz content exceeds 95 percent. Only member S1 of the Sugarloaf Quartzite is similar in texture and composition (relict detrital grains are visible in S1 on careful inspection). Faint laminations are the only visible indication of bedding in the Zabriskie Quartzite, and small scale trough cross-stratification can sometimes be recognized. The Zabriskie Quartzite is the most resistant unit at Delamar Mountain, where it underlies ridges and steep slopes, and can be seen from considerable distance. Scolithus tubes are present in the lower Zabriskie Quartzite at Chicopee Canyon (Stewart and Poole, 1975); Tyler, 1975), but no convincing Scolithus tubes were recognized

in the other sections. A 64 m thick section is present at Peak 7856' near Delamar Mountain and a minimum thickness of 36 meters of Zabriskie Quartzite occurs at Sugarloaf. The Zabriskie Quartzite is locally missing near Rose Mine, as it is cut out by faults along the strongly sheared overturned limb of the Rose Mine Synform below the Doble Thrust. The upper and lower contacts of the Zabriskie Quartzite are faults in Section 13 (T2N, R3E).

Age and Correlation. In the southern Great Basin, the Zabriskie Quartzite contains no fossils except for Scolithus tubes. It is dated by its stratigraphic position between Lower Cambrian rocks of the uppermost Wood Canyon Formation and Lower Cambrian rocks of the lower Carrara Formation (Stewart, 1970). This distinctive orthoquartzite is easily recognized as it separates a primarily clastic sequence below from a predominantly carbonate succession above. Eastward, the Zabriskie Quartzite correlates with the upper Tapeats Sandstone of the cratonic sequence, exposed in southern Nevada and easternmost southern California. Based on faunal zones, Stewart (1970) has suggested the Zabriskie Quartzite is not time transgressive to the east. Rocks in the Big Bear area are assigned to the Zabriskie Quartzite because of their lithologic similarity, stratigraphic position between the Wood Canyon and Carrara formations, and the local presence of Scolithus tubes within and just below the Zabriskie Quartzite.

Carrara Formation

Distribution and Description. Metasedimentary rocks correlated with the Carrara Formation (original reference: Cornwall and Kleinhampl, 1961; type area: Bare Mountain, Nevada) are exposed at Delamar Mountain, Sugarloaf and below the Doble Thrust near Rose Mine. These strata conformably overlie the Zabriskie Quartzite in all areas. The Carrara Formation is overlain with apparent conformity by the Papoose Lake Member of the Bonanza King Formation at Delamar Mountain and below the Doble Thrust. The Carrara includes rocks previously assigned to the lowermost Furnace Formation (Richmond, 1960) or Furnace Limestone (Dibblee, 1964a,b;

1967a,b).

In the Big Bear area, the Carrara consists of recessive, interlayered mica schist and phyllite, thin laminated calc-silicate rock, more resistant grey and white banded calcite marble, crepe weathering thin laminated calc-silicate marble, and micaceous quartzite. The protoliths included siliceous and calcareous siltstones and shales, mottled (?) and cherty limestone, and rare interbedded sandstone. Few primary sedimentary structures remain as bedding in these rocks is often tectonically transposed, particularly in the marbles. The tectonite banding in the marbles developed from tight to isoclinal folding of original bedding, and rootless fold hinges are common. This transposition is identical to that seen during progressive deformation of Carrara and Bonanza King mottled limestones in the Clark Mountain region (B. C. Burchfiel, personal comm., 1977). Similar transposition occurs in the calc-silicate rocks of the Carrara Formation below the Doble Thrust.

A ledge of resistant, color-banded calcite marble (up to 10 m thick) occurs regularly near the base of the Carrara Formation throughout the Big Bear area. Another thinner ledge of marble is present near the top of the Carrara Formation below the Doble Thrust and locally at Delamar Mountain. In general, schists predominate in the lower part of the Carrara Formation and calc-silicate rocks in the upper part. No fossils were found during this study but concretionary algal balls called Girvanella, common in the Carrara Formation, were found in float at Delamar Mountain. A section at Peak 7856' in the Delamar Mountain area includes 177 m of Carrara Formation, and a minimum of 88 m of Carrara Formation is present at Sugarloaf.

Age and Correlation. The Carrara Formation in the southern Great Basin is assigned an Early and Middle Cambrian age on the basis of trilobites (Stewart, 1970). This recessive unit is distinctive in the desert ranges because it forms orange-weathering slopes separating the white Zabriskie Quartzite cliffs below from the thick, cliff-forming Bonanza King Formation carbonates above. The Carrara Formation marks the

top of the Upper Precambrian-Lower Cambrian clastic wedge of the miogeocline. Lithologically, it forms a transitional facies between these lower clastics and the thick Middle-Upper Cambrian carbonate succession above, and typically consists of siltstone and shale (often calcareous), and interbedded limestone.

In the eastern, cratonal facies, the Carrara Formation is correlative to the Bright Angel Shale. In the Providence and Marble Mountains in the eastern Mojave Desert, strata correlative with the Carrara Formation include three conformable formations: the Latham Shale (less than 30 m thick) and Chambless Limestone (30-60 m thick) of Early Cambrian age and the Cadiz Formation (siltstone and limestone, 180 m thick) of Middle Cambrian age (Stewart, 1970). Stewart has recognized this three-fold division in strata mapped as Carrara Formation further north in the eastern Mojave Desert of California, but cannot trace these units into southern Nevada or Death Valley.

Strata in the Big Bear area are assigned to the Carrara Formation on the basis of lithologic similarity and stratigraphic position above the distinctive Zabriskie Quartzite and below the Bonanza King Formation marbles. Only the Bonanza King Formation has similar color banded marble. In contrast to the predominantly dolomitic marbles of the Big Bear Group, calcite marbles of the Carrara and Bonanza King Formations were derived from limestone. The thick section of laminated calc-silicate rocks in the upper Carrara Formation is the most distinctive part of this unit.

It is suggested that the lower banded calcite marble which is widely recognized in Carrara sections in the Big Bear area may be correlative with the Chambless Limestone. Stewart and Poole (1975) suggested that Latham, Chambless and Cadiz equivalents might be present at Chicopee Canyon. I agree that this three-fold division is locally possible. However, it cannot be established conclusively, partly because of poor outcrop and partly because of internal structural complexity. Thus the name Carrara Formation is appropriate for these rocks. Future workers, however, may elect to apply Latham, Chambless, Cadiz nomenclature to strata here assigned to the Carrara Formation.

Bonanza King Formation

Distribution and Description. Rocks here assigned to the Bonanza King Formation (original reference: Hazzard and Mason, 1936; type section: Providence Mountains, California) occur at Delamar Mountain, below the Doble Thrust and at Sugarloaf. In the former two areas the Bonanza King is subdivided into two conformable members, the lower Papoose Lake Member and upper Banded Mountain Member (Barnes and Palmer, 1961). The Papoose Lake Member conformably overlies the Carrara Formation. In the Sugarloaf area, the Bonanza King is not subdivided. The top of the Bonanza King was not recognized in any of these areas. The Bonanza King includes rocks previously assigned to the Furnace Formation (Richmond, 1960) or Furnace Limestone (Dibblee, 1964a,b; 1967a,b).

The Papoose Lake Member consists of blue-grey and white thin banded calcite marble. The protolith was a sequence of limestones. The color banding is the distinctive feature of the Papoose Lake Member, and represents tectonically transposed bedding. Rootless fold hinges are numerous with axial surfaces parallel to layering. Primary sedimentary structures are not preserved. At Delamar Mountain, the Papoose Lake Member has a structural thickness of 88 m. Below the Doble Thrust, the Papoose Lake Member is isoclinally infolded with the upper Carrara Formation. A minimum structural thickness of 200 m of Papoose Lake is present near Rose Mine.

The overlying Banded Mountain Member is characterized by its lithologic heterogeneity. At its base, a recessive horizon (of variable tectonic thickness) consisting of thin layered quartzite and quartz schist is recognized. Above is a lithologically diverse sequence of primarily calcite marble. Color varies from white to light and dark grey. Massive, thin layered, color-banded and cherty marbles occur. The chert consists of calc-silicate nodules, lenses and irregular stringers and is often abundant. Thin color-banded marble interbeds are similar to those in the Papoose Lake Member and Carrara Formation. These different lithologies alternate in beds generally between 1-5 m thick. Occasional thin, recessive interbeds of calc-silicate rock or

phyllite are present, usually only as float blocks. This sequence was derived from a section of limestones (often siliceous) locally interbedded with siltstone. At least 170 m of Banded Mountain Member are present at Delamar Mountain. The Banded Mountain Member has a minimum structural thickness of 300 m or more below the Doble Thrust, however, because these marbles are complexly folded, this figure is only a crude approximation.

Marbles mapped as Bonanza King Formation at Sugarloaf are lithologically similar to the Banded Mountain Member in the other localities and are in tectonic or intrusive contact with other units. Discontinuous intervals of color-banded marble, similar to marbles of the Papoose Lake Member, are present within this complexly folded sequence. As similar marbles occur within the Banded Mountain Member elsewhere, it is not clear if these are infolds of Papoose Lake rocks or part of the Banded Mountain Member. The latter interpretation was adopted here and is supported by evidence further west. Rocks believed to belong to the same structural plate as those discussed above occur on the ridge crest west of Sugarloaf Peak (Section 34, T2N, R1E). Here, an apparently comformable sequence of Carrara Formation, Papoose Lake Member and the lower part of the Banded Mountain Member is exposed and easily differentiated. In the Sugarloaf area, the Papoose Lake Member has apparently been cut out along intruded low angle normal faults.

Age and Correlation. In the southern Great Basin the Bonanza King Formation is assigned a Middle to Late Cambrian age (Palmer and Hazzard, 1956) and conformably overlies the Carrara Formation or its equivalents. The Bonanza King Formation is overlain conformably by the fossiliferous Upper Cambrian Dunderburg Shale Member of the Nopah Formation. The Papoose Lake Member is lithologically homogeneous, consisting of grey, massive dolomite, or less commonly limestone. A regionally extensive thin siltstone unit occurs at the base of the Banded Mountain Member. The remainder of the Banded Mountain consists of a lithologically heterogeneous sequence of massive, mottled and cherty dolomites with some silty interbeds (Gans, 1974). Metasedimentary

rocks in the Big Bear area are assigned to these two members of the Bonanza King Formation on the basis of their striking lithologic similarity and equivalent stratigraphic position. Even the silty unit at the base of the Banded Mountain Member can be recognized (the recessive quartzite-phyllite unit).

A surprising lithologic difference in the Bonanza King Formation at Big Bear (and Victorville as well; see E. Miller, 1977) from typical sections elsewhere is the paucity of dolomite. The Bonanza King Formation in the Big Bear area consists primarily of calcite marble. The lack of dolomite could reflect in part metamorphic breakdown of dolomite, but this is not supported by the relative scarcity of Mg-rich metamorphic minerals in these marbles. It appears the protoliths were limestones, not dolomites. However, much of the Bonanza King dolomite in the southern Nevada region appears to be secondary, replacing calcite. This is evident in laminated Bonanza King limestones with mottles of secondary dolomite present in the southern Spring Mountains (J. Southard, personal comm., 1978). The Bonanza King Formation in the western Mojave Desert was apparently not as thoroughly dolomitized, and in this respect is similar to the more cratonal Cambrian carbonate sections, such as rocks in the Grand Canyon area.

Nopah (?) Formation

Distribution and Desription. Rocks possibly correlative with the Upper Cambrian Nopah Formation (original reference: Hazzard, 1937; type area: Nopah Range, California) are exposed near Bertha Peak in the Delamar Mountain area (Section 5, T2N, R1E). They are not in sequence with nearby exposures of the Bonanza King Formation, but have faulted or intruded contacts. Rocks included in the Nopah (?) Formation consist primarily of massive, coarse white dolomitic marble. Occasional chert (calc-silicate) lenses or laminae are the only vestiges of original bedding. This lithology is locally overlain (structurally) by thin color-banded and cherty grey dolomitic marbles (no facing indicators are preserved). This sequence has a minimum structural thickness of ∿100 m.

Age and Correlation. In the southern Great Basin the Bonanza King Formation is typically overlain by the fossiliferous Dunderburg Shale Member of the Nopah Formation which is overlain by thick massive dolomite of the upper part of the Nopah Formation. The Nopah Formation is of Late Cambrian age. In marginal miogeoclinal sections the upper Nopah Formation is a white or buff, coarse grained massive dolomite (Gans, 1974). In the Victorville area (at Sidewinder Mountain), E. Miller (1977) has recognized rocks correlative with the Dunderburg Shale Member and overlying rocks of the Nopah Formation depositionally overlying rocks correlative with the Banded Mountain Member of the Bonanza King Formation. The Nopah Formation here occurs as a buff-weathering, massive dolomitic marble, distinctive from the predominantly calc-marbles below in the Bonanza King Formation and above in the overlying Sultan Limestone (of Middle Devonian age). A complete Bonanza King-Dunderburg-Nopah section has not yet been recognized in the Big Bear area. Thick sections of white dolomitic marble like those at Bertha Peak are not typical of the Bonanza King Formation at Delamar Mountain or elsewhere in the study area. These marbles may be equivalent to the Nopah Formation. However, without fossil evidence or an intact stratigraphic sequence this cannot be demonstrated. It is intriguing, however, that a thin sequence of calc-silicate rocks (poorly exposed and tightly folded) occur near the Nopah (?) Formation immediately west of Bertha Peak (they are intruded by the Bertha Diorite along the jeep trail). These may represent a Dunderburg equivalent. Alternatively, rocks mapped here as the Nopah (?) Formation may be a part of the lithologically heterogeneous Banded Mountain Member.

The grey dolomites overlying the Nopah (?) Formation are of particular note. If the Nopah correlation is correct, these may be correlatives of a higher unit such as the Upper Ordovician Mountain Springs Formation, a grey cherty dolomite that overlies the Nopah Formation in transitional miogeoclinal-cratonal sections (Gans, 1974). These rocks could conceivably correlate in some way with the Devonian Sultan Limestone, although absence of stromatoporoids which are characteristic of the lower Sultan Limestone, argues against this.

Only the northwestern periphery of the Bertha Ridge marble section was examined in this study. Structural complexities (mainly low-angle normal faults) have dismembered the section there, but this area is one of the most likely locales for revealing the Lower Paleozoic stratigraphic sequence in the Big Bear area, albeit in pieces.

Depositional Environments

Big Bear Group

Several factors indicate the Big Bear Group is predominantly, if not entirely, marine in origin. These include the relative textural and mineralogical maturity of protolith sandstones, the sequence and types of lithologies as well as sedimentary structures observed, the presence of thick, in part algal, carbonate buildups, and general lack of evidence of continental (fluviatile or lacustrine) deposition. Stewart (1970) reached a similar conclusion concerning the Upper Precambrian strata of the southern Great Basin and concluded the clastic components had a cratonal provenance. Later, he suggested these strata constituted the basal, predominantly clastic wedge of the Cordilleran miogeocline (Stewart, 1972), an interpretation which is now generally accepted (Burchfiel and Davis, 1972, 1975). The Big Bear Group represents the western equivalent of the Great Basin Upper Precambrian sequence and is also interpreted to represent the oldest preserved post rift deposits along the ancient margin.

The collection of detailed quantitative sedimentologic data (e.g. paleocurrent variations) was not an objective of this study. However, qualitative observations assembled during the course of mapping are pertinent, as they bear on the evolving depositional environments recorded within the Big Bear Group. This in turn bears on regional Late Precambrian facies variations (discussed below). Possible interpretations of sedimentary depositional environments for each formation based on protolith types and sedimentary structures are discussed below. Emphasis is placed on the less tectonized lower part of the section.

Wildhorse Quartzite. In the basal portions of the Wildhorse Quartzite, locally derived metamorphic clasts and feldspar (from the paleoweathered zones?) are reworked with fine grained, mature quartz sand. Low-angle, accretionary cross-stratification seen at and near the basal contact probably formed in beach deposits transgressing over a low relief basement surface. These gritty sands locally occur in lenticular ripple laminated beds within fining up sequences, capped by mudcracked siltstones. The conglomeratic beach sands may have interfingered with sandy tidal flats.

Upsection, locally derived clasts quickly disappear and fine, mature quartz sands and lesser siltstone predominate. Evidence of wave-induced transport is lacking. Single or multiple large scale, tabular tangential cross sets are typically truncated by lenticular bedded quartzites and siltstones, often with ripples indicating reversed current directions. Mudcracks are sometimes seen.

The large bedforms could represent migrating sandwaves, longshore or tidal bars. Similar bedforms occur in deltaic and fluvial environments (Heckel, 1972) however absence of coarsening up sequences or channelling suggests these settings are unlikely. A tidally dominated shallow marine shelf is thought to be the most likely environment of deposition. Absence of hummocky cross-stratification and scarcity of oscillation ripples suggests wave activity was insignificant, indicating a restricted basin geometry. The large scale cross sets are interpreted as migrating offshore tidal sand waves or bars, overlain by prograding sandy tidal flats (often showing reverse tidal current flow). Large scale "cross sets" of lenticular-bedded ripple laminated sand and laminated silty sands are similar to prograding tidal creek channel point-bar deposits recognized by Reineck and Singh (1975, p.90). The abundance of possible tidal flat deposits may be underestimated, as non-outcropping siltstone and shale may also represent such deposits. Much of member W1 may represent cyclic sand body transgression and tidal flat progradation.

In the upper Wildhorse Quartzite (member W2), alternating tabular sets of trough and tangential or low-angle cross strata are conspicuous.

Lenticular bedding is less common. Medium scale and larger trough cross-stratification occurs in backshore beach (dune) settings, spillover lobes, tidal and/or alluvial channel deposits (Heckel, 1972). Other evidence for alluvial deposition is lacking. The strata may represent channel deposits within an intertidal sand body complex (as described by Klein, 1977). Alternatively, the alternating bedforms described may represent accretionary beach and backshore dune deposits, perhaps or barrier islands.

Lightning Gulch Formation. The Wildhorse Quartzite interfingers locally with the overlying Lightning Gulch Formation. Lithologies within the latter unit are much finer grained, and again show little evidence of wave activity. Predominant lithotypes are laminated mudstone and siltstone with subordinate thin lenticular beds of ripple laminated sandstone, and sequences of sandstone, siltstone and mudstone displaying pinstripe tidal bedding, lenticular and locally flaser bedding. Grading is common and ripple cross lamination is present in lenticular and flaser bedded sands. These lithologies could have been deposited below wave base in an offshore shelf setting, and represent a transgressive sequence overlying the Wildhorse Quartzite. These lithologies are also identical to those recognized in North Sea tidal flat deposits (see Reineck and Singh, 1973; also see Klein, 1977: Tidal Flat Facies Model). The common occurrence of mudcracks (in members L2 and L3) and soft sediment dewatering or animal escape structures supports interpretation as tidal flat deposits. Loading structures (such as soft sediment folds and pseudo-nodule formation) are common in tidal flat deposits (Klein, 1971) but not diagnostic. Ripple cross laminated sands probably represent migrating tidal current ripples, formed when fine grained sediment, carried in suspension, is deposited during slack water. Some semicontinuous pinstripe sand bodies are also probably deposited in part from suspension as tidal currents wane. These occur in graded sequences, and in thin section they often sharply overlie current transported sand ripples (with foreset laminae preserved). Thus, both tidal current traction and suspension transport are recognized. The

great thickness of the Lightning Gulch Formation, occurring without obvious evidence of changing environments, requires that subsidence was vigorous during its deposition.

An intertidal setting for the Lightning Gulch Formation is supported by the lack of submarine textures (e.g. pillows) in the basalt flow(?) (Wildhorse Greenstone) which occurs at or near its base. The greenstone may have flowed across the transition zone between member L1 tidal flats and member W2 barrier island(?) deposits. Quartzite xenoliths could then have been picked up from the sands of member W2. Occasional tuffaceous horizons in the Wildhorse Quartzite and Lightning Gulch Formations attest to episodic mafic-intermediate volcanic activity in the region.

Sugarloaf Quartzite. Members S2 and S4 of the Sugarloaf Quartzite are lithologically identical to the underlying Lightning Gulch Formation (pinstripe tidal bedding and lenticular bedding, grading, mudcracks, and soft sediment deformation features are present). Overlying and separating members L3, S2 and S4 are three sheets of highly mature quartz sand (members S1, S3 and S4 respectively). In all three cases, the sand bodies overlap a recently emergent mudcracked surface. Member S3 has rip-up clasts of member S2 at its base. These are interpreted as transgressive sands. They are characterized by large scale low-angle cross-stratification (although smaller scale, high-angle and trough sets are present). Their mature composition suggests these are marine sands. Accretionary low-angle cross-stratification is common in beach deposits (Elliot, 1978), and in view of their transgressive setting, these may represent migrating barrier island beach sands. Members S2 and S4 are interpreted as prograding tidal flat deposits, which may have advanced seaward during post-transgression still stands. The laminated dolomites occurring locally at the top of member S4 represent the first of several episodes of carbonate deposition recorded. These underlie transgressive sands of member S5, which laterally overlie mudcracked tidal flat deposits contiguous with those below the carbonates. These relations suggest the member S4 carbonates, at least, were

inter- or supratidal deposits (algal mat dolomites?).

Green Canyon Formation. The depositional setting of the overlying Green Canyon Formation is more difficult to constrain. Little remains of primary sedimentary structures in the marbles, and interbedded metaclastic rocks are generally not well exposed. The presence of silicified columnar and algal mat stromatolites in members G1 and G5 indicates these rocks were probably deposited in relatively shallow water. Many of the laminations recognized in marble and calc-silicate rocks in other members (G2, G3, G6, G7, G9) may represent algal mats. Algal mats and stromatolites in general are commonly found in restricted upper intertidal and supratidal settings in the Recent (Wilson, 1975). They occur commonly along arid coastlines or in restricted shallow waters of carbonate platforms (Till, 1978; Sellwood, 1978). Stromatolite deposition since the Cambrian has occurred primarily in similar restricted settings (Heckel, 1974). However, stromatolite facies associations analogous to those described from various Phanerozoic carbonate platform deposits have been widely recognized in the Precambrian by Hoffman (1974). Precambrian stromatolites may have inhabited a wider spectrum of environments than their modern descendants. The algal mats and columnar stromatolites from the Green Canyon Formation were almost certainly deposited in low energy environments, but with sub- to supratidal range possible. Structures or lithologies suggestive of high energy reef complexes were not recognized, although the protoliths of the coarse massive marbles are uncertain. A lacustrine setting for the Green Canyon carbonates seems unlikely as the unit is overlain and underlain by shallow marine clastics.

The interbedded clastics within the Green Canyon Formation are probably marine deposits as well. The fine grained clastics (siltstones and lesser mudstones) in members G3, G4 and G6 are generally laminated and in member G6, thin lenticular bedded sandstones are present locally (similar to those in the Lightning Gulch Formation and Sugarloaf Quartzite). These occur with locally thick interbeds of mature quartz

sand in member G6, which display large scale low-angle cross sets. The sand bodies may represent beach accretion deposits, or migrating offshore bars. Evidence of wave activity is lacking. The laminated finer grained clastics could represent offshore shelf deposits, laid down below wave base, or lagoonal or intertidal deposits. These fine grained clastics separate the mature sands from laminated carbonates of member G6. Whether the vertical sequence, quartz sandstone-graphitic siltstone and mudstone-carbonate, is transgressive (beach, offshore fines, carbonate platform) or regressive and progradational (barrier beach, lagoon or clastic tidal flat, algal tidal and supra-tidal flat) is not clear. In either case, the high carbon content of the pelitic rocks suggests an anoxic, restricted environment of deposition.

In the upper Green Canyon Formation coarse arkosic sands of member G8 interfinger with carbonates. The influx of detrital K-feldspar, metamorphic clasts and coarse (pebble to cobble size) quartzite clasts indicates a new and in part proximal source terrane. Both low- and high-angle tabular cross sets are recognized. These clastics may be in part fluviatile or deltaic, interfingering laterally with marine carbonates.

Delamar Mountain Formation. The lower Part of the Delamar Mountain Formation is transitional between the underlying dolomites of member G9 of the Green Canyon Formation and the overlying arkosic sands of member D2. Interbeds of dolomite and sandstone occur together with laminated marls and calcareous siltstones, tidal bedded and flaser/lenticular-bedded sand, and siltstone and mudstone. The clastic rocks resemble those of the Lightning Gulch Formation and are probably tidal flat deposits, which interfinger with inter- to supratidal(?) carbonates and thin offshore(?) sand bodies. These deposits are overlapped by the well bedded, often coarse sands of member D2. Unlike member G8 of the Green Canyon Formation, the detrital feldspar in member D2 is predominantly plagioclase. Large scale tabular low-angle

and tangential cross sets are typical, and superposed oscillation ripples are present. These sands may represent accretionary beach deposits or migrating offshore sand bodies. Wave activity was locally important. This marks a change from predominantly restricted marine, tide dominated conditions prevailing earlier in the depositional history of the Big Bear Group.

Uppermost Precambrian-Cambrian Rocks

The conformably overlying uppermost Precambrian-Cambrian section at Big Bear was not examined in as much detail. Some of these formations have been studied by sedimentologists at localities in the southern Great Basin. Klein (1971, 1977) has interpreted the lower and middle members of the Wood Canyon Formation as, in part, intertidal deposits. Correlative rocks at Big Bear have many similar characteristics, including pinstripe tidal bedding and lenticular bedding, Klein's "B-C sequences", and occasional herringbone cross-stratification. These may represent intertidalites as well. Lenticular beds and rip-up clasts in the upper Wood Canyon Formation are also suggestive of an intertidal environment. Periodic emergence is indicated by the presence of rip-up clasts of upper Wood Canyon Formation at the base of the transgressive Zabriskie Quartzite at Chicopee Canyon (Tyler, 1975).

Few primary structures can be recognized in the orthoquartzites of the Zabriskie Quartzite and its exact environmental setting is uncertain. Lobo and Osborne (1976) suggested the Zabriskie Quartzite consists of prograding shelf sands. In the Death Valley region, tidal sand body and tidal flat environments are recognized in the Upper Zabriskie (Klein, 1977). The presence of low-angle cross-stratification (at Big Bear) and exceptional compositional maturity are also suggestive of beach deposits.

The depositional settings of the Carrara and Bonanza King formations have been related to Cambrian grand cycles (Aitken, 1966) by several geologists. Aitken proposed the concept of grand cycles to account for cyclic variations in Cambro-Ordovician clastic and

carbonate deposition in the Canadian Cordillera. A grand cycle begins with deposition of shallow marine clastic sediments (of the inner detrital belt) during rapid transgression. These are gradationally overlain by shallow marine carbonates, often very thick, which belong to the middle carbonate belt. The latter constitute offshore carbonate platforms or islands which separate the inner and outer (mud and silt dominated) detrital belts (see Fig. 19). Regression and exposure ends the cycle, which begins again with overlying transgressive clastic deposits. Halley (1975) and Mount and Rowland (1979) have applied the grand cycle concept to Cambrian deposition in the southern Cordillera.

Halley (1975) has suggested the Carrara Formation records multiple grand cycles. Two and perhaps more cycles may be present at Big Bear. The lower marble horizon (Chambless equivalent?) defines the top of a cycle which begins with Zabriskie Quartzite deposition. An upper cycle continues through deposition of the overlying Papoose Lake Member of the Bonanza King Formation. The silty unit at the base of the Banded Mountain Member and the Dunderburg Shale Member represent basal deposits of higher grand cycles.

Clastic deposits within the Carrara and Bonanza King formations are typically laminated in the Big Bear area, and rarely show evidence of migrating bedforms or any current-traction activity. Evidence of intertidal deposition was not observed. These may represent shelf silts and muds deposited below wave base.

Further east, dolomites and limestones of the Bonanza King and Nopah formations show numerous features indicating shallow marine deposition (Gans, 1974). The presence of laminations, possible silicified stromatolites and algal mats in correlative marbles at Big Bear is consistent with such an environment.

Summary and General Characteristics

The Big Bear Group and overlying uppermost Precambrian-Cambrian strata are almost exclusively shallow marine deposits. The lower clastic section of the Big Bear Group shows little evidence of open

Figure 19.

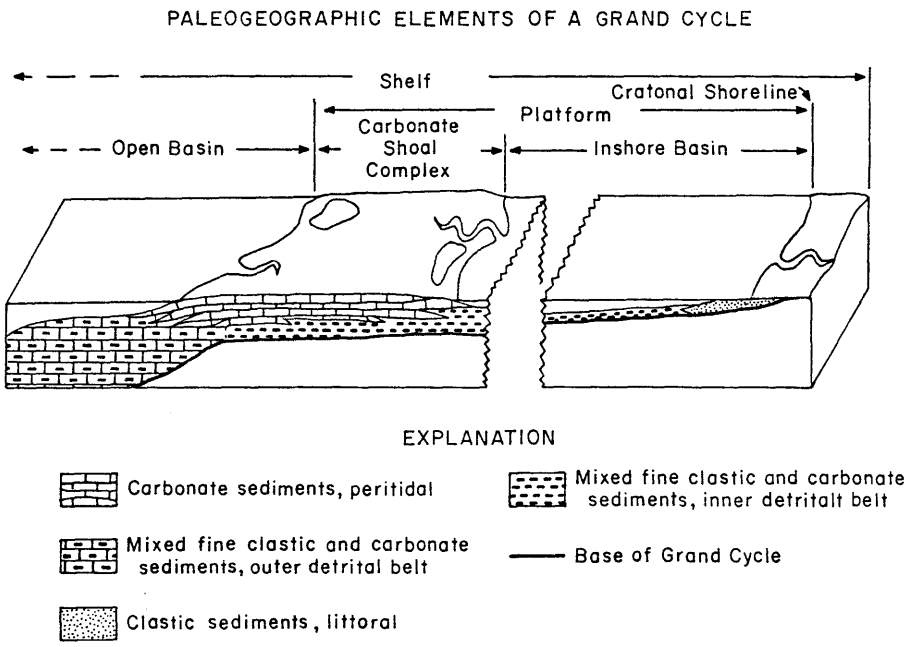

Modified after Aitken (1978).

marine conditions, where storm-driven wave traction transport is a dominant influence. Instead, tidal currents controlled sediment transport. This suggests a relatively restricted initial basin geometry, such as a gulf, isolated from the effects of storm activity. Vigorous subsidence, combined with moderate sea level fluctuations, is necessary to explain the considerable thicknesses of units like the Lightning Gulch Formation. These units were deposited across a broad, low relief shelf. Deposition of large sand bodies is associated with transgression, suggesting these offshore sands fringed the broad tidal flats (analogous to modern tide dominated environments, where coarsening offshore is the rule; see Klein, 1977).

Carbonate deposition dominates the upper part of the Big Bear Group. Again, there is little evidence of wave activity and a restricted basin geometry is suggested. The thick algal dolomite successions probably represent, at least in part, progradation of intertidal to supratidal algal flats into the basin. Other environments may also be represented. Carbonates interfingered complexly with shallow marine clastics deposited in beach and intertidal environments among others.

Gradual incursion of coarse arkosic sands (Delamar Mountain Formation) ended carbonate deposition. These transgressive sands exhibit some evidence of wave traction transport. The upper part of the Delamar Mountain Formation may signal the end of a restricted, tide-dominated basin and record the transition to open marine conditions.

The conformably overlying intertidalites of the Wood Canyon Formation are the oldest strata which definitely extend beyond the Big Bear area (discussed below). The Wood Canyon Formation and overlying Cambrian units can be traced eastward to the southern Great Basin, and are lithologically uniform over thousands of square kilometers. Until Wood Canyon deposition, the Big Bear depocenter evolved separately from the southern Great Basin; subsequently, regionally uniform marine deposition is in both areas. At Big Bear, the transition from a restricted to an open marine setting may have begun with transgression of the upper Delamar Mountain sands.

The provenance of the fine-grained, mature quartz sands in the lower three quarters of the Big Bear Group is almost certainly cratonal. Locally derived clastics, including granitic pegmatite, vein quartz, coarse quartzite clasts and detrital K-feldspar are restricted to the base of the sequence. Another minor incursion occurs at the top of member W2 of the Wildhorse Quartzite. Quartzite is not prominent in the basement complex here, although it may be locally important elsewhere in the range (see discussion above). However, it seems unlikely the mature orthoquartzites in the Sugarloaf Quartzite, for example, were locally derived.

Member G8 of the Green Canyon Formation includes coarse arkosic sands which may have had a local source. Clasts of metamorphic microcline similar to those in the Precambrian gneiss complex are recognized. It is unlikely that pebbles and rare cobbles of quartzite in this unit travelled very far. Member G8, in part, may represent an interfingering of fluvial-deltaic and marine carbonate environments.

Arkosic sands return with deposition of the Delamar Mountain Formation, and persist until Zabriskie Quartzite deposition. Unlike member G8, detrital plagioclase is evident in the Delamar Mountain Formation. Orthoquartzite typically underlies the Wood Canyon Formation in the southern Great Basin (Stewart, 1970; see below). As is the case there, the uppermost Precambrian-Cambrian sands at Big Bear are almost certainly of cratonal origin.

Upper Precambrian-Cambrian Rocks of the Big Bear Area and Their Relation to the Cordilleran Miogeocline

Introduction

The Wood Canyon Formation and overlying Cambrian rocks in the Big Bear area are equivalent in lithology and sequence to Cambrian miogeoclinal formations in the southern Nevada-southern Death Valley-eastern Mojave Desert region. The Big Bear Group, however, is distinct from stratigraphically equivalent Upper Precambrian formations recognized to the east. This areal variation in Upper Precambrian stratigraphy probably reflects rapid facies changes along the ancient continental margin early in its development. By Latest Precambrian-Early Cambrian time, relatively uniform depositional conditions were established across the southern Great Basin-Mojave Desert region. This indicates that Late Precambrian paleogeography was considerably more complex in the Mojave Desert region than previously suspected. The recognition of significant Late Precambrian facies variations across the Mojave Desert suggests that other enigmatic quartzite and marble sections may include unrecognized Upper Precambrian rocks of the Cordilleran miogeocline.

Paleogeographic Setting of Uppermost Precambrian-Cambrian Rocks

The Uppermost Precambrian-Cambrian rocks at Big Bear and correlative rocks at Victorville tie this region to the Cordilleran miogeocline and indicate that the miogeoclinal terrane extends westward across the northern Mojave Desert (Stewart and Poole, 1975; Tyler, 1975; E. Miller, 1977). The underlying Big Bear Group and older Precambrian gneiss complex are likewise tied paleogeographically to the miogeocline (Cameron, 1980). The Uppermost Precambrian-Cambrian rocks at Big Bear are most similar to rocks along the eastern margin of the miogeocline in the eastern Mojave Desert (Figs. 20, 21 and 22).

Comparing structural thicknesses of internally deformed carbonate

Figure 20: Location map of pre-Mesozoic rocks in the Mojave Desert-Death Valley-southern Nevada region.

Rock Units

Precambrian crystalline rocks: dots

Precambrian crystalline rocks of the San Gabriel terrane: diagonal rule

Precambrian Pahrump Group: horizontal rule

Upper Precambrian-Paleozoic rocks of the Cordilleran miogeocline and craton: white

Lower Paleozoic continental slope and rise sequences (allochthonous): black

Paleozoic rocks of the western Mojave terrane: vertical rule

Localities and specific features:

B: Baker
BM: Big Maria Mountains
C: Clark Mountains
Ch: Chuckwalla Mountains
DV: Death Valley
E: Eagle Mountains
EP: El Paso Mountains
F: Funeral Mountains
FM: Frenchman Mountain
G: Goldstone
gf: Garlock fault
I: Inyo Mountains
K: Kingston Range
Ke: Kelso
Ki: Kilbeck Hills
LA: Los Angeles
LC: Last Chance Range
M: Marble Mountains
N: Nopah Range
NY: New York Mountains
P: Providence Mountains
Pa: Panamint Range
S: Soda Mountains
saf: San Andreas fault
SB: San Bernardino Mountains
SD: San Diego
SG: San Gabriel Mountains
SH: Silurian Hills
SM: Spring Mountains
V: Victorville
W: White Mountains
Sh: Shadow Mountains

The outlines of the Sierra Nevada, Peninsular Ranges and eastern Transverse Ranges are shown for reference.

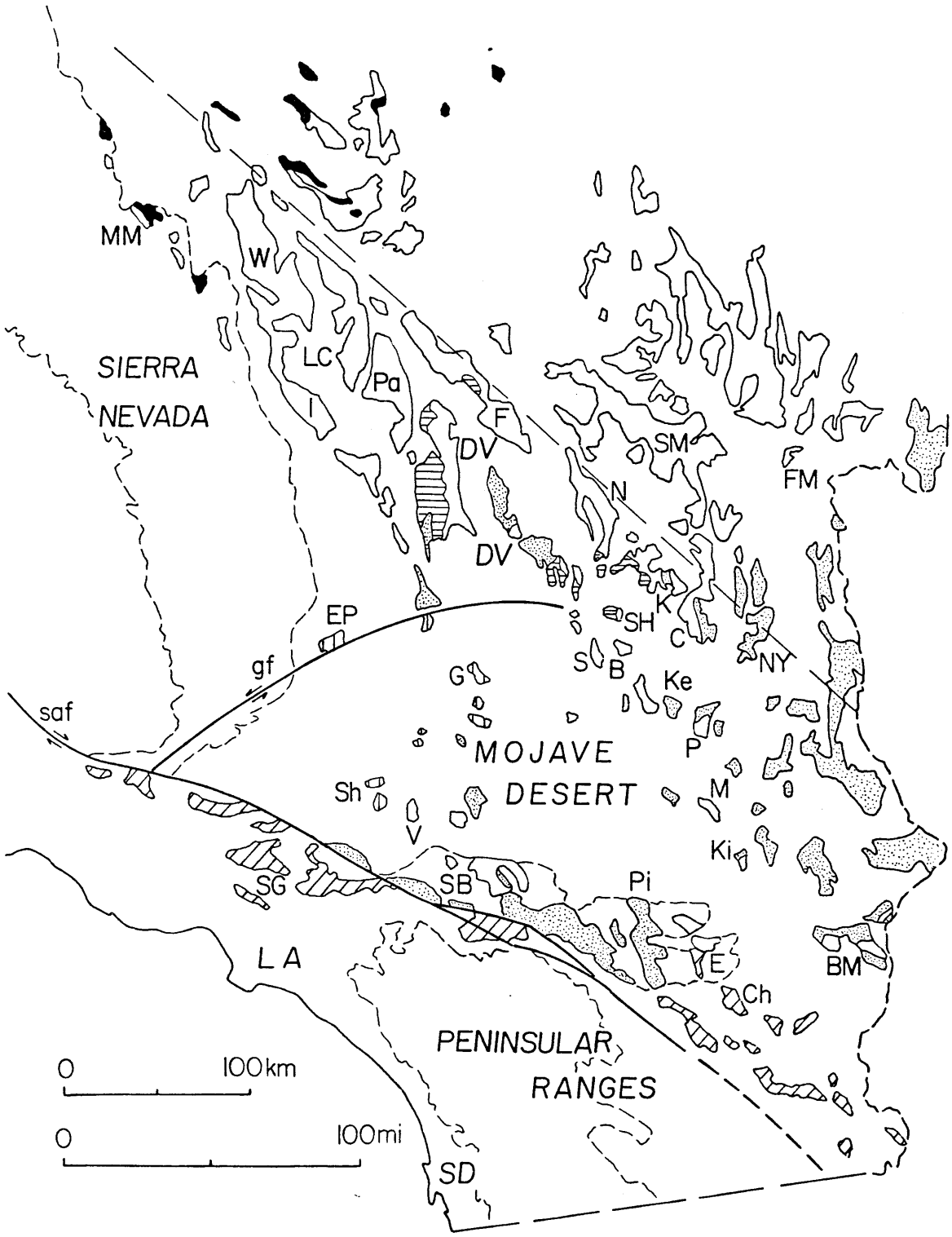
MM
W
SIERRA
NEVADA
LC
Pa
I
F
DV
DV
SM
N
FM
EP
gf
saf
SH
K
C
NY
S
B
Ke
G
MOJAVE
DESERT
P
M
Sh
V
Ki
SG
SB
Pi
LA
E
BM
Ch
PENINSULAR
RANGES
0
100km
0
100mi
SD

Figure 21: Isopach trends of the Cordilleran miogeocline in southern California and southern Nevada

p€s: Stirling Quartzite
€wc: Wood Canyon Formation
E limit Late p€: eastern limit of upper Precambrian miogeoclinal strata
SE limit Ord: SE limit of Ordovician strata (∿Paleozoic miogeocline-craton hingeline)
P-Tr Truncation Boundary: inferred western limit of Precambrian continental crust in southern Sierra Nevada based on Sr isotopic data ($r_i \geq 0.706$)
E Limit Lower Pz Slope Facies: E limit of Lower Paleozoic deep water facies rocks thrust over the miogeocline in mid-Paleozoic time

Isopachs after Stewart (1970), Burchfiel and Davis (1981), B. C. Burchfiel (personal comm., 1981)

Localities
FM: Frenchman Mountain
K: Kelso
M: Mount Morrison
N: Nopah Range
P: Providence Mountains
Pi: Pinto Mountains
Q: Quartzite Mountain (Victorville)
S: Soda Mountains
SB: San Bernardino Mountains
SH: Silurian Hills

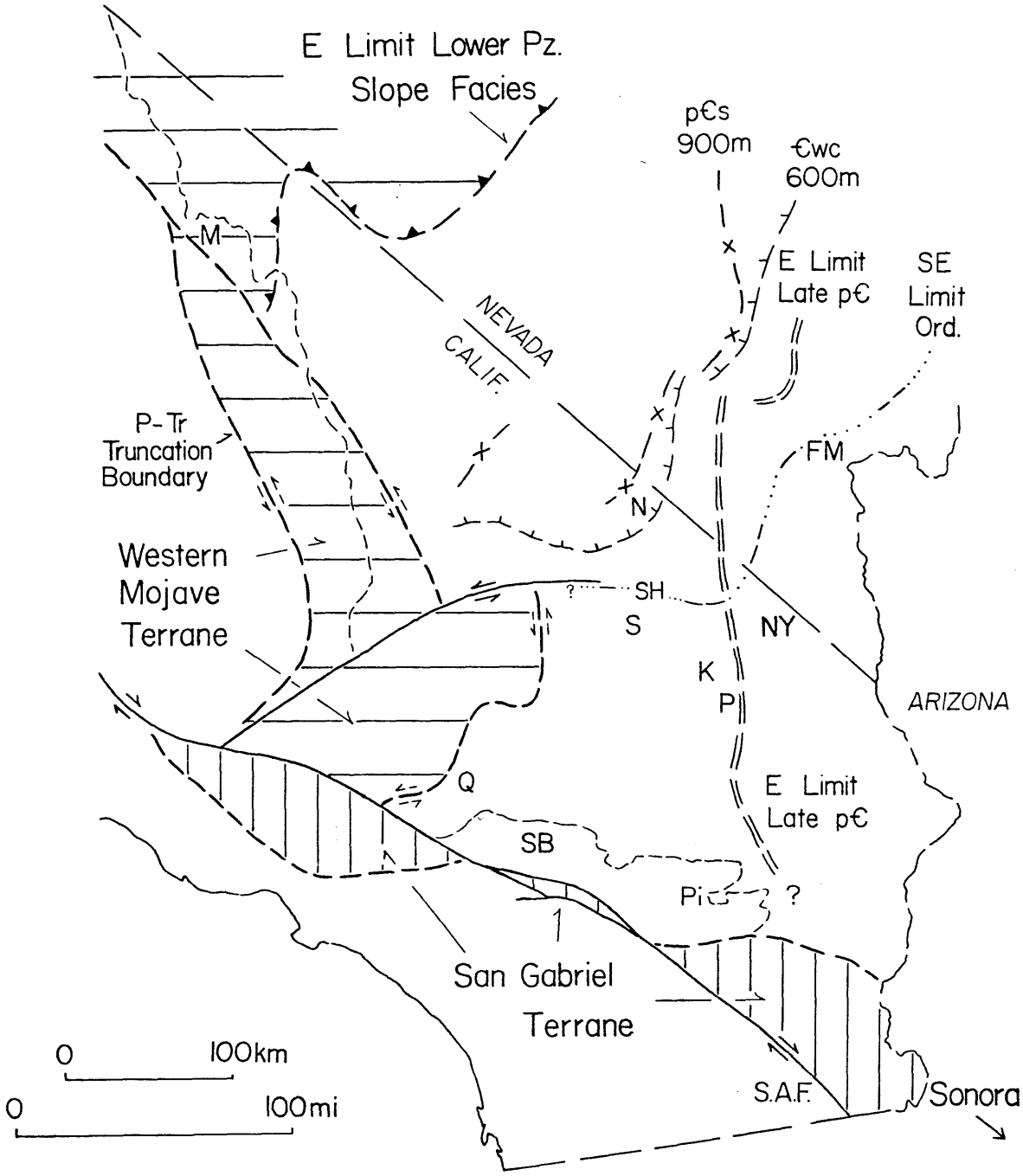
E Limit Lower Pz.
Slope Facies
pЄs
900m
Ewc
600m
E Limit
Late pЄ
SE
Limit
Ord.
M
NEVADA
CALIF.
P-Tr
Truncation
Boundary
FM
N
Western
Mojave
Terrane
SH
S
NY
K
P
ARIZONA
Q
E Limit
Late pЄ
SB
Pi
?
San Gabriel
Terrane
0
100km
0
100mi
S.A.F.
Sonora

Figure 22: Stratigraphic sections of Upper Precambrian-Cambrian rocks from the northern Mojave Desert region.

Thicknesses shown are in most cases structural thicknesses. Older Precambrian crystalline rocks denoted by diagonal waves.

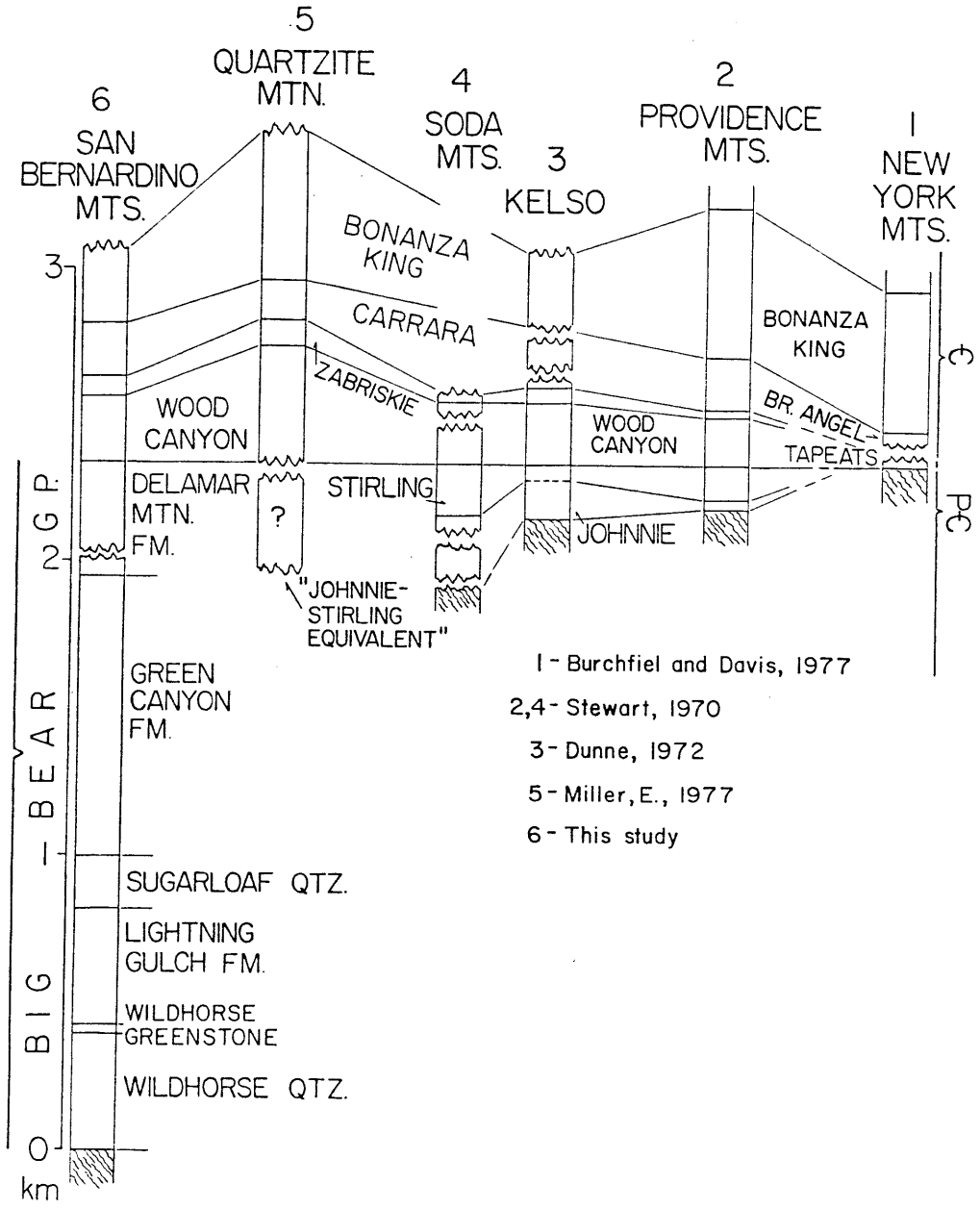

units, such as the Bonanza King, is probably meaningless; however, the measured structural thicknesses of predominantly quartzite units, such as the Wood Canyon and Zabriskie formations, may locally approximate original thicknesses. In terms of unit thicknesses, the Big Bear section matches well with the same formations in the eastern Mojave. In contrast, the Wood Canyon, Zabriskie and Carrara formations thicken significantly further north in the Death Valley region (Stewart, 1970).

The presence of possible Latham, Chambless and Cadiz equivalents within the Carrara Formation at Big Bear supports correlation with the eastern Mojave Desert sections, as does the general absence of carbonate rocks in the upper Wood Canyon Formation. By contrast, the Wood Canyon Formation at Quartzite Mountain near Victorville contains numerous interbeds of marble, typical of a more basinward miogeoclinal facies (Stewart and Poole, 1975; E. Miller, 1977).

The Zabriskie Quartzite at Quartzite Mountain is somewhat thicker (90 m) than at Big Bear (50-64 m) which Stewart and Poole (1975) also attributed to the former locality's more basinward paleogeographic setting. However, at Sidewinder Mountain, 22 km east of Quartzite Mountain, the Zabriskie Quartzite is only 2-6 m thick. Zabriskie thickness variations can be attributed to rapid lateral pinch-outs, tectonic telescoping of the sections along thrusts, or structural thinning (as seen at Big Bear).

Such paleogeographic details are probably unresolvable due to the structural complications and scarcity of pre-Mesozoic rocks in this region. However, the overall similarity of all the Big Bear-Victorville sections to those in the eastern Mojave argues for a marginal miogeoclinal setting. The pinch-outs and minor facies variations recognized here are common in sections near the miogeocline-craton hingeline elsewhere.

Upper Precambrian Rocks of the Southern Great Basin

Figure 23 is a generalized Upper Precambrian-Paleozoic stratigraphic transect across the miogeocline from southern Nevada through Death Valley (from Burchfiel and Davis, 1981). The section

Figure 23: Generalized stratigraphic framework of Upper Precambrian-Paleozoic rocks on a transect from Frenchman Mountain (southern Nevada) to Mount Morrison in the eastern Sierra Nevada (other localities shown in Figure 20; Figure 23 from Burchfiel and Davis, 1981). Transect crosses the miogeocline, extending from the cratonal margin (Frenchman Mountain) to the northwesternmost exposures of miogeoclinal rocks in the Inyo-White Mountains. Structural relations between rocks at Mount Morrison and rocks in the Inyo-White Mountains are unknown. Lower Paleozoic slope or rise(?) facies rocks at Mount Morrison may correlate with rocks of the Roberts Mountain allochthon. No Pennsylvanian-Permian rocks are exposed in the vicinity of the Funeral Mountains and hence are not shown in this section.

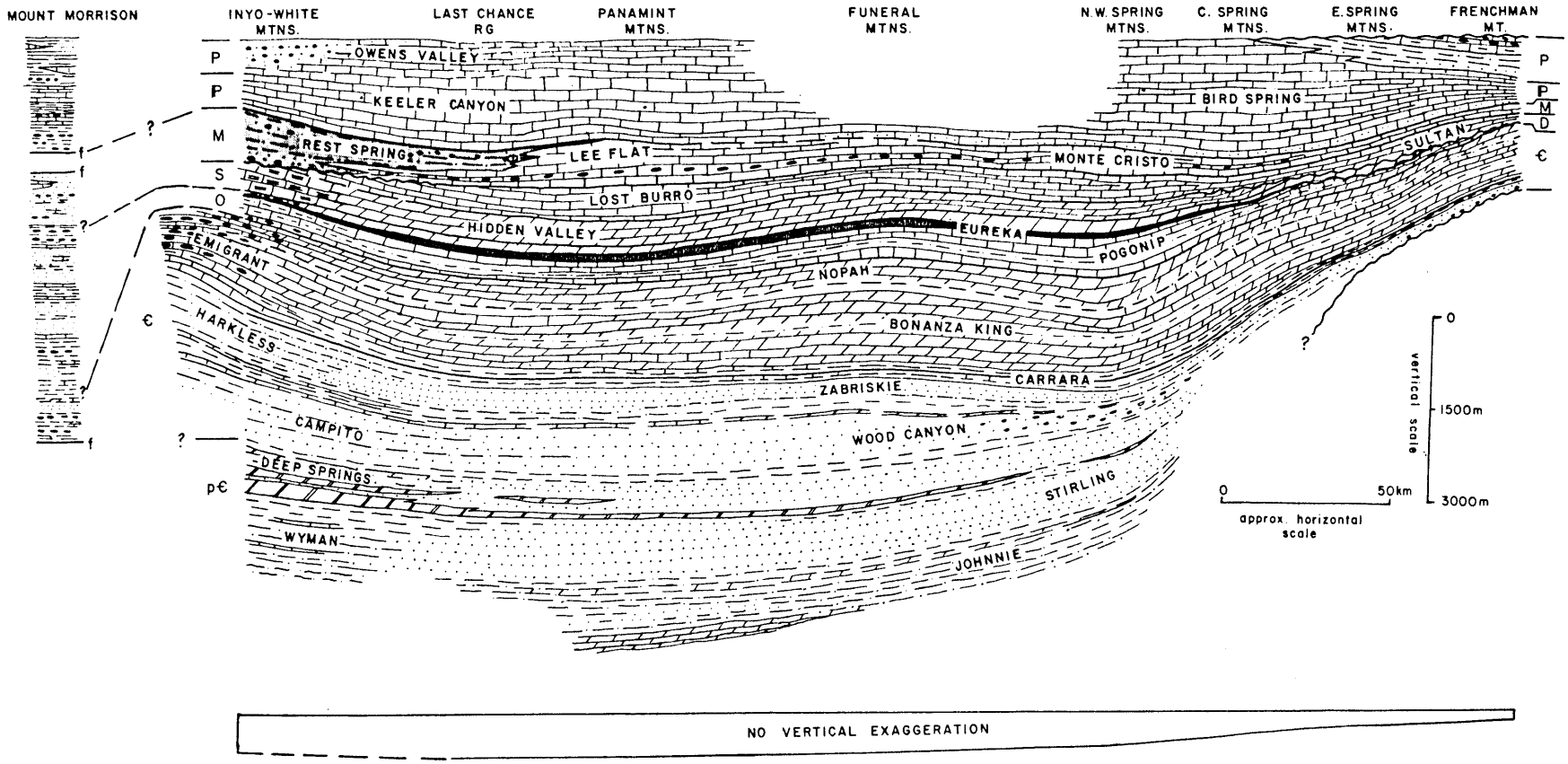
MOUNT MORRISON
INYO-WHITE MTNS.
LAST CHANCE RG
PANAMINT MTNS.
FUNERAL MTNS.
N.W. SPRING MTNS.
C. SPRING MTNS.
E. SPRING MTNS.
FRENCHMAN MT.
P
P
M
S
O
€
pC
f
?
OWENS VALLEY
KEELER CANYON
REST SPRING
LEE FLAT
LOST BURRO
HIDDEN VALLEY
EMIGRANT
HARKLESS
CAMPITO
DEEP SPRINGS
WYMAN
JOHNNIE
STIRLING
WOOD CANYON
ZABRISKIE
NOPAH
EUREKA
BONANZA KING
CARRARA
POGONIP
MONTE CRISTO
BIRD SPRING
SULTANT
P
P
M
D
€
0
1500m
3000m
vertical scale
0
50km
approx. horizontal scale
NO VERTICAL EXAGGERATION

runs from Frenchman Mountain (near Las Vegas) at the craton margin to the Mount Morrison area (east-central Sierra Nevada) where allochthonous Lower Paleozoic slope facies rocks are exposed (see Fig. 20 for locations). This west-northwest-trending section is nearly perpendicular to regional Upper Precambrian-Cambrian isopachs and facies trends.

Miogeoclinal strata correlative with Cambrian rocks at Big Bear (Wood Canyon Formation, Zabriskie Quartzite, Carrara Formation, Bonanza King Formation) conformably overlie a thick, regionally extensive Upper Precambrian clastic sequence. The Upper Precambrian rocks of the Death Valley region have been described by Stewart (1970) and most of the following is a summary of his work. The Upper Precambrian sequence locally includes the Noonday Dolomite at its base, but more typically the Johnnie Formation is the lowest unit exposed, and is overlain conformably by the Stirling Quartzite. The Johnnie (or the Noonday) unconformably overlies older crystalline rocks in the Death Valley and the eastern Mojave Desert regions. These basement rocks have locally yielded radiometric ages ranging from 1.4 to 1.7 b.y. (Wasserburg and others, 1959; Silver and others, 1961; Lanphere and others, 1963; Lanphere, 1964). In the central and southern Death Valley region sedimentary rocks of the Pahrump Group underlie the Johnnie or Noonday formations and overlie older crystalline rocks. In southern Nevada, the Last Chance Range and White-Inyo Mountains, the base of the Upper Precambrian sequence is not exposed.

The Johnnie Formation consists predominantly of siltstone and shale with interbeds of carbonate rocks, and lesser amounts of quartz arenite and subarkosic sandstone. The Stirling Quartzite consists of quartz arenite and subarkosic sandstone, with local interbeds of siltstone and carbonate (Stewart, 1970; Lobo and Osborne, 1976). The five members of the Stirling Quartzite can be recognized throughout the southern Nevada-Death Valley-eastern Mojave Desert region. Likewise, the uppermost Rainstorm member of the Johnnie Formation is regionally extensive. Lithologically the lower Johnnie Formation is regionally heterogeneous. However, in the southern Death Valley area, six members can be recognized from range to range (Stewart, 1970). The

uniformity of the upper Johnnie Formation and the Stirling Quartzite in this part of the miogeocline is striking.

Together with the Wood Canyon, Zabriskie and Carrara formations, these Upper Precambrian strata constitute the basal clastic wedge of the Cordilleran miogeocline (Stewart, 1972; Stewart and Suczek, 1977). As such they represent the initial deposits along the rifted southern Cordilleran margin. Diamictites in the upper part of the Pahrump Group (Kingston Peak Formation) are included with this sequence by Stewart and Suczek (1977).

To the west-northwest, this Upper Precambrian-Lower Cambrian sequence grades laterally into the fine grained clastic and carbonate units of the White-Inyo Mountains. Eastward, the transition from the thick Upper Precambrian-Lower Cambrian miogeoclinal clastic wedge to the thin Lower-Middle Cambrian basal sequence on the craton, consisting of Tapeats Sandstone and Bright Angel Shale, is not exposed in southern Nevada. The transition must occur in the subsurface and across several major thrust faults between the northwest Spring Mountains and Frenchman Mountain where the Tapeats and Bright Angel formations overlie crystalline basement rocks.

In the eastern Mojave Desert, a miogeocline to craton transition can be recognized. South from Death Valley both Lower Cambrian and particularly Upper Precambrian formations thin in the vicinity of Baker, California. The Johnnie and Stirling rocks thin from more than 2 km in thickness in Death Valley to 150 m in the Providence Mountains. Individual members of the Johnnie and Stirling formations known from southern Death Valley have been recognized in the Baker region by Stewart (1970). He suggested the Johnnie-Stirling contact is unconformable in the Providence Mountains (Stewart, 1970), east of which Upper Precambrian strata are absent (Burchfiel and Davis, 1981). The Upper Precambrian sections near Baker are the nearest to the San Bernardino Mountains of any known. They are transitional in facies to cratonal sections in the New York and Marble Mountains.

Comparison with the Big Bear Group

Figure 22 compares stratigraphic sections of Upper Precambrian-Cambrian rocks across the northern Mojave Desert. Cratonal facies Tapeats Sandstone and Bright Angel Shale are recognized in the New York Mountains. Westward, a typical marginal-miogeoclinal Cambrian stratigraphy (Wood Canyon, Zabriskie, Carrara, Bonanza King formations) extends across the northern Mojave. These units thicken northward in the Death Valley region. In the eastern Mojave, the Wood Canyon Formation overlies a thin Johnnie-Stirling sequence, which also thickens dramatically to the north. Westward, however, the Wood Canyon Formation overlies a thick and very different sequence of Upper Precambrian rocks in the San Bernardino Mountains (Cameron, 1980).

The Big Bear Group is stratigraphically equivalent to the Johnnie and Stirling formations. Both the Big Bear and Death Valley sequences consist of shallow marine deposits which overlap crystalline rocks yielding 1.7 b.y. ages. However, the Upper Precambrian lithologic sequence in the Big Bear area is distinct from that to the east, and requires separate nomenclature. In general the Big Bear Group is distinguished from rocks of the Johnnie and Stirling formations by 1) a different lithologic sequence, 2) higher proportion of carbonate rocks, 3) mafic volcanic rocks in the lower part of the sequence, and 4) predominance of pure quartz sandstone in the lower two-thirds of the section, and feldspathic sandstone at the top.

Tyler (1975) suggested the rocks here assigned to Delamar Mountain Formation correlated with the D and E members of the Stirling Quartzite. The sandstone protoliths of the Delamar Mountain Formation were rich in feldspar, however, the uppermost Stirling Quartzite (E member) is typically an orthoquartzite (Stewart, 1970; Lobo and Osborne, 1976). Interbedded carbonates are important locally in the upper Stirling (D member), but only in the northern Death Valley-Nevada Test Site region. The D member is not prominant in the southern Death Valley area, and is often absent in sections in the eastern Mojave Desert. Also, no unit correlative with the Green Canyon Formation is

recognized in the eastern Mojave Desert, in the sections closest to Big Bear. As the Stirling Quartzite is noted for its regional lithologic uniformity, it is suggested that the lithologic contrasts between typical Stirling Quartzite and the upper Big Bear Group preclude using the term Stirling Quartzite in the San Bernardino Mountains.

Rocks in the lower part of the Johnnie Formation do exhibit wide facies variations, but more so in areas outside southern Death Valley. Carbonate rocks occur in the Johnnie Formation, but are normally present throughout the section, not locally as in the Big Bear Group. No rocks similar to the regionally extensive Rainstorm Member (which includes the distinctive "Johnnie oolite") are recognized at Big Bear. Although little detailed sedimentological work on the Johnnie and Stirling formations has been published, intertidal facies rocks similar to those of the Big Bear Group have not been described from either unit (see Lobo and Osborne, 1976). One might argue that the Johnnie Formation is lithologically heterogeneous enough that the name could be applied to rocks of the Big Bear Group. However, the absence of the Stirling Quartzite, the apparent lack of erosional breaks within the Big Bear Group, and its conformable upper contact with the Wood Canyon all preclude using the name Johnnie Formation to describe any part of the Big Bear Group. Rocks correlative with the Noonday Dolomite and Pahrump Group are clearly not present in the San Bernardino Mountains. Johnnie-Stirling nomenclature is not appropriate to describe this lithologically distinctive Upper Precambrian sequence. Use of this terminology at nearby Quartzite Mountain (Stewart and Poole, 1975; E. Miller, 1977) may not be justified either, and Upper Precambrian strata there may correlate with parts of the Delamar Mountain or Green Canyon formations.

It is proposed that the name Big Bear Group be formally adopted to describe all Upper Precambrian strata conformably underlying the Wood Canyon Formation in the San Bernardino Mountains and vicinity. It is further proposed that the six units of the Big Bear Group recognized in the San Bernardino Mountains are deserving of formational

rank. These propositions will be submitted to the U.S. Committee on Stratigraphic Code.

Late Precambrian Paleogeography and Facies Variations

The Big Bear Group is the only complete Upper Precambrian section presently known south and west of Baker, California, and northwest of Caborca, Sonora, Mexico. It provides key data concerning paleogeography along the ancient continental margin. The Big Bear Group and the Johnnie and Stirling formations occupy equivalent stratigraphic positions and are broadly time equivalent. Stewart (1972) included the Johnnie-Stirling sequence in the basal clastic wedge of the Cordilleran miogeocline, and suggested these rocks were among the initial deposits of the newly rifted Late Precambrian continental margin. It is suggested that the Big Bear Group was deposited in a similar setting.

Accumulation of thick shallow marine deposits, such as the Big Bear Group and Upper Precambrian strata in the Death Valley region, requires vigorous subsidence during deposition. Studies of modern divergent margins, such as the Red Sea (Lowell and others, 1975), suggest the stages of continental breakup include: thermal expansion and regional doming of the continental lithosphere above upwelling asthenosphere; crustal rifting and attentuation, manifested at shallow levels by listric normal or block faulting; and eventual drifting of the separated continental plates as oceanic crust forms along the rift axis. Evidence from Mesozoic and younger margins suggests that thick shallow marine sequences are primarily early drift-phase deposits, whereas underlying rift-stage deposits (often non-marine) are more rarely preserved in the stratigraphic record (Lowell and others, 1975; Kinsman, 1975; Schuepbach and Vail, 1980). Models of Sleep (1971) and Sleep and Snell (1976) support this conclusion, and suggest subsidence along divergent "Atlantic-type" margins is most pronounced during the early drift-phase. As the diverging continental plates drift from the ridge-centered region of asthenospheric upwelling and high heat flow, the lithosphere of the continental

margin cools, contracts and subsides. After drifting begins, the rate of subsidence declines exponentially.

Stewart and Suczek (1977) applied this subsidence model to Upper Precambrian-Lower Paleozoic miogeoclinal rocks in the White-Inyo Mountains region. They concluded that stratigraphic thickness variations through time there agreed well with model thickness changes predicted if the subsidence rate decayed exponentially. Based on this comparison, they suggested clastic wedge deposition along the Cordilleran margin began between 600-650 m.y. ago. Thus, the thick Upper Precambrian sequences at the base of the Cordilleran miogeocline were deposited in a relatively short time (between 30 and 80 m.y.).

The Big Bear Group was deposited in a vigorously subsiding basin. The persistence of restricted, tide dominated shallow marine environments and interfingering of facies observed in the Big Bear Group is consistent with rapid deposition. If the analogies drawn from modern divergent margins are applicable, it is likely that the Big Bear Group and correlative Upper Precambrian strata in the southern Great Basin represent initial drift-phase deposits of the miogeocline.

Stewart and Suczek (1977) proposed the early history of the miogeocline was profoundly influenced by margin-parallel, basement highlands uplifted during the doming and rift stages (Fig. 24). Analogous basement uplifts are found along the modern Red Sea margin (Lowell and others, 1975). In their view these highlands were the source terrane for the basal clastic wedge. Subsequent thermotectonic contraction and subsidence, combined with erosion, removed these uplifts so by middle Cambrian time shorelines transgressed far to the east and carbonate deposition dominated the ancient shelf. This model has considerable intuitive appeal. However, several important aspects of Late Precambrian paleogeography are not dealt with. In the lower Big Bear Group, mature, medium to fine grained orthoquartzite makes up much of the section. It is difficult to envision these sands as being derived via short river systems from nearby Red Sea-like basement highlands. These and similar mature quartz sandstones in the Precambrian of the southern Great Basin almost certainly had a

Figure 24: Model for the Late Precambrian-Cambrian tectonic framework of miogeoclinal deposition in the southern Cordillera (modified after Stewart and Suczek, 1977).

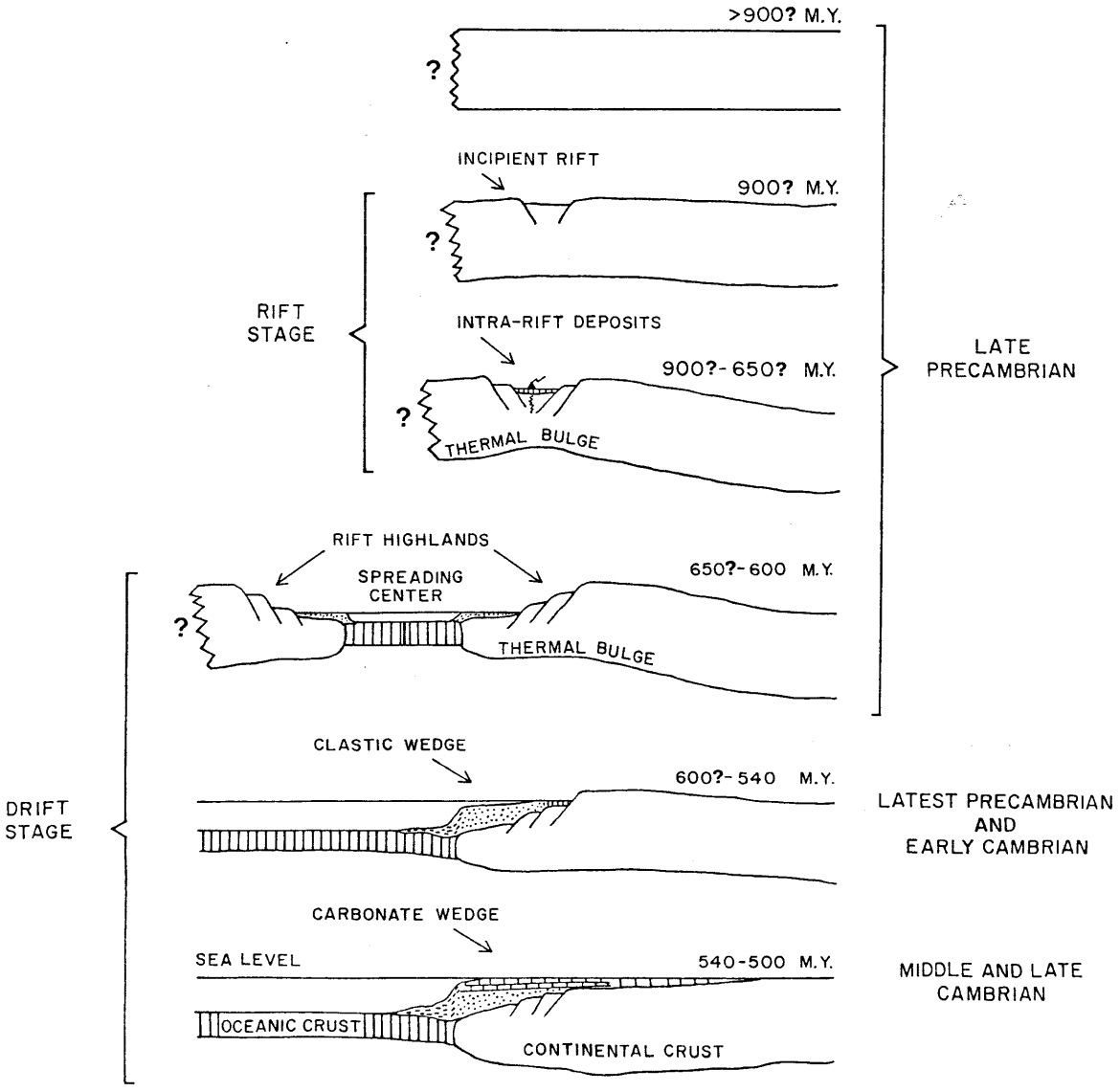

cratonal source (Stewart, 1970). Major drainage systems from the craton probably provided a significant amount of this mature terrigenous sediment. A modern analogy can be drawn from the Colorado River, which carries mature continental debris into the rift-drift basin in the northern Gulf of California. Also puzzling are the locally thick accumulations of carbonate rocks, both in the Big Bear Group and particularly in Sonora, where the Upper Precambrian section is dominated by shallow marine carbonates (discussed below). In the Green Canyon Formation, possible locally derived clastics appear in association with carbonates, only when more typical tide dominated clastic sedimentation is interrupted. Overall, the relative scarcity of coarse clastics or evidence of interfingering fluvial deposits at Big Bear or in the southern Great Basin (Stewart, 1970) suggests that nearby basement highlands were not the principal clastic sediment source. In the Big Bear Group, coarsening offshore is noted, suggesting that lateral basin transport of clastics was important there.

It is suggested that during the early drift stages of divergent margin evolution, rapid lateral facies variations, producing regional stratigraphic variation, are to be expected. Variables such as local basin structure and topography, source areas, marine circulation patterns, water temperature, salinity and nutrient supply help control clastic and carbonate sedimentation on continental margins. Complex depositional patterns are more likely early in a margin's evolution, when local structural control of basin geometry is still pronounced, than at later, more mature stages when erosion and thermotectonic subsidence combine to produce regional low relief such as present along the mature Atlantic margin of North America.

Upper Precambrian-Cambrian regional stratigraphy in the southern Cordillera reflects divergent margin evolution from a late-rift to mature-drift stage. Depositional patterns were most complex during initial phases of miogeoclinal sedimentation.

The western Mojave Desert and the southern Great Basin were independent depocenters until Wood Canyon time. In the east, the Kingston Peak Formation records deposition during late stage rift

tectonism (Wright and others, 1974; Stewart and Suczek, 1977). It contains coarse, locally-derived clastics and its basin is in part fault controlled (Wright and others, 1974). The overlying Noonday Dolomite is similarly areally restricted, and clastic rocks of its basinal facies were derived from local source areas to the southwest (the Mojave Upland of Wright and others, 1974). The overlying lower Johnnie Formation is present over a wide region but is lithologically heterogeneous from range to range (Stewart, 1970). In contrast, the uppermost part of the Johnnie, the Rainstorm Member, and overlying Stirling Quartzite are uniform over a wide region (Stewart, 1970). This transition probably reflects infilling of local Late Precambrian basins over a wide area in the southern Great Basin. Even so, the western Mojave deposystem still remained independent. This lasted until Latest Precambrian time, when deposition of Wood Canyon strata across this entire region signalled a mature depositional setting.

Stratigraphic variations across the Mojave Desert suggest the existence of a long-lived tectonic feature there, a paleogeographic high or arch, trending transverse, not parallel, to isopachs in the southern Great Basin. Dramatic north to south thinning of the Johnnie-Stirling sequence, and the appearance of thick Upper Precambrian strata of contrasting facies to the west (Big Bear Group) and south (see below) suggest a paleogeographic high was present in the eastern Mojave Desert (Fig. 25). This tectonic high persisted until Latest Precambrian-Early Cambrian time when clastic and later carbonate units of regionally uniform thickness overlapped the eastern and western Mojave regions.

Renewed epeirogenic activity along this "Mojave high" may have caused the westward deflection of middle and late Paleozoic isopachs and facies belts across the northern Mojave (Fig. 26) which was first noted by Gans (1974), and later substantiated by E. Miller (1977). Though most of the Mojave Desert lay in a marginal miogeoclinal setting during the Cambrian, in post-Cambrian time and certainly in the Late Paleozoic both the eastern Mojave region (Burchfiel and Davis, 1981) and the San Bernardino Mountains-Victorville area (E. Miller,

Figure 25: Stratigraphic sections of Upper Precambrian-Cambrian rocks from the southern Death Valley region to the San Bernardino Mountains. Sources:

1. Stewart, 1970
2. Kupfer, 1960; Stewart, 1970
3. Stewart, 1970
4. Dunne, 1972
5. Stewart, 1970
6. this study

Thicknesses shown are often structural thicknesses. Older Precambrian crystalline rocks denoted by diagonal waves.

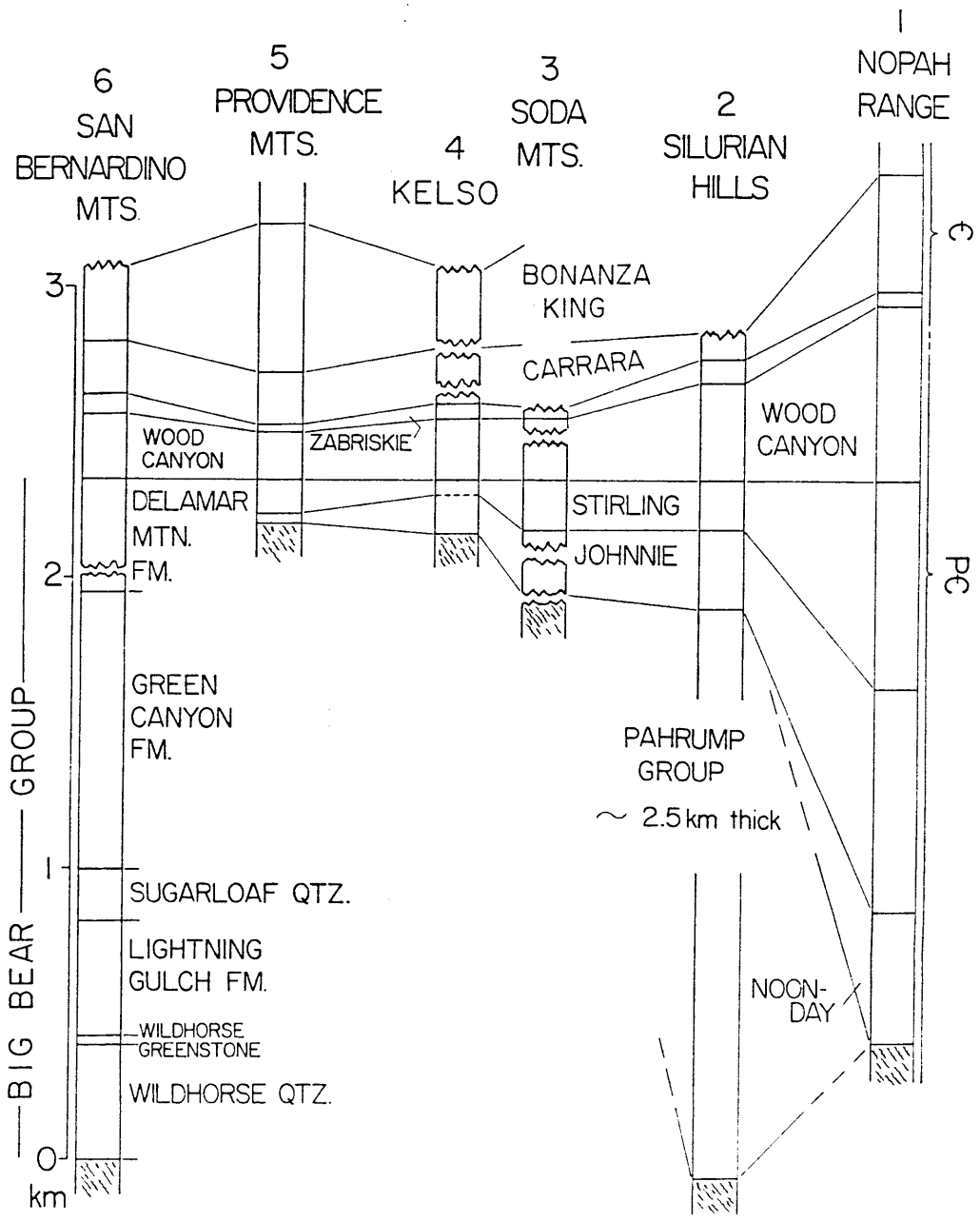

Figure 26: Interpretive map of Late Precambrian-Paleozoic paleogeographic elements in the Mojave Desert region.

AA: Armogossa Aulacogen of Wright and others (1974)
gf: Garlock fault
p€-€wc: Wood Canyon Formation
saf: San Andreas fault
SB: San Bernardino Mountains
SN: Sierra Nevada

Facies and isopach lines are from Burchfiel and Davis (1981), Wright and others (1974), B. C. Burchfiel (pers. commun., 1981), this study.

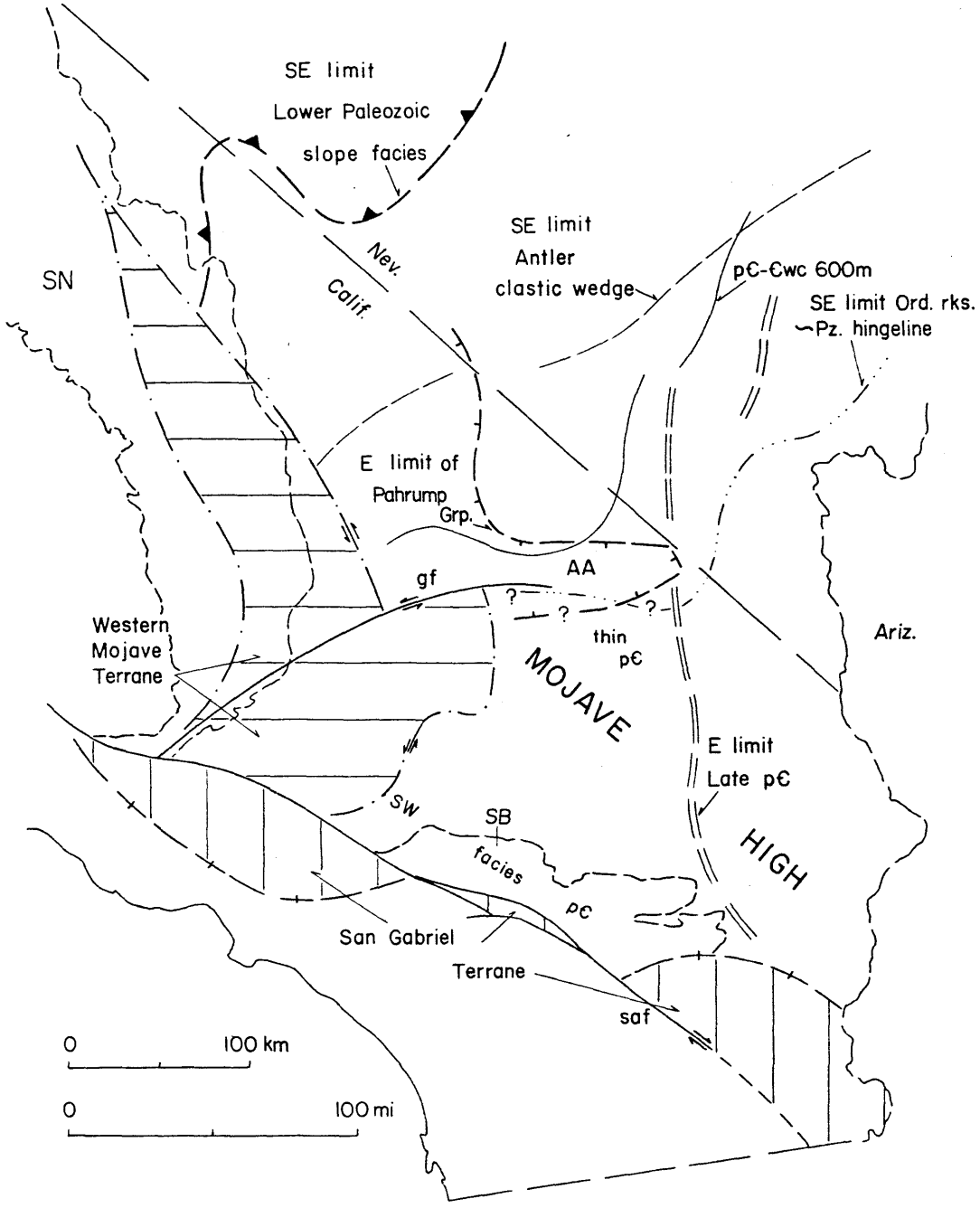
SE limit
Lower Paleozoic
slope facies
SE limit
Antler
clastic wedge
pC-Cwc 600m
SE limit Ord. rks.
Pz. hingeline
SN
Nev.
Calif.
E limit of
Pahrump
Grp.
AA
gf
?
?
?
thin
pC
Western
Mojave
Terrane
MOJAVE
Ariz.
E limit
Late pC
HIGH
SW
SB
facies
pC
San Gabriel
Terrane
saf
0
100 km
0
100 mi

1977; 1981) lay in a cratonic or marginal miogeoclinal setting.

The northern boundary of this high, defined by marked thinning of Precambrian-Cambrian isopachs and the deflection of later Paleozoic facies trends, closely approximates the southern limit of rocks of the Armagossa Aulacogen (Wright and others, 1974) and the overlying Noonday Dolomite. Wright and others (1974) suggested these rocks were deposited in a structurally controlled trough. They postulated that recurring tectonism within this trough subtly influenced depositional patterns of the overlying Johnnie, Stirling, and Wood Canyon formations in the southern Death Valley region. It is unknown whether the southern limit of the trough recognized by Wright and others (1974) is fault bound, or whether broad arching controls the distribution of the Pahrump Group and Noonday Dolomite.

It is suggested here that recurrent tectonism, either faulting or broad warping, near the southern boundary of the Armagossa Aulocagen, localized the northern boundary of the paleogeographic high recognized in the Mojave Desert. Rift related structures which bounded the Kingston Peak basin may have had persistent effect on miogeoclinal paleogeography.

The nature of the southwestern boundary of the Late Precambrian paleogeographic high in the Mojave is unknown, and unfortunately few outcrops of pre-Mesozoic rocks are known between the Baker area and the Big Bear-Victorville region. Whether the intervening area was locally emergent during deposition of the Big Bear Group and the Johnnie and Stirling formations is uncertain.

The southeastern continuation of this high is not well constrained. Its southwestern boundary lay west of the Marble Mountains, Kilbeck Hills, and Big Maria Mountains where Upper Precambrian rocks are absent (Stone and Howard, 1979; Burchfiel and Davis, 1981) and east of suspected Upper Precambrian rocks in the Pinto Mountains (discussed below).

The Mojave high trended obliquely to northeast trending miogeoclinal isopachs and facies boundaries in the southern Nevada-Death Valley region. Its northern boundary may be localized along

faults or flexures which probably originated during initial rifting of the margin (Wright and others, 1974) but record a long history of later epeirogenic tectonism. The effects of early drift stage thermo-tectonic subsidence, which culminated with the major Cambrian transgression (Stewart and Suczek, 1977), were superposed on the more fundamental structural control of this transverse, northwest(?) trending paleogeographic high in the Mojave region. The postulated Mojave high appears to be a long-lived tectonic element in the history of the southern Cordillera. It may have exerted profound control on Precambrian-Paleozoic sedimentary deposition, and hence on subsequent Mesozoic and Cenozoic tectonics. It may be analogous to the Salmon River Arch of Idaho. Similarities between these regions were first noted by Armstrong (1975). Possible relationships between these features and the geometry of Late Precambrian rifting, suggested by Dickinson (1981), are considered below.

Enigmatic Miogeoclinal Rocks of the Southern Cordillera

West and south of Baker, the rocks at Big Bear and Victorville are the only confirmed Upper Precambrian strata in southern California. Cratonal facies Cambrian clastics (Tapeats-Bright Angel) occur in southeastern California, and are exposed in the Clark Mountains, New York Mountains, Marble Mountains, Kilbeck Hills, and Big Maria Mountains (Burchfiel and Davis, 1981). Similar rocks are found in southern Arizona. The Upper Precambrian hinge line lies west of these exposures. The nearest confirmed Upper Precambrian strata southeast of Big Bear crop out some 600 km away in Mexico, near Caborca, Sonora (Fig. 27). Recognition of Upper Precambrian facies variations across the Mojave Desert region may help explain the unusual Upper Precambrian section in Sonora.

The presence of fossiliferous miogeoclinal strata at Carborca has long been known (Cooper and others, 1952). Eells (1972) recognized a fossiliferous Cambrian section which included units similar in lithology and sequence to the Wood Canyon-Zabriskie-Carrara-Bonanza King succession of the southern Great Basin (Fig. 28). The Wood

Figure 27: Major pre-Mesozoic paleogeographic and tectonic elements of the southern Cordillera.

B: Baker
C: Caborca
gf: Garlock fault
LA: Los Angeles
LV: Las Vegas
?ms: approximate trace of Mojave-Sonora megashear through central Mojave Desert as postulated by Silver and Anderson (1974)
PR: Peninsular Ranges
saf: San Andreas fault
SB: San Bernardino Mountains
SF: San Francisco
SGT: San Gabriel terrane
sjf: San Jacinto fault
SN: Sierra Nevada
V: Victorville
WMT: western Mojave terrane

Pz (Paleozoic) hingeline = SE limit of Ordovician rocks
Inferred limit Precambrian continental crust based on surface geology and Sr isotopic data
Antler terrane (Roberts Mountain allochthon and equivalents, accreted in Mid-Paleozoic): vertical rule
Sonoma terranes (Golconda allochthon and "Sonomia arc", accreted in Permo-Triassic): diagonal rule
San Gabriel terrane: horizontal rule
Salinian block crystalline rocks: dots

Mojave-Sonora megashear includes labelled segment from Caborca to SE California, segment labelled ?ms, and the eastern boundary of the western Mojave terrane.

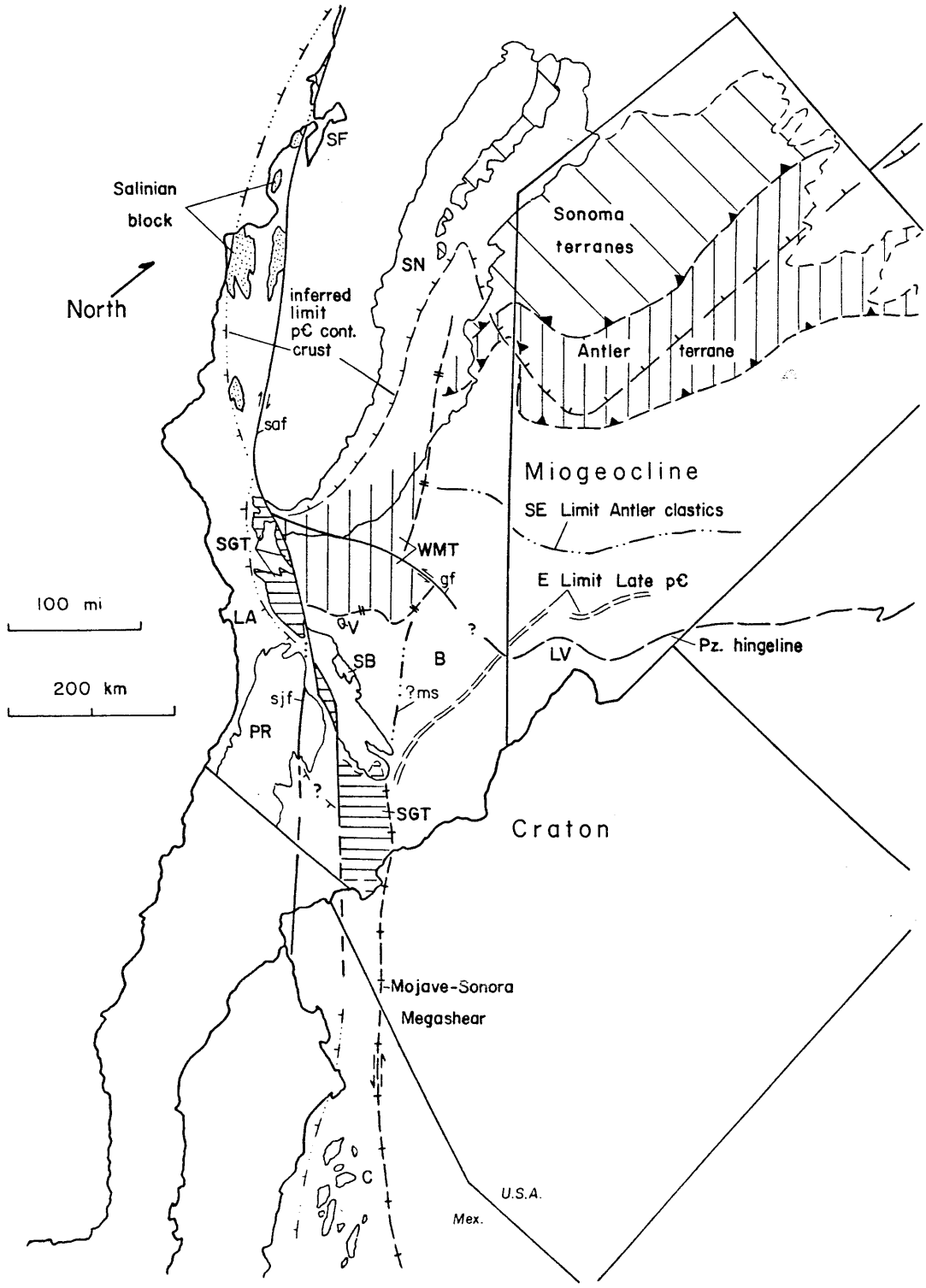
Salinian
block
North
SF
SN
inferred
limit
pC cont.
crust
saf
Sonoma
terranes
Antler
terrane
Miogeocline
SE Limit Antler clastics
E Limit Late pC
Pz. hingeline
SGT
WMT
gf
LA
V
SB
B
?ms
LV
sjf
PR
SGT
Craton
100 mi
200 km
Mojave-Sonora
Megashear
C
U.S.A.
Mex.

Figure 28: Correlation and comparison of Upper Precambrian-Cambrian formations in the Caborca region, Sonora, Mexico and in the Nopah Range, California. Figure 28 is from Eells (1972). (For scale, note that Noonday - Stirling sequence in Nopah Range is 1940 m thick.)

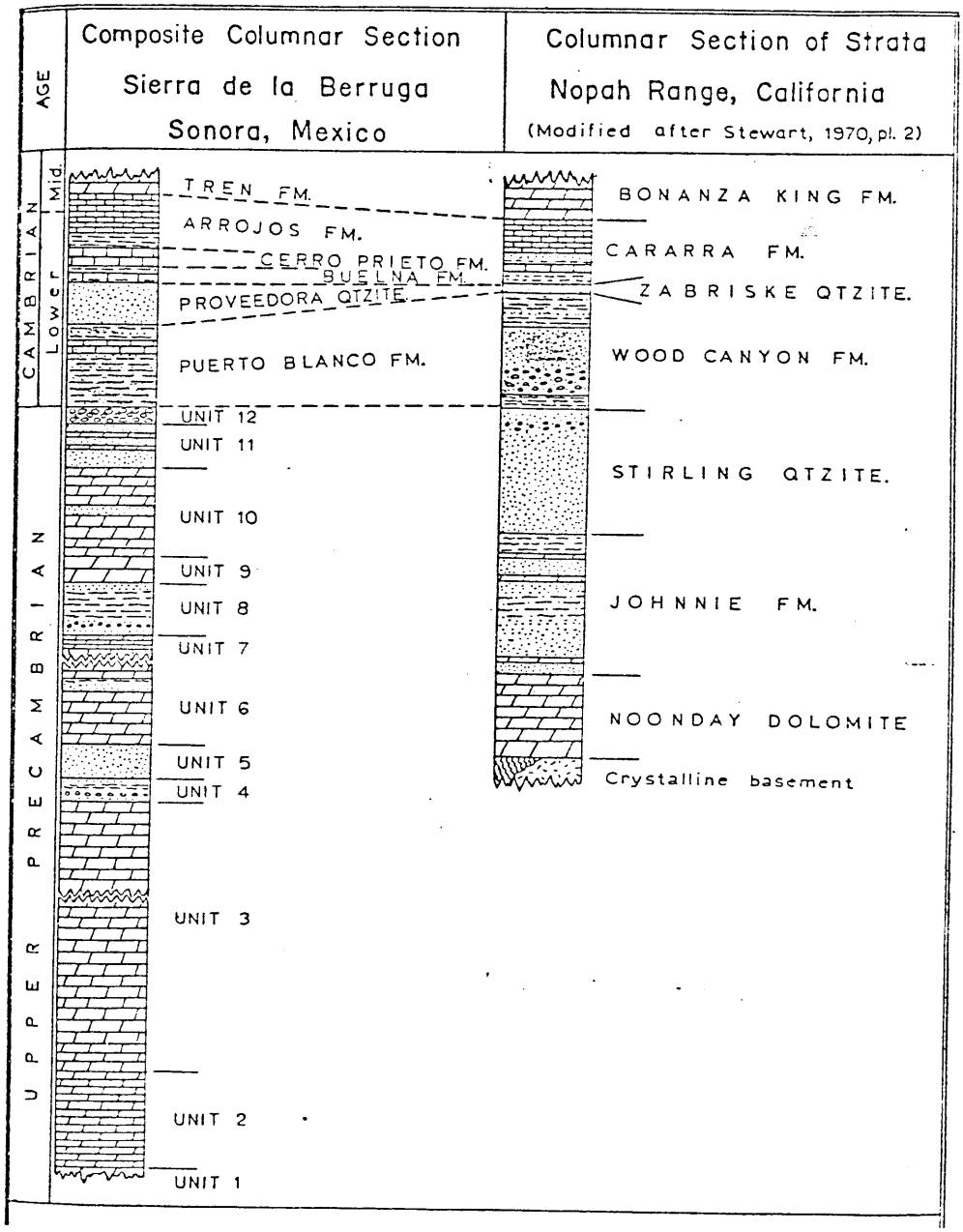

Canyon equivalent conformably overlies a thick sequence of Upper Precambrian strata, primarily dolomite and limestone, but with mafic volcanic rocks at the top. This section is discontinuous, and not exposed in a single complete section. Later, Anderson and others (1979) reported that this Upper Precambrian sequence overlies a basement complex whose oldest rocks yield 1.7 b.y. U/Pb zircon ages, similar to ages of older basement gneisses in the Mojave-Death Valley region. The minimum thickness of the composite Upper Precambrian section at Caborca is 4 km (Anderson and others, 1979).

Similar Cambrian stratigraphy ties Caborca to the Cordilleran miogeocline. It has long been suggested that these rocks are in place and represent the southern continuation of the Cordilleran miogeocline (Kay, 1951; King, 1959, 1969). Some recent paleogeographic interpretations have reiterated this theme (Stewart and Poole, 1975). The marked lithologic contrast between the predominantly clastic Upper Precambrian sequence in the southern Great Basin and the predominantly carbonate sequence at Caborca has caused some reluctance about accepting this interpretation. In view of significant Upper Precambrian facies variations now recognized in the Mojave, this issue seems less troublesome. The Big Bear Group, in fact, may represent a transitional facies between primarily clastic deposits to the north and prolific carbonate deposition to the south. By Wood Canyon time, uniform depositional conditions occur in all three areas.

An alternative interpretation has been presented by Silver and Anderson (1974). They suggest that the rocks at Caborca are out of place along a major left-lateral strike slip fault, the Mojave-Sonora megashear. Recognition of the megashear is based in large part on apparent offsets of Precambrian age provinces in crystalline basement rocks.

Silver and others (1977a) have recognized a southwest trending age province boundary striking from north New Mexico to southwestern Arizona. A terrane yielding ages of 1.75 b.y. is exposed to the northwest, and a terrane yielding ages of 1.65 b.y. is exposed to the southeast. The 1.75 b.y. terrane extends into southern California and

underlies the miogeoclinal and cratonal facies rocks (Silver and others, 1977a; Silver, 1971). Lithologically, the two terranes are similar, consisting of eugeosynclinal paragneisses and schists intruded by (quartz monzonite) augen orthogneisses. The ages of the granitic rocks differ by about 100 m.y. across the boundary. Both terranes are intruded by voluminous 1.4 b.y. anorogenic granites (Silver and others, 1977b).

The miogeoclinal Upper Precambrian-Cambrian sequence at Caborca overlies rocks of the older terrane (Anderson and Silver, 1977). To the northwest, rocks of the younger terrane are found, and are overlain by a cratonal sequence in southern Arizona (130 km away). No transitional facies of Upper Precambrian-Cambrian strata are known in between. Silver and Anderson (1974) and Anderson and Silver (1979) suggest these terranes are separated by the megashear, with a postulated 700-800 km of left-lateral offset. The displacement on the megashear is Early to Middle Mesozoic.

Although the mismatch of Precambrian terranes (minimum 500 km offset) suggested by Silver and Anderson is impressive, it is necessary to demonstrate offset of overlying Upper Precambrian and Paleozoic strata to show the megashear is an important Phanerozoic tectonic feature. Without such evidence, one can argue the apparent basement offset is Precambrian in age, and that the close juxtaposition of thick miogeoclinal and thin cratonal sequences occurred during Mesozoic thrusting (a similar juxtaposition occurs over a distance of 80 km in the southern Nevada thrust belt). Such an argument is difficult to counter considering the lack of detailed mapping and extensive post-orogenic cover between Caborca and known outcrops of cratonal rocks.

Silver and Anderson (1974) obtain a 700-800 km figure for offset on the megashear by matching Upper Precambrian-Cambrian strata in Caborca with similar age strata in the Death Valley region. They suggest the megashear trends northward through the central Mojave Desert and northward through Owens Valley. However, the continuation of miogeoclinal and cratonal facies rocks across the Mojave Desert to the San Bernardino Mountains-Victorville area does not permit such a

trajectory. Any major discontinuity must run west and south of the San Bernardino Mountains. Further, the Upper Precambrian rocks of Sonora do not match lithologically with the Johnnie-Stirling sequence, nor can Caborca stratigraphy by matched with Upper Precambrian and Cambrian units in the White-Inyo Mountains which are markedly different from those in Sonora.

The best correlation occurs between rocks in Caborca and rocks in the San Bernardino Mountains-Victorville area. The Upper Precambrian Big Bear Group is transitional to the carbonate-rich sequence at Caborca and the Cambrian stratigraphy is quite similar. During the Middle-Late Paleozoic, the San Bernardino Mountains-Victorville area lay in a cratonal setting. A Middle-Late Paleozoic cratonal setting for rocks in the Caborca area is not certain, but the absence of Ordovician and Silurian strata, or rocks of the Antler clastic wedge (Poole and Hayes, 1971), suggests this is the case. Displacement of Caborca sequence from the San Bernardino Mountains area would require approximately 600 km of left-lateral offset.

Davis and others (1978) and Burchfiel and Davis (1981) have suggested that the western Mojave terrane and perhaps the Caborca sequence were fault-bounded slivers, transported to their present relative positions during a Permo-Triassic left-lateral transform faulting event which truncated the old margin (see also Hamilton and Myers, 1966; Burchfiel and Davis, 1972). This faulting must occur prior to Permo-Triassic regional metamorphism and arc activity which affects the western Mojave terrane and adjacent areas (see below) but is not recognized at Caborca.

A more perplexing piece in the megashear puzzle is the San Gabriel terrane (Silver, 1971). This distinctive assemblage of Precambrian crystalline rocks is known only from southern California and is exposed on both sides of the San Andreas Fault. When viewed on a mid-Tertiary palinspastic base (Fig. 29), the San Gabriel terrane is located between the San Bernardino Mountains and Caborca, and west of the only known cratonal or miogeoclinal strata in southeastern California.

The San Gabriel terrane consists of older eugeosynclinal

Figure 29: Pre-Mesozoic palinspastic base map of southern California and vicinity. Effects of Miocene and younger faulting are removed. Figure 29 is simplified from an unpublished 1978 palinspastic reconstruction by the author, published elsewhere by Burchfiel and Davis (1981).

Allochthonous Lower Paleozoic slope and rise(?) rocks and equivalents(?) in the western Mojave terrane: wide diagonal rule
San Gabriel terrane: narrow diagonal rule
Terranes accreted in Early Mesozoic: vertical rule
Franciscan complex and equivalents (accreted in Late Mesozoic): horizontal rule
Great Valley Sequence and correlative Late Mesozoic fore-arc basin deposits: dots
Salinian block granitic rocks: crosses
Metamorphic rocks of the Santa Lucia Range: cross-hatch
P.Tr.T.B.: Permo-Triassic truncation boundary (inferred western limit of Precambrian continental crust based on surface geology and $^{87}Sr/^{86}Sr = 0.706$.

SB: San Bernardino Mountains
P: Pinto Mountains
SL: Santa Lucia Mountains

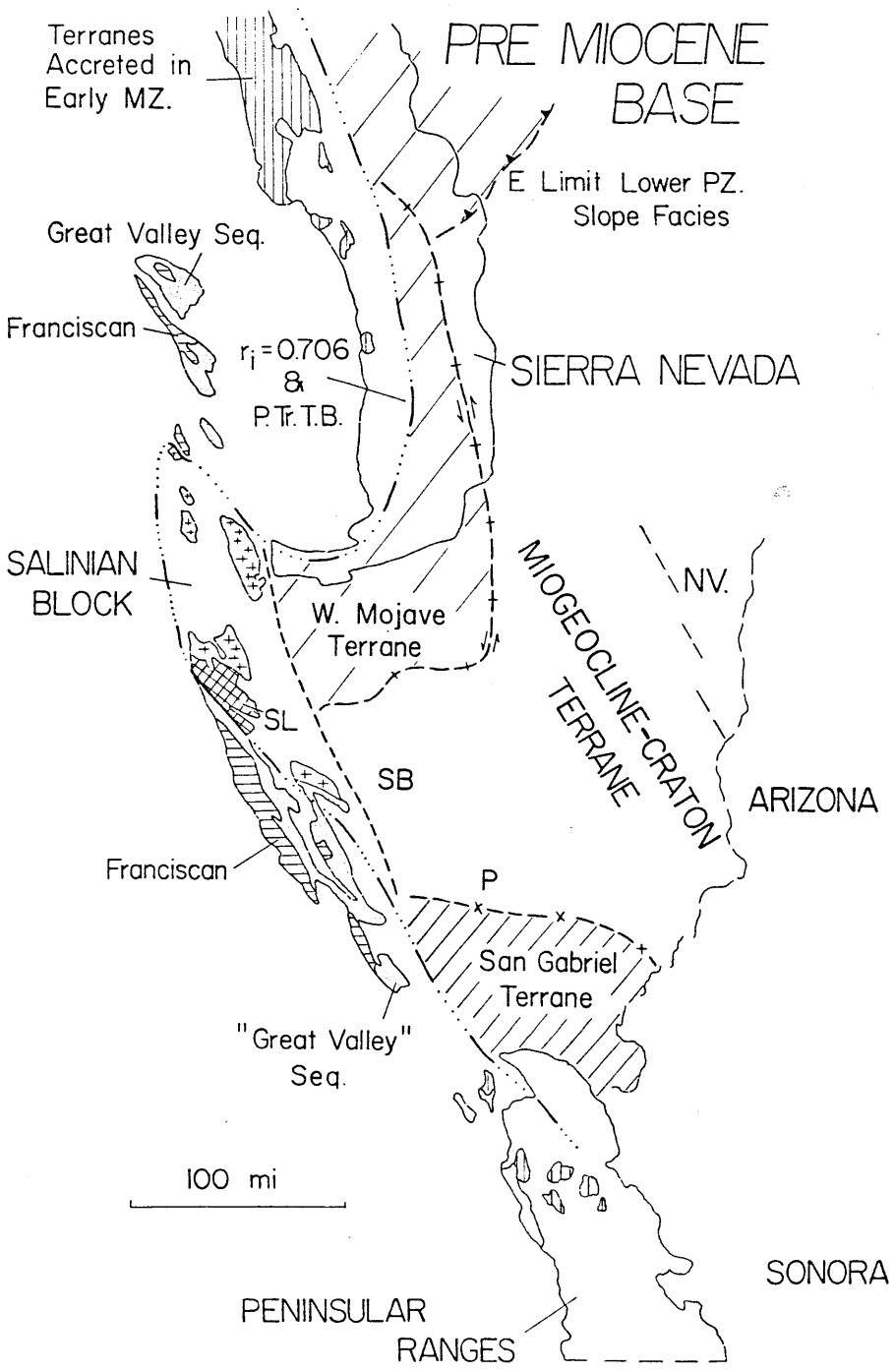
Terranes
Accreted in
Early MZ.
PRE MIOCENE
BASE
E Limit Lower PZ.
Slope Facies
Great Valley Seq.
Franciscan
r_i=0.706
&
P.Tr.T.B.
SIERRA NEVADA
SALINIAN
BLOCK
W. Mojave
Terrane
MIOGEOCLINE-CRATON
TERRANE
NV.
SL
SB
ARIZONA
Franciscan
P
San Gabriel
Terrane
"Great Valley"
Seq.
100 mi
SONORA
PENINSULAR
RANGES

paragneisses and intrusive augen orthogneisses which were deformed together. The orthogneisses have yielded 1.65 b.y. old U/Pb zircon ages (Silver, 1971). The protoliths, early deformational history, and ages of the rocks are the same as in the "younger" basement terrane recognized to the southeast. Unlike those rocks, the San Gabriel terrane was subsequently metamorphosed at granulite facies (now retrograded), intruded by orogenic 1.4 b.y. old granites, and then intruded by a 1.2 b.y. old anorthosite-syenite complex (Silver, 1971; Silver and others, 1977a). With the exception of the last event, the similar timing of events in the San Gabriel terrane and the 1.65 b.y. old basement complex in southern Arizona is striking.

Silver and Anderson (1974) suggest the San Gabriel terrane is highly exotic and include it with the block displaced left-laterally along the megashear. I suggest an alternate interpretation, that the San Gabriel terrane was displaced right-laterally to its present relative position along a Precambrian strike-slip fault.

Warren Hamilton (personal communication, 1980) has suggested the lithologic contrasts between the San Gabriel terrane and nearby basement outcrops reflect contrasting level of exposure, not widely separated points of origin. I concur and suggest these rocks represent the lower crustal part of the younger Precambrian terrane. The early histories are similar, however San Gabriel basement rocks were buried at a deeper level than present exposures of the 1.65 b.y. suite. They experienced a granulite facies overprint. During widespread plutonism 1.4 b.y. ago, the country rocks at the deeper level were deformed, whereas rocks at a shallower level were passively intruded. Finally, the fact that anorthosite-syenite magmatism 1.2 b.y. ago is only recorded in the deeper level San Gabriel rocks is to be expected, as such intrusives rarely rise above lower crustal levels (Hyndman, 1972). I suggest the San Gabriel terrane was offset right-laterally from original continuity with the younger Precambrian terrane of Silver and others (1977a). Its present anomalously high level of exposure may be due to its upper plate position with respect to a major regional thrust in the Chuckawalla-Eagle Mountains area

(Powell and Silver, 1979). I suggest that the overlying supracrustal rocks of the San Gabriel terrane were stripped off then and during regional Cretaceous uplift (see below). No Upper Precambrian-Paleozoic cover strata are known overlying the San Gabriel terrane. Possible exceptions may be some of the highly deformed metamorphic rocks in the northeastern Peninsular Ranges, especially a sequence of marbles and other metamorphic rocks at Travertine Rock, on the west side of the Salton Sea.

Unresolved here is the paleogeographic position of the Caborca sequence. If this block is in place, and has not moved laterally relative to the craton or miogeoclinal strata in the Mojave Desert-Death Valley region, the present distribution of thick sequences of miogeoclinal strata may be a primary feature of the margin. The bend of the miogeocline around the Salmon River Arch and the Mojave Desert may be related to marginal offsets (Dickinson, 1981), irregularities in the shape of the margin due to transform-rift-transform segmentation. In this model the Mojave high would be bounded on the southwest by a relict transform fault zone, along which the San Gabriel terrane may have been displaced. If however, the Caborca rocks are out-of-place along a left-lateral fault, as basement ages indicate, then the evidence for a marginal offset disappears. In this case, the redistribution of major blocks during Permo-Triassic strike-slip faulting precludes a reconstruction of Precambrian rift geometry in the southern Cordillera. These two alternative hypotheses cannot be resolved at present.

The recognizition of significant facies variations between Upper Precambrian sections in the Mojave region opens the possibility that other enigmatic quartzite and marble sequences in this region may include Upper Precambrian strata of the Cordilleran miogeocline. A likely candidate is a thick undated sequence of quartzite, conglomerate, and phyllite which overlies an undeformed porphyritic granite in the Pinto Mountains (Figs. 20 and 29). These rocks, studied by Powell and Silver (1979), are equivalent to high grade metamorphic rocks which structurally underlie rocks of the San Gabriel terrane in the Eagle

and Chuckawalla Mountains. Powell and Silver suggest this section does not correlate with the Big Bear Group but I disagree. I have visited the Pinto Mountains sequence with Powell and was impressed by similarity between its lower part and the Wildhorse Quartzite. The lithologies and sedimentary structures are similar. Considering the contrasts between the Big Bear Group and previously described sections to the east, the similarity of the Pinto Mountains sequence is even more striking. I believe any differences between the Pinto Mountains sequence and the rocks at Big Bear can be attributed to local lateral facies variations. I see no reason to believe this sequence is exotic, and suggest these rocks are Upper Precambrian strata of the Cordilleran miogeocline.

The undated metasedimentary rocks of the Salinian block (Fig. 1) have long puzzled California geologists. These rocks are strongly deformed and metamorphosed at upper amphibolite facies (Compton, 1966). Cretaceous batholithic rocks which intrude metasedimentary rocks in the Salinian block have yielded high initial Sr^{87}/Sr^{86} ratios, suggesting the terrane is underlain by Precambrian crust (Kistler and others, 1973). The metasedimentary sequence includes quartzite (often feldspathic), quartzo-feldspathic paragneiss, schist and phyllite (often graphitic) and marble. Definite metavolcanic rocks are rare (Ross, 1977). Compton (1966) and Weibe (1970) suggested that Salinian metasedimentary rocks were the offset continuation of miogeoclinal rocks in the western Mojave Desert (which were at that time poorly known).

Ross (1977) has more recently pointed out difficulties in correlating rocks in the Salinian block with known Upper Precambrian-Paleozoic miogeoclinal sequences in the southern Great Basin. In particular, nothing correlative with the thick Paleozoic carbonate succession is present in the Salinian block. Some geologists have recently suggested the Salinian block is an exotic microplate (Blake and others, 1979).

I suspect much of this confusion results from trying to correlate the wrong sequences. Figure 29 is a mid-Tertiary palinspastic reconstruction of California. Prior to Late Cenozoic transform tectonism,

the Salinian block lay opposite the western Mojave Desert-eastern Transverse Range area. Comparing Salinian block rocks with Death Valley stratigraphy is erroneous. I have visited localities studied by Compton and Weibe in the Santa Lucia Mountains and am impressed that these rocks could correlate with Upper Precambrian sequences in the Big Bear or Pinto Mountain areas. This evaluation is based on types and proportions of lithologies present, not on a stratigraphic sequence because none exists in these complexly deformed rocks in the Santa Lucia Mountains. However, the recognition of pronounced Upper Precambrian facies variations in the Mojave requires that the paleogeographic setting of the Salinian block be reevaluated. All reasonable correlations should be tested before this terrane is assigned an exotic origin.

Upper Paleozoic Rocks on the North Slope

Study of Upper Paleozoic marbles exposed on the north flank of the San Bernardino Mountains was not a major focus of this investigation but they are described briefly here since these rocks provide important constraints concerning the Late Paleozoic paleogeographic setting of the Victorville-San Bernardino Mountains region. Stratigraphic correlations suggested here are provisional, as they are based on limited detailed mapping in the Cushenbury Canyon-Furnace Canyon area, and reconnaissance mapping north of Holcomb Valley, undertaken at the initial stages of my field work in the Big Bear area.

Marbles of known and suspected Late Paleozoic age are widespread on the north flank of the San Bernardino Mountains (Plate I). Based on rock stratigraphic sequence and limited paleontologic data these marbles are believed to be correlative with Devonian-Permian(?) formations of marginal miogeoclinal or cratonic facies which are recognized in southern Nevada and the eastern Mojave Desert. At least locally, the Upper Paleozoic marbles structurally underlie the Precambrian-Cambrian rocks discussed above where they are juxtaposed along a major thrust (this fault contact is largely intruded by Cretaceous granite however). The Upper Paleozoic marbles are inferred to have conformably overlain the Upper Precambrian-Cambrian miogeoclinal sequence exposed in the Big Bear area, but such a relationship has not (to my knowledge) yet been recognized in the San Bernardino Mountains. An intact Cambrian to Devonian stratigraphic section may be present on the north slope or in other areas near Big Bear which I have not examined.

In the Cushenbury Canyon-Marble Canyon area (Plate I), the Upper Paleozoic section is largely overturned, lying in the south or southwest dipping, overturned limb of a recumbent antiform (Furnace Canyon Anticline of Hollenbaugh, 1968). Original bedding is transposed. Units are internally isoclinally folded (mesoscopic F_1 axial surfaces are parallel to original bedding) and this transposed bedding was refolded by macroscopic and mesoscopic tight to isoclinal F_2 folds during formation of the antiform. Nevertheless, the general stratigraphic sequence is preserved.

The base of the section is intruded at Burnt Flats (NW1/4 Section 23, T3N, R1E, Big Bear City, 7.5' quadrangle). The lowest unit exposed here consists of marbles which are tentatively correlated with the Middle-Upper Devonian Sultan Limestone (Fig. 23; original reference: Hewett, 1931). Cherty (calc-silicate) marbles, perhaps correlative with the middle Valentine Member of the Sultan Limestone, are overlain by very pure calcite marble which may correlate with the upper Crystal Pass Member of the Sultan Limestone. Rocks similar to the lower Ironside Member of Sultan Limestone, which usually contains distinctive silicified stromatoporoids, are not present.

Overlying the Sultan(?) marbles are calcite marbles containing abundant chert (calc-silicate) nodules. These cherty marbles bear close resemblance to the nodular chert-bearing limestones of the Anchor Member of the Monte Cristo Limestone of Early to Middle(?) Mississippian age (Fig. 23; original reference Hewett, 1931). These cherty marbles are believed to correlate with the lower Dawn and Anchor members of the Monte Cristo, and along with the underlying Crystal Pass Member-equivalent marbles are the key units for correlations proposed here. Coarsely crystalline, massive calcite marble overlies the Dawn-Anchor equivalent marbles, and is here tentatively correlated with the upper Bullion and Yellowpine Members of the Monte Cristo Limestone.

The Monte Cristo(?) marbles are overlain by a very thick sequence of calcite marble (sometimes cherty) and subordinate interlayered calc-silicate rock, phyllite and quartzite which is here correlated with the Bird Spring Formation (original reference: Hewett, 1931) of Mississippian-Permian age. The basal Bird Spring Formation in the Cushenbury Canyon-Marble Canyon consists of calcite marble with interlayered lenses of fine-grained quartzite. Conspicuously absent at this stratigraphic level are conglomerates or any significant thickness of metaclastic rocks. Terrigenous rocks are present at the base of the Bird Spring Formation in typical miogeoclinal facies sections in the southern Nevada region (the Indian Spring Member). Poorly preserved fossils are present in marbles

included in the lower Bird Spring in the Cushenbury Canyon-Marble Canyon area. These include crinoid fragments, corals and brachiopods, the latter of which are of Carboniferous (possibly Mississippian) age (Hollenbaugh, 1968). Recrystallized fusilinid(?) tests are present at higher stratigraphic levels. Marbles exposed east of Cushenbury Canyon are presumed to stratigraphically overlie the rocks described here, and may include rocks of Permian age. The uppermost Fairview Valley Formation (Early Triassic in age?) exposed near Victorville contains clasts of limestones containing Wolfcampian faunal assemblages typical of the Bird Spring Formation (reported by E. Miller, 1978; personal communication, 1980). The existence of these locally derived clasts indicates that Permian limestones were present somewhere in the Victorville-Big Bear region.

Southwest of Marble Canyon, overturned Bird Spring(?) marbles structurally underlie the Cushenbury Thrust (Plate I). Upper plate rocks include complexly imbricated marbles, calc-silicate rocks and phyllites here assigned to the Carrara and Bonanza King Formations of Cambrian age. This thrust zone is intruded by Cretaceous granitic rocks, but may have originally continued eastward. Above and southwest of Cushenbury Canyon, Precambrian-Cambrian rocks mapped by Tyler (1975) sit topographically above Upper Paleozoic marbles, and these sequences are separated by intrusive rocks (locally sheared). Where they come in closest proximity (NE1/4 of Section 23, T3N, R1E) the Precambrian-Cambrian rocks (including the basement gneisses) are complexly interleaved in what may be a schuppen zone above an intruded thrust fault. Cretaceous granitic rocks may have intruded along a thrust which emplaced Precambrian-Cambrian rocks over Upper Paleozoic marbles. This thrust may have been the continuation of the Cushenbury Thrust. Southeast of Cushenbury Canyon, suspected Upper Paleozoic marbles are present northeast of the Helendale Fault (Plate I). These marbles may also belong in the lower plate of the Cushenbury Thrust. Cambrian rocks exposed southwest and northeast of the Helendale Fault near Rose Mine may lie in the upper plate of this thrust, whose trace is concealed or intruded.

West of Furnace Canyon and north of Holcomb Valley, calcite marbles have yielded fossils including crinoid fragments, and corals and brachiopods of Carboniferous (possibly Mississippian) age (Richmond, 1960). The fossiliferous section at John Peak (Plate I) is correlated with the Bird Spring Formation, and resembles Bird Spring rocks in the Cushenbury Canyon-Marble Canyon area. The John Peak section is upright, however, and is not as strongly deformed as the section of Upper Paleozoic marbles exposed further east. Primary sedimentary structures including laminations and rare cross beds are locally preserved. These rocks may lie in the upright limb of a major W-NW trending antiform whose overturned limb is exposed in the Cushenbury Canyon-Marble Canyon area. If so, Devonian and older rocks might be exposed in the core of this fold, in the canyons north of John Peak. Low-angle faults carry marbles tentatively assigned to the Cambrian Bonanza King Formation over the Upper Paleozoic section at localities south and west of John Peak; these may represent segments of the Cushenbury Thrust. The westward continuation of these thrust(?) is not certain.

Although Upper Paleozoic rocks are apparently widespread in the north central San Bernardino Mountains, their original relationship to structurally overlying Upper Precambrian-Cambrian miogeoclinal rocks remains unresolved. Evidence from the Victorville area suggests that the Upper Precambrian-Cambrian sequence and the Upper Paleozoic sequence may have originally been in stratigraphic continuity, and that the thrust (or thrusts) juxtaposing these sections need not be of large displacement. In the Sidewinder Mountain area (Fig. 2), E. Miller (1977) recognized that stromatoporoid-bearing marbles, correlative with the Ironside Member of the Devonian Sultan Limestone, disconformably overlie marbles correlative with the Upper Cambrian Nopah Formation. The Devono-Cambrian disconformity is typical of cratonic facies stratigraphic sections in the southern Nevada-eastern Mojave Desert region (Gans, 1974). In the transition zone between typical miogeoclinal sections and typical cratonic sections, Lower Devonian, Silurian and finally Ordovician strata are

progressively cut out beneath the Middle Devonian Sultan Limestone and its equivalents. E. Miller (1977) concluded that the Victorville area lay in a cratonic paleogeographic setting during the Early Paleozoic, and in a marginal miogeoclinal setting during the Cambrian. This resulted from a crosscutting of paleogeographic trends, perhaps related to recurrent regional epeirogenic tectonism in the Mojave region (as discussed above). A similar relationship may hold in the San Bernardino Mountains. The apparent absence of post-Cambrian, pre-Devonian rocks in the range may be real; this part of the section may be missing beneath the Middle Devonian disconformity. Stewart and Poole (1975) pointed out that the apparent absence of distinctive Lower Paleozoic miogeoclinal units like the Ordovician Eureka Quartzite from previously described Paleozoic sections in the Big Bear area probably indicates a transitional miogeoclinal-cratonal facies setting for the Big Bear area during the Early Paleozoic. Present data are consistent with such an interpretation.

The predominance of carbonate rocks in the Carboniferous and Permian(?) section on the north slope is suggestive of a marginal miogeoclinal-cratonal depositional setting during the Late Paleozoic as well. The paucity of clastic rocks at the base of the Bird Spring(?) Formation is particularly significant in this respect. In typical miogeoclinal sections, terrigenous influx from the northwestward thickening Antler clastic wedge occurs at this interval (Burchfiel and Davis, 1981). The Indian Spring Member of the Bird Spring Formation has been interpreted as a distal facies of the Antler clastic wedge (Poole and Sandburg, 1977). By analogy with the miogeoclinal terrane of the southern Great Basin, the absence of Antler clastic wedge deposits within the Upper Paleozoic section near Big Bear is suggestive this terrane lay in a marginal miogeoclinal-cratonal setting in the Late Paleozoic, and far from the uplifted Antler orogenic belt.

Although no record of proximity to the Antler highlands is present in the Upper Paleozoic section near Big Bear, rocks correlative with proximal Antler clastic wedge or overlap deposits of inferred Late

Paleozoic age are now present nearby in the Shadow Mountains (Fig. 20; see Poole, 1974), and are part of the enigmatic western Mojave terrane (E. Miller and others, 1979). Similar rocks are present in the El Paso Mountains (Poole and Sandburg, 1977), where they overlie or are structurally interleaved with complexly imbricated Early Paleozoic deep water facies rocks correlative with allochthonous units of the Antler orogenic belt (Poole and Christiansen, 1980). No transitional facies is presently known between Late Paleozoic rocks of the western Mojave terrane and those of the miogeoclinal-cratonal terranes to the southeast.

The apparent eastern boundary of the western Mojave terrane cuts at high angle across Late Paleozoic facies trends of the miogeoclinal terrane in the Death Valley-Mojave region, including isopach trends for the Antler clastic wedge (Figs. 25 and 27). This apparent truncation of facies trends, and the absence of clastic wedge deposits in miogeoclinal sections in the central Mojave and Big Bear-Victorville area led Davis and others (1978) and Burchfiel and Davis (1981) to suggest that the rocks of the western Mojave terrane are out of place, and were displaced southward along a major left-lateral strike-slip fault from an original position in continuity with the Antler orogenic belt (Fig. 27). They hypothesized this faulting was related to complex Permo-Triassic transform tectonism leading to tectonic truncation of the old continental margin. They visualize the western Mojave terrane as a fault-bounded crustal sliver, left stranded along the transform zone while outboard blocks continued to move southward (Permo-Triassic tectonics is discussed further in Chapter VI). Later Mesozoic and Cenozoic deformational events have greatly modified the original eastern boundary of the western Mojave terrane. Its present tortuous trace through the Mojave probably reflects the combined effects of Mesozoic plutonism and faulting, and latest Cretaceous-early Tertiary oroclinal bending (Burchfiel and Davis, 1981).

Quaternary Surficial Deposits

A variety of surficial deposits of Quaternary age are present in

the map areas. Quaternary alluvium (Qa -- including lake deposits) is widespread within active drainage systems. Talus deposits (Qt) are present on steep slopes on either flank of the Sugarloaf Ridge area. The talus consists almost entirely of blocks of Wildhorse and Sugarloaf Quartzite which cap much of the ridge crest. Landslide deposits (Qls), consisting of lithologically diverse clasts, are also present. Larger, coherent blocks within a landslide or gravity slide mass are often mapped separately.

Older fanglomerate deposits of Quaternary age (Qof) are widespread in the map areas. The poorly sorted fanglomerate deposits often contain clasts which are not of local derivation, or whose source area cannot be explained by existing topographic or structural relief, or by present drainage systems. Deposition of these older fanglomerates predates later Quaternary uplift of the Big Bear area (discussed in Chapter IV). Older fanglomerate deposits perched on ridges north and south of Wildhorse Meadow have been isolated from their source areas by rapid Quaternary uplift. The same is true of older fanglomerate exposed north of Sugarloaf Mountain in the vicinity of Hill 8220'. These deposits constitute the Sugarloaf fan, which dips gently northward off the north flank of the mountain. Erosion has beheaded this fan from its source area, which may have been at an elevation well above the present ridge crest above Hill 8220'.

CHAPTER III: IGNEOUS ROCKS

General Statement

Igneous rocks are widely exposed in the study areas and intrude the Precambrian-Cambrian succession. These rocks are part of an extensive batholithic complex that constitutes the majority of the bedrock outcrops in the San Bernardino Mountains. This complex is part of the Mesozoic batholithic terrane which encompasses much of the Mojave Desert and extends northward into the Sierra Nevada-western Death Valley regions. Earlier workers thought the Mesozoic igneous rocks in the Big Bear area constituted a magmatic suite of Late Jurassic to Early Cretaceous age (Richmond, 1960; Dibblee, 1964a,b). Reconnaissance K/Ar dating by Armstrong and Suppe (1973) indicated the voluminous quartz monzonite and granite batholith which underlies the bulk of the range (and much of the western Mojave Desert) is probably of Late Cretaceous age.

Older igneous rocks of variable composition are locally present, and are spatially associated with the pre-Mesozoic country rocks. These intrusive rocks may represent remnants of an earlier batholith complex, preserved along with pre-Mesozoic rocks as roof pendants over the Cretaceous batholith. The results of K/Ar and $^{40}Ar/^{39}Ar$ geochronometric studies of some of these older plutons are discussed in Chapter V.

In this study, examination of the Mesozoic intrusive rocks focused on their relationship to the overall structural evolution of the Big Bear area. Lithologic characteristics and contact relationships are discussed in this chapter; consideration of the chronology and mechanisms of emplacement and relationships to country rock deformation are reserved for Chapter IV. Detailed petrogenetic and geochemical studies are beyond the scope of this project. Map units are defined on the basis of field and petrographic observations. Modes were estimated visually from thin sections and classification is according to Streckeisen and others (1973) and Streckeisen (1979). As far as is possible, units are discussed in order of relative age, the oldest units first.

Sugarloaf Area

Introduction

Igneous rocks in the Sugarloaf area are divided into four petrologic-geographic groups: the Sugarloaf Intrusive Complex (predominantly quartz diorite), the Wildhorse Road Sequence including porphyritic dikes and sills of dacitic composition and associated granitoid dikes, muscovite-bearing granitic intrusives near Route 38 on the east side of the area, and garnet-muscovite granite below the Doble Thrust. Rocks in the latter two groups are probably part of the Cretaceous batholith and are not in direct contact with rocks of the other two groups. The relative ages of the Sugarloaf Intrusive Complex and the dacite porphyries are ambiguous. Emplacement of these intrusives postdates a synmetamorphic polyphase folding event. Their relationship to subsequent normal faulting and their contact metamorphic effects are described in Chapter IV. Geochronologic data is discussed in Chapter V.

Sugarloaf Intrusive Complex

Introduction. The Sugarloaf Intrusive Complex is exposed in the southwestern part of the map area, north of Sugarloaf Mountain. It includes the compositionally variable Sugarloaf Quartz Diorite, a breccia unit in part coeval with the Diorite, and several younger bodies of quartz monzodiorite-quartz monzonite. All of these rocks were included in Dibblee's (1964a) quartz diorite unit. His map shows the unit exposed for another 3 to 4 km west of Sugarloaf Mountain.

Sugarloaf Quartz Diorite. The Sugarloaf Quartz Diorite (units Sqd and Sqmd) comprises the bulk of the complex. This unit may be a composite pluton. It underlies much of the area north of Sugarloaf Mountain and Peak 9433'. Other exposures are present east of Hill 8055', on Green Spot Hill and the west end of Deadman's Ridge. The Sugarloaf Quartz Diorite intrudes the pre-Mesozoic succession. Emplacement is structurally controlled, since these rocks intrude along low- and

moderate-angle normal faults, which themselves cut earlier folds and faults. The Sugarloaf Quartz Diorite is in part coeval with the breccia unit (Sb), which was also injected along faults. Small bodies of leucocratic quartz monzodiorite and quartz monzonite (Sqm) intrude hornblende quartz diorite of Sqd north of Sugarloaf Mountain. The age relations of these younger bodies to the Cretaceous granite and quartz monzonite batholith are not known.

The Sugarloaf Quartz Diorite actually includes a range of rock types, although quartz diorite predominates. Principal lithologies include: hornblende biotite diorite, hornblende biotite quartz diorite, biotite quartz diorite, and biotite quartz monzodiorite. Less common rock types include hornblende diorite, biotite diorite and hornblende monzodiorite. Quartz content averages about 10%, but ranges from <5-20%. Mafic minerals range from 10-30%. Hornblende ranges from 0->15%. Biotite is almost always present, and typically averages 10-15%. Although euhedral hornblende is present, many grains are ragged and are often intergrown with fine-grained biotite. Biotite is frequently chloritized. Plagioclase shows normal and reverse zoning. Sericitization is ubiquitous and saussuritization is typical. When present, K-feldspar is interstitial between plagioclase and mafic phases, and often intergrown with micrographic quartz. Abundant accessories (3-6%) include magnetite, sphene (often rimming magnetite), and apatite.

These rocks are typically medium-grained. Hypidiomorphic granular textures predominate. Intrusive contacts with the country rocks are sharp, and there is little reduction in grain size near the contacts. The development of a conspicuous chill zone is not typical. Narrow skarn zones are recognized at many marble contacts (typically 1 m or less wide). Xenoliths of metasedimentary rocks are frequently present, including quartzite, marble and pelitic lithologies. Elongate xenoliths (particularly phyllite) are often aligned subparallel to a crude primary igneous foliation defined by plagioclase laths. This flow fabric was recognized only in float blocks, typically where narrow bodies of diorite are intruded along fault zones.

Evidence of post-crystallization deformation is common. In thin

section, quartz is often undulatory and quartz and feldspar grain boundaries are sutured. Epidote-filled fractures and small-displacement shear zones are common north of Sugarloaf Mountain. This deformation is probably related to emplacement of younger plutons. Two mapped faults of small displacement cut unit Sqd.

Despite its lithologic variability, most of the Sugarloaf Quartz Diorite is shown as a single unit (Sqd) on the geologic map. Only the larger bodies of the more leucocratic biotite quartz monzodiorite facies are shown separately (Sqmd). In general, hornblende biotite quartz diorite predominates north of Sugarloaf Mountain, and west of Hill 8055'. Biotite quartz diorite predominates adjacent to lower Green Canyon.

More detailed subdivision is hindered by the discontinuous nature of outcrop within this unit. In the field, changes in lithology (such as the disappearance of hornblende, appearance of K-feldspar, and increase in quartz content) often can be recognized as occurring over distances of a few meters. In many cases these changes appear to be gradational and may be due in part to igneous differentiation. The replacement of hornblende by biotite often appears to be a magmatic phenomenon. Variable assimilation of country rock material may also be a factor in compositional variability. It seems most likely, however, that much of the unit's variability is the result of multiple episodes of intrusion that formed a composite quartz diorite pluton. Some exposures of hornblende biotite quartz diorite record multiple episodes of intrusion. For example, north of Sugarloaf Mountain several small hornblende diorite dikes (too small to be shown on the map) intrude the marbles, and are themselves crosscut and contact metamorphosed by the emplacement of the main body of hornblende biotite quartz diorite (hornblende and plagioclase are partially replaced by actinolite and epidote). Northeast of Hill 8055', porphyritic dikes of hornblende biotite quartz diorite intrude a diorite of a more typical medium-grained facies. It seems likely that a similarly complex history may be present elsewhere in the Sugarloaf Quartz Diorite.

The Cienga Seca Quartz Diorite is exposed just south of the

Sugarloaf map area. It has yielded Late Cretaceous K/Ar ages on hornblende and biotite (77.7 ± 1.0 m.y. and 68.5 ± 1.0 m.y. respectively; Armstrong and Suppe, 1973). It is intruded by granitic rocks similar to those seen along Route 38 in the study area. Dibblee (1964a) grouped the Sugarloaf and Cienga Seca diorites as a single unit. However, based on thin section and reconnaissance field study, the Cienga Seca pluton shows little evidence of the post-crystallization alteration and deformation which is typical of the Sugarloaf Diorite. Geochronologic data suggest these plutons are of different ages.

Breccia Unit. The breccia unit (Sb) is at least partly of igneous origin and is coeval with portions of the Sugarloaf Quartz Diorite. It is exposed in the NE1/4 of Section 6 (T1N, R2E), northeast of Sugarloaf Mountain. Other good exposures, too small to be shown on the map, occur along the NE trending fault cutting marbles of the Green Canyon Formation. Float of Sb is found among outcrops of Sqd immediately north of Sugarloaf Mountain, where Sqd intrudes numerous faults. It is also recognized in float in the area underlain by Sqmd north and west of Peak 9433', where Sqmd intrudes the Green Canyon Fault. Similar rocks are present as xenoliths in the quartz monzodiorite-quartz monzonite body (Sqm) in the SW1/4 of Section 31 (T1N, R2E).

Rocks of the breccia unit are typically found along exposed or inferred fault zones that displace pre-Mesozoic rocks. Foliation is common and is defined by matrix minerals and preferred orientation of elongate clasts. This foliation is in part tectonic and in part magmatic in origin, as discussed below. Where it can be measured, foliation parallels the known or inferred strike and dip of the fault zones.

The breccia unit is lithologically heterogeneous and texturally complex. Typical exposures contain a variety of clasts which are very poorly size sorted (average range: 2 mm to many cm). Rock fragments present as clasts include: metasedimentary rocks (quartzite, phyllite and calc-silicate rocks) which typically occur as elongate slivers;

medium-grained biotite quartz diorite and its finer-grained equivalents; and autoliths of the breccia. The most abundant clasts are finer-grained single crystals and small aggregates of plagioclase, quartz and biotite (Fig. 30). The fine- to very fine-grained matrix includes these three components, and white mica, in variable proportions. Mica content ranges from 10-20% up to 50%.

Textures recognized in rocks of the breccia unit indicate origin by both magmatic and tectonic-metamorphic processes; these two textural types often grade into one another within a single thin section. Where matrix textures appear to be primarily magmatic, the rock is a quartz diorite in composition. Evidence of high intracrystalline strain is lacking. Relict igneous textures, including oscillatory zoning in plagioclase, are preserved. The foliation appears to be an igneous flow fabric, aligning biotite and plagioclase "phenocrysts", as well as larger clasts. Possible vesicles are sometimes present. These dioritic rocks grade into breccias with a more micaceous matrix and which are better foliated. In the case of the latter rocks the high percentage of biotite, white mica and quartz (70% total) in the matrix might suggest locally significant assimilation of metasedimentary wall rock material by the breccia unit; however, much of the white mica present is metamorphic, forming from sericitization of plagioclase. Often, sericitization occurred synchronously with shearing. This can be recognized in thin section where quartz-biotite-white mica-rich layers enclose augen-like clasts of dioritic composition (Fig. 31). These highly strained biotite-plagioclase-quartz aggregates grade into the phyllitic matrix, as quartz decreases in grain size and plagioclase is progressively sericitized. Here, the breccia unit's foliation is locally tectonic, having developed by synmetamorphic shearing of dioritic rocks.

Some of the sheared diorite clasts present represent more tectonized equivalents of larger biotite quartz diorite xenoliths recognized within the breccia unit. Elsewhere, however, similar biotite quartz diorite, itself containing a variety of xenoliths, grades into rocks of the breccia unit. In these cases the flow foliation in the diorite (defined by biotite and plagioclase) parallels that in the

Figure 30: Photomicrograph of the breccia unit of the Sugarloaf Intrusive Complex. Quartz and plagioclase crystals and aggregates are surrounded by matrix of fine-grained quartz, plagioclase, biotite and white mica. Note zoned (partially sericitized) plagioclase in left center. Quartz grains are undulatory and often highly fractured. Length of photo equals 5 mm. Crossed polars. Sample is from NE1/4 of Section 6 (T1N, R2E).

Figure 30.

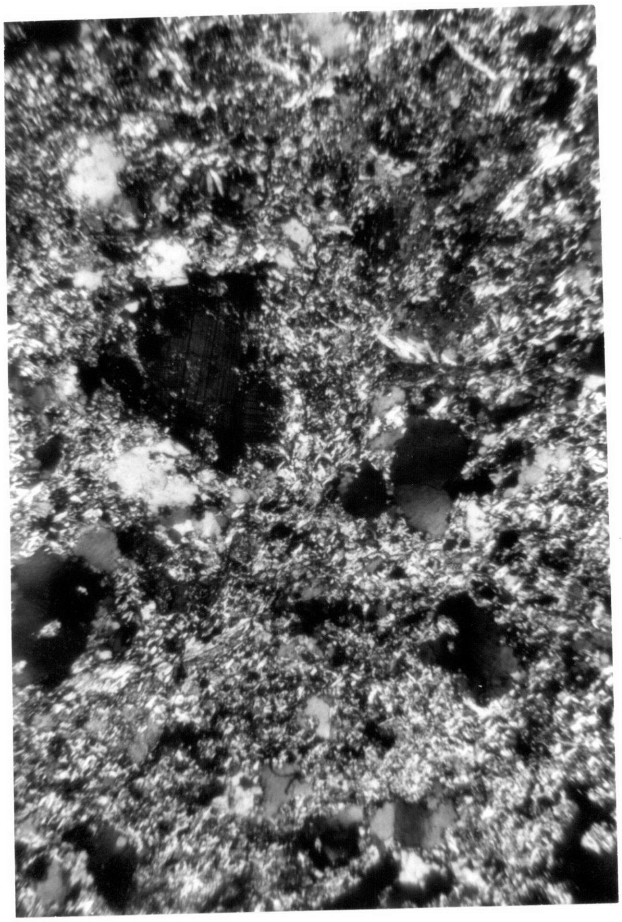

Figure 31: Photomicrograph of the breccia unit of the Sugarloaf Intrusive Complex. Plagioclase within dioritic aggregate (center) is partially replaced by white mica; quartz ± biotite remains. Foliation in matrix outside field of view is parallel to length of photo. Length of photo equals 2 mm.

a) plane polarized light
b) crossed polars
Sample is from NE1/4 of Section 6 (T1N, R2E).

Figure 31a.

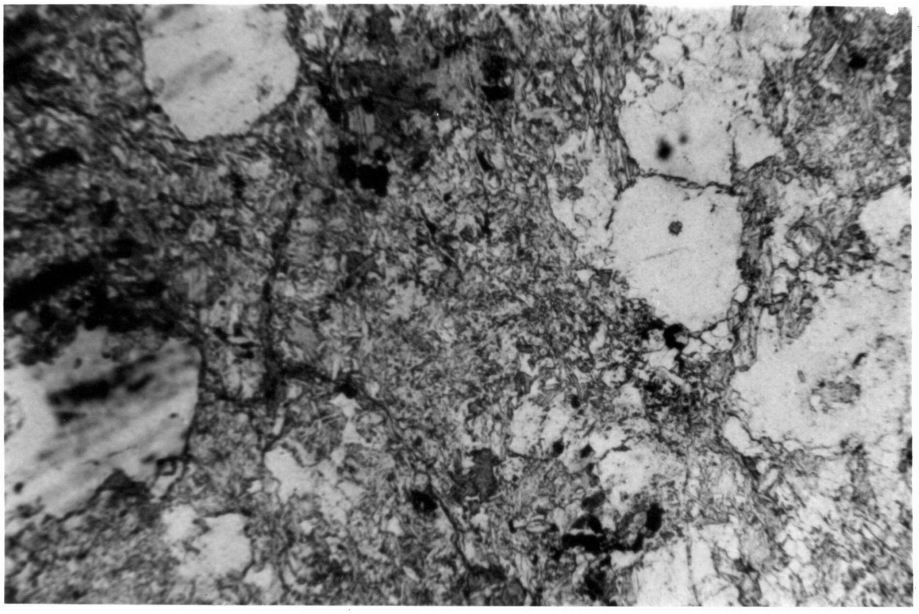

Figure 31b.

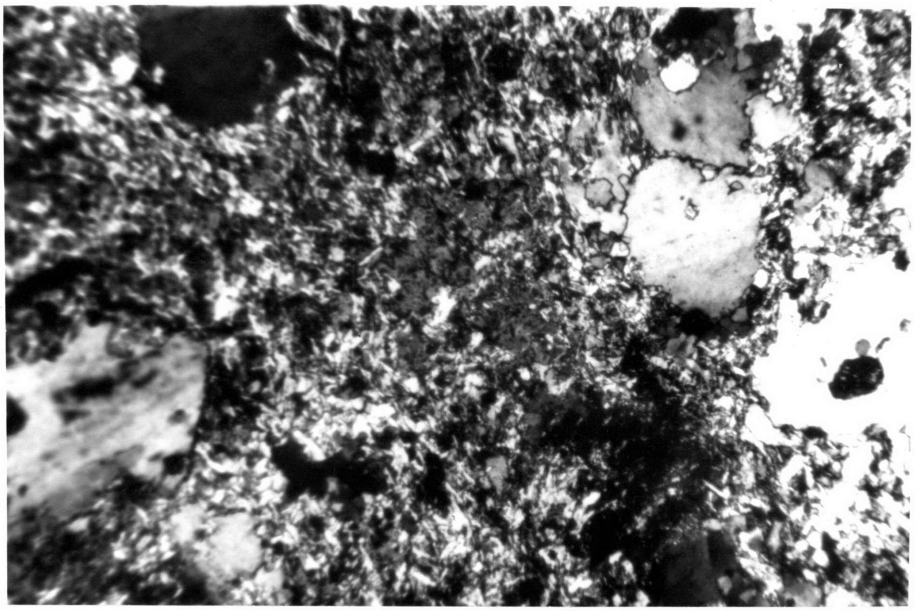

breccia unit. Previously mentioned float blocks of the breccia unit found within intruded fault zones were probably xenoliths within the local diorite and monzodiorite bodies. It appears that the rocks included in the breccia unit formed while the Sugarloaf Quartz Diorite was being emplaced.

It is suggested that the breccias, containing both igneous and sedimentary clasts and matrix material in part of igneous origin, are intrusive injection breccias. They formed as dioritic magma was repeatedly and forcibly injected along fault zones. The dikes picked up country rock xenoliths and assimilated some of the finer-grained material. These intrusions also carried xenoliths of earlier intrusives of the complex and autoliths. Many of the euhedral plagioclase crystals may represent phenocrysts carried by the dioritic magmas and subsequently mixed with exotic fragments. The presence of possible vesicles and the fine-grained character of the magmatic matrix indicates a shallow level of emplacement.

The origin of the locally preserved tectonite fabrics is uncertain. Deformation occurred synmetamorphically. These sheared dioritic rocks may represent earlier dikes, deformed during recurring fault movements between periods of magmatic injection. Alternatively, these may be xenoliths carried with the magma and deformed protoclastically.

It is of note that no xenoliths of hornblende-bearing plutonic rocks were recognized, nor was hornblende observed in the magmatic matrix. The absence of hornblende phenocrysts or hornblende-bearing xenoliths further supports a composite origin for the Sugarloaf Quartz Diorite. This suggests either: 1) the magma chambers and conduits for biotite-rich and hornblende-rich dioritic magmas were independent; or 2) that hornblende biotite quartz diorite exposed north of Sugarloaf Mountain is younger than the breccia unit and coeval biotite quartz diorite (this is considered more likely here).

Not all the rocks included in the breccia unit contain abundant igneous clasts or have igneous matrix material. Recrystallized fault gouge and cataclastic breccia is sometimes prevalent. In the NE1/4 of Section 6 (T1N, R2E) exposures of the breccia unit are in contact with

Lightning Gulch Formation and Sugarloaf Quartzite. Large slivers (several meters in size) of these units are recognized within the breccia unit (one is shown on the geologic map). Some of the breccia unit matrix consists of quartz muscovite phyllite, with much less plagioclase and biotite than usual. These rocks contain variably sized clasts of quartzite and phyllite but clasts of igneous derivation are not evident. They are believed to represent recrystallized fault gouge and breccia formed during low-angle faulting of the Lightning Gulch Formation and Sugarloaf Quartzite. Rocks of this lithology appear to grade into more typical igneous breccias. It is suggested the cataclastic breccias formed first, during low-angle faulting. Similar rocks are found along a low-angle fault contact along Wildhorse Road (discussed in Chapter IV). Subsequently, the igneous breccias were injected along the fault zone. Faulting, recrystallization and intrusion may have been broadly contemporaneous.

Quartz Monzodiorite-Quartz Monzonite. Several small bodies of quartz monzodiorite and quartz monzonite exposed north of Sugarloaf are here considered as a single unit (Sqm). They intrude hornblende biotite quartz diorite of unit Sqd and locally contain xenoliths of the breccia unit. These are the youngest rocks in the Sugarloaf Intrusive Complex.

The quartz monzodiorite-monzonites are more leucocratic than any rocks included in the Sugarloaf Quartz Diorite. They typically contain $\leq$5% mafic minerals. Biotite (often chloritized) is the only mafic phase. Quartz ranges from 15-20%. These rocks typically contain twice as much K-feldspar (about one-third of the total feldspar) as the biotite quartz monzodiorite unit (Sqmd). Coarse graphic intergrowths of quartz and K-feldspar are common. Sphene and traces of magnetite are present. Plagioclase sericitization and saussuritization are common.

Rocks belonging to this map unit are medium- to coarse-grained, and display hypidiomorphic granular texture. Unlike the Sugarloaf Quartz Diorite, their emplacement is not obviously controlled by faults.

These intrusions were apparently emplaced as discordant plugs.

The quartz monzodiorites and quartz monzonites are intermediate in composition between other rocks of the Sugarloaf Intrusive Complex and the widespread granite-quartz monzonite batholithic rocks. Whether they represent more differentiated, late stage magmas of the Sugarloaf Complex, or are plugs of the younger batholith is uncertain. However, the presence of postcrystallization hydrothermal alteration, accessory sphene, and the nested position of these rocks within the Sugarloaf Intrusive Complex suggest to me that the former interpretation is more likely.

Wildhorse Road Sequence

Dacite Porphyries. Porphyritic dikes and sills of intermediate composition (dp), along with related(?) coarse-grained dikes (gu) crop out in the center of the study area. Exposures are best along Wildhorse Road, but outcrops also occur on lower slopes above Route 38. These rocks are undoubtedly far more prevalent than the geologic map indicates; however, outcrop control is generally poor in this area underlain primarily by Precambrian gneisses. Contacts between these rocks and granitic rocks to the east were not observed. Exposures of dacite porphyry in the S center of Section 29 (T2N, R2E) are adjacent to slopes apparently underlain by hornblende biotite quartz diorite of unit Sqd. The latter unit does not crop out here, and the contact relations were not determined.

The dacite porphyries occur as thin tabular bodies, which are both discordant and concordant to country rock fabric. These dikes and sills generally dip moderately to the west, northwest, or southwest, and often display foliation parallel to the contact.

Many of the bodies were emplaced along moderate- to low-angle faults which cut the Precambrian gneisses. These faults also generally dip west. Intricate tectonic slivering of basement gneisses is present along Wildhorse Road. The magnitude of displacement is usually unknown. Only more prominent faults are shown on the geologic map.

The dikes and sills are typically porphyritic, with a fine- to very fine-grained groundmass. Compositionally these rocks are primarily dacites,

and are light grey in fresh exposures. The groundmass consists of 25-30% quartz, and 5-10% biotite. Biotite frequently displays a flow foliation. Plagioclase is the only feldspar recognized in fine-grained rocks, and probably predominates in very fine-grained lithologies. The groundmass is not sericitized. Accessory sphene and zircon are present.

The dacite porphyries contain up to 30% phenocrysts and xenoliths, which are typically 2-3 mm in length, and are primarily euhedral plagioclase and quartz prisms. Plagioclase phenocrysts are typically sericitized. Plagioclase-quartz aggregates are present, and may be cognate inclusions. Xenoliths of quartzite and phyllite are also sometimes present. Rare aggregates of microcline and quartz occur, and may be xenoliths of the gneiss complex. Phenocrysts and xenoliths are sometimes aligned parallel to a magmatic flow foliation in the groundmass. This primary foliation is not always present, particularly in rocks further to the east (Fig. 32).

In some cases the foliation in these rocks is tectonic. Dacite porphyry dikes adjacent to the Sugarloaf Quartz Diorite in Section 29 (T2N, R2E) are mineralogically similar to those elsewhere. However, phenocrysts and xenoliths are strongly deformed and flattened parallel to the matrix foliation. Quartz displays evidence of plastic deformation, including thorough polygonization, mortar texture, and ribbon textures. Elongate muscovite-quartz aggregates are present and probably represent deformed metasedimentary xenoliths. The matrix foliation is defined by dimensional preferred orientation of biotite, and to a lesser extent, quartz and plagioclase. This foliation wraps around the deformed phenocrysts and xenoliths (Fig. 33). Deformation postdates crystallization of the porphyry, and may be superposed on an earlier magmatic flow fabric. Along strike in outcrops on Wildhorse Road, dacite porphyry dikes show only a primary flow foliation, and phenocrysts are not deformed. Deformed dikes were also recognized north of Wildhorse Road, along northwest trending faults in the S center of Section 29 (T2N, R2E).

The origin of this local tectonite fabric is uncertain. It may be due to local renewed movement along the faults after dike emplacement, and suggests dike emplacement may have been broadly contemporaneous

Figure 32: Photomicrograph of non-foliated dacite porphyry. Plagioclase (variably sericitized) and prismatic quartz phenocrysts are not strained. Matrix minerals (plagioclase, quartz and biotite) are not aligned. Length of photo equals 5 mm.

a) plane polarized light
b) crossed polars
Sample is from outcrop on Wildhorse Road in the NW1/4 of Section 33 (T2N, R2E).

Figure 32a.

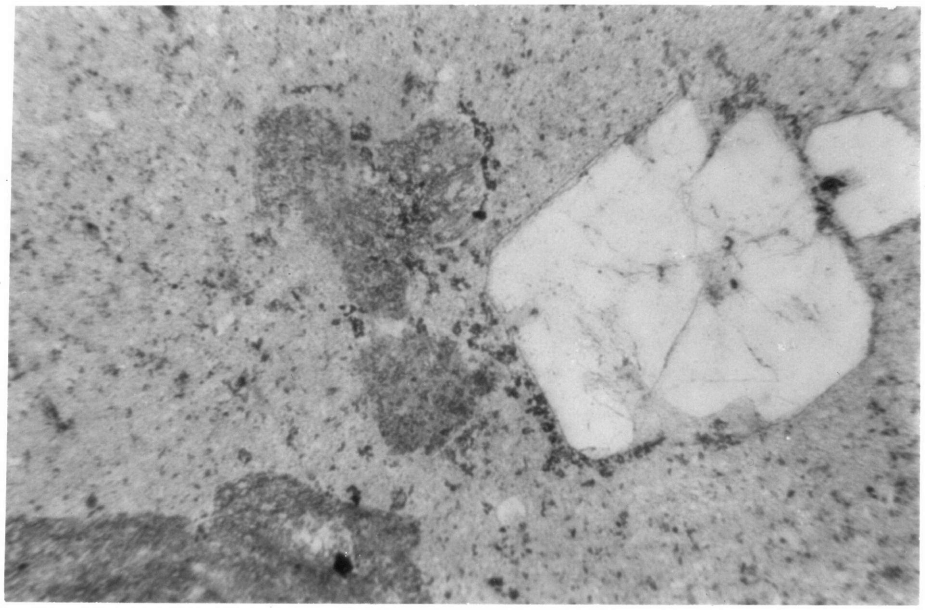

Figure 32b.

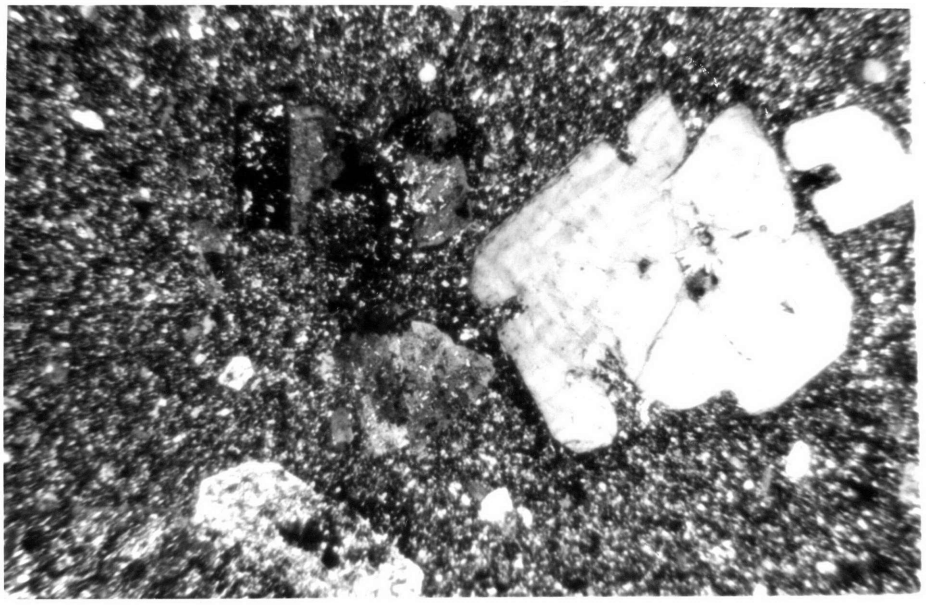

Figure 33: Photomicrograph of tectonized dacite porphyry. Foliation is parallel to width of photo. Matrix micas are aligned; quartz and feldspar are dimensionally elongate. Quartz phenocrysts are dimensionally elongate parallel to foliation, and are undulatory and/or polygonized. Mortar texture is locally present as well. Metasedimentary xenolith (quartz + muscovite) in lower right center is also oriented parallel to foliation. Length of photo equals 5 mm.

a) plane polarized light
b) crossed polars
Sample is from dike along trace of fault four, S center of Section 29 (T2N, R2E), collected at 7460' elevation.

Figure 33a.

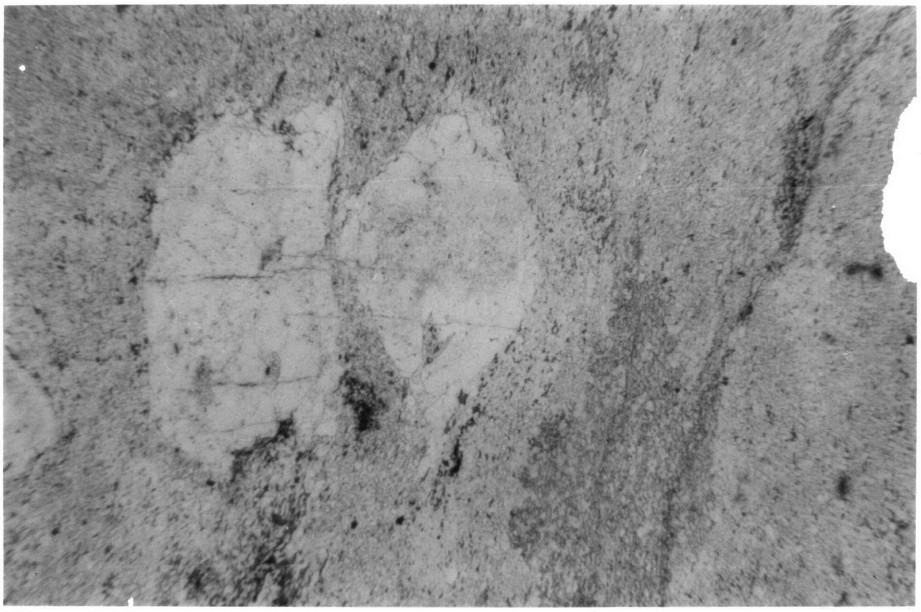

Figure 33b.

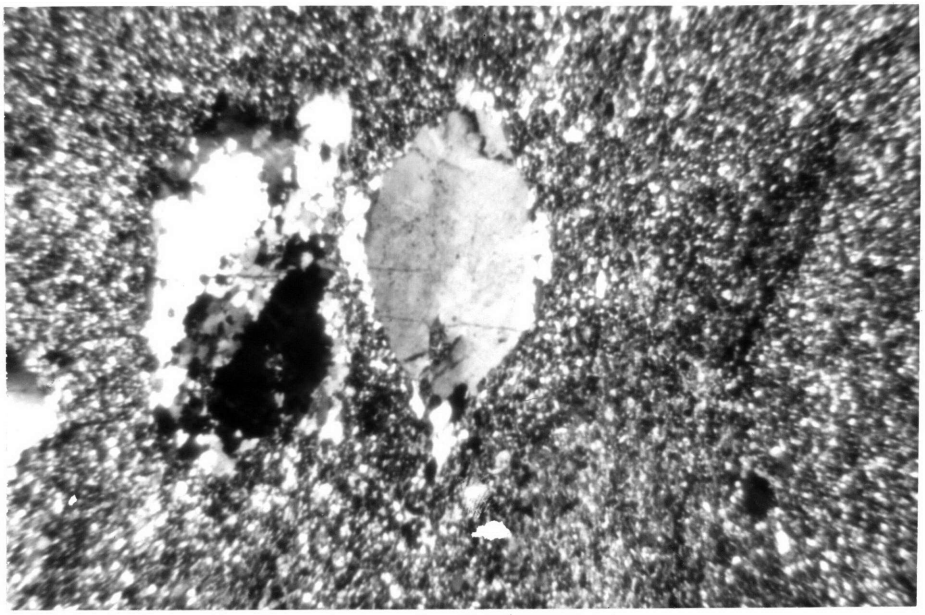

with faulting. Alternatively, the local deformation may be related to emplacement of later plutons, perhaps the Sugarloaf Quartz Diorite. Nearby outcrops of the latter do not record this tectonite fabric. Because of their compositional similarity to nearby non-tectonized dikes which intrude rocks of the Big Bear Group, it seems unlikely that these porphyries are part of the Precambrian basement complex.

Undifferentiated Granitoids. Numerous medium- to coarse-grained dikes intrude the Precambrian gneisses in this area and are grouped together as undifferentiated granitoids (gu). They include biotite quartz diorite, quartz monzodiorite and quartz monzonite(?). They locally intrude the dacite porphyries and may in part be comagmatic. Compositionally, some of these rocks resemble those of the granite-quartz monzonite batholith; however, the latter is in a porphyritic facies where exposed in the study area, so these quartz monzonite(?) dikes are included in unit gu. It is possible that unit gu is related to the Sugarloaf Intrusive Complex.

Locally, the granitoids are also emplaced along faults, some certainly of Mesozoic age, and rarely they display a crude primary igneous foliation. In the N center of Section 33 (T2N, R2E), a granitoid dike intrudes Precambrian gneisses and is itself cut by a northwest trending high-angle fault zone. Textures suggest intrusion may have occurred during an earlier episode of faulting. For example, detached and irregular shaped bodies of relatively undeformed intrusive are found floating in a matrix of highly sheared gneiss. This suggests magma was emplaced, then sliced from its feeder dikes prior to final crystallization.

Undifferentiated Diorite. Badly sheared medium-grained hornblende-biotite plagioclase rock (du) is exposed along Wildhorse Road in the SE1/4 of Section 29 (T2N, R2E). This diorite(?) appears to intrude the basement gneisses and is cut by quartz monzodiorite(?) of unit gu. Its age and affinity is unknown. Lithologically similar fine-grained diorite is

present in float along the trace of the Deer Spring Fault in the W center of Section 33 (T2N, R2E). These rocks are not sheared, and probably were emplaced along the fault. The diorite there is certainly of Mesozoic age, and perhaps is related to the Sugarloaf Quartz Diorite.

Muscovite-bearing Granite and Quartz Monzonite

Porphyritic granitic rocks (g) are exposed in dikes, sills and small discordant bodies near Route 38 in the southeastern portion of the Sugarloaf area. They are the northwestern continuation of Cretaceous "quartz monzonite" batholithic rocks mapped by Dibblee (1967a) in the Onyx Summit area, further southeast along Route 38. According to the classification scheme of Streckeisen and others (1973), rocks in both areas are granites. In the study area they intrude (and locally engulf) the basement gneisses and the Wildhorse Quartzite.

The linear distribution of these exposures is suggestive that they may in subsurface crosscut several major faults in the country rocks. Evidence is discussed in Chapter V which indicates these granites and a larger exposure at Onyx Summit were emplaced along a pre-existing low-angle fault.

Quartz is abundant in these leucocratic rocks, ranging from 20-30%. K-feldspar and plagioclase occur in approximately equal amounts. Biotite (sometimes chloritized) is the only mafic phase, ranging from 3-10%, averaging about 5%. Muscovite is present in all thin sections, and ranges from 1-3%. Magnetite and zircon occur in trace amounts, but sphene is absent. In the matrix, graphic intergrowths are ubiquitous, and myrmekite is sometimes present. Feldspars show only slight sericitization. Little evidence of post-crystallization deformation is seen. Some phenocrysts may actually be xenocrysts. These include highly strained quartz and ragged sericitized plagioclase crystals. These textures contrast sharply with those in the matrix. Polycrystalline aggregates of quartz-feldspar-muscovite may be xenoliths or cognate inclusions.

These granitic rocks are distinctive from other leucocratic granitoids in the map area. They contain more quartz, K-feldspar, fewer

mafics, no sphene, lack alteration and in particular, contain primary muscovite.

Exposures of quartz monzonite intruding the basement gneisses in Sections 27 and 28 (T2N, R2E) are tentatively included in this suite. They are shown separately on the geologic map (unit 9m). These porphyritic rocks locally display primary flow banding defined by alignment of biotite and muscovite. They contain more mica than the typical granites, between 10-15%; biotite and muscovite occur in equal proportions. Quartz averages 15-20%. Approximately 15% of the rock consists of plagioclase phenocrysts, many thoroughly sericitized. However, the presence of abundant muscovite suggests these quartz monzonites are probably related to the granites.

Garnet-bearing Muscovite Granite and Quartz Monzonite

Medium-grained garnet-bearing muscovite granite and quartz monzonite (mg) intrude the Bonanza King Formation below the Doble Thrust. Elsewhere, similar rocks are part of the Cretaceous granite-quartz monzonite batholith. They contain 1-2% garnet, 5-10% muscovite, traces of biotite, 20-30% quartz, and unaltered plagioclase and microcline in approximately equal proportions. Some garnet occurs in aggregates surrounded by highly deformed quartz and may be xenolithic. Other, finer-grained garnets occur in aggregates with quartz-microcline-muscovite and may also be xenoliths. Most of the muscovite is magmatic, however. These bodies are not foliated.

Elsewhere below the Doble Thrust, near Smart's Ranch in Section 3 (T2N, R2E) and east of Onyx Summit in Sections 6 and 7 (T1N, R3E), foliated garnet-bearing muscovite granite and quartz monzonite was also recognized during reconnaissance mapping. Tyler (1975) recognized similar rocks below the Doble Thrust with foliation subparallel to that in the intruded marbles. He concluded the foliation formed synchronously with the major deformation of the country rocks. In areas mentioned above, foliation in the intrusives does parallel that of intruded marbles, and the intrusives are locally sheared. However foliation

is not always present and disappears as these rocks grade into massive granite and quartz monzonite away from the contact. The local development of foliation may be an emplacement fabric, perhaps protoclastic, which is localized along the batholith's margins. In the map area, these rocks are massive and clearly postdate earlier penetrative deformation.

Delamar Mountain Area

Introduction

Intrusive rocks underlie much of the Delamar Mountain area. These rocks crosscut earlier folds and faults which affected the upper Precambrian-Cambrian strata. Richmond (1960) first recognized many of the igneous units described here, but reached different conclusions concerning the sequence of intrusive events. Dibblee (1964b) included Richmond's mapping in his compilation of the Lucerne Valley 15' Quadrangle. He did not discuss contact relationships; however, the sequence of emplacement depicted on his map legend parallels that presented here.

Fawnskin Monzonite

The oldest pluton in the Delamar Mountain area is here referred to as the Fawnskin Monzonite (fm). It is a large body which can be traced discontinuously for several kilometers northwest of the map area. C. Miller (1977) examined this pluton in his study of early Mesozoic alkalic monzonites of southern California, and his dissertation includes major and trace element data, as well as Rb/Sr and U/Pb isotopic data. The Fawnskin Monzonite is equivalent to the hornblende quartz monzonite unit of Richmond (1960) and Dibblee (1964b). It underlies Delamar Mountain and adjacent slopes, although bedrock exposures are discontinuous. The main body is intruded by biotite quartz monzonite on its southern flank, and by a dike complex to the north; in between, the Fawnskin Monzonite intrudes the west limb of the Delamar Mountain Antiform.

To the east, a separate smaller body of the Fawnskin Monzonite is exposed in Section 7 (T2N, R1E) and is intruded by the Bertha Diorite and a biotite quartz monzonite(?) dike. This body intrudes downfaulted Cambrian rocks.

The Fawnskin Monzonite includes monzonite (sensu stricto) and quartz monzonite, containing from less than 5-20% quartz. Plagioclase and K-feldspar (orthoclase and microcline) occur in equal proportions. Mafic minerals account for 15->25% of the rock. Hornblende predominates (10-15%), and sometimes includes clinopyroxene cores. Pyroxene-bearing monzonites are more prevalent northwest of the map area (C. Miller, 1977). Brown biotite is common, and ranges up to 5%, especially in quartz-rich rocks. Biotite is sometimes chloritized. Magnetite, apatite, zircon and sphene are common accessories (1-3% total). Abundant and conspicuous euhedral sphenes, up to 3 mm in length, are characteristic of the Fawnskin Monzonite. These rocks are medium- to coarse-grained. Textures are typically hypidiomorphic granular. Pyroxene, hornblende and plagioclase were early crystallizing phases, followed by K-feldspar, biotite and quartz. Quartz is typically anhedral and interstitial.

The most distinctive feature of this unit is its marked primary foliation defined by alignment of hornblende and feldspars (including K-feldspar megacrysts up to 5 cm in length). This foliation is generally but not always present; sometimes only a subvertical hornblende lineation is recognized. Rootless flow folds are common, defined by swirling of hornblende and feldspar.

No penetrative fabric is present to indicate a post-crystallization deformational origin of the foliation. Minor post-crystallization strain is indicated by suturing of interstitial quartz and feldspar grain boundaries, undulatory extinction of quartz, and local subgrain development. This deformation probably occurred during the emplacement of younger plutons.

There is no evidence for a metamorphic origin of the aligned minerals. The presence of complex zoning and perthite suggests both plagioclase and K-feldspar are magmatic in origin. The replacement

of clinopyroxene by hornblende and locally of hornblende by biotite are probably late stage magmatic reactions. The only evidence of metamorphism is local chloritization of biotite, the sericitization of feldspars, and local saussuritization of plagioclase. This probably resulted from later low grade hydrothermal metamorphism.

The foliation is interpreted to be a primary magmatic texture of the monzonite. This flow fabric was imparted during the final stages of the monzonite's emplacement, while the body was a crystal mush. The abundance of oriented minerals indicates that crystals made up a high proportion (about 50%) of the magma body. A subvertical flow direction is indicated by the typically steep plunge of hornblende lineations. C. Miller (1977) suggested a similar origin for this foliation.

Miller differentiated several subunits within the Fawnskin Monzonite. In particular, he differentiated a quartz monzonite unit that lacked foliation, and he suggested these rocks might be younger than the rest of the pluton. He recognized this unit along the easternmost margin of the main body in the Delamar Mountain area. I was not able to differentiate these rocks from other exposures of the pluton. The foliation was recognized throughout. Compositional variations were recognized between quartz-rich, mafic-poor quartz monzonites and more mafic, quartz-poor monzonites, but these occur gradationally. No evidence was seen to indicate a composite origin for the Fawnskin Monzonite at its southeastern end, although this may not be the case elsewhere.

Bertha Diorite

The Bertha Diorite (bd) is exposed along the southeastern portion of the map area, and includes rocks of Richmond's (1960) tonalite porphyry. It was intruded along faults which downdrop Bonanza King marbles to the southeast against Upper Precambrian-Cambrian rocks to the northwest. Contrary to Richmond's (1960) conclusion, I suggest the Bertha Diorite also intrudes the isolated body of the Fawnskin Monzonite (contact discussed below). It is itself intruded by a biotite quartz monzonite

dike(?) along Holcomb Valley Road and a younger diorite (hbqd) in Section 12 (T2N, R1W).

The Bertha Diorite consists primarily of quartz diorite, although diorite and quartz monzodiorite also are present. Quartz ranges from <5-15%. Mafic minerals include hornblende and biotite in varying proportions, and account for up to 20% of the rock. Biotite clusters often rim hornblende, and coarse biotite is frequently chloritized. Accessories include magnetite, apatite, zircon and sphene (the latter often occurs as large euhedral grains). Plagioclase phenocrysts are zoned and sericitization is typical. Saussuritization is ubiquitous in the porphyritic facies. Xenocrysts of carbonate are sometimes present in thin section in the coarser facies.

Two facies are recognized within the Bertha Diorite. The porphyritic border facies is most typical of the unit, and consists of diorite and quartz diorite. The porphyritic facies locally grades into a coarser-grained interior facies, consisting of quartz diorite and quartz monzodiorite. The porphyritic facies contains 5-10% phenocrysts. These are predominantly euhedral zoned plagioclase and lesser hornblende. The groundmass consists primarily of fine-grained randomly oriented plagioclase, and also includes hornblende, biotite, epidote and quartz. No evidence of flow foliation is present. The medium-grained interior facies has hypidiomorphic granular texture. Vestiges of the porphyritic texture persist: the early plagioclase phenocrysts can still be recognized and randomly oriented fine-grained plagioclase occurs as inclusions. Interstitial K-feldspar and micrographic quartz are often present. The latter shows evidence of postcrystallization deformation including undulatory extinction and sutured grain boundaries.

The contact between the Bertha Diorite and Fawnskin Monzonite is not directly exposed in the map area, although outcrops are separated by only a few meters. Based on the presence of "diorite" xenoliths in the monzonite, Richmond (1960) concluded the monzonite intruded the diorite here. He was the first to suggest the small monzonite body near Holcomb Valley Road correlated with the outcrops of the Fawnskin Monzonite to the west. It is quartz monzonite, with 5-15% hornblende and the large

sphenes typical of the Fawnskin Monzonite, however, it lacks the foliation so common elsewhere. Nevertheless, it is so similar in other respects that Dibblee (1964b) and C. Miller (1977) also assigned it to the Fawnskin Monzonite.

During this study, mafic xenoliths were recognized within blocks of the monzonite near its contact with the Bertha Diorite. Petrographic examination revealed these were coarse-grained hornblende-rich (>60%) lithologies, also including microcline, plagioclase and quartz. This lithology grades locally into one typical of the Fawnskin Monzonite. These xenoliths resemble mafic cognate inclusions locally seen elsewhere in the Fawnskin Monzonite, and not the porphyritic facies of the Bertha Diorite.

Thin sections of the monzonite here also contain numerous fractures filled with veins of very fine-grained feldspar and quartz. These features increase in abundance as the diorite is approached. Locally, float blocks of the monzonite show pronounced shearing with a reduction of grain size along closely spaced zones. These shear zones are often filled with veins of fine-grained feldspar and quartz, as described above. These post-crystallization deformation features in the monzonite are distinct from its typical igneous flow fabric.

Outcrops of the Bertha Diorite at the intersection of the Delamar Mountain and Holcomb Valley roads are no finer-grained than elsewhere, although the monzonite is exposed only 4-5 meters across the road. Along the trace of the contact and east of Holcomb Valley Road, float blocks contain the contact relations. Here, hornblende quartz monzonite is assimilated into the diorite. Within individual hand specimens, the diorite first loses its phenocrysts, then the groundmass decreases in grain size. The margin facies of the diorite and the contact zone are no more than a few meters wide at most. Within rocks of the margin facies, weathering pits resembling vesicles, 2-10 mm in diameter, are occasionally present and relicts of possible amygdaloidal filling (of calcite?) are also present locally. This very fine-grained margin facies of the diorite engulfs stoped crystals and lithic fragments of

the monzonite (Fig. 34). These are spalled off along feldspar-quartz filled fractures like those described above.

Significant amounts of wall rock contamination of the Bertha Diorite probably have not occurred at this structural level. In thin section, coarse hornblende and feldspar crystals derived from the monzonite cannot be recognized within the diorite's margin facies more than a few cm from their source. Elsewhere, xenolithic clots of hornblende and epidote (up to 2 cm in diameter) are recognized in diorite float blocks immediately adjacent to the contact, but are not present in diorite outcrops a few meters further within the pluton. If major amounts of monzonitic material were assimilated by the diorite, it would be expected that its marginal portions would be more contaminated and thus more silicic than its interior. The reverse appears to be true in the case of the Bertha Diorite.

The contact with the Fawnskin Monzonite is interpreted to represent a relatively narrow chill margin along which small amounts of detached wallrock material have been assimilated or entrapped. Carbonate xenoliths are locally recognized in the interior facies of the pluton. They occur in an area where small marble pendants are common, however, so this material need not have come far.

Hornblende Biotite Quartz Diorite

Several small bodies of a quartz diorite (hbqd) are exposed in the NE1/4 of Section 12 (T2N, R1W). These are intruded by granite and biotite quartz monzonite, and intrude the Bonanza King and Carrara formations. The northernmost exposures of this unit intrude the porphyritic facies of the Bertha Diorite and locally contain xenoliths of its coarser interior facies. The interior facies of the Bertha Diorite crops out locally, but its contact with the hornblende biotite quartz diorite is not exposed.

In thin section the younger quartz diorite is distinctive. It has hypidiomorphic granular texture and is medium- to coarse-grained. It contains 10% quartz and almost no K-feldspar. Plagioclase is zoned, and unlike the older units this diorite shows little sericitization and contains

Figure 34: Rock chip showing Bertha Diorite intruding Fawnskin Monzonite. Base of chip is 33 mm long. Dark-colored very fine-grained marginal facies of the diorite in the photo's lower half contains partially assimilated feldspar xenocrysts (white) derived from monzonite. Dark grains in monzonite are hornblendes. Sample collected in NW1/4 of Section 7 (T1N, R1E) in upper Polique Canyon.

Figure 35: Vesicular andesite of dike complex containing xenoliths of Fawnskin Monzonite (in center and in upper right of block). Coarse-grained, felsic xenolith is present between these. Plagioclase phenocrysts (white) are abundant. Block is 20 cm in length. Sample collected in the NW1/4 of Section 36 (T3N, R1W).

Figure 34.

Figure 35.

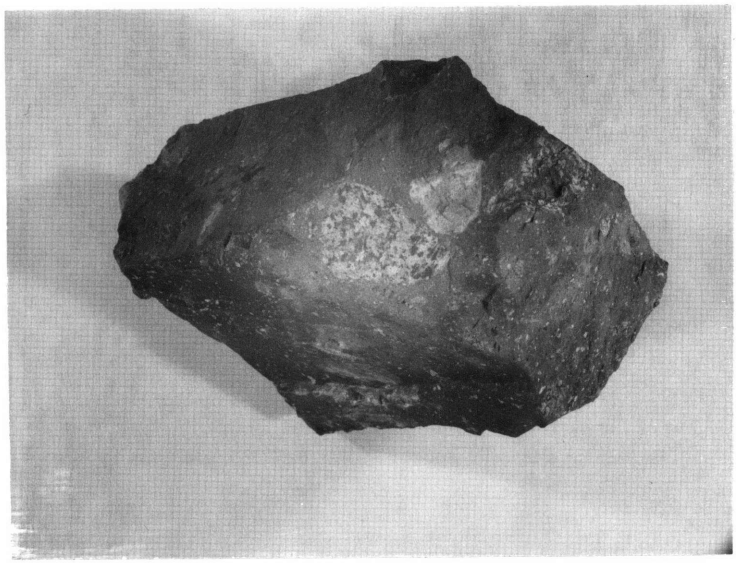

no epidote. Coarse hornblende (10%) and biotite (15%) are the mafic phases (the latter is locally chloritized). Large and abundant euhedral sphene is a distinctive feature.

The relative lack of alteration or evidence of post-crystallization deformation features differentiate this quartz diorite from the earlier plutons and suggest it may be significantly younger. Petrographically, it is indistinguishable from the Cienga Seca Quartz Diorite exposed south of the Sugarloaf area.

Dike Complex

In the northern part of the area a dike complex (dc) invades the Fawnskin Monzonite and Bonanza King Formation marbles, and has spread these units apart. Individual dikes are often several meters wide, and extend several tens of meters. They generally strike northwest and dip vertically.

Richmond (1960) considered these rocks as part of a metavolcanic complex; he recognized quartz latite porphyry, crystal and crystal lithic quartz tuff, and amygdaloidal trachyandesite. His descriptions are more complete than those presented here. He believed these rocks were intruded by Fawnskin Monzonite, and were the earliest Mesozoic igneous rocks in the Big Bear area. During this study, dikes of the complex were repeatedly observed cutting the Fawnskin Monzonite. Andesitic dikes (believed to be the earliest in the complex) contain partially assimilated xenoliths of Fawnskin Monzonite, from a few cm in diameter up to mappable scale (Fig. 35). The dike complex is elsewhere intruded by rocks of the granite and quartz monzonite batholith (Richmond, 1960; Dibblee, 1964b).

The dike complex displays a great range of textural and compositional types. Dike rocks include porphyritic andesite (locally vesicular), latite, and quartz latite. Phenocrysts (average length 2 cm) form from 5-15% of the rock. These include zoned plagioclase (predominant), K-feldspar, quartz and hornblende. Xenoliths of calc-silicate and carbonate rocks, quartzite, and monzonite are seen. Some andesitic rocks

may contain glass shards. Corroded phenocrysts of feldspar and quartz may be xenocrysts. Clots of euhedral hornblende-K-feldspar-plagioclase-quartz may be plutonic xenoliths or cognate inclusions.

The fine- to very fine-grained matrix of these rocks contains up to 15% quartz. Hornblende is the principal mafic phase (5-15%) and biotite is common. Sphene is a typical accessory. Feldspar content is variable. Micrographic textures are often present, and plagioclase is commonly sericitized. Epidote (after plagioclase) is also recognized. Evidence for significant metamorphism including biotite growth, suggested by Richmond (1960), was not seen.

Based on crosscutting relationships, it appears the more mafic dikes were generally emplaced earlier than the more acid ones. Andesite dikes, which contain most of the Fawnskin Monzonite xenoliths, are typically separated from that unit by younger dikes. Younger dikes apparently spread apart the earlier andesitic dikes and the Fawnskin Monzonite.

Vesicular textures and fragments of glass recognized in some dikes during this study support Richmond's conclusion that this complex was emplaced in a shallow level sub-volcanic environment. So too does the porphyritic character of these rocks and their sharp chill margins. The compositional range of the dike complex is similar to that of the Bertha Diorite. Both units show textural evidence of emplacement at shallow plutonic or sub-volcanic levels, presumably along faults. It is possible they were emplaced at the same time and may be comagmatic.

Granite and Quartz Monzonite

The voluminous Cretaceous batholith that underlies much of the San Bernardino Mountains is represented in the southwest part of the Delamar Mountain area by granite and quartz monzonite (g). This resistant unit forms distinctive outcrops, with rounded edges and granular surfaces. These rocks were previously described as biotite quartz monzonite by Richmond (1960) and Dibblee (1964b). This unit intrudes the Fawnskin Monzonite, the hornblende biotite quartz diorite

and the Carrara and Bonanza King formations. Dike rocks similar to this unit crosscut the Fawnskin Monzonite-Bertha Diorite contact along Holcomb Valley Road. North of the map area, correlative rocks intrude the dike complex (Richmond, 1960). Its intrusive contacts are not generally marked by a fine-grained chill zone. Rather, grain size remains relatively coarse. This unit often contains 20-30% quartz, and would be classified according to Streckeisen and others (1973) as a granite. Some quartz monzonite (<20% quartz) is also recognized. Biotite ($\leq$5%) is the mafic phase. K-feldspar and plagioclase occur in roughly equal proportions. Micrographic and myrmekitic textures are common. Accessory magnetite and apatite are not abundant, and sphene is generally absent. Hypidiomorphic granular textures are predominant.

North of Bertha Peak, porphyritic granite (gp) intrudes outcrops of Wood Canyon Formation. These intrusives were not examined in detail and their age relations to other igneous units in the map area is uncertain. Based on observations outside the map area Richmond (1960) suggested these granites were the youngest igneous rocks in the Holcomb Valley area. Dibblee (1964b), however, concluded these porphyritic granitic rocks were related to the dike complex, and were intruded by Cretaceous granite and quartz monzonite.

Elsewhere in the range similar granite and quartz monzonite have yielded Late Cretaceous K/Ar ages on biotite (Armstrong and Suppe, 1973). The significance of these dates, and the age of these batholithic rocks is discussed in Chapter V.

CHAPTER IV: DEFORMATIONAL HISTORY

Introduction

Reconstruction of the deformational history of the Big Bear area is a major objective of this study. Precambrian, Mesozoic and Cenozoic deformational events are present, although analysis of Mesozoic tectonism is particularly stressed in this investigation. The emphasis of this chapter is descriptive, focussing on the sequence, geometry and style of deformational events recognized. Interpretation of the deformational history of the Big Bear area, in particular the character of Mesozoic intra-arc tectonism here and its regional setting and significance, is deferred until Chapter VI.

As a convention in this thesis, Precambrian fold phases and foliations are denoted by lower case letters (f_1, s_1) while Mesozoic structures are identified by capital letters (F_1, S_1). It is understood that the reader will refer to the appropriate maps and cross sections as required. The tectonic map for the Sugarloaf area (Plate VI) shows the locations of folds and faults described here, as well as the various structural blocks identified in the Sugarloaf area. Contoured pole diagrams (i.e. $\perp S_0$) were used to determine the plunges of macroscopic cylindrical folds cited in the text (Turner and Weiss, 1963).

Precambrian Events

Rocks of the Precambrian gneiss complex record a complex deformational history prior to deposition of the overlying Upper Precambrian Wildhorse Quartzite. The earliest structures recognized are f_1 isoclinal folds. The s_1 foliation, the predominant fabric present in these rocks, is axial planar to the f_1 folds. The s_1 foliation is defined by alignment of metamorphic micas in schists and paragneisses, and alignment of augen and mafic minerals in orthogneisses. Compositional layering (relict bedding?) was transposed into parallelism with s_1.

Granitic augen gneisses and pegmatites which intrude the older

basement rocks also contain the s_1 foliation, and may have been emplaced prior to or during f_1. Xenoliths, locally found within the orthogneisses, are flattened parallel to s_1. These often contain an earlier foliation that is truncated by s_1 (see Chapter III). This truncated planar fabric could be pre-f_1. Alternatively, these relations could result from a progressive f_1 deformation sequence including early folding and shear flattening, intrusion, and further folding and flattening. This interpretation is favored here. Only rarely were f_1 fold hinges observed in the field, although intrafolial folds are common.

The s_1 foliation and f_1 folds are refolded by f_2 folds, which are tight or isoclinal. The s_2 cleavage is axial planar to f_2 folds and is defined by coarse biotite and finer grained muscovite. In thin section s_2 cross-cuts the s_1 foliation. The s_2 cleavage is typically subparallel to local s_1 foliation. Thus, s_2 cleavage is difficult to recognize except in fold hinges. This suggests that the axial surfaces of f_1 and f_2 may have been subparallel. f_1 and f_2 may be coplanar deformations and represent progressive folding events in a single episode of deformation. f_1 hinges could not be measured owing to poor exposure, thus it is unknown if f_1 and f_2 fold axes were coaxial as well.

Crudely foliated late synkinematic and non-foliated post-kinematic granitic dikes and veins cut f_1 and f_2 structures, but do not intrude the overlying Wildhorse Quartzite. Macroscopic post-metamorphic folds (f_3?) may also be locally present but did not develop a related axial planar cleavage. The existence of such folds is suggested by local predepositional warping of s_2 surfaces below the Wildhorse Quartzite. In the E1/2 of Section 33 (T2N, R2E) for example, east-dipping rocks of member W1 overlie gneisses with s_1 and s_2 surfaces which are "folded" in what appears to be a west southwest plunging antiform.

Mesozoic Events

The geology of the Big Bear area was largely shaped by Mesozoic deformational events. As such, they receive particular attention here. The sequence of structural events varies somewhat between the Rose

Mine, Sugarloaf, and Delamar Mountain map areas. The deformational history of each area is reviewed separately, and summarized briefly at the beginning of each section. Only a brief summary of Mesozoic structural events in the study areas is presented in this chapter. Structural and geochronologic data (presented in Chapter V) are more completely synthesized in a discussion of Mesozoic tectonics in the Big Bear area, in Chapter VI.

The terms "block" and "sub-block", used in discussing Mesozoic events in the Sugarloaf area, refer to the numerous structural plates identified on the tectonic map for this area (Plate VI). Blocks (e.g. block VII) may consist of several sub-blocks (sub-blocks VIIa, VIIb, VIIc, ...) which in turn are occasionally further differentiated (sub-blocks VIIb1 and VIIb2).

Rose Mine Area

Introduction. West of Rose Mine, the Doble Thrust carries Precambrian gneisses and Wildhorse Quartzite in the overturned limb of the Arrastre Creek Antiform over uppermost Precambrian-Cambrian rocks of the overturned limb of the Rose Mine Synform. Final emplacement of the Doble Thrust culminated a complex, progressive sequence of deformational events including polyphase folding, thrusting and high-angle faulting. These events occurred under metamorphic conditions transitional between greenschist and amphibolite facies. Mesoscopic crenulation folds and macroscopic NE-SW trending open folds refold the Doble Thrust and appear largely post-metamorphic. Emplacement of Cretaceous granitic rocks is thought to postdate all these events. The sequence of structural events is summarized in Fig. 36.

Event 1: Synmetamorphic Polyphase Folding and Thrusting. The earliest Mesozoic structures recognized are synmetamorphic folds and minor thrusts. In rocks below the Doble Thrust, two fold phases are locally present. F_1 folds are isoclinal and cause transposition of

Figure 36: Sequence of Structural Events at Rose Mine

1. Synmetamorphic polyphase folding and thrusting
   Metamorphism: at least greenschist facies (biotite grade)
   F_1: zonally developed isoclinal folds
   F.A. vary in orientation but are locally parallel to F_2 axes
   A.P. and S_1 cleavage are approximately parallel to S_0
   F_2: tight to isoclinal folds, involve Precambrian gneisses
   F.A. trend N-NW, plunge varies
   A.P. and S_2 cleavage dip SW and W
   Vergence is to NE
   Minor associated thrusting
2. High-angle faulting (affects rocks below Doble Thrust)
3. Emplacement of the Doble Thrust
   Thrusting is synmetamorphic and involves Precambrian gneisses
   F_2 Arrastre Creek Antiform may be thrust ramp antiform
   S_2 cleavage in gneisses is best developed immediately above thrust
4. Crenulation cleavage (F_3; folds Doble Thrust)
   F.A. plunge NW
   A.P. and S_3 cleavage dip NE or NNE
5. Open folding (F_4; folds Doble Thrust)
   F.A. trend NE-SW, plunge varies(?)
   A.P. are upright, no cleavage
6. Intrusion of Cretaceous granitic rocks

F.A. = fold axes

A.P. = axial planes

bedding in the Bonanza King and Carrara formations. They may be present, but have not been recognized in stratigraphically lower units. F_1 folds are refolded by NW plunging, NE vergent F_2 folds which include the Rose Mine Synform. Minor F_2 thrusts are present along the synform's overturned limb. Both fold phases were synmetamorphic and associated microfabrics are characterized by the growth of oriented metamorphic minerals including tremolite, biotite and muscovite and plastic flow of quartz and feldspar and calcite and dolomite (metamorphic grade is discussed below). Polyphase folding and associated thrusting are considered part of a single progressive deformational event.

Above the Doble Thrust, the eastern, overturned limb of the Arrastre Creek Antiform is present in the Rose Mine area. This fold appears to trend N-S to NW-SE and its plunge is uncertain (probably variable). It is interpreted as an F_2 generation fold, and may be a ramp antiform for the Doble Thrust. F_1 structures were not recognized in rocks of the overturned limb, but their presence may be obscured by strong F_2 deformation.

F_1 folds are recognized with certainty only in rocks of the Carrara and Bonanza King formations. Mesoscopic F_1 folds cause transposition of original bedding in these units, however, the proper stratigraphic sequence has apparently been preserved. This is most easily explained if F_1 folds formed by bedding-parallel slip, causing internal transposition of the individual formations. Mesocopic F_1 folds are isoclinal, with typical short limb lengths of a few cm. The axial surfaces of F_1 folds (S_1) are parallel to bedding (S_0). S_1 cleavage is present in pelitic rocks. $S_0 \times S_1$ lineations are conspicuous in the marbles, where they are defined by color bands. These lineations are parallel to exposed F_1 fold axes. Larger amplitude folds (short limb lengths of several m) are present in Bonanza King marbles northeast of the Helendale Fault but are difficult to trace owing to lack of distinctive marker horizons. Southeast of the Helendale Fault, F_1 folds of more than a few cm in amplitude are difficult to differentiate from coaxial F_2 folds. However, macroscopic F_2 folds are present along the overturned Carrara

Formation-Papoose Lake Member contact in the center of Section 19 (T2N, R2E). F_1 folds here have clockwise asymmetry, while F_2 folds are of the reverse orientation. F_1 folds have not been recognized in the Zabriskie and Wood Canyon formations, although folds are not well exposed in these units. F_1 folds may have been restricted by rock type to the more ductile marbles and calc-silicate rocks overlying the Zabriskie Quartzite. Similarly, F_1 folds have not been recognized in Wildhorse Quartzite above the Doble Thrust. However, F_1 structures are present in less deformed rocks inferred to be offset from the east limb of the antiform (discussed below) and their presence on the antiform's overturned east limb here may have been obscured by severe F_2 deformation.

F_2 folds form the major macroscopic structures, and refold F_1 folds and S_1 cleavage. S_2 axial-planar cleavage is recognized in association with F_2 folds. The Rose Mine Synform is an F_2 fold and is exposed beneath the Doble Thrust. Along its southwest limb, second order, tight to isoclinal F_2 folds plunge NW and are NE vergent. Minor F_2 thrusts cut this limb. Rocks northeast of the Helendale Fault may have lain in the synform's core, and record later complex deformation. Above the thrust, the basement-cored Arrastre Creek Antiform may be an F_2 generation fold. The antiform is east vergent, but its axial plunge is uncertain. F_2 folds have been refolded and rotated by later structures.

Rocks southeast of the Helendale Fault lie in the overturned limb of the Rose Mine Synform. These include uppermost Precambrian-Cambrian formations which are in inverted sequence. These rocks record complex second-order F_2 folding and thrusting. F_2 folds on the overturned limb fold bedding in the Wood Canyon and Zabriskie formations and fold transposed bedding in the Carrara and Bonanza King formations. These F_2 folds are tight to isoclinal. Axial planar cleavage and axial surfaces of mesoscopic folds trend NW and dip moderately (about 40-50°) SW. These are best exposed in the Carrara and Bonanza King formations; their contact is complexly folded by NW plunging F_2 folds. Mesoscopic isoclinal F_2 folds are also present within the Wood Canyon Formation, however

hinges are rarely exposed. Where closure can be determined these folds face upward to the northeast, consistent with F_2 folds elsewhere on this limb. Exposed F_2 fold axes in Sections 18 and 19 plunge WNW (about 30°/N70W). These folds are essentially colinear with F_1 folds and S_0 x S_1 lineations (Fig. 37). Colinearity of F_1 and F_2 folds, at least in this area, would make the former more difficult to recognize in the poorly exposed rocks of the Wood Canyon Formation.

The overturned limb of the synform contains several minor thrusts which cut out most formational contacts. The Zabriskie Quartzite is often sliced out completely, and rocks of the Papoose Lake Member and much of the Carrara Formation are progressively cut out along strike to the northwest. These small thrusts are believed to have formed when folding could no longer accommodate strain accumulated during development of the synform so that portions of the overturned limb deformed by faulting. Quartzites of the Zabriskie and Wood Canyon formations in particular were unable to shorten by folding as readily as interbedded marbles and pelitic rocks.

Bonanza King marbles northeast of the Helendale Fault may lie in the core of the Rose Mine Synform. They are complexly folded and further disrupted by NW trending high-angle faults. Owing to general lithologic homogeneity, fold geometry was not mapped in detail. Tight, NW trending (F_2?) folds were recognized which refold transposed bedding and mesoscopic F_1 folds, and are themselves refolded. F_1 fold axes and S_0 x S_1 lineations are plotted in Fig. 38. They are dispersed along a NW trending small circle girdle. As F_1 and F_2 folds appear to be approximately colinear along the overturned limb of the Rose Mine Synform, it is suggested this rotation of F_1 fabrics is the result of post-F_2 folding. Geometric analysis suggests refolding by horizontal, NE-SW trending flexural slip folds (Turner and Weiss, 1963). These folds are discussed further below. Fault-bound Carrara Formation rocks may have lain in the east limb of the Rose Mine Synform.

The basement-cored Arrastre Creek Antiform trends N to NW and may be an F_2 generation fold. Only a portion of its eastern, overturned

Figure 37: Equal-area plot of F_1 linear elements west of the Helendale Fault and below the Doble Thrust in the Rose Mine area.

(note that all equal-area plots are lower hemisphere projections)

Figure 38: Equal-area plot of F_1 linear elements east of the Helendale Fault in the Rose Mine area.

Rose Mine - E. of Helendale Fault

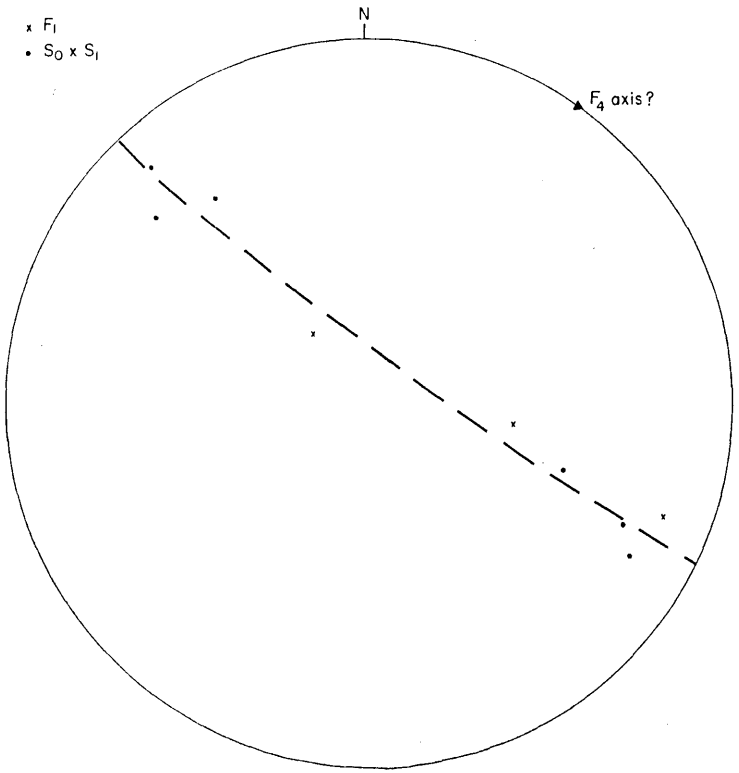

Rose Mine-W. of Helendale Fault, below Doble Thrust

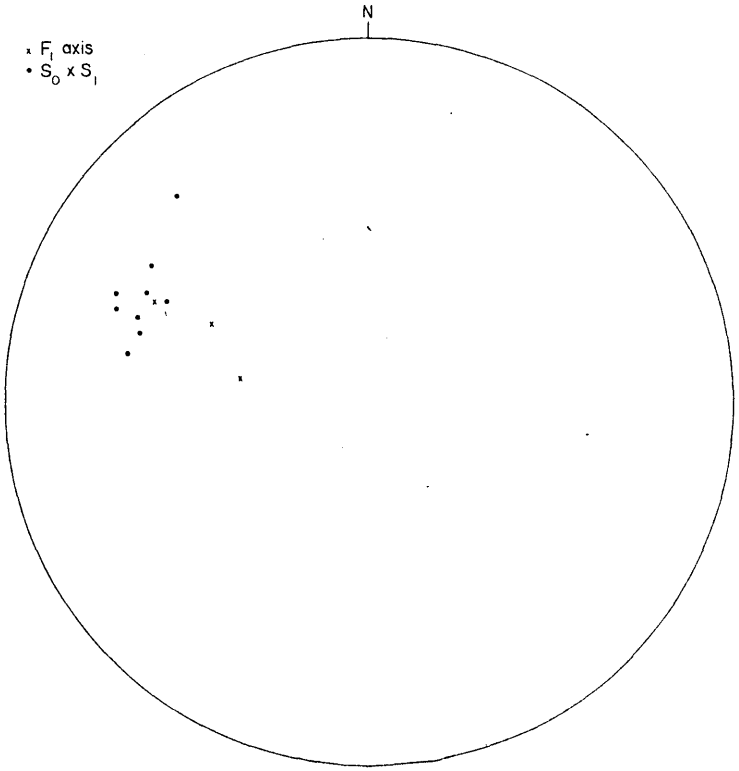

limb is described here; the western continuation of this structure is described below. In the Rose Mine area, Precambrian gneisses in the core of the antiform structurally overlie overturned Wildhorse Quartzite. This contact is depositional (see discussion below) and is overturned to the east through 40° or more. The underlying Wildhorse Quartzite is isoclinally folded on a mesoscopic scale, as indicated by facing reversals present in outcrop and fold hinges recognized in float. These are believed to be second-order F_2 folds related to the antiform. Fold axes were not directly observed, and the plunge of the antiform is not known. Where closure could be recognized (only in a few cases) the folds are overturned, isoclinal and face ENE.

The quartzites in the SE1/4 of Section 13 (T2N, R3E) have a NW trending, SW dipping cleavage that is presumably axial-planar to F_2 folds. This S_2 cleavage is formed by metamorphic biotite and muscovite and flattening of quartz grains (Fig. 39). Overlying gneisses have an S_2 cleavage as well (discussed below) which is subparallel to that in the quartzites. The overturned limb of the antiform is cut by the Doble Thrust. Folding, thrust detachment, and recrystallization of cover and basement rocks are thought to have occurred during a progressive deformational episode, as discussed below.

Quartzite pebble elongation lineations plunge down the dip of cleavage (50-60°/S75W) in the Wildhorse Quartzite. These lineations may approximate the direction of the principal elongation axis of the finite strain ellipsoid associated with the F_2 folds, however structural data are too incomplete for substantive conclusions.

Event 2: High-angle Faulting. Several high-angle faults cut folds and minor thrusts of Event 1 on the overturned limb of the Rose Mine Synform. The traces of several of these faults trend toward the Doble Thrust but do not appear to offset it. Of note are faults a and b which merge below the Doble Thrust. The NW trending faults (a, b, c, d) show variable separation. One of the NW trending faults, d, is cut by a NE trending fault which may continue northeast to cut the

Figure 39: Photomicrograph of S_2 cleavage in Wildhorse Quartzite (member W1) above Doble Thrust. Cleavage parallels length of the photo and is best identified by orientation of biotite and muscovite. Quartz is dimensionally elongate and polygonized. Photo length equals 5 mm.

a) plane polarized light
b) crossed polars
Sample is from SE1/4 of Section 13 (T2N, R2E).

Figure 39a.

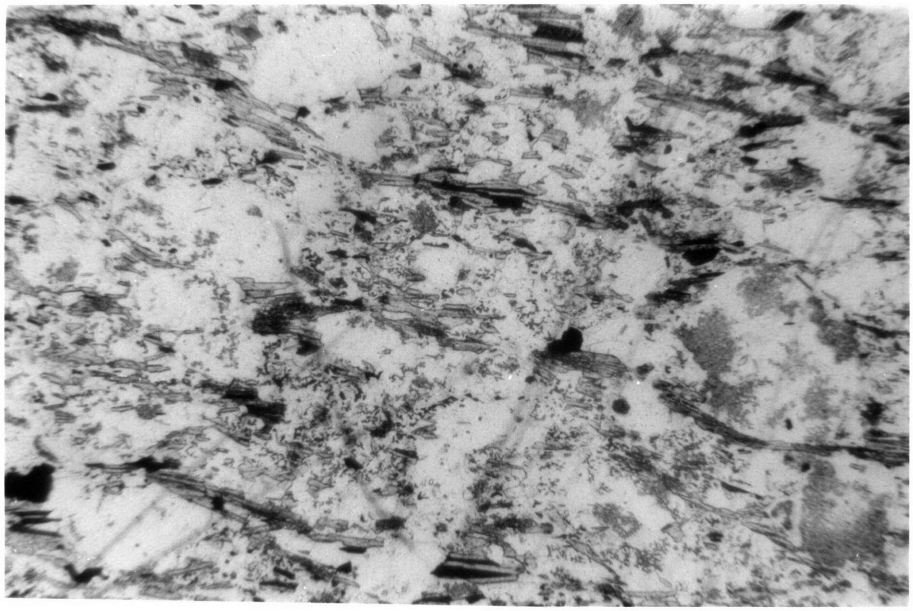

Figure 39b.

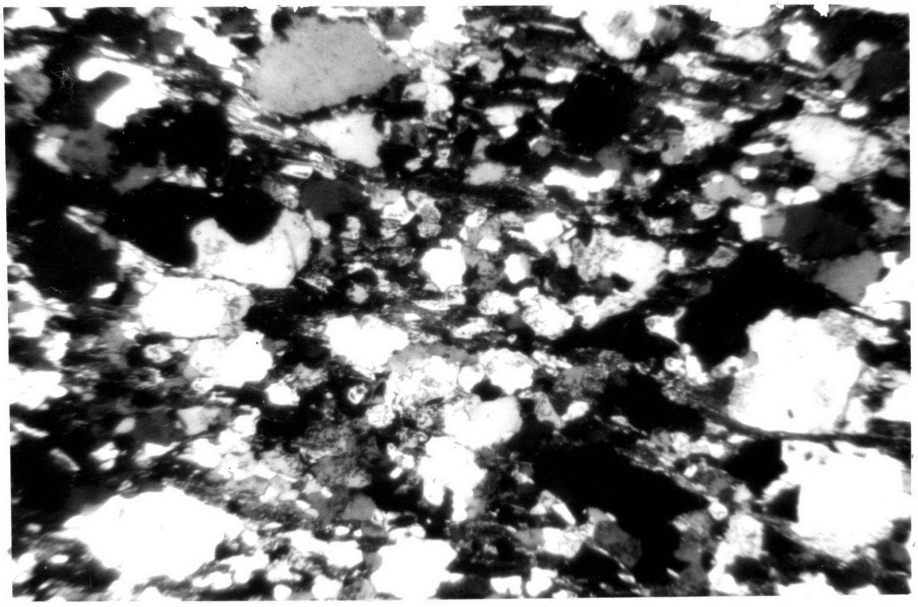

Round Valley Fault and intrusive unit mg. The NE trending faults have displacements of less than 5-10 m, and could be younger than the Doble Thrust, and yet not offset it. The NW trending faults have greater minimum dip-slip separation (40-100 m), and of these, faults a and b are probably truncated by the Doble Thrust.

Event 3: Emplacement of the Doble Thrust. The Doble Thrust is one of the major Mesozoic structural features in the Big Bear area. It was first recognized as a thrust fault by Tyler (1975) in the Baldwin Lake area northwest of Rose Mine (Plate I). Along much of its length there the thrust juxtaposes Precambrian gneisses over an overturned section of uppermost Precambrian-Cambrian rocks. These lower plate rocks continue to the Rose Mine area. In the map area, the thrust is interpreted as cutting upsection in its upper plate. It slices through the eastern overturned limb of the Arrastre Creek Antiform.

Dibblee (1964b, 1967a,b) had a different interpretation for the continuation of the Doble Thrust into this area. He located a fault contact along the gneiss-Wildhorse Quartzite contact, and suggested the fault died out along strike south of the Rose Mine area, where he recognized the gneiss-quartzite contact as depositional. My mapping suggests that the gneiss-quartzite contact is an unconformity in the Rose Mine area as well, and that the continuation of the Doble Thrust is further east at the Wildhorse Quartzite-Wood Canyon Formation contact. Rocks assigned to the lower Wildhorse Quartzite are overturned along the contact with the gneisses. These quartzites are lithologically similar to rocks of member W1 elsewhere, and locally lenses of quartz and quartzite pebble conglomerate are found near the gneiss-quartzite contact. The basement-Wildhorse Quartzite contact may indeed be locally faulted here, however minor shearing is not surprising as the quartzites and the gneisses were strongly deformed during F_2 folding. Any shearing along the basement-quartzite contact is of small displacement, since in the NE1/4 of Section 25 (T2N, R2E),

south of Hill 7492', conglomeratic quartzite of member W1 unconformably overlies basement gneisses.

The Doble Thrust cuts across the overturned Wildhorse Quartzite-basement contact in the SE1/4 of Section 13. At this point, the apparent, stratigraphic throw across the fault is approximately 2 km. The thrust is easy to overlook here, as quartzites above and below the fault dip to the SW. Geologic reconnaissance indicates the Doble Thrust continues south to Onyx Peak (Plate I) where upper and lower plate rocks are cut by granitic rocks of the Cretaceous batholith (Dibblee, 1967a). Near Onyx Peak, upper Wildhorse Quartzite (member W2) is thrust over Wood Canyon Formation.

Tyler (1975) interpreted the Doble Thrust near Baldwin Lake as a shallowly SW dipping thrust fault. Gilliou (1953) and Dibblee (1964b, 1967a,b) interpreted this structure as a steeply dipping reverse fault. In a NE trending gully in the SE1/4 of Section 13 (T2N, R2E), outcrop geometry indicates the fault dips shallowly SW at 30° or less. A fault contact is locally exposed, and dips 15-20° SW, however, this outcrop may be out of place (Fig. 40). A three-point construction of the fault surface yielded a fault attitude of N22W/19SW.

A Mesozoic cleavage (S_2) is recognized in rocks of the Precambrian gneiss complex adjacent to the Doble Thrust. The older Precambrian foliation (s_1) dips steeply to vertically above the thrust. Where recognized furthest from the thrust, the Mesozoic cleavage is irregularly developed, crosscuts s_1 and parallels bedding and cleavage in the Wildhorse Quartzite (Fig. 41). The Mesozoic S_2 cleavage in the SE corner of Section 13 (T2N, R3E) dips 40-55° SW. The S_2 cleavage is associated with growth of fine-grained white mica and biotite. Transposition of the older s_1 fabric is recognized, and incipient metamorphic differentiation of micaceous and quartzo-feldspathic or quartz-feldspar layers is apparent (Fig. 42). Quartz and feldspar display polygonization; coarse K-feldspar grains are highly strained. Closer to the thrust fault, dip of the S_2 cleavage decreases to 20-40°, and more closely parallels the dip of the thrust. The S_2 cleavage appears

Figure 40: Exposure of Doble Thrust. Thrust juxtaposes Precambrian gneisses (pЄgn) over Wood Canyon quartzites (Єwc). Thrust zone consists of quartzo-feldspathic schist (a few cm in thickness) separating gneiss and quartzite. Thrust zone dips gently to SW, is recrystallized and cross-cut by F_3 crenulation cleavage. Hammer handle is 28 cm long. Photo taken in SE1/4 of Section 13 (T2N, R2E).

Figure 41: Mesozoic S_2 cleavage in Precambrian gneisses above the Doble Thrust. Precambrian s_1 foliation dips vertically; S_2 cleavage dips to right (less steeply than prominent weathering surfaces). Hammer handle is present in upper center. Photo taken in the SE1/4 of Section 13 (T2N, R2E).

Figure 40.

Figure 41.

Figure 42: Photomicrograph of S_2 cleavage in Precambrian gneisses above the Doble Thrust. Cleavage defined by fine-grained biotite and muscovite is parallel to width of photo. Note metamorphic differentiation of anastomosing mica-rich layers. K-feldspar grains are undulatory, quartz is dimensionally elongate and polygonized. Length of photo equals 5 mm.

a) plane polarized light
b) crossed polars
Sample is from SE1/4 of Section 13 (T2N, R2E).

Figure 42a.

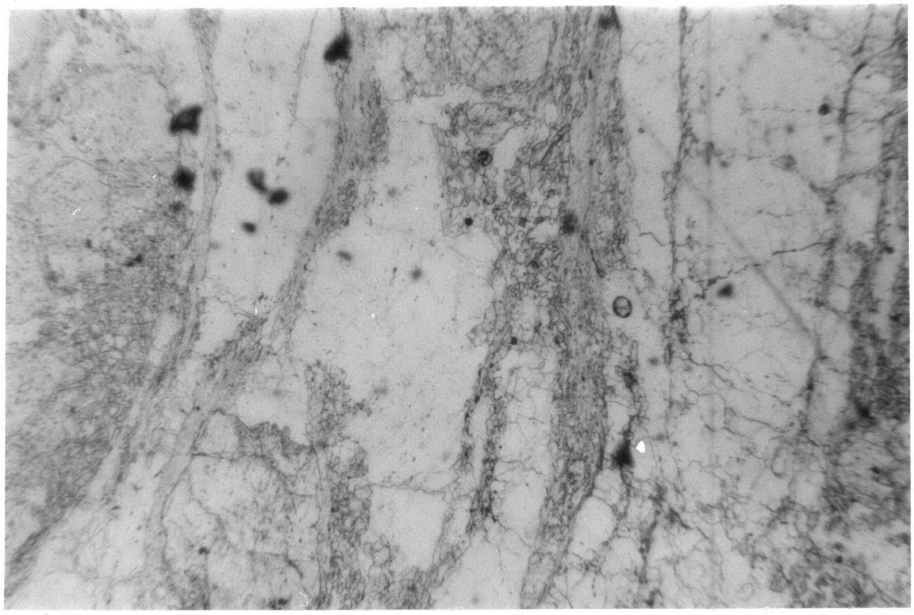

Figure 42b.

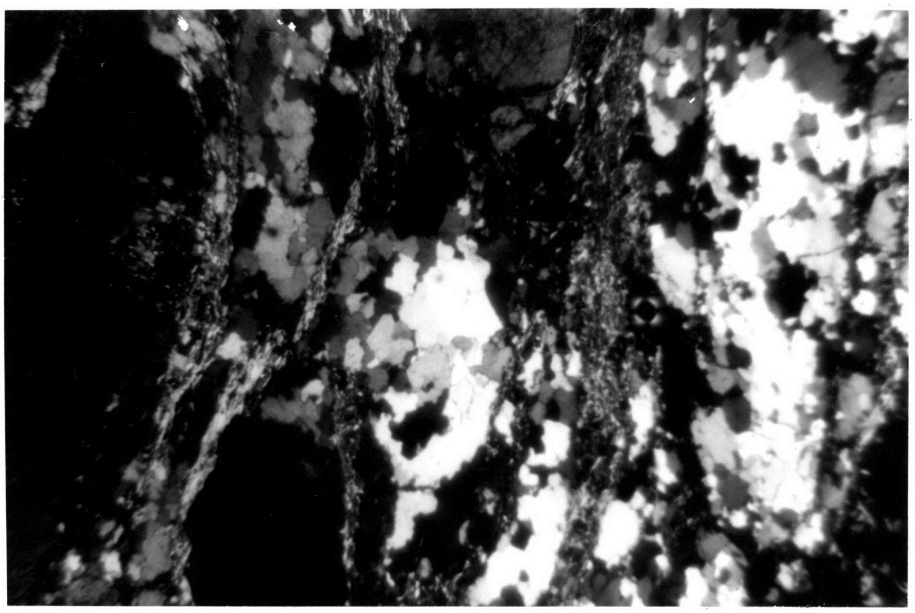

more penetrative closer to the thrust. Within approximately 20 m of the fault, a well-developed crenulation cleavage(S_3, an event 4 fabric) is present which crosscuts the steeply dipping Precambrian fabric and more gently dipping Mesozoic S_2 cleavage. Although locally obscured, the earlier S_2 fabric can nevertheless be followed to the thrust contact. Adjacent to the Doble Thrust, S_2 cleavage strikes NW and dips 20-40° SW, subparallel to the fault.

The Doble Thrust was a synmetamorphic fault, and recrystallization apparently outlasted translation. Rocks within a few cm above and below the fault show no evidence of cataclasis. Where exposed, the fault contact has a welded appearance. Overlying gneissic rocks and underlying quartzite grade into a few cm thick section of quartzo-feldspathic schist (syntectonically recrystallized gouge?), and the contact is warped by event 4 crenulation folds. Quartzite from less than a meter below this contact shows little evidence of high intragranular strain (grain size is not reduced nor are grains particularly dimensionally elongate). It is suggested that upper plate translation occurred along a narrow, ductile thrust fault zone.

Event 4: Folding and Crenulation Cleavage. Locally well-developed crenulation cleavage (S_3) and associated chevron folds (F_3) are recognized affecting upper and lower plate rocks immediately adjacent to the Doble Thrust, as well as the rocks in the fault zone itself. Mesoscopic event 4 structures are restricted within 20-30 m of the thrust. These post-thrust structures are best exposed in Section 13. Here, the cross-cutting crenulation cleavage strikes NW and dips steeply to moderately NE. The axes of crenulation folds trend NW and are sub-horizontal or gently plunging (10-20° NW). Below the thrust, small amplitude (1-3 cm) chevron folds are present in pelitic layers. Some mica growth occurred during crenulation cleavage formation, and event 4 is believed to have occurred during the waning stages of the syn-metamorphic contractional deformation during which the Doble Thrust was emplaced.

The crenulation cleavage is not developed in interbedded quartzites. It is not surprising then, that event 4 structures are not obvious further south, where quartzite is the principal lithology on either side of the fault. However, local warping of the Wildhorse Quartzite southeast of Hill 7233', and rare NW plunging small-scale folds in the underlying Wood Canyon (such as seen northeast of Hill 7492') may be F_3 generation folds. Axial planar cleavage associated with the latter folds dips steeply NNE.

Event 5: Open Folding. NE-SW trending open folds of uncertain age refold the Doble Thrust and earlier folds. The relative age relations with event 4 folding and later plutonism are not clear. Some of these folds could be of Cenozoic age.

The Doble Thrust is warped into a SW plunging synform whose hinge is present in the Rose Mine area. Both upper and lower plate rocks appear to be refolded. A $\perp S_0$, S_2 plot for upper plate rocks in the hinge area yields a fold axis plunging 50°/S62W. This synform is one of the major structures in the Big Bear area (see Plate I); the Doble Thrust trace trends WNW along the fold's NW limb, and S along its SE limb. As discussed below, folds believed to be of this generation are present further west and are important in controlling outcrop pattern.

The inferred NE trending folds which refold F_1 and F_2 structures in rocks northeast of the Helendale Fault may be F_4 folds. The trace of the Helendale Fault appears to cut the F_4 folds; their plunge varies across this fault.

Event 6: Intrusion of Cretaceous Granitic Rocks. Pre-Mesozoic rocks in the Rose Mine area are intruded by muscovite granite and associated granitic-quartz monzonitic rocks of the Cretaceous batholith. These plutons intrude the Rose Mine Synform; elsewhere associated granitic rocks crosscut the Doble Thrust. They are inferred to postdate event 4 and event 5 folds. Granitic rocks in the Rose Mine map area are not foliated.

Geometry of the Doble Thrust at Baldwin Lake. It is believed that events 1, 2, 3 and 4 represent progressive events in a single deformational episode, accompanied by dynamothermal metamorphism. Field relationships in the Rose Mine area alone permit an interpretation in which the Arrastre Creek Antiform and Rose Mine Synform formed as a conjugate fold pair, whose common overturned limb was breached by the Doble Thrust. This simple geometry is precluded by geologic relations near Baldwin Lake, described by Tyler (1975).

Tyler recognized the Doble Thrust crosscuts earlier formed folds and faults in the lower plate (Plate I). Overturned uppermost Precambrian-Cambrian rocks below the Doble Thrust northeast of Baldwin Lake may represent the continuation of the overturned limb of the Rose Mine Synform. North of Gold Mountain, the NW trending doubly plunging Chicopee Canyon Antiform, cored by rocks of the Delamar Mountain Formation, appears below the Doble Thrust. This (F_2?) fold is separated from the overturned limb of the synform to the northeast by a complex, NW trending fault zone. This fault zone braids to the northwest, and includes slivers of basement rocks and overturned Upper Precambrian and Cambrian rocks. Both reverse and normal sense separations are observed along the fault zone. To the southeast, a thrust sheet of Upper Precambrian(?) quartzite overrides this fault zone and is itself overridden by the Doble Thrust.

Tyler suggested a structural sequence in which synmetamorphic folds, including the Chicopee Canyon Antiform, formed first. He interpreted the complex fault zone to have initiated as a reverse fault, breaching the fold's overturned limb. Subsequently, normal faulting or "backsliding" occurred locally along the fault zone, giving rise to the complex separations now observed. This fault zone and the earlier folds were then overridden by the Doble Thrust and the subsidiary thrust slice below it.

Tyler believed this complex sequence of events occurred during a single, protracted contractional deformation. The sequence of events at Baldwin Lake is similar to that at Rose Mine: early NE to E vergent folding, faulting, and emplacement of the Doble

Thrust. The relation of these events to the overall Mesozoic deformational evolution at Big Bear is discussed below.

Distribution of Mesozoic S_2 Cleavage in Precambrian Gneisses.

Other basal contacts along the east limb of the Arrastre Creek Antiform were examined in reconnaissance for evidence of either S_2 or S_3 cleavage in the Precambrian gneisses. These fabrics were not observed, either near Broom Flat (Section 36, T2N, R2E), or at Onyx Summit. In these areas, the overlying Wildhorse Quartzites are not overturned as far, nor deformed as intensely, as near Rose Mine.

Tyler (1975) recognized a gently dipping Mesozoic cleavage (S_2) in basement gneisses immediately above the Doble Thrust north of Baldwin Lake. This cleavage strikes parallel to the thrust trace, and dips 10-20°S or SSW. The fabric crosscuts steeply dipping Precambrian foliation, and is defined by new biotite growth in augen gneisses. It is more sporadically developed than at Rose Mine (B.C. Burchfiel, personal comm., 1980). The relation of Mesozoic cleavage development to folding and thrusting of Precambrian gneisses is discussed below.

Sugarloaf Area

Introduction. Rocks in the Sugarloaf area lie above the Doble Thrust and record dynamothermal metamorphism and polyphase folding similar to the rocks at Rose Mine. Metamorphic assemblages (discussed below) are indicative of low P, intermediate T conditions, transitional between greenschist and amphibolite facies. Metamorphism and folding are thought to have occurred during a single, progressive deformational episode. This complexly folded terrane was subsequently disrupted by low-angle normal faulting, which shuffled these rocks into an overlapping stack of younger-over-older allochthons. Low-angle, younger-over-older faulting caused significant east-west extension in this area. The higher allochthons, exposed to the west, include progressively younger rocks. Basement-cored antiforms exposed in the lower blocks may be offset from

the crest of the Arrastre Creek Antiform. The emplacement of the higher allochthons was associated, in part, with magmatism related to the Sugarloaf Intrusive Complex. The highest allochthons are in many places engulfed by intrusive rocks. The relationship between magmatism and emplacement of the lower allochthons is uncertain. Plutonism associated with the Cretaceous batholith postdates these earlier structures. The sequence of structural events is summarized in Fig. 43.

Event 1: Metamorphism and Polyphase Folding. Metamorphism and polyphase folding are the earliest Mesozoic deformational events recognized in the Sugarloaf area. These events are interpreted to have occurred during a single, progressive deformational episode. Metamorphism began prior to penetrative deformation and continued during much of event 1 folding. The highest grade metamorphic assemblages indicate low P, intermediate conditions and are pre-kinematic with respect to folding. Three phases of folding are recognized. F_1 and F_2 folds formed synmetamorphically. The axial orientation of F_1 isoclinal folds is not certain. They are refolded by F_2 folds which trend NNW-NW and are E or NE vergent. F_3 folds are largely postmetamorphic, upright, and trend NE-SW. The general characteristics of each fold phase are summarized briefly below. The sequence and geometry of event 1 folding is then discussed for each structural block, along with kinematic data where available. The relationship between metamorphism and folding and the nature of basement involvement are discussed at the end of this section. Much of the complexity and confusion concerning the sequence and geometry of event 1 folding is the result of tectonic disruption due to later low-angle faulting and intrusion. Often, only fragments of the overall event 1 fold history are present in any one low-angle fault block. Because of this, the fold sequence in each block is described individually, as it is from these pieces of information that the interpretive sequence of event 1 folding is reconstructed. In a later section, the geometry of event 1 folds is used to palinspastically remove the effects of later faulting. Speculations concerning correlation of

Figure 43: Sequence of structural events in the Sugarloaf area

1. Metamorphism and polyphase folding
   Metamorphism: low-P, intermediate-T (greenschist-amphibolite facies transition); peak is locally prekinematic

   F_I: zonal tight to isoclinal asymmetric folding of miogeoclinal rocks
   F.A. orientation is variable (SW to NW trend); probably not initially homoaxial
   A.P. and S_1 cleavage dip parallel or at low angle to bedding (S_0)
   vergence is variable (S-NE)

   F_2: tight to open folds, involve Precambrian gneisses
   F.A. trend N-NW, plunge varies
   A.P. dip W or SW, or upright; S_2 cleavage present with asymmetric folds
   vergence is to E-NE; tectonic transport to NE

   F_3: typically open folds, involve Precambrian gneisses
   F.A. trend NE-SW, plunge varies
   A.P. typically upright, without associated cleavage
   (SE vergent F_3(?) folds are locally recognized and are associated with NW dipping S_3 cleavage)

2. High-angle faulting

3. Low-angle, younger-over-older faulting (normal faulting)
   a. lower structural blocks (I-VI) emplaced: transport generally to W, relation to magmatism is uncertain
   b. high-angle faulting
   c. higher structural blocks (VId-IX) emplaced: transport to W and N; faulting in part contemporaneous with emplacement of Sugarloaf Intrusive Complex

4. Emplacement of Sugarloaf Intrusive Complex

5. Emplacement of Cretaceous granite-quartz monzonite

F.A. = fold axes

A.P. = axial planes

event 1 structures between structural blocks is reserved until then.

F_1 folds and axial-planar (S_1) cleavage are the earliest event 1 structures recognized. Macroscopic and mesoscopic F_1 folds are tight to isoclinal, with short overturned limbs. Their axial orientations are variable, in part because of later refolding and tectonic rotation. It appears however, that F_1 folds are not strictly coaxial. NW and SW trending folds are present. Where closure is observed, F_1 folds are NE or SE vergent. S_1 cleavage dips at low angle to bedding on the limbs of F_1 folds. F_1 folding was synmetamorphic. F_1 folds and S_1 cleavage are irregularly developed, being most conspicuous in pelitic rocks and marbles. In some cases formations or members record internal isoclinal folding, in which original bedding is transposed but stratigraphic sequence is maintained. The axial surfaces of the F_1 folds are sub-parallel to bedding. F_1 folds are disharmonic. In general, macroscopic F_1 folds are most conspicuous in higher structural blocks, which were downdropped from higher stratigraphic-structural levels during event 3 low-angle faulting (discussed below). In lower structural blocks, macroscopic F_1 folds are rarer, although mesoscopic folds and S_1 cleavage are widespread. Throughout the map area, most rocks lie on the upright limbs of F_1 folds. No large amplitude recumbent isoclinal folds are recognized. It may be that F_1 structures in the map area formed in the upright limb of a large F_1 fold, perhaps involving basement gneisses, and that the hinge of this fold is not exposed in the study area. Alternatively, F_1 folding may have been confined to the Upper Precambrian-Paleozoic cover sequence, perhaps resulting from non-homogeneous bedding-parallel slip which died out at deeper structural levels (the latter interpretation is favored here).

F_2 folds refold F_1 structures and produce many of the macroscopic structures recognized here. F_2 folds typically trend NW-SE or N-S and usually plunge NW or N. The variation in trend and plunge of F_2 folds probably reflects rotation by later folds and faults. Both open and tight F_2 folds are present; many folds are overturned and are NE or E vergent. The overturned limbs are sometimes breached by F_2 reverse faults. Overturned folds have an irregularly developed axial planar cleavage

(S_2, sometimes a microscopic crenulation cleavage). Tectonic transport of overturned F_2 folds was apparently to the northeast. Upright F_2 folds have no penetrative cleavage. Precambrian gneisses are present in the cores of several F_2 folds, and in some cases Precambrian foliations are refolded.

NE-SW trending open folds refold F_1 and F_2 folds and S_1 and S_2 cleavage and are here assigned to an F_3 event. In some cases it is uncertain if these late folds belong to event 1, or are significantly younger. Because of similar style and orientation, all of these folds are discussed here. F_3 folds are typically upright and S_3 axial-planar cleavage is rare. Precambrian gneisses are involved in some F_3 folds and have been refolded along with overlying rocks.

F_2 folds in the Rose Mine area, including the Arrastre Creek Antiform, and F_2 folds in the Sugarloaf area are thought to have formed during the same fold phase. The Arrastre Creek Antiform has similar trend and vergence to F_2 folds in the Sugarloaf area. In fact, several basement-cored F_2 antiforms recognized in higher structural blocks in the Sugarloaf area may be offset from the crestal region of the Arrastre Creek Antiform along later low-angle normal faults. F_2 folds in the Sugarloaf and Rose Mine areas refold earlier isoclinal (F_1) folds and are themselves refolded by generally NE-SW trending open folds (F_3 and F_4 folds).

S_1 cleavage and possible F_1 folds are locally present in block I. S_1 cleavage-bedding relations at the east and west end of Deadman's Ridge indicate these rocks lie in the upright limbs of F_1 folds. Overturned quartzites exposed adjacent to the Erwin Fault (west segment) in Section 20 (T2N, R2E) may lie in the overturned limb of an F_1 syncline; the plunge of this syncline is unknown. The continuation of this fold across the Woodlands Fault is not certain. The lack of overturned beds in block I suggests that this syncline, and any other unrecognized F_1 folds, are of small amplitude, with short overturned limbs.

The complex outcrop pattern in block I has resulted from superposition of N-NW trending F_2 folds and NE-SW trending F_3 folds. The latter set of open, upright folds is here included with F_3, rather than F_1

largely on the basis of style. The NE trending folds are interpreted to refold F_2 folds, although unambiguous crosscutting relations are not present. Variation in trend and plunge of F_2 folds suggests they are refolded, however.

F_2 folds may have formed as an en echelon set. F_2 folds include the Gold Hill Synform and associated minor folds west of the Ranch Fault. These are truncated to the northwest by the Baldwin Fault and are underlain by the low-angle Shay Fault. East of the Ranch Fault, refolded F_2 folds are present on the east end of Gold Hill. These F_2 folds involve Precambrian gneisses. Correlative or en echelon F_2 folds south of the Erwin Fault include the Gocke Synform and Antiform at the east end of Deadman's Ridge. These folds plunge S and are truncated by the Arrastre Fault to the south and Erwin Fault (east segment) to the north. A gentle, NNW plunging antiform at the west end of Deadman's Ridge is considered an F_2 fold. Other F_2 folds may be present just south of Erwin Lake.

NE trending F_3 folds are interpreted to warp the F_2 folds, but the geometry of F_3 folds is disrupted by later faulting, particularly by the Erwin and Stray Cat faults. Prominent F_3 folds include the Erwin Antiform and Deadman's Synform, which plunge NE at 10-15°. Their common limb is locally cut by the Erwin Fault (west segment). These folds are interpreted to refold the inferred F_1 syncline in the upper plate of the Woodlands Fault. The Erwin Antiform is apparently cored by Precambrian gneisses; gneisses exposed east of the Stray Cat Fault on Deadman's Ridge are believed to lie in the core of this fold. This fold may cause the deflection in the trend and plunge of F_2 folds between Gold Hill and Deadman's Ridge. This basement-cored antiform may re-emerge northeast of the intersection of the Erwin and Stray Cat faults, the vicinity of Hill 7081'. South of the Erwin Fault (east segment) an open, WNW trending synform may be an F_3 fold. Gently NE plunging F_3 folds are also present southeast of the Deadman's Synform, and west of the Stray Cat Fault. On Gold Hill, northeast trending F_3 folds also involve Precambrian gneisses and appear to refold F_2 folds.

In blocks II and III, no clear examples of F_1 fabrics were recognized, although upright bedding indicates these rocks would lie in the upright limbs of any major F_1 folds. Basal quartzites in block II generally dip northwest, and southeast of Balky Horse Canyon may be folded into a gently north plunging (F_2?) synform. Younger faults have cut block III into three sub-blocks. In sub-block IIIa, a major F_2 structure, the basement-cored May Van Antiform, is exposed. The antiform plunges 15°/N30W in the May Van Canyon area. Precambrian foliations appear to be refolded by this structure, although shortening by reverse faulting may have occurred as well (the steeply SW dipping fault zone in May Van Canyon may have had its initial movements during event 1). Cleavage related to this upright fold was not recognized. Generally NE dipping Wildhorse Quartzite in sub-blocks IIIb and IIIc is believed to be downfaulted from the northeast limb of the antiform. Quartzites on this limb extend southeast of the Balky Horse Fault and beyond the map area. Dibblee (1964a, 1967a) has traced these quartzites to the vicinity of Onyx Summit (Plate I). He mapped the contact with underlying gneisses (exposed southeast of the Lightning Gulch Fault) as depositional, but McJunkin (1976) recognized a low-angle fault contact below these quartzites. Thus, it is uncertain if the gneisses in the core of the May Van Antiform extended south of the map area, to re-emerge beneath blocks V and VI. The northeast limb of this fold, however, does appear continuous to the southeast.

The northeast limb of the May Van Antiform is refolded by F_3 open folds which plunge NE at 20-30°. Locally, in sub-block IIIb, a refolded F_2 fold plunges gently southeast. F_3 folds may warp the southwest limb of the May Van Antiform as well. In general, the map pattern suggests the presence of a fold-interference dome here, but lack of quartzite outcrop on the southwest limb makes this difficult to demonstrate.

The presence of a nearly isoclinal F_1 fold, the Wildhorse Road Syncline, is inferred in the northwestern part of sub-block Va. The hinge of this refolded fold is not exposed; its presence is suggested by outcrop pattern, facing reversals and mesoscopic structures. The

syncline is cored by member W2 of the Wildhorse Quartzite where sub-block Va reappears beneath sub-block VIc on the north slope of Hill 8055'. Its axial trace disappears beneath allochthonous rocks of sub-block VIc when followed along trend. The syncline is refolded by a moderately NW plunging F_2 synform-antiform pair, and is further disrupted by complex faulting. On the synform's east limb, S_1 cleavage dips 40-58° NW and $S_0 \times S_1$ lineations plunge about 45°/S70W. It is not known if a conjugate F_1 anticline is present in rocks immediately to the northwest of the Wildhorse Road Syncline. S_1 cleavage here still dips to the NW, and is subparallel to bedding. The poorly exposed quartzites north of Wildhorse Road lie in the limb of an F_1 fold, but facing could only be recognized in one locality (top to the SE). These quartzites could be complexly folded by F_1 folds.

Southeast of Hill 8055', rocks of sub-block Va lie in the upright limb of the F_1 syncline, as presumably do the rocks of block IV. S_1 cleavage in the Green Canyon area dips at a low angle to bedding, and appears to be folded by the Green Spring Antiform, an F_2 fold.

F_2 folds trend NW. The Green Spring Antiform is an open fold, which plunges NW at about 10-20°. Its hinge area is covered, and may be cut by an F_2 reverse fault (southwest side up). The northeast limb of the Green Spring Antiform continues southeast of the Balky Horse Fault, and near Wildhorse Meadows Precambrian gneisses are exposed in the core of the antiform. NW dipping Wildhorse Quartzite in block IV may have lain in the west limb of the Green Spring Antiform. West of the antiform, tighter F_2 folds, plunging NW at about 25-40°, refold the Wildhorse Road Syncline. Unfortunately, the nature of the F_1-F_2 fold interference pattern here could not be determined. S_2 cleavage was not observed in the quartzites of block Va.

F_3 open folds trend NE-SW and refold F_2 structures. A NE plunging fold refolds the northeast limb of the Green Spring Antiform in the Wildhorse Spring area; on the southeast limb of this F_3fold, $\perp S_0$ plots indicate F_2 folds plunge SE. On the opposite limb of the Green Spring Antiform, F_3 folds plunge WSW in the lower Green Canyon area. F_3 folding

may be responsible for the steepening of F_2 fold axes in the Hill 8055' area.

All three fold phases are recognized in sub-block VIa, and their superposition has produced some interesting fold interference relations. Precambrian gneisses in the southwest portion of the map area may be in an interference dome. Unfortunately, my mapping does not extend south of here, so I must rely on pre-existing maps to interpret the continuation of event 1 structures I recognized into areas of sub-block VIa I did not map. The geometry of event 1 folding proposed for these areas of sub-block VIa should be considered speculative.

F_1 cleavage and mesoscopic folds are present in sub-block VIa. These fabrics are refolded by F_2 and F_3 folds. Macroscopic F_1 folds were not recognized in this sub-block within the map area. North of the Balky Horse Fault, S_1 cleavage typically (but not always) dips slightly less steeply than bedding. Mesoscopic isoclinal folds are NE vergent and plunge NW on the upright, N to NW dipping limbs of F_2 folds. These are Z folds. Overturned limb length is very short, and bedding is almost always upright where facing indicators are present.

South of the Balky Horse Fault, more severe F_1 deformation has resulted in transposition of original bedding in pelitic rocks of the Lightning Gulch exposed on the northeast limb of the F_2 Lightning Antiform. Mesoscopic F_1 folds are present in float blocks of the Wildhorse Greenstone and in outcrops of pelitic rocks (axial orientations could not be observed however). Although sedimentary features are frequently obliterated, proper stratigraphic sequence is maintained. S_1 foliation or cleavage here dips parallel to or slightly shallower than bedding. The variable development of F_1 fabrics within single formations in sub-block VIa indicates inhomogeneous distribution of strain during F_1 folding. Rocks south of the Balky Horse Fault may have been closer to a macroscopic F_1 fold hinge. F_1 lineations appear to be refolded along with S_1 cleavage.

Precambrian gneisses in the southwest portion of sub-block VIa and southeast of the Balky Horse Fault lie in the core of an E-W trending antiform mapped by McJunkin (1976). South of the map area, these gneisses

structurally overlie an overturned, N dipping sequence of quartzites. McJunkin interpreted the gneiss-quartzite contact as depositional, and suggested the quartzites (= Wildhorse Quartzite?) lay in the overturned south limb of an E-W trending antiform. According to McJunkin's map, upper Precambrian rocks of sub-block VIa mapped in this study would lie in the antiform's upright limb. The orientations of F_1 fabrics in this "limb" suggest this antiform is not an F_1 structure. S_1 cleavage typically dips shallower than bedding. The opposite would be expected if S_1 cleavage was axial planar to a S vergent anticline. Mesoscopic F_1 folds are NE vergent, not S vergent as would be expected. It is suggested the antiform recognized by McJunkin is a post-F_1 fold. Its possible relation to later F_2 and F_3 folds in the study area is discussed further below. McJunkin suggested the S vergent antiform might be related to the late Cenozoic Santa Ana Thrust, which cuts the fold's overturned limb. This is possible based on data available to me.

F_2 folds in sub-block VIa plunge NNW to NW and refold S_1 cleavage. West of the Trail Fault, the Sugarloaf Antiform and Synform are major F_2 structures. Their common, overturned limb is breached by a steeply SW dipping (F_2?) reverse fault. West of the antiform, the Sugarloaf Saddle Synform is also breached by an F_2 reverse fault. The Sugarloaf Antiform is cored by Precambrian gneisses which are folded by the F_2 fold but contain no penetrative F_2 cleavage. The fold axis of the antiform varies in orientation down plunge, from 40°/NNW in the southeast to 25°/N36W at the crest of Sugarloaf Ridge. The hinge of the adjacent Sugarloaf Synform is tectonically duplicated across a NW trending, largely concealed fault. The F_2 fold axis is essentially coincident in both outcrop areas, plunging about 20°/N58W. An S_2 cleavage (often a microscopic crenulation cleavage) is recognized in the hinge area, and dips about 20°W. $S_0 \times S_2$ lineations parallel the macroscopic F_2 fold axis, as do many F_1 fold axes in the core of this fold. The upright limb of the Sugarloaf Synform is locally warped by F_3 folds which fold S_2 cleavage and produce a basin-like fold interference pattern west of the Trail Fault.

A highly questionable F_2 transport direction for the Sugarloaf Synform (southern fault block) was determined by using the method of folded lineations (Turner and Weiss, 1963). F_1-related lineations plunge WNW (sub-parallel to the F_2 fold axis) on the northwest and north dipping limbs of the fold. One $S_0 \times S_1$ lineation plunges east, on the northeast dipping limb (Fig. 44). These lineations lie on a great circle girdle which is essentially defined by the single east plunging lineation. If the lineations were colinear and were reoriented by F_2 similar-type folding, then the F_1-related lineations should lie along a great circle girdle (Turner and Weiss, 1963). The intersection of this great circle with the F_2 slip plane (average S_2 cleavage orientation in the synform) yields the F_2 transport direction, ESE in this case (Fig. 44). I am skeptical about the validity of this determination. The great circle girdle is defined by a single data point in this case, and all other F_1-related lineations are nearly co-axial with the F_2 axis. Owing to the sporadic development of F_2 cleavage I am skeptical that this synform developed as a similar-type fold (flexural-slip or flexural-fold folding appears more likely to me). Finally, the deduced F_2 transport direction parallels the F_2 fold axis. This phenomenon is recognized for folds found in zones of high F_2 strain (such as mylonite zones) where progressive deformation causes rotation of early-formed fold axes into near parallelism with the direction of tectonic transport (Hobbs and others, 1976). Such an explanation does not appear likely in this case however. I suspect a more likely explanation is that F_1-related lineations were not strictly colinear prior to F_2 folding.

F_2 folds are also thought to be present east of the Trail Fault, but their geometry is not as certain. Rocks north of the Balky Horse Fault are warped by an open F_2 fold, the Meadows Antiform, which plunges 40°/NNW. Mesoscopic F_2 folds here have a similar plunge (Fig. 45). The inclination of plunge may decrease southwards. South of the Balky Horse Fault, northeast dipping Wildhorse Quartzite overlying the Pre cambrian gneisses may lie in the offset, northeast limb of the Meadows Antiform. An open F_2 synform separates this limb of the Meadows Antiform and the NNW plunging Lightning Antiform, whose northeast limb is locally overturned. In places

Figure 44: Equal-area plot of mesoscopic structural data from the Sugarloaf Synform (south block) in sub-block VIa.

Figure 45: Equal-area plot of mesoscopic structural data from sub-block VIa, east of the Trail Fault.

Sub-block VI a - E. of Trail Fault

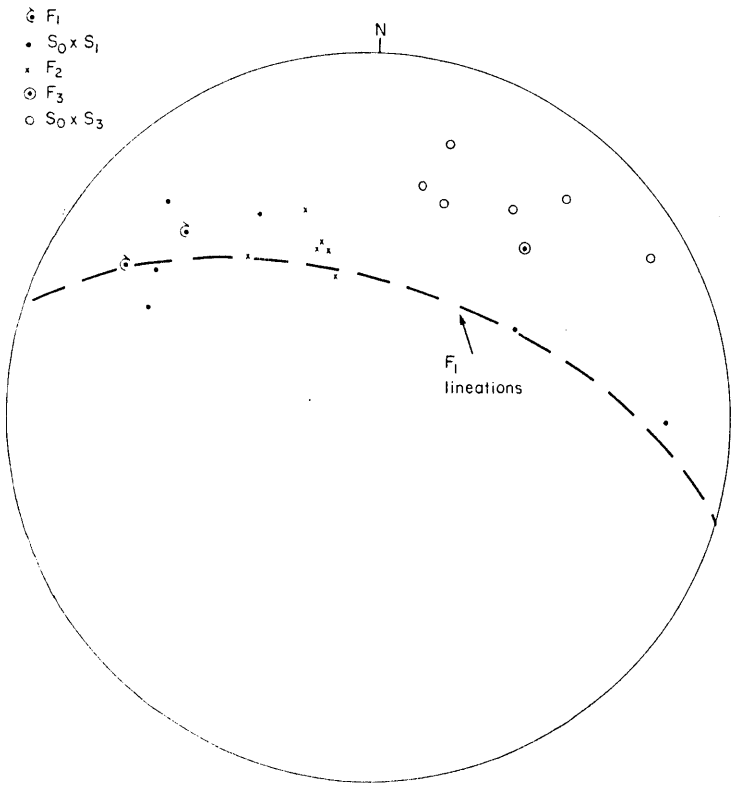

Sub-block VI a Sugarloaf Synform - S. block

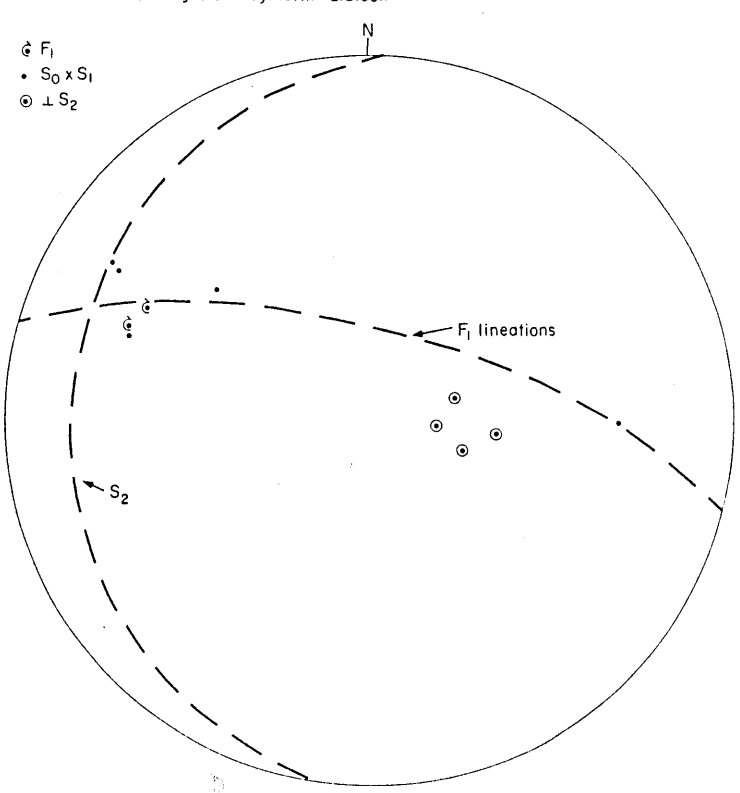

along this limb, bedding in pelitic rocks is completely transposed into an S_1 foliation, but stratigraphic sequence is preserved. Mesoscopic F_1 isoclinal folds are present in the Wildhorse Greenstone and Lightning Gulch Formation. These are interpreted as F_1 fabrics, even though similarly severe transposition of bedding is not recognized elsewhere in sub-block VIa, even on the overturned limbs of other F_2 folds. Strain associated with F_1 folding is not homogeneously distributed, but is localized lithologically and areally as discussed above. F_3(?) folds also refold F_1 fabrics on the northeast limb of the Lightning Antiform. No F_2 axial-planar cleavage is recognized in association with F_2 folds in sub-block VIa east of the Trail Fault.

The Meadows Antiform and Sugarloaf Synform are interpreted to share a common limb, based on stratigraphic and structural similarities. The Trail Fault is believed to be primarily a left-slip fault. When slip across this fault is restored, the plunge of F_2 folds within sub-block VIa is seen to change progressively, from NNW to NW, down plunge from SE to NW. This may reflect the effects of F_3 folding.

F_3 folds are present in sub-block VIa. Gently W-SW plunging folds which warp the upright limb of the Sugarloaf Synform and refold F_2 cleavage there were mentioned above. F_2-F_3 superposition here produces a Ramsay (1967) type I fold interference basin (F_2 and F_3 axes intersect at close to 90°; F_3 transport direction is at a high angle to S_2). Mesoscopic (northeast plunging) F_3 folds are recognized in the northeast limb of the Sugarloaf Antiform.

East of the Trail Fault, NE plunging F_3(?) folds and associated cleavage are present. These structures are interpreted to postdate F_2 structures, but this relationship cannot be clearly demonstrated based on my data. Disharmonic F_3(?) folds affect rocks of the Lightning Gulch Formation on the northeast limb of the Lightning Antiform. These locally overturned folds plunge at 25-35°NE. Irregularly developed axial-planar S_3 cleavage is locally associated with these folds, and dips moderately NW. $S_0 \times S_3$ lineations here also plunge NE (Fig. 45). As other F_3 folds are generally upright and lack cleavage, these folds are rather distinctive. North of the Balky Horse Fault, a subvertical or NW dipping spaced fracture

cleavage is recognized in rocks on the west limb of the Meadows Antiform which may also be related to F_3(?) folding. This cleavage dips steeper than bedding, and bedding-cleavage intersections plunge NE (Fig. 45). Based on analogy with fold superposition recognized elsewhere in the Sugarloaf area, it is suggested that NE trending F_3(?) folds here are superposed on earlier F_2 folds. F_3(?) linear elements from sub-area VIa east of the Trail Fault do not appear to be refolded by F_2 folds, but rather, maintain a consistent NE plunge on both NE and NW dipping limbs of F_2 folds (Fig. 45).

In contrast, F_1 linear elements from this area plunge NW on northwest dipping limbs of F_2 folds and E on northeast dipping limbs (Fig. 45). I suggest this is due to rotation by F_2 folding. The limited mesoscopic data permit a great circle girdle to be fitted to the F_1 lineation data, suggesting F_2 folds are of similar type. Owing to the limited data base and uncertainty concerning the additional effects of F_3(?) related rotation on the E plunging points I don't attach much kinematic significance to this girdle. I suspect these F_2 folds are more likely flexural-slip or flexural-flow folds rather than similar folds.

Superposition of F_2 and F_3(?) folds may have resulted in the dome-like outcrop pattern of Precambrian gneisses in the SW portion of sub-block VIa (both in the map area and beyond; see Plate I). It is possible that the NW dipping S_3 cleavage and SE vergent F_3(?) folds are related to the S vergent basement-cored antiform recognized south of the map area (McJunkin, 1976). Perhaps the overturning recognized by McJunkin (1976) is related to Mesozoic, rather than Cenozoic folding. As mentioned above, the variations in F_2 fold plunge in sub-block VIa may be related to later tectonic rotation, perhaps due to F_3(?) folding. The northward steepening in dip recognized in rocks of sub-block VIb (cross sections B-B', C-C'), might be due to NE trending F_3(?) folding. It is possible that Precambrian gneisses in the SW1/4 of section 4 (T1N, R2E) might be in the nose of an open, gently NE plunging F_3(?) antiform.

Because of extreme tectonic disruption by later faulting, the reconstruction of event 1 folding in sub-blocks VIc and VId is more tentative. In sub-block VIc, rare mesoscopic isoclinal folds of F_1 generation are present in phyllites of the Lightning Gulch Formation. These can be recognized in exposures along Green Canyon, above fault c-1 (see Plate VI for location). F_1 fold axes and $S_0 \times S_1$ intersection lineations plunge moderately W or WSW on the limbs of F_2 folds. S_1 cleavage parallels bedding except in F_1 fold hinges. Mesoscopic F_1 folds are apparently restricted to the poorly exposed pelitic rocks, and are not recognized in the massive quartzite members of the Sugarloaf Quartzite. Tectonic decoupling between rocks of the Lightning Gulch Formation and overlying Sugarloaf Quartzite is common in the study area, and in many cases may have first occurred during disharmonic F_1 folding. Later younger-over-older fault block displacements were often localized along these sheared contacts. In a younger-over-older fault block of Sugarloaf Quartzite (member S1) just north of Hill 8055', overturned beds dip 70° N. This overturning could be related to an F_1 fold, as this sense of vergence is not typical of F_2 or F_3 folds in sub-block VIc.

Both macroscopic and mesoscopic F_2 folds are present, along with S_2 axial-planar cleavage. The plunge of F_2 folds and orientation of S_2 cleavage varies either due to F_3 refolding or later fault block rotations. Tight F_2 folds are overturned to the NE or E; they plunge between 0 - 30° W or NW. A W-plunging synform cored by Sugarloaf Quartzite is the most conspicuous F_2 fold. Bedding-S_2 cleavage relations indicate this fold is overturned to the N-NE. To the east and west of this fold, other E vergent F_2 folds are recognized in rocks of the Lightning Gulch Formation. These folds plunge NW or S, with axial surfaces and S_2 cleavage dipping shallowly W. Low-angle and high-angle faults separate Lightning Gulch rocks with NW plunging F_2 folds from the W plunging F_2 synform described above. This variation in F_2 fold plunge is probably the result of later tectonic rotations.

Above fault c-1, F_1 linear fabrics refolded by S plunging F_2 folds can be fitted to a NE trending great circle, permitting the interpretation that these F_2 folds approximate similar fold geometry. Using the method of refolded lineations to determine the transport direction for similar folds (Turner and Weiss, 1963) yields an ENE transport direction for these F_2

folds (Fig. 46). However, considering the limited spread of points defining the F_1 lineation great circle, this local F_2 transport direction should be regarded with caution.

The presence of F_3 folding in sub-block VIc is uncertain. F_2 fold axes and $S_0 \times S_2$ lineations from sub-block VIc as a whole lie along a small circle girdle with a SW trending, horizontal axis (Fig. 46). This dispersal could be the result of rotation during F_3 flexural slip folding (Turner and Weiss, 1963), or, perhaps more likely reflects fault block rotations, unrelated to folding. There is some evidence for minor later folding of sub-block VIc, discussed below.

F_1 and F_3 folds are present in sub-block VId. Lightning Gulch Phyllites on the north slope structurally underlie numerous, younger-over-older fault slivers of Sugarloaf Quartzite. These phyllites are depositionally(?) overlain by upright quartzites of member S1, which cap the ridge to the south. The phyllites are disharmonically folded into tight, nearly isoclinal, mesoscopic F_1 folds with well-developed axial planar S_1 cleavage. One well-exposed F_1 anticline plunges gently SSW and verges E. These F_1 folds and S_1 cleavage are folded by F_3 folds. Overlying rocks of the Sugarloaf Quartzite in the south are folded into an F_3 synform, and apparently lie in the upright limb of a macroscopic F_1 anticline. The overturned limb of this anticline is exposed south of a NE trending high-angle(?) fault. Rare crossbeds and bedding-S_1 cleavage relations suggest the rocks south of the high-angle fault lie in the overturned limb of an F_1 anticline. The hinge of this fold is not exposed. An $S_0 \times S_1$ lineation on the overturned limb plunges 31°/S29W. An outlier of sub-block VId rocks, downdropped along the Woodlands Fault, consists of overturned Lightning Gulch Formation and Sugarloaf Quartzite. These rocks may also have lain in the overturned limb of the F_1 anticline, as may have rocks exposed between fault segments n and g4 (see plate VI for location).

F_3 folds plunge SW and refold S_1 cleavage. F_1 fold axes and $S_0 \times S_1$ lineations from sub-block VId lie along a small circle girdle, about a SW plunging, near horizontal axis (Fig. 47). The open F_3 synform which folds Sugarloaf Quartzites in the upright limb of the F_1 anticline also plunges SW.

Figure 46: Equal-area plot of mesoscopic structural data from sub-block VIc.

F_3? axis represents pole to small circle girdle fitted to F_2 linear elements. F_2 transport direction determined for folds above fault C-1.

Figure 47: Equal-area plot of mesoscopic structural data from sub-block VId.

F_3 axis represents pole to small circle girdle fitted to dispersed F_1 linear elements.

Sub-block VI d

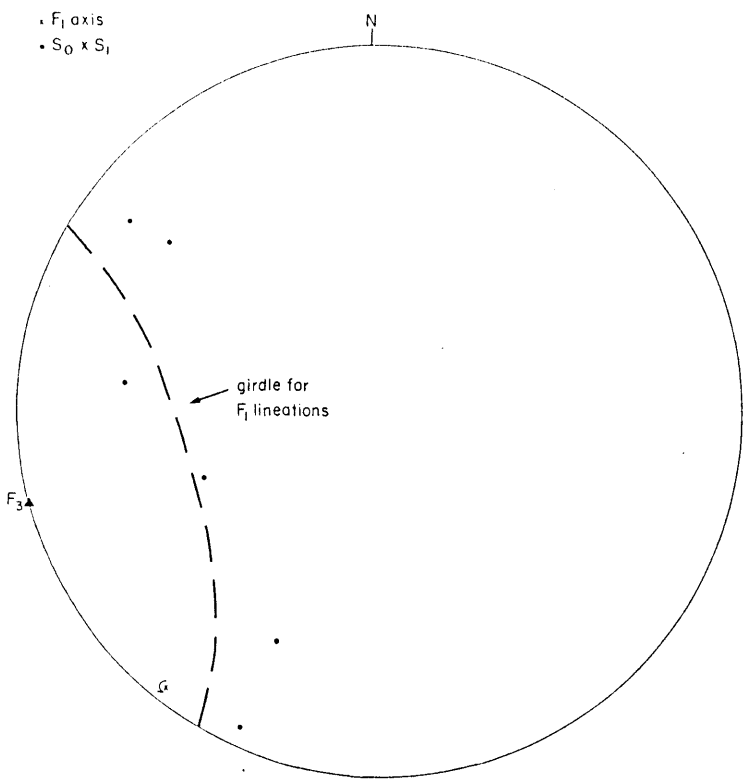

Sub-block VI c

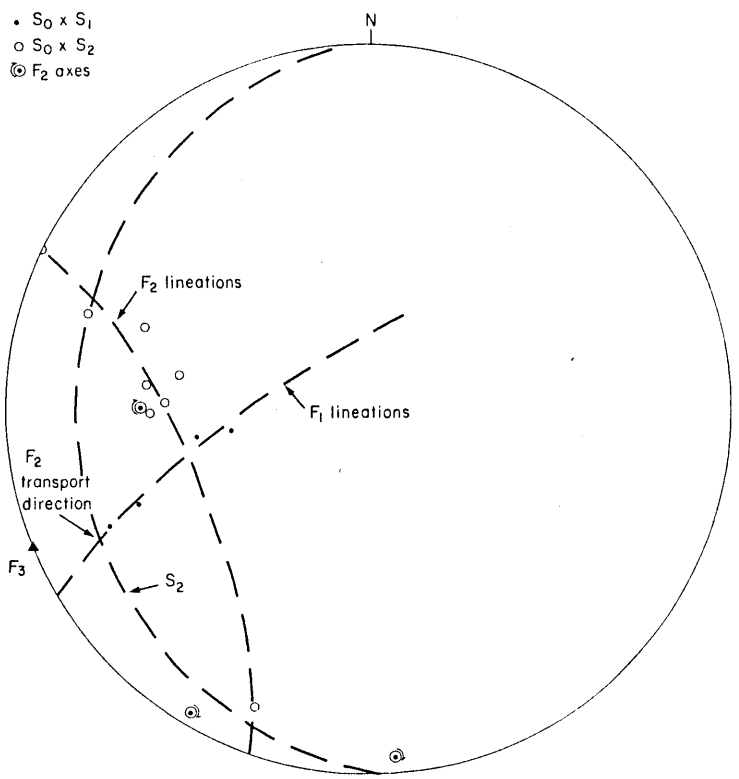

Event 1 structures in the highest blocks, VII, VIII and IX, have been particularly disrupted by later deformational events. In some cases, the sequence and geometry of early folding events cannot be reconstructed with any certainty. Elsewhere, these rocks record a sequence of polyphase folding similar to that in lower structural blocks. Here, F_1 and F_2 folds are tight and locally isoclinal. Both have associated axial-planar cleavage. Thus in cases where superposition of folds is not present or not obvious, it is generally not possible to differentiate F_1 and F_2 folds based on style alone. Fold axial orientation is also a questionable criteria in several cases where rotation across later low-angle faults is a possibility.

Rocks of sub-block VIIa are so disrupted by later faulting and intrusion that event 1 fold phases could not be subdivided. A minor thrust here is probably an F_2 structure. Evidence of macroscopic F_1 folds is lacking. However, mesoscopic F_1 folds and S_1 cleavage are recognized in isolated exposures of Lightning Gulch Formation in the NE1/4 of Section 6 (T1N, R2E). S_1 cleavage and F_1 folds are refolded by gently NNW plunging F2 folds. These outcrops may be downdropped from the nose of the Sugarloaf Antiform in block VIa.

In rocks included in sub-blocks VIIb and VIIc, three phases of event 1 folding are locally present. F_1 is represented by several macroscopic tight to isoclinal folds, as well as mesoscopic isoclinal folds. The latter are irregularly developed, being most common in thick units of marble or phyllite where original bedding is typically transposed into parallelism with F_1 axial surfaces and S_1 cleavage. Mesoscopic F_1 folds are rare in quartzite units, where stratigraphic facing remains consistent on the limbs of later F_2 and F_3 folds. In quartzites and sometimes in marbles and phyllites as well, primary sedimentary structures are preserved. Here, S_1 cleavage is axial-planar to macroscopic F_1 folds and dips at a low angle to bedding on fold limbs.

Macroscopic F_1 folds are present in sub-block VIIc. Rocks of members G4 and G5 of the Green Canyon Formation, exposed in the southern portions of sub-blocks VIIc-1 and VIIc-2, are interpreted to lie in the core of an F_1 anticline. This anticline is refolded by NW plunging F_2 folds (in particular the Green Canyon Synform) and locally by a NE plunging F_3 synform;

all three fold sets are cut by younger low-angle faults which have disrupted the fold interference patterns. S_1 cleavage, F_1 fold axes and $S_0 \times S_1$ intersection lineations are refolded. The original orientation of the F_1 fold is uncertain. Geometric analysis is complicated by F_3 folding of the west limb of the F_2 synform.

Immediately to the south, rocks of sub-block VIIb-2 are in fault contact with the steep S limb of the F_1 anticline. Rocks of members G1 through G3 are internally isoclinally folded, and are interpreted to lie in the upright limb of a macroscopic F_1 fold. These same units are folded into an overturned, isoclinal F_1 anticline-syncline pair in sub-block VIIb-1; the rocks in sub-block VIIb-2 may have lain in the upright lower limb of the syncline of this fold couple and were offset by later faulting. The axial surfaces of the F_1 folds in sub-block VIIb-1 dip moderately NW, and their common limb is cut by a complex fault zone which includes segments of F_1 thrust faults. The plunge of these F_1 folds is not certain; however, it may parallel the plunge of the $S_0 \times S_1$ intersection lineation (30°/N75W) in a thrust sliver. S_1 cleavage in this sliver parallels the axial surface of the major F_1 folds. Rocks here assigned to sub-block VIIb-1 extend further west, but are so discontinuous that their fold geometry could not be determined.

The above interpretation is based on the favored stratigraphic reconstruction of the Green Canyon Formation, discussed in Chapter II. If the alternative correlations discussed there are used (members G1=G5, G2=G6, G3=G7), then a somewhat different tectonic reconstruction emerges (Fig. 48). In this case, an F_1 anticline-syncline pair is recognized in the southern portion of block VII. The low-angle fault separating sub-block VIIc-1 and sub-block VIIb-2 (Plate VI) is interpreted as an F_1 thrust rather than a later, low-angle normal fault. This thrust may be the same thrust cut by the NE trending fault in sub-block VIIb-1. The F_1 thrust breaches the overturned, common limb of the F_1 anticline-syncline pair, and these structures are refolded by NW plunging F_2 folds. This alternative interpretation of F_1 fold geometry is compatible with observations concerning later event 1 folding and younger faulting events (discussed below).

Figure 48: Alternative geologic-tectonic map for portions of sub-blocks VIIb and VIIc. This map is based on alternative stratigraphic interpretations for the Green Canyon Formation discussed in Chapter II ($g_1 = g_5$, $g_2 = g_6$, $g_3 = g_7$). In this interpretation, member g_4 is lowest unit of the Green Canyon Formation exposed in the Figure 48 map area. Unit symbols and structural symbols are the same as in Plates II and VI. Mesozoic igneous rocks and surficial deposits are omitted.

Fig. 48

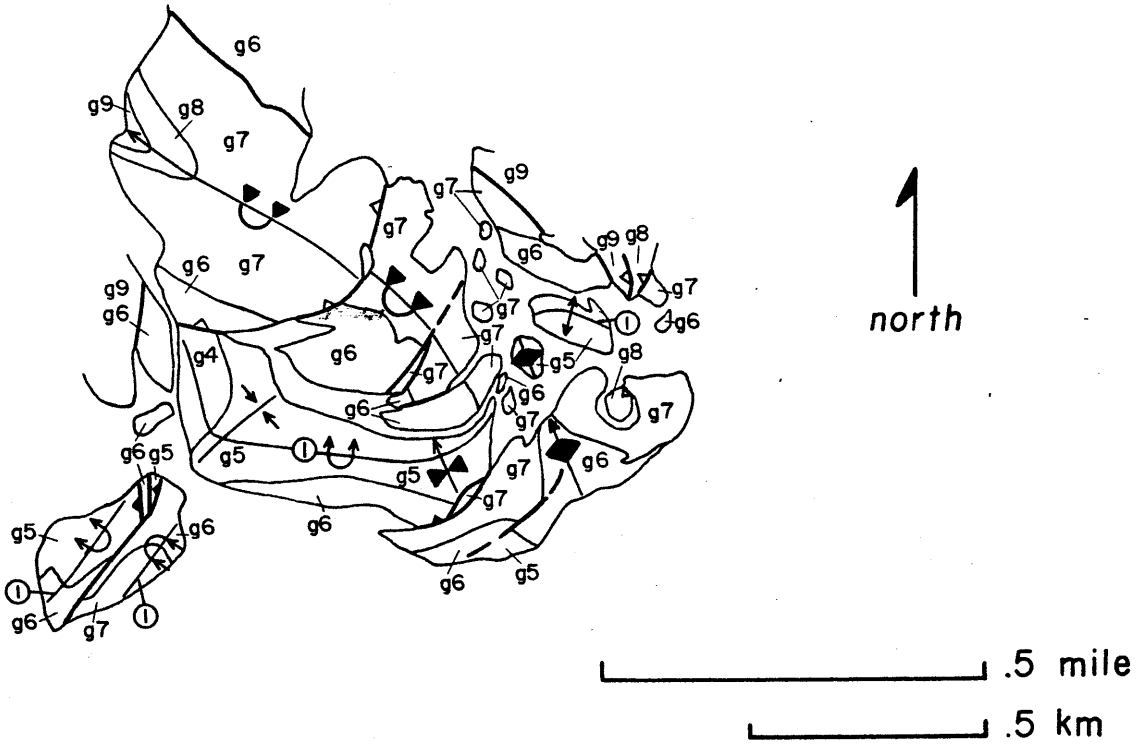

Other macroscopic F_1 folds may be present in sub-block VIIc-1, particularly in the marble members G7 and G9 of the Green Canyon Formation. However a lack of stratigraphic markers makes such folds difficult to recognize. Member G8 quartzites in the southwestern portion of sub-block VIIc-1 are complexly folded and faulted. Some of the tight folding here is probably F_1 folding.

F_2 folds in sub-blocks VIIc-1 and VIIc-2 plunge NW, and include the Green Canyon Synform, a tight fold which is overturned to the NE. An adjacent F_2 antiform to the northeast is also inferred to refold the F_1 anticline. Rocks in sub-block VIIc-2 lie in this antiform's northeast limb. Its western limb, common to the Green Canyon Synform, appears in part to be faulted out. In the lower Green Canyon area, a complexly folded and fault-bounded sequence of rocks, assigned to member G6 of the Green Canyon Formation, is interpreted to lie in the upright, NE limb of the Green Canyon Synform based on bedding-S_2 cleavage relations. Southwest of the Green Canyon Synform, rocks of member G6 may lie within another NW plunging F_2 antiform. These rocks are down-faulted against older rocks to the southeast which lie in the F_1 anticline's core. Younger rocks of the Green Canyon Formation are down-faulted to the west, and perhaps originally lay in the southwest limb of this F_2 antiform. In rocks of sub-block VIId, a NW plunging F_2 synform is recognized.

Geometric analysis was attempted for F_2 folds which refold the F_1 anticline in sub-blocks VIIC-1 and VIIC-2 (Fig. 49). This is complicated however, because F_1-related lineations are dispersed on the west limb of the Green Canyon Synform. In part, this may be due to F_3 refolding of this limb. In addition, however, F_1 fold axes may not have been strictly coaxial. This can be seen in outcrops of member G5 where F_1 fold axes vary in plunge although the axial surfaces of these folds dip consistently to the NE. In a general way, however, the present dispersal of F_1-related linear elements is suggestive that prior to F_3 folding they lay along a crude great circle girdle, rather than a small circle girdle about the NW plunging F_2 axes. If similar-type folding is assumed for these tight F_2 folds, then an approximate F_2 transport direction can be obtained. A

Figure 49: Equal-area plot of mesoscopic structural data from F_1 anticline refolded by F_2 folds in sub-block VIIc.

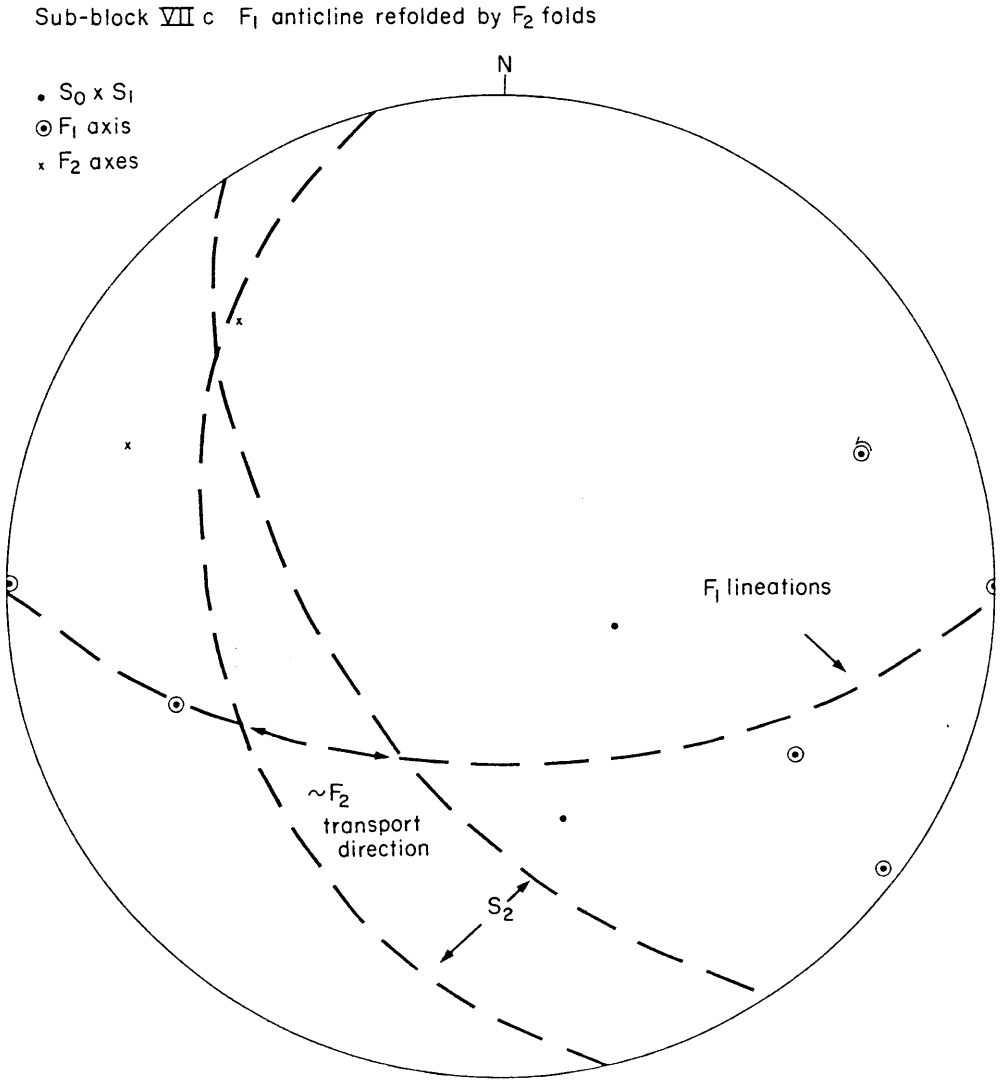

great circle can be fitted to F_1 lineations within the F_1 anticline by ignoring the local scatter on the west limb of the synform. The intersection of this great circle and the F_2 slip plane (average S_2 axial-planar cleavage orientation) yields an ENE F_2 transport direction, consistent with the vergence of F_2 folds.

F_3 folds are locally present in the sub-block VIIc. Rocks in the core of the F_1 antiform, lying in the west limb of the F_2 Green Canyon Synform, are locally refolded by a NE plunging open fold which refolds S_1 cleavage and axial surfaces of F_1 folds. Other F_3 folds warp rocks in member G6 along this limb. Intruded low-angle faults which cut F_1 and F_2 folds here also appear to postdate these F_3 folds. Other W or SW plunging F_3 open folds locally affect rocks on the northeast limb of the Green Canyon Synform.

In sub-block VIIe, macroscopic event 1 folds are present but it is difficult to differentiate F_1 and F_2 folds. On the southwest end of Deadman's Ridge, a tight, nearly isoclinal synform within Green Canyon Formation rocks trends N and is overturned to the E. A similar tight, NW plunging synform is found in an overlying low-angle fault block. Whether these are F_1 or F_2 folds is not known. Both SW and NW trending folds are recognized on Green Spot Hill, but later faulting has obscured their relative time relationships. The central fault block of Delamar Mountain Formation rocks may be folded into a SW trending synform; rocks on the north side of the hill at least locally top to the southeast. It is suspected that NW dipping quartzites there are overturned, and lie in the overturned limb of a major fold, perhaps an F_1 syncline. The southeast limb of this "fold" is refolded by NW plunging (F_2?) folds. The relation of these folds to synforms in adjacent fault blocks is unknown.

Event 1 fold geometry of block VIII is particularly disrupted by later intrusive activity. Nevertheless, outcrop distribution and bedding-cleavage relations suggest the existence of tight W-SW plunging folds. Axial-planar cleavage dips steeply N or is sub-vertical. Although this

orientation is similar to that of F_3 folds in other blocks, the style of folds in block VIII is that of F_1 or F_2 folds. As their plunge and vergence is unlike that of other F_2 folds, these are tentatively assigned to the F_1 phase.

In block IX, F_1 folding is represented by mesoscopic isoclinal folds which have transposed original bedding. The axial surfaces of these folds was parallel to original bedding. These folds are refolded by SW plunging, SE vergent folds with locally developed axial-planar cleavage. Here, although the orientation of these later folds is more typical of F_3 structures, their tight, locally isoclinal form is not. These may be F_2 folds, in which case block IX has rotated significantly with respect to other blocks. Alternatively, these folds may represent a second stage of F_1 folding, formed during progressive F_1 deformation.

In this section, the textural evidence bearing on event 1 metamorphism and folding is summarized. The P, T conditions of metamorphism in the Big Bear area are discussed in a later section. In the Sugarloaf area, event 1 metamorphism began prior to F_1 folding. In pelitic and mafic rocks, the highest grade assemblages recognized are prekinematic with respect to F_1-related fabrics. Metamorphic conditions persisted during F_1 and F_2 folding. This is indicated by the development of penetrative fabrics associated with the growth of metamorphic minerals and evidence of rock flowage during deformation. F_3 folding may have been largely post-metamorphic.

Locally, metamorphic mineral growth is recognized which is prekinematic with respect to F_1 folds and fabrics. This is most clearly indicated by pelitic rocks, particularly those of the Lightning Gulch Formation and Sugarloaf Quartzite in sub-block VIa. These rocks often contain prophyroblasts of andalusite, biotite and chlorite and pseudoporphyroblasts of quartz and micas. In hand specimens from the upright limbs of F_1 folds, they appear randomly oriented. In thin section however, most of these porphyroblasts are deformed. Prekinematic biotite and chlorite formed in random orientation and were deformed by kink bands or kink folds as they rotated toward parallelism with S_1 cleavage (Fig. 50).

Figure 50: Photomicrographs of deformed prekinematic porphyroblasts from the Lightning Gulch Formation (member L2), Sugarloaf area.

a) Prekinematic biotite porphyroblast is deformed by kink folds. Trace of variably developed S_1 cleavage approximately parallel axial trace of kink folds ($\sim$ parallel to width of photo), and subparallel to bedding (defined by quartz inclusions in biotite) which dips steeply to left. Stratigraphic top is to left.

b) Kinked prekinematic biotite porphyroblast is partially enclosed by prekinematic andalusite porphyroblast. S_1 cleavage in matrix is parallel to NE-SW diagonal of photo. That portion of biotite not enclosed by andalusite grain was kink-folded during development of S_1. Stratigraphic top is toward NW corner.

Both a) and b) are from same thin section. Length of photos equals 2 mm. Both were taken in plane polarized light. Sample collected from the W1/2 of Section 4 (T1N, R2E).

Figure 50a.

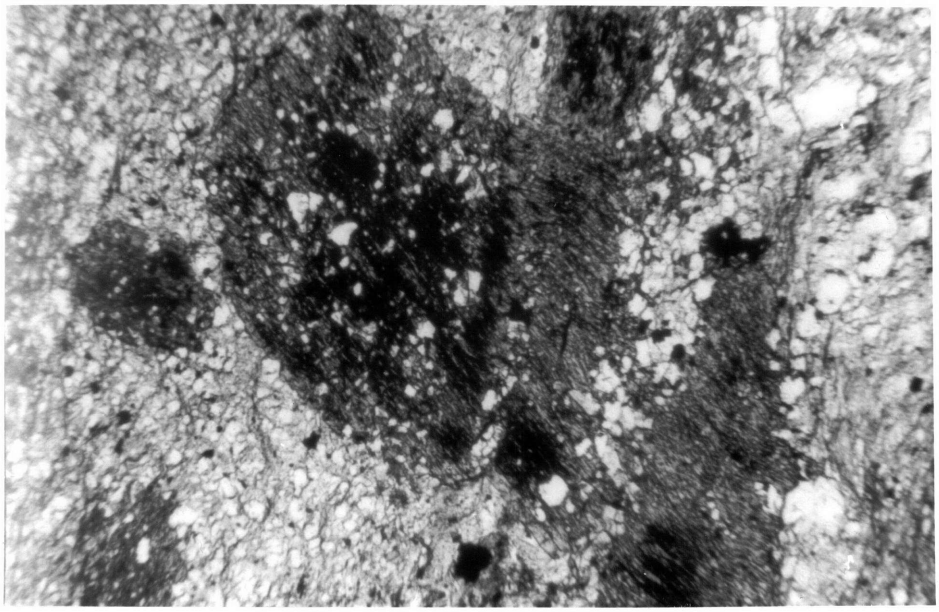

Figure 50b.

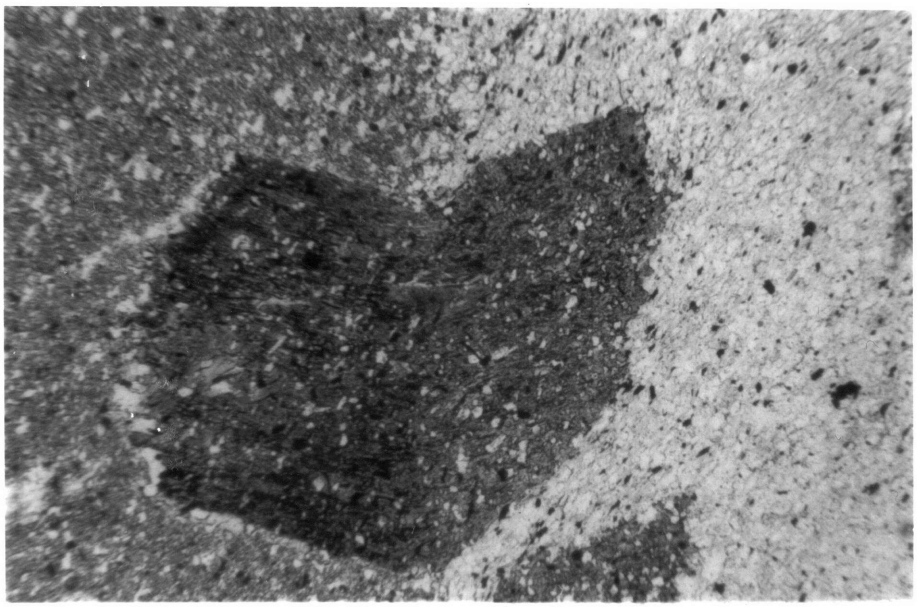

Those which were oriented with basal cleavage planes subparallel to S_1 cleavage in the matrix usually were not deformed.

Andalusite porphyroblasts contain numerous inclusions of rounded, undeformed quartz grains, distinct from recrystallized, often highly strained quartz in the matrix. Inclusions of earlier-formed biotite and chlorite porphyroblasts are sometimes present. Andalusite porphyroblasts are cut by tension gashes, often sigmoidal, which are usually filled with chlorite or biotite (Fig. 51). S_1 cleavage is defined by synkinematic fine-grained muscovite, chlorite, and biotite, and wraps around prekinematic porphyroblasts. Synkinematic andalusite was not recognized.

More intense F_1 deformation is locally recognized, such as on the northeast limb of the Lightning Antiform. Here, prekinematic biotite and andalusite porphyroblasts and quartz-muscovite pseudoporphyroblasts were rotated during development of an S_1 foliation which transposes bedding (Fig. 52). Rotation is indicated by faint heavy mineral inclusion trains in andalusite, defining original bedding, which are now inclined at variable angles to the tectonite fabric. The S_1 foliation is formed by synkinematic biotite and muscovite, and by highly strained, elongate quartz grains.

Some pelitic rocks do not show any obvious mesoscopic S_1 cleavage oblique to bedding, but rather display well-preserved sedimentary structures and a bedding-parallel slaty cleavage. In thin section, prekinematic porphyroblasts reveal numerous microstructures, including kink folds and sigmoidal tension gashes. Their orientation suggests that the bedding-parallel cleavage formed by layer-parallel shear rather than by vertical loading. This cleavage is often refracted; it intersects contacts with interbedded quartzites at an acute angle and is quickly deflected into parallelism with bedding. Much of the mesoscopic bedding-parallel cleavage probably formed during layer-parallel shear during F_1 deformation.

Pseudoporphyroblasts in pelitic rocks formed by retrogression of andalusite and perhaps other metamorphic minerals (cordierite?) and show similar textural relations with respect to S_1 fabrics as do the prekinematic porphyroblasts. Retrograde metamorphism, then, locally predated F_1 folding.

Figure 51: Photomicrograph of deformed prekinematic porphyroblast from the Lightning Gulch Formation (member L2), Sugarloaf area. Prekinematic andalusite porphyroblast (same grain as in Figure 50b) is cut by chlorite-filled sigmoidal tension gashes. S_1 cleavage is parallel to length of photo. Stratigraphic top is toward top of page. Counter-clockwise sense of shear is the same as in Figure 50b. Andalusite encloses partially chloritized prekinematic biotite porphyroblasts. Length of picture is 5 mm, plane polarized light. Sample is from W1/2 of Section 4 (T1N, R2E).

Figure 52: Photomicrograph of S_1 transposition foliation in the Lightning Gulch Formation (member L2), Sugarloaf area. S_1 foliation is parallel to width of photo and causes transposition of original bedding. Prekinematic andalusite, biotite, and quartz-muscovite pseudo-porphyroblasts are surrounded by S_1 and locally rotated. Length of photo is 5 mm. Plane polarized light. Sample is from SW1/4 of Section 3 (T1N, R2E).

Figure 51.

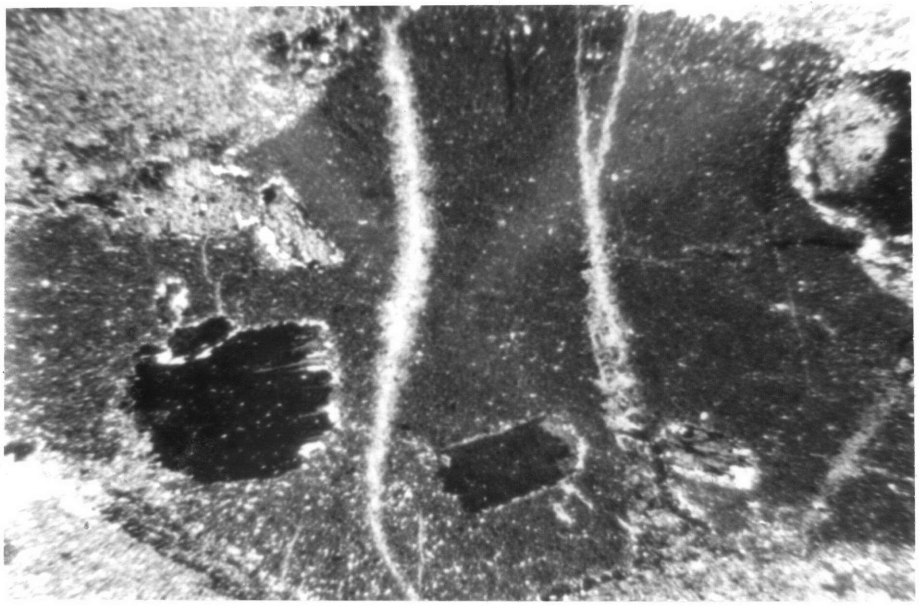

Figure 52.

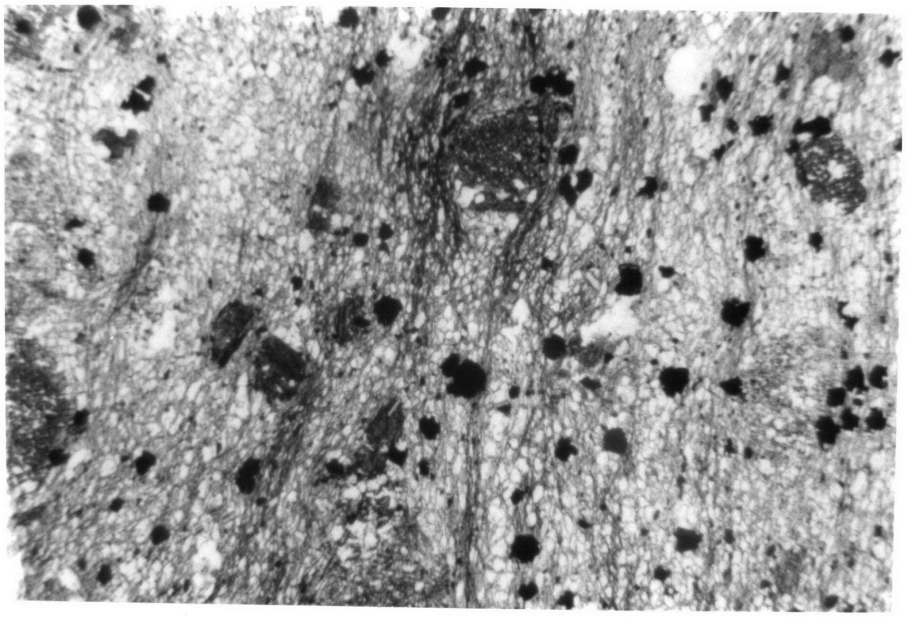

The metamorphic assemblage recognized in the matrix of the Wildhorse Greenstone also appears to be prekinematic with respect to F_1 folding. On the upright limbs of F_1 folds, the greenstone matrix is essentially massive, and shows no conspicuous S_1 cleavage. However, quartzite xenoliths and quartz-filled amygdules within the greenstone often show inter- and intracrystalline strain which appears to be related to F_1 deformation. Dimensional elongation of these aggregates probably represents the combined effects of a primary flow fabric and superposed F_1 deformation. It is believed that recrystallization in the matrix took place prior to F_1 folding, and that the greenstone behaved as a massive unit during F_1 deformation.

Mafic and pelitic rocks are the key rock types in constraining metamorphic conditions attached in the Sugarloaf area. In both rock types, textural relations indicate the highest grade assemblages (discussed below) were formed prior to F_1 folding; the metamorphic peak here was prekinematic. In marbles and calc-silicate rocks, sedimentary structures, including stromatolitic and algal mat laminations, are outlined by various calc-silicate minerals. Metamorphic replacement of siliceous carbonate rock by calc-silicate assemblages occurred prior to F_1 folding. Metamorphic assemblages formed prior to F_1 folding are similar to synkinematic assemblages for marbles, calc-silicate rocks and quartzites.

Metamorphic conditions continued during F_2 folding. S_2 axial-planar cleavage is recognized in the cores of tight F_2 folds, and is associated with the growth of metamorphic minerals. In pelitic rocks, S_2 cleavage is formed by domainal growth of white mica, chlorite and biotite. In quartz-rich phyllites, a microscopic crenulation cleavage is common, and is associated with some new growth of muscovite, chlorite and biotite. The presence of these fine crenulations often cannot be recognized mesoscopically. The crenulation axes parallel mesoscopic F_2 folds, and the cleavage parallels the axial planes of macroscopic F_2 folds. In marbles, S_2 axial-planar cleavage is defined by dimensional preferred orientation of calcite, dolomite and tremolite grains. Metamorphic conditions during F_2 folding were such that some ductile flowage occurred in marbles and in

quartzites. Evidence of penetrative fabrics associated with F_3 folding is generally lacking. The exception occurs along the northeast limb of the Lightning Antiform, where growth of fine-grained mica is associated with a locally developed S_3 cleavage. As discussed above, these folds are exceptional with respect to other F_3 folds. In general, F_3 folding appears to be postmetamorphic.

Precambrian gneisses are involved in several event 1 folds. These include F_2 and F_3 folds in Blocks I, III, Va and Via. No unambiguous examples of Mesozoic fabrics related to event 1 folding were recognized in the gneisses. The absence of Mesozoic fabrics in gneisses within the Sugarloaf area makes it unlikely that these rocks deformed by distributed shear. Rather, basement shortening apparently occurred by folding and/or faulting. In the case of the F_2 Sugarloaf Antiform, for example, gneisses are folded with overlying cover rocks, but on the overturned limb are cut by a reverse fault. Faulting may be associated with F_2 folding in the case of the May Van Antiform as well.

The general scarcity or absence of event 1 fabrics in the basement gneisses in the Sugarloaf area is surprising. These rocks were folded and faulted at this time, but show no conspicuous evidence of penetrative fabric development or retrogression. At the same time overlying cover rocks were metamorphically reconstituted during event 1 deformation. The relationship between Mesozoic deformation and metamorphism is discussed further in Chapter VI.

Event 2: High-angle Faulting. Event 2 structures include high-angle faults which cut event 1 folds and faults, and are cut themselves by event 3 structures. These cross cutting relationships can only be identified in a few places. Thus event 2 structures may be much more widespread than can be presently demonstrated.

Structures of this generation are clearly present south of Route 38. In block III, high-angle faults cut by the May Van and Deadman's faults are event 2 structures. High-angle faults in block V which cut the northeast

limb of the Green Spring Antiform are included in this event. In sub-block VIa, the Trail Fault, and other north and northwest-trending high-angle faults are of this generation. Some of these structures could also be interpreted as tear faults, formed during F_2 or F_3 folding.

High-angle faults of event 2 are suspected in the higher structural blocks, VII, VIII, and IX, but because of structural disruption during later events, this cannot be proved. Since event 3 involves both low-angle and high-angle faulting, it is frequently impossible to differentiate event 2 and 3 high-angle faults. One likely event 2 structure is the northwest-trending fault which cuts the northwest limb of the Green Canyon Synform in the NE1/4 of Section 31 (T2N, R2E). High-angle faults on Green Spot Hill may include event 2 structures.

In block I, the Stray Cat Fault and related structures might be of event 2 generation. Northward across the valley, a north to northwest-trending fault may be the continuation of the Stray Cat Fault. It cuts several northwest and east-trending faults. The Erwin Fault is believed to cut the Stray Cat Fault, and could be an event 2 or 3 structure. Minor event 2(?) faults are cut by the Arrastre Fault.

Event 3: Low-angle, Younger-over-older Faulting. Event 3 structures consist of low-angle and associated moderate- and high-angle faults which typically juxtapose younger rocks over older rocks. The major structural blocks recognized in the Sugarloaf area formed during event 3. The blocks are interpreted as allochthons, bound at their bases by low-angle faults. In some cases, the bounding low-angle faults are covered by alluvium or are intruded. Here the concealed or original contact relationships must be inferred. These faults are interpreted as extensional features. McJunkin (1976) recognized the presence of allochthonous sheets bounded by low-angle faults, which he interpreted as Quaternary landslides. He apparently did not recognize that many of these faults are intruded by Mesozoic igneous rocks. Some of his landslides are reinterpreted as event 3 structures in discussions below.

Final emplacement of the highest structural blocks, including VId, VII, VIII and IX, postdates transport of the lower allochthons (blocks I - VIa-c), and may be associated with emplacement of the Sugarloaf Intrusive Complex which intrudes these and underlying blocks. It is uncertain if emplacement of the lower allochthons was associated with magmatism. All these structures may have formed during one complex event. Alternatively, the two low-angle faulting episodes may have been separated significantly in time, as discussed below. Because of structural similarity this progressive sequence of events is discussed together. Three phases of event 3 are recognized. During event 3a, the lower allochthons were emplaced. High-angle faulting during event 3b locally disrupted these lower blocks. Event 3c includes a complex sequence of faulting that led to final emplacement of the higher allochthons.

Event 3 faults share some important characteristics. Younger rocks are typically faulted over older rocks. Older-over-younger faults of this generation are rare. These allochthons do not show mesoscopic features characteristic of surficial gravity slides. Chaotic interleaving of rocks of different formations, or intraformational megabrecciation, is not present. The blocks and sub-blocks moved as coherent plates. Translation of the allochthons occurred along narrow fault zones. Evidence of syn- or post-kinematic recrystallization is found along some event 3 fault zones.

During event 3a blocks I-VI were detached along low-angle faults. These are the "lower allochthons". South of Route 38, blocks II-VI (a, b, c) constitute a stack of structural plates. Their contact with block I is not exposed, therefore, the contact relations depicted in the cross sections are interpretive (see discussion below). Fault dips used for cross sections and cited in discussions below are constrained principally by three-point construction, since fault zones are rarely exposed. The distribution and geometry of event 3a faults is discussed first, followed by speculations concerning the kinematics of faulting and palinspastic reconstructions.

Block I is detached above the Arrastre Fault. This low-angle fault is exposed east of Gocke Valley where Wildhorse Quartzite sits discordantly above Precambrian gneisses. As mapped here, the Arrastre Fault is offset by a WNW trending high-angle fault, northeast of which the Arrastre Fault cuts downsection in the upper plate, and juxtaposes Precambrian gneisses against Precambrian gneisses. Its trace north of the center of Section 23 (T2W, R2E) is not known. I initially placed the Arrastre Fault contact at the Wildhorse Quartzite-Precambrian gneiss contact in Section 23, largely because basal conglomerate is rare here. This contact is presently interpreted as depositional. Bedding in the overlying quartzites is concordant to the contact. Rare clasts of quartzite are present in the basal quartzite and locally, conglomerate is found in float. At two localities, depositional contacts are exposed, both with and without well-developed basal conglomerate (in the former case, the exposure is a slump block). The Arrastre Fault is covered by alluvium in Gocke Valley. The contact between blocks I and II and III is not exposed. Other possible event 3a faults include the Shay Fault and low-angle, younger-over-older faults at the west end of Gold Hill.

The basal fault for block II is not exposed. The granitic rocks which underlie block II are inferred to have intruded along a SW dipping low-angle fault, here referred to as the Onyx Summit Fault.

Blocks II and III are separated by the 38 Fault, here interpreted as the basal fault for block III. Three-point construction yields a SW dip of 7-10° for the 38 Fault. East of Balky Horse Canyon, the trace of the 38 Fault is crosscut by granite. The 38 Fault is thought to cut the May Van and Deadman's faults but alluvium covers these contacts. The May Van and Deadman's faults dip N and NE, and flatten downdip; they are interpreted as earlier event 3a structures. These are younger-over-older faults, and are the detachment faults for sub-blocks IIIb and IIIc. Wildhorse Quartzite in these sub-blocks may be downdropped from the northeast limb of the May Van Antiform.

NE dipping Wildhorse Quartzite of sub-block IIIa extends SE of my map area to the Onyx Summit area. It structurally overlies Precambrian gneisses in the NE1/4 of Section 2 (T1N, R2E) just above Route 38. Bedding attitudes cited by Dibblee (1967a) and McJunkin (1976) for quartzites above the gneisses are discordant to the contact and suggest this may be a younger-over-older fault contact. This fault(?) contact is crosscut by granitic rocks. It may be the continuation of either the 38 Fault or the Onyx Summit Fault. Precambrian gneisses underlie sub-block IIIa quartzites to the southwest as well. Dibblee (1967a) mapped this contact as depositional. If so, then these gneisses belong to sub-block IIIa which may project beneath block V to emerge below the Lightning Gulch Fault (these gneisses then lie in the core of the May Van Antiform). McJunkin (1976) has mapped the quartzite-gneiss contact as a low-angle, younger-over-older fault in the western portion of Section 2. This fault cuts downsection in its upper plate to the east, placing gneisses on top of gneisses, and locally on top of quartzites. If this interpretation is correct, the gneisses in Lightning Gulch structurally underlie block III, as well as blocks V and VI. McJunkin's fault may be correlative with the Lightning Gulch Fault, which may be a late-stage event 3a fault cutting blocks III, V and VI. Dibblee's interpretation is followed here (see cross section GG'), however the alternate interpretation indicated by McJunkin's mapping is certainly a possibility.

The 38 Fault is concealed west of the Deadman's Canyon area; its trace may parallel Route 38. Generally W dipping faults which cut Precambrian gneisses in the western part of sub-block IIIa may include event 3a structures. These faults are locally intruded by dacite porphyry tectonite (discussed in Chapter III). Overlying sub-block IVa is bound at its base by a fault dipping 35° NW. Sub-blocks IVa, b and c are thought to have constituted a single plate prior to later faulting and intrusion.

Sub-block Va is bound at its base by the Deer Spring Fault, which dips no more than 18°SW in the Green Canyon area. A NW trending fault cuts the Deer Spring Fault in Section 33 and locally downdrops sub-block Va. The NW trending fault is inferred to be a normal fault of minor displacement and variable SW dip. The NW dipping Lightning Gulch Fault bounds sub-block Va on the southeast. This fault may be the continuation of the Deer Spring Fault, and if so, the basal detachment fault for sub-block Va is trough-shaped, and plunges W. Out-of-place member W2 quartzites assigned to block Vb are believed to be underlain by a low-angle fault.

The Wildhorse Fault underlies sub-block VIa. Three-point construction indicates this fault dips SW at about 30° south of the Balky Horse Fault. A SW dip of 15° is calculated in upper Green Canyon. It is not clear if the Wildhorse Fault merges with or is cut by the Lightning Gulch Fault. The Sugarloaf Saddle Fault separates sub-blocks VIa and VIb. This younger-over-older fault flattens rapidly down dip, and could not be traced southward within the poorly outcropping Precambrian gneisses. The nature of its intersection with the Wildhorse and Lightning Gulch faults is not known, but it is considered an event 3a structure.

To the northwest, sub-block VIa is overlapped by rocks of block VII along an intruded fault zone (Green Canyon Fault). West of Green Spring, the Wildhorse Fault is overlapped by a gravity slide. Rocks of the Lightning Gulch Formation exposed west of the slide are in low-angle fault contact with rocks of sub-block Va and are intruded by monzodiorite of the Sugarloaf Intrusive Complex. These rocks are thought to represent the continuation of sub-block VIa downdropped on a concealed fault in the N trending gully.

Rocks of the Lightning Gulch Formation and Sugarloaf Quartzite constitute sub-block VIc. Upper and lower plate rocks are similar to those juxtaposed across the Wildhorse Fault to the south, and sub-block VIc is correlated with sub-block VIa. Sub-block VIc was complexly

faulted during event 3b. Outcrop patterns indicate the basal detachment fault is subhorizontal. Locally, the basal fault cuts earlier (event 2?) high-angle faults in the lower plate. Sub-block VIc is a klippe, and its subhorizontal fault geometry suggests the Wildhorse Fault may flatten at depth beneath sub-block VIa as well. Intraplate younger-over-older detachment has locally occurred between the Lightning Gulch Formation and member S1 of the Sugarloaf Quartzite. Similar intraplate detachment faulting is recognized in sub-block VId, at the west end of Deadman's Ridge. Although the rocks of sub-block VId correlate with those in sub-blocks VIa and VIc,the basal fault there is not an event 3a structure, but is younger (discussed below).

Fault blocks detached during event 3a moved as coherent plates as internal brecciation is lacking. Outcrops within a few meters of faults typically show no evidence of brecciation. Movement was confined to narrow fault zones. At an exposure of the Wildhorse Fault along Wildhorse Road (N center of NW1/4, Section 32, T2N, R2E), poorly exposed quartz-biotite-muscovite schist is found within a 0.5 m wide fault zone separating overlying Sugarloaf Quartzite from underlying Wildhorse Quartzite (Fig. 53). Bedding in the quartzites is highly discordant to the fault. Schistosity in the schist parallels the fault, and these schists are crudely lineated (lineation was not seen in outcrop however). The foliation in the matrix here is not as well-developed as in nearby metasedimentary rocks. Angular quartz grains and quartzite clasts are present in the micaceous matrix. Individual quartz grains display undulatory extinction. These clasts may have been derived from adjacent, previously deformed quartzites. Unlike the quartz in nearby quartzites, these grains are also highly fractured (Fig. 54). These schists are interpreted as recrystallized fault gouge. The fault gouge formed along a narrow zone of cataclastic shear constituting the Wildhorse Fault. It is unknown whether growth of metamorphic mica in the matrix occurred during shearing or only afterward. The absence of annealed quartz suggests to me that recrystallization was primarily syn-kinematic. Minor post-recrystallization slip parallel to the fault zone caused local kinking of biotite.

Figure 53: Exposure of an event 3a low-angle normal fault. This fault is correlated with the Wildhorse Fault, and juxtaposes a small klippe of Sugarloaf Quartzite (member S1, white rocks) over Wildhorse Quartzite (grey rocks below, largely covered). Upper plate rocks are upright(?) and dip moderately to left; lower plate rocks dip steeply to right (facing unknown). Quartz schist is found along fault zone, which dips 38°/N80W. Note conjugate joints in upper plate quartzites. Hammer in left center for scale. Photo taken along Wildhorse Road in the NW1/4 of Section 32 (T2N, R2E).

Figure 53.

Figure 54: Photomicrograph of quartz-biotite muscovite schist interpreted as recrystallized fault gouge formed along the Wildhorse Fault. Schistosity is parallel to the width of the photo. Angular, often undulatory quartz grains and aggregates are conspicuously fractured. Biotite is locally kinked, indicating minor post-recrystallization deformation occurred. Length of photo equals 2 mm.

a) plane polarized light
b) crossed polars
Sample is from roadcut along Wildhorse Road in the NW1/4 of Section 32 (T2N, R2E).

Figure 54a.

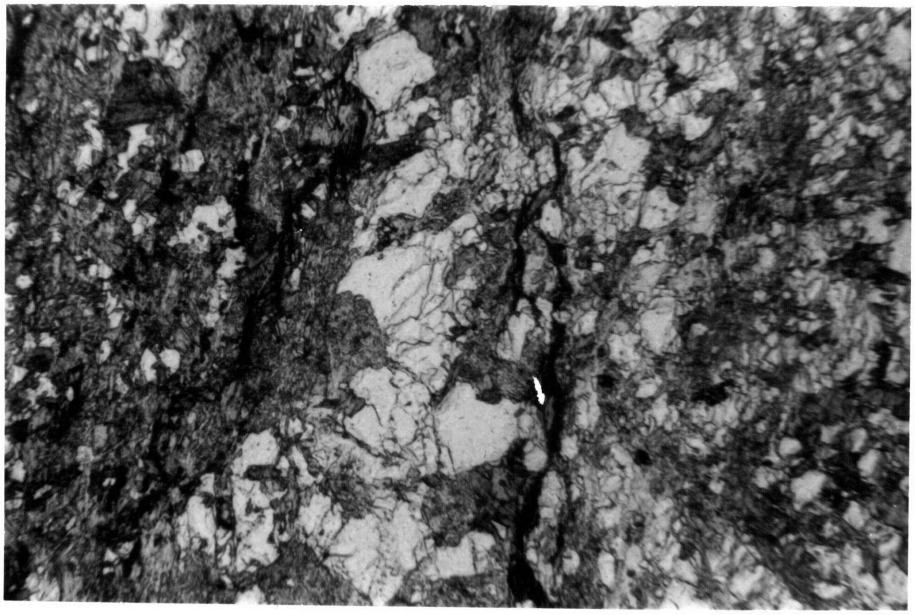

Figure 54b.

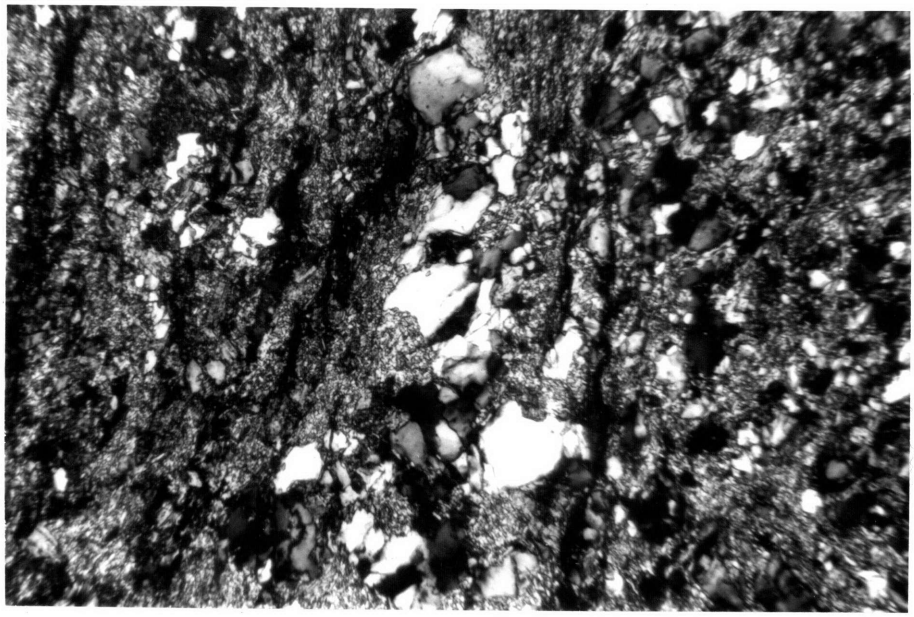

Intraplate deformational fabrics related to event 3a faults are not conspicuous. Mesoscopic folds definitely related to event 3a were not recognized, however they would be hard to differentiate from event 1 folds. Jointing is often well-developed in quartzites adjacent to detachment faults (Fig. 53). Precambrian gneisses within a few meters of the trace of the Wildhorse Fault southeast of Wildhorse Meadow may contain an event 3a fabric. A poorly developed cleavage is locally present which dips SW at approximately 40°. This cleavage appears to be defined by very fine-grained mica. It cross cuts S_1 and S_2 fabrics of Precambrian age. It may be this cleavage is an event 1 fabric. It is, however, only recognized immediately below the Wildhorse Fault, an event 3a structure.

In his discussion of Cenozoic younger-over-older faults in the Great Basin, Armstrong (1972) noted that extension by listric or low-angle normal faulting provides the simplest geometric explanation for such structures. Low-angle younger-over-older faults can form during compressional thrusting by beheading folds, but in such cases older-over-younger faults are equally developed. At Sugarloaf, older-over-younger low-angle faults are conspicuously absent even though event 3a faults cut earlier folds. However, apparent offsets of event 1 structures can be recognized which indicate the younger-over-older faults are extensional in origin.

Event 3 faults are superimposed on a terrane that underwent polyphase folding during event 1. Offset of event 1 structures can be used to palinspastically remove the effects of event 3 low-angle faulting. For palinspastic purposes, F_2 and F_3 folds are most useful. F_1 folds are apparently disharmonic and irregularly developed from block to block. Palinspastic reconstructions based on matching offset F_2 folds suggest that event 3a faulting involved significant east-west extension.

I suggest that blocks I-IX originally lay in the upper plate of the Doble Thrust. The major event 1 fold above the thrust is the Arrastre

Creek Antiform. Wildhorse Quartzite along its eastern overturned limb crops out for some 8 km, from Rose Mine to Onyx Summit. West of these exposures, Wildhorse Quartzite crops out in the eastern portions of blocks I, II, III, V and VI. These rocks do not constitute the westward dipping, upright limb of the Arrastre Creek Antiform. Rather, these quartzites typically lie in E or NE dipping limbs of F_2 antiforms.

Between the east limb of the Arrastre Creek Antiform and Arrastre Creek, Wildhorse Quartzite crops out in two localities (see Plate VI) mapped by Dibblee (1967a) and McJunkin (1976). One locality lies within the Broom Flat Slide of McJunkin (1976). This slide or allochthon is apparently overlapped by blocks I and is itself detached above a W dipping low-angle fault which I believe is an event 3a structure. The sheet includes Precambrian gneisses and depositionally(?) overlying quartzites which dip E from 30-40° (McJunkin, 1976). North of Broom Flat, the basal fault juxtaposes these quartzites over gneisses along the Arrastre Creek Antiform's east limb. The Broom Flat allochthon has apparently been downdropped from that limb. Southwest of Broom Flat, a small outcrop of quartzite of basal conglomerate facies (Wildhorse Quartzite?) overlies Precambrian gneisses (Dibblee, 1947a; McJunkin, 1976). The outcrop pattern indicates the quartzite-gneiss contact is subhorizontal although bedding in the overlying quartzites dips 35-65°E. Either these quartzites are detached above a low-angle, younger-over-older fault, or the quartzites and underlying gneisses are relatively downthrown by an unrecognized normal(?) fault along the quartzite outcrop's eastern edge.

South of these exposures, the dip of bedding locally decreases along the east limb of the Arrastre Creek Antiform (to 25-35° E, upright) and outcrop patterns locally indicate a decrease to near horizontal dips (Dibblee, 1967a; McJunkin, 1976). However, in the area east of Arrastre Creek, the W dipping limb of the Arrastre Creek Antiform has not been recognized. Instead, the E dipping limb of the antiform appears to be structurally repeated by younger-over-older faulting.

I suggest that the E and NE dipping quartzites in blocks I-VI were also offset from the east limb of the Arrastre Creek Antiform and

that tectonic disruption of this fold took place during event 3a. In other words, the Gocke Antiform, May Van Antiform, Green Spring Antiform and Lightning-Meadows Antiforms, which are beheaded F_2 folds and are cut by low-angle faults, are here thought to be offset from the crest of the Arrastre Creek Antiform. The Arrastre Creek Antiform is believed to be of the same fold generation as F_2 folds in the Sugarloaf area. Its upright, W dipping limb has been transported far to the west, and is now exposed as the west limbs of F_2 folds in blocks I-VI.

In general, event 3a low-angle normal faulting is interpreted to have formed a complexly overlapping stack of allochthonous sheets bound by gently W dipping faults. Complexly folded rocks in the upper plate of the Doble Thrust have been pulled apart by extensional faulting. In detail, palinspastic restoration is far more complex, in part since many key contacts are not exposed. An additional uncertainty is the fold geometry of the Arrastre Creek Antiform. Was it a single cylindrical fold, or was a set of en echelon folds present, similar to the F_2 Meadows and Lightning antiforms in sub-block VIa? Because of these uncertainties, a unique palinspastic reconstruction cannot be espoused based on available data. Two models are presented here, which differ mainly in the original location of blocks II, III and V (see Figs. 55,56). The original positions of blocks I and VI are similar in both reconstructions. Between the west end of Deadman's Ridge and the Doble Thrust near Rose Mine the maximum extension during event 3a is approximately 60% (an area has been extended from about 5 to 8 km in an east-west direction). South of Route 38 the amount of extension between the Doble Thrust east of Broom Flat and the west edge of block IV may have been 100% or more during event 3a (Fig. 55).

North of Route 38, the Gocke Antiform may be offset from 1.5 to 3.2 km westward, from an original position in the crest of the Arrastre Creek Antiform. Block I originally overlay the Broom Flat slide, which may have moved only a short distance. The open F_3 synform present to the northeast of the Erwin Antiform may correlate with the SW plunging F_4 synform which refolds the Doble Thrust near Rose Mine.

Figure 55: Schematic palinspastic map removing effects of event 3a normal faulting: model A. In model A it is assumed the Gocke Antiform correlates with the May Van Antiform. Symbols are the same as in Plate VI.

Figure 56: Schematic palinspastic map removing the effects of event 3a normal faulting: model B. In model B it is assumed that the May Van Antiform correlates with the NNW plunging F_2 antiform at the west end of Deadman's Ridge (block I). Symbols are the same as in Plate VI.

ACA: Arrastre Creek Antiform
GHS: Gold Hill Synform
EA: Erwin Antiform
WDR: West end of Deadman's Ridge
DS: Deadman's Synform
AF: Arrastre Fault
GS: Gocke Synform
GA: Gocke Antiform
DT: Doble Thrust
BFS: Broom Flat Slide
OSF: Onyx Summit Fault
38 F: 38 Fault
MVA: May Van Antiform
WF: Wildhorse Fault
SS: Sugarloaf Synform
SA: Sugarloaf Antiform
MA: Meadows Antiform
LA: Lightning Antiform

Fig. 55

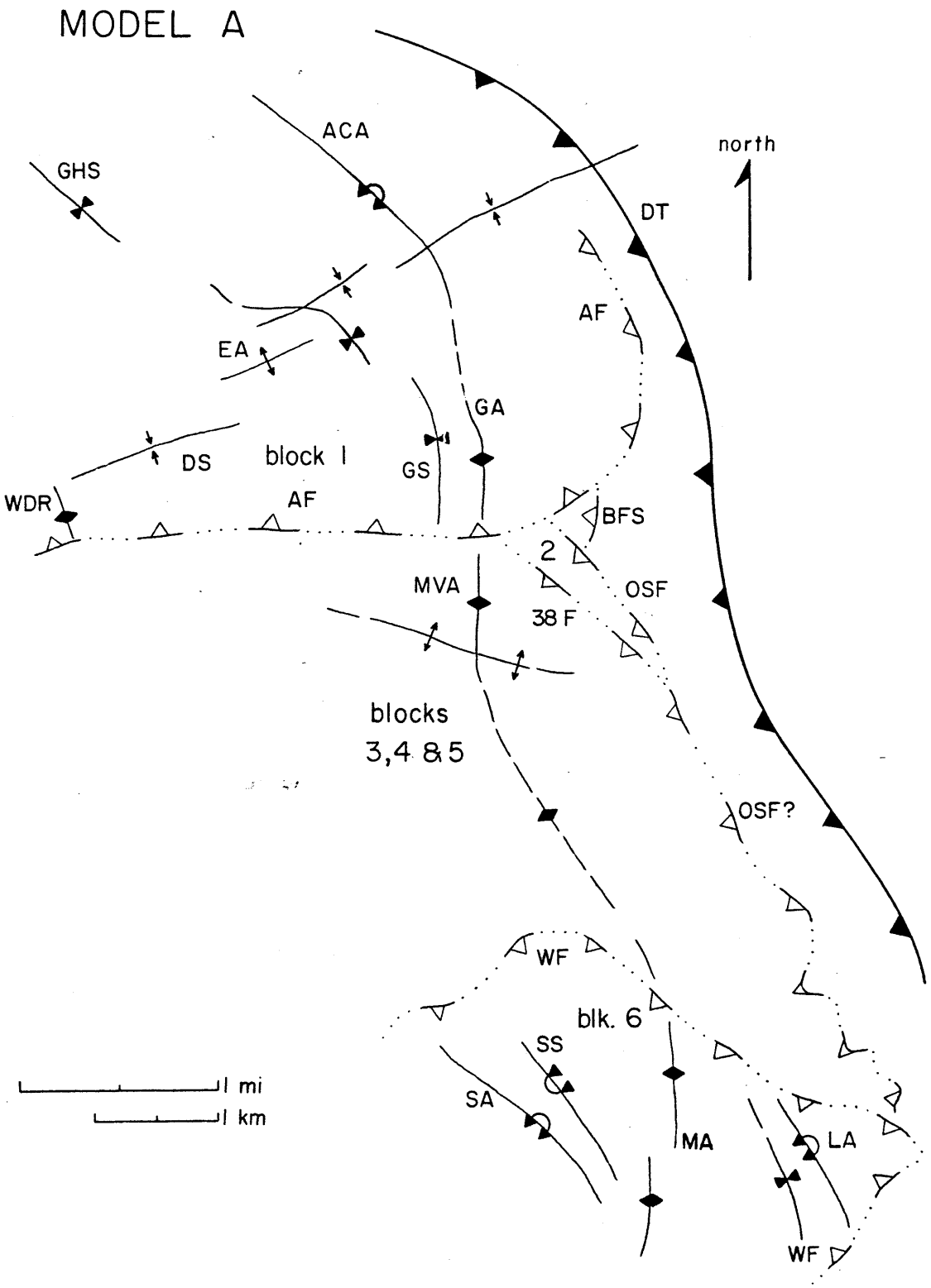
MODEL A
ACA
GHS
north
DT
AF
EA
GA
DS
block 1
GS
WDR
AF
BFS
2
MVA
OSF
38 F
blocks
3,4 &5
OSF?
WF
blk. 6
SS
SA
MA
LA
WF
1 mi
1 km

Fig. 56

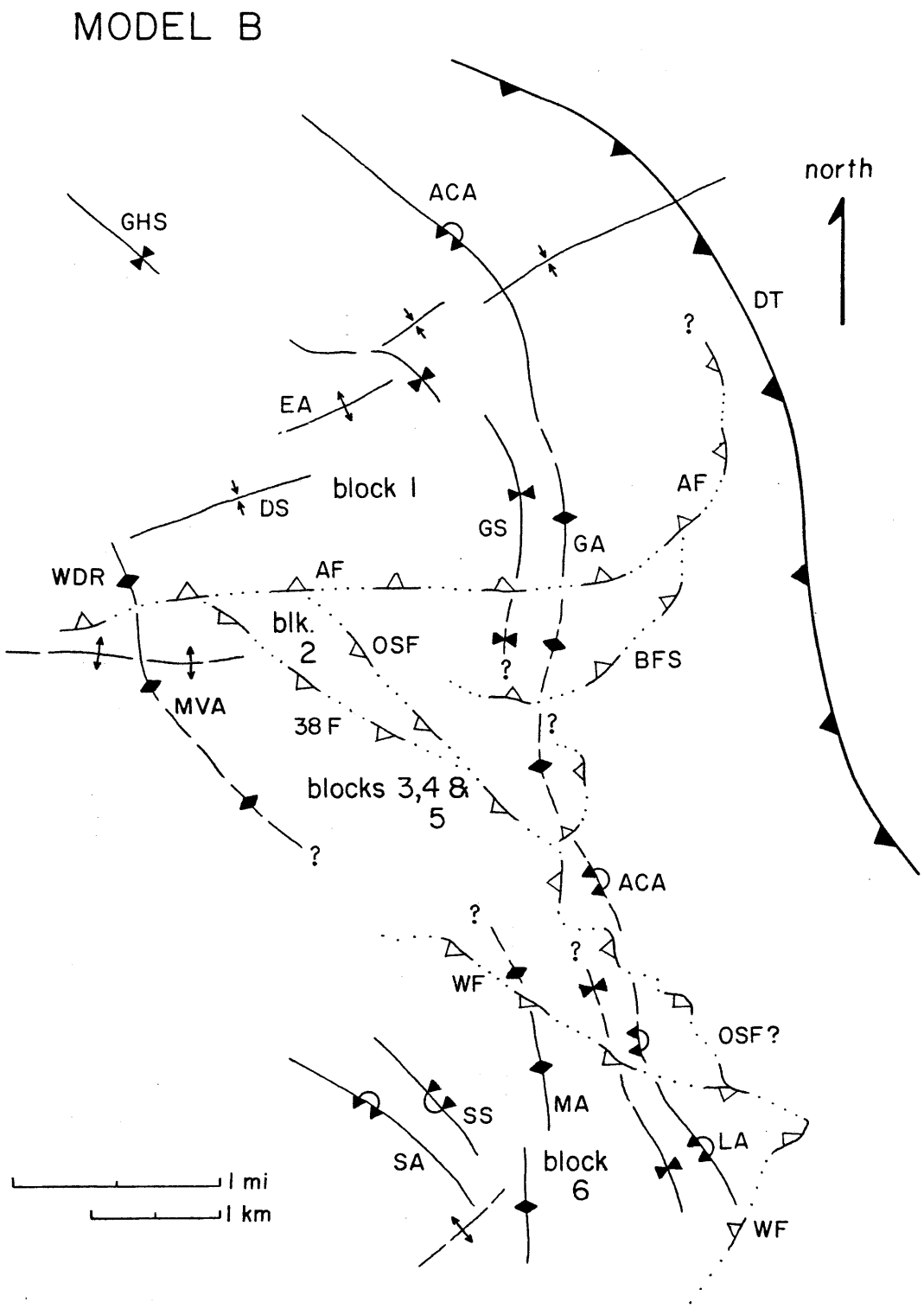
MODEL B
north
GHS
ACA
DT
EA
block 1
DS
AF
GS
GA
WDR
AF
blk.
2
OSF
BFS
MVA
38 F
blocks 3,4 &
5
ACA
WF
OSF?
SS
MA
SA
block
6
LA
WF
1 mi
1 km

The kinematics of event 3a faulting south of Route 38 is far more uncertain. It appears likely that the Green Spring Antiform (sub-block Va) is offset from the crest of the May Van Antiform (sub-block IIIa). Cross sections AA', HH' and GG" indicate between 1-1.6 km of westward displacement on the Deer Spring-Lightning Gulch faults given this match. This direction of transport is consistent with the possible west-plunging trough-like geometry of sub-block Va's detachment surface (for a similar example see Proffett, 1977). If sub-blocks IIIb and IIIc are downfaulted from the east limb of the May Van Antiform then the 38 Fault may have as little as 0.5 km dip slip offset to the west (section HH').

The kinematic relation between blocks I and III is an important unknown. In Fig. 55, it is assumed that the May Van Antiform is offset from the Gocke Antiform. In this case, block III is offset perhaps 2.5 km further west than block I. Some of this additional displacement occurred along the 38 Fault, but most occurred along the Onyx Summit Fault. This reconstruction implies a complex movement history for blocks I-III. Their initial westward displacement may have been as a single block above a proto-Onyx Summit-Arrastre fault system. Later, block I and sub-blocks IIIb and IIIc detached from blocks II and IIIa along younger-over-older faults. Blocks I, IIIb and IIIc may at one time have constituted a coherent sheet. Later displacement on the Onyx Summit and 38 faults cut these earlier faults and resulted in westward relative transport of block II and sub-block IVa.

Major translation on the Onyx Summit Fault may explain the different orientation of F_2 and F_3 folds in block I and in blocks II-V. In block I, F_2 folds on Deadman's Ridge trend nearly north-south and parallel the trend of the Arrastre Creek Antiform, thus requiring little relative rotation across the Arrastre Fault. F_3 folds trend NE on Deadman's Ridge. Above the Onyx Summit Fault, F_2 folds trend NNW to NW in blocks II-V, and F_3 folds trend NNE on the east limbs of F_2 folds. This difference in fold orientation can be particularly explained by counterclockwise rotation of blocks II-V above the Onyx Summit Fault, which is required if the May Van Antiform is offset from the Gocke Antiform.

An alternative reconstruction (Fig. 56) results if the May Van Antiform is correlated with the NNW plunging F_2 fold at the west end of Deadman's Ridge. In this case, only one episode of westward displacement of a coherent terrane consisting of blocks I-V occurred along a proto-Onyx Summit-Arrastre fault system. The principal relative movement between blocks I and blocks II and III occurred along the Arrastre Fault, a younger-over-older fault which downdropped block I northward relative to blocks II and III and the Broom Flat sheet. This fault may have cut or partially reactivated the earlier proto-Arrastre Fault segment. Sub-blocks IIIb and IIIc may be klippen of block I, downdropped by later displacement on the 38 Fault, which presumably cuts the Arrastre Fault as well. In Fig. 56, it is assumed Green Spring Antiform is offset from the crest of the May Van Antiform. This model requires that the variation in F_2 and F_3 fold orientation between blocks I and III and V must occur by rotation above the 38 Fault and above the Deer Spring Fault.

My major objection to the second reconstruction is the lack of evidence for an F_2 synform separating the May Van Antiform and Arrastre Creek Antiform, which is required by this model. It seems ad hoc to argue that the west dipping limb which must have separated the east dipping limbs of the Arrastre Creek and May Van antiforms has been completely removed by erosion. However, this objection could be alleviated if these F_2 folds formed en echelon . At present, both reconstructions appear tenable.

In both reconstructions, block VIa is assumed to be derived from an original position above the gneisses in the Lightning Gulch area. Block VI cuts down section from north (sub-blocks VIc and VId) to south. Although its northern portion may have overlain rocks of block V for example, rocks in sub-block VIa must have been derived from an area that is now tectonically denuded of Upper Precambrian cover rocks. In these reconstructions, the eastern, locally overturned limb of the Lightning Antiform is correlated with the east limb of the Arrastre Creek Antiform near Onyx Summit. The match-up of other folds is uncertain, and depends

on whether the Meadows and Lightning Antiforms merge or diverge down plunge.

The original position of the higher structural blocks (VII-IX) prior to event 3a faulting is not well constrained. They presumably lay in the upper plate of the Doble Thrust, and on top of the lower allochthons. They record evidence of event 3a faulting, but as these structures are truncated by and transported above younger low-angle faults (of event 3c) their geometric relations to event 3a faults in the lower blocks are not known.

After the emplacement of the lower allochthons, but prior to final emplacement of the higher blocks, complex event 3b faulting disrupted the lower allochthons near Hill 8055'. This event affected rocks in an area where the Sugarloaf Intrusive Complex subsequently invaded the lower structural blocks. The locations of structures here are labelled in plate VI. Constant reference to the geologic and tectonic maps, as well as cross sections EE", FF", and II"' is required to follow the discussion below.

Four of the lower allochthons are present in lower Green Canyon: blocks III, IV, V and VI. They are separated by faults at the base of block IV (four in plate VI), the Deer Spring Fault (ds) and the Wildhorse Fault (segments labelled w). The Wildhorse Fault locally cuts older high-angle faults in sub-block Va (z).

The earliest event 3b structures are high- and moderate-angle faults of generation a (faults a1 - a9) which clearly cut the Wildhorse and Deer Spring faults. A northwestward continuation of fault a9 to cut the basal fault of block IV is assumed but is not certain. In some cases, only short segments of generation a faults are preserved. Segments a3, a4, a5, a6 and a7 are thought to be remnants of a zone of west-dipping faults along which normal and reverse displacements of blocks IV, V and VI occurred. This zone was later intruded by the Sugarloaf Quartz Diorite and cut by a minor fault s. Also cut by generation a faults were intra-

plate detachment faults of block VIc. Fault a5 cuts north-dipping fault y, believed to be a minor imbrication formed late during event 3a. Faults a1 and a1', and a2 and a2' are thought to correlate respectively.

Faults b1 and b2 cut generation a structures. Relative uplift of underlying block Va quartzites occurs on both of these faults. Fault b1 dips shallowly northwest and truncates a1, a2, and a5. Fault b2 dips southwest, and is thought to cut faults a1', a2' and a3.

Low-angle faults of generation c cut b1 and b2. The rocks above fault c1 are thought to have been downfaulted from an original position above the Wildhorse Fault in block VIc. Small low-angle fault blocks of Sugarloaf Quartzite overlie sub-block Va to the north and may have been emplaced at this time or later. Structures of all three generations, a, b and c are intruded by Sugarloaf Quartz Diorite.

Minor folding may be associated with event 3b. Wildhorse Quartzite appears beneath sub-block VIc rocks exposed between faults a2 and a3. The presence of this window indicates the Wildhorse Fault is gently warped here (cross section FF"). This warping may reflect open folding, prior to high-angle faulting. Such minor folding might be associated with event 3b faulting, which I see as a distinct possibility. Alternatively, it might be argued that some F_3 folding actually postdates event 3a low-angle faulting. This appears unlikely to me. In the lower Green Canyon area the outcrop pattern of the various structural blocks is largely a result of event 3b faulting, not folding. I suggest the event 3 low-angle fault blocks are bound by curviplanar fault surfaces. An excellent example, the basal fault for block VII, is discussed below.

Emplacement of the higher allochthons, sub-block VId and blocks VII, VIII and IX occurred during event 3c. Because event 3b faulting jostled the lower allochthons, and because of multi-stage fault block movement during event 3c, the higher allochthons overlap many of the lower blocks (I, III, V and VI) and the faults that juxtapose them. Like the earlier low-angle faults, these too place younger rocks over older

rocks, and are believed to be related to extension. In these allochthons the youngest rocks in the Sugarloaf area are exposed, and some of the largest stratigraphic separations (up to two km) are recognized across event 3c faults. These allochthons are intruded by, and form the roof for, the Sugarloaf Intrusive Complex. The emplacement of these plutonic rocks and extensional, younger-over-older faulting are thought to be related. Event 3c structures are believed to have formed, in part, as the roof rocks extended during intrusion of the shallow-level plutonic complex.

The complex sequence and geometry of event 3c structures is best preserved in the lower Green Canyon area. To the west, the higher allochthons are more engulfed by rocks of the Sugarloaf Intrusive Complex, and many important contacts are covered by talus. In Green Canyon, and presumably to the west, older structures in the lower blocks are apparently truncated by the Green Canyon basal fault (GCF - see Plate VI). This composite fault forms the base for block VII. It is probably not a single fault, but a composite younger-over-older detachment surface along which several faults have merged. These faults may have formed at different times during event 3c. From north to south, sub-blocks exposed below the GCF include VId, Va, VIc, Va again VIa and VIb. The base of block VII, where bound by the GCF, or intruded, defines a convex, trough-like surface which apparently plunges westward. The inclination of this surface decreases down-dip. This surface dips N (in cross sections BB', CC'), NW (DD', II'''') and SW (EE"). Cross section FF" crosses near the hinge of this trough. A trough-like geometry is inferred for the Green Canyon basal fault as well.

Only three segments of the Green Canyon basal fault surface are exposed in Green Canyon. Along segment g1, rocks of sub-block Va underlie the fault. Along fault g2, Lightning Gulch phyllites of sub-block VIc, which were downdropped by fault c1 are found below the basal fault. Along segment g3, sub-block Va rocks uplifted by fault b2 are present below the basal fault. In intervening areas, the trace of the Green Canyon basal

fault is covered or intruded. Outcrop geometry suggests that lower plate structures formed during events 3a and 3b were truncated by the Green Canyon basal fault.

The Green Canyon basal fault also cuts structures in the upper plate, some of which perhaps formed during events 3a and 3b. In the SW1/4 of Section 32 (T2N, R2E), rocks of members G7, G8 and G9 of the Green Canyon Formation constitute sub-block VIId, and are juxtaposed above rocks of the middle and lower Green Canyon Formation (in sub-blocks VIIc2 and VIIb2 respectively) along locally exposed low-angle, younger-over-older faults (d1-3). High-angle fault e postdates an associated low-angle fault, d4, and a suspected normal fault, d5. The emplacement of sub-block VIId postdates juxtaposition of lower plate sub-blocks VIIb2 and VIIc2 along an intruded fault. This sequence of low-angle and high-angle faults predates emplacement of the Green Canyon basal fault, and may include event 3a and 3b structures.

Further north, within sub-block VIIc1, faults h, i1, i2, j and low-angle normal fault k are all believed to predate the Green Canyon basal fault. To the south, in sub-block VIIc1, a sequence of low-angle younger-over-older faults (f1-4) disrupts rocks in the Green Canyon Synform and adjacent F_2 antiforms; fault f1 downdrops these rocks with respect to sub-block VIIb2 rocks (an alternate interpretation is discussed under event 1, above). Faults f2-4 may predate fault f1 and the Green Canyon basal fault. Fault f1 could be an event 3c structure, and might merge with the GCF. It is the bounding fault for sub-block VIIc1.

There is evidence near Green Canyon to suggest a second episode of low-angle faulting occurred during event 3c, postdating the Green Canyon basal fault and fault f1. At this time, sub-blocks VIIe and VId were carried relatively northward and locally overlapped block I at the west end of Deadman's Ridge. Fault segment g4 is inferred to represent the offset continuation of the Green Canyon basal fault, juxtaposing rocks of the upper Green Canyon Formation (sub-block VIIe) and Sugarloaf Quartzite (sub-block VId). Fault m, another low-angle younger-over-older fault, may

have formed at this time or earlier. Both are cut by an intruded, locally southwest-dipping normal fault, n. All of these structures are believed to be cut by a low-angle normal fault along which northward relative transport of sub-blocks VId and VIIe occurred. Exposed segments of this fault are believed to include L1, L2, and L3. A klippe of Sugarloaf Quartzite underlain by fault L4 is included with the composite VId-VIIe allochthon. The detachment fault for this allochthon is cut by high-angle faults p1 and p2. Lower plate Wildhorse Quartzite on either side of fault p1 is in a basal conglomerate facies, thus dip slip offset on these two faults is minor. Outcrop geometry suggests faults L2-L3 dip gently northwest here.

Rocks in sub-block VId do not show the complex internal disruption of rocks in sub-block VIc, where event 3b structures are present. The absence of such structures, as well as the units juxtaposed across fault g4, suggest that the sub-block VId-VIIe allochthon may have been derived from a position near Green Spring where sub-block VIId overlies VIa. This match indicates approximately 2.5 km of N-NW transport. It is inferred that this allochthon was intruded by rocks of the Sugarloaf Intrusive Complex after transport.

In the Green Canyon area, emplacement of the higher allochthons involved a complex sequence of low-angle and high-angle faulting events. Rocks of block VII record an earlier episode of low-angle faulting, suggesting these rocks may have been deformed during event 3a as well, but at a higher structural level. The detailed geometry and sequence of events involved in the emplacement of the higher blocks north of Sugarloaf Mountain is obscure, primarily owing to plutonic disruption. In three dimensions, the pre-Mesozoic rocks are interpreted to form thin, locally overlapping sheets, roofing the plutonic rocks (see cross sections BB', CC', DD', EE''). Locally preserved fault contacts, outcrop geometry and analogy with the Green Canyon area suggest these rocks are the intruded remnants of a stack of younger-over-older allochthons emplaced along faults which at least locally flattened down dip to the N and W. The

Sugarloaf Intrusive Complex is believed to have been emplaced along the bounding faults, thus spreading these allochthonous sheets apart and warping them.

As in Green Canyon, the inferred trace of the Green Canyon basal fault cuts lower plate structure, here trending obliquely across the trace of the Sugarloaf Saddle Fault, and northwest-trending faults cutting sub-block VIa. The basal fault is exposed on the north slope of Sugarloaf Mountain (segments g5 and g6). Sugarloaf Quartzite (sub-block VIIa) is juxtaposed against Wildhorse Quartzite (sub-block VIb). The base of sub-block VIIa appears to dip northward, off the mountainside (Fig. 57). Sugarloaf Quartz Diorite intrudes the basal fault. The igneous rocks are locally present in outcrop, and are found in float elsewhere along the fault's trace.

The Green Canyon basal fault is almost certainly a composite fault here. Emplacement of block VII and higher blocks involved a complex sequence of faulting, as was the case in Green Canyon. Sub-block VIIa is the lowest "plate" here. Rocks of sub-block VIIa project beneath younger rocks of sub-block VIIb1, inferred to have been a higher allochthon or allochthons. To the north, rocks of the upper Green Canyon Formation constitute the western continuation of sub-block VIIc1, which is inferred to have overlain sub-blocks VIIa and VIIb1. Still higher is block VIII. These uppermost Precambrian-Cambrian rocks are believed to be the remains of an allochthon which overlay nearby Upper Precambrian rocks of sub-blocks VIIb1 and VIIc1. The highest block, IX, consists of Cambrian Bonanza King Formation marbles and overlaps older rocks of blocks VII and VIII.

In spite of plutonic disruption, it is possible to partially reconstruct the complex sequence of events involved in final emplacement of the upper allochthons. Cross-cutting relationships suggest that the fault blocks were emplaced progressively, from lowest to highest. Sub-blocks VIIa and VIIb1 are believed to have been emplaced first. Green Canyon basal fault segment g5 is thought to dip northward and may be cut by fault

Figure 57: Blocks VI and VII, juxtaposed across the Green Canyon basal fault (GCF) on the north slope of Sugarloaf Mountain. Wildhorse Quartzite of block VI underlies summit as well as tree- and talus-covered slopes to left. Light-colored rocks of block VII (Sugarloaf Quartzite and Green Canyon Formation) in center and right of photo are underlain by the GCF or dioritic rocks which intrude the fault. View is from NE; photo taken on NW ridge of Peak 9433'.

Figure 57.

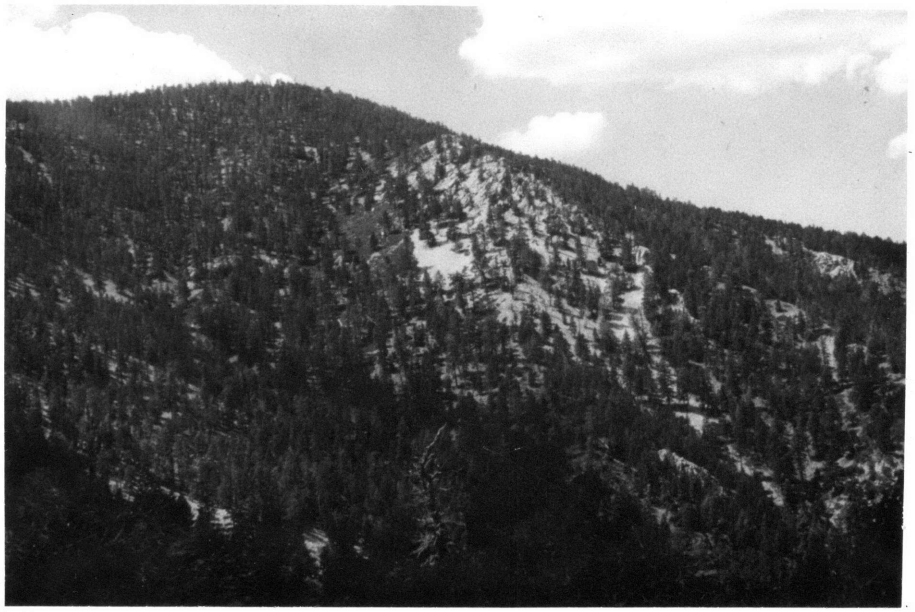

g6, which is thought to flatten down-dip to the north. Rocks of members L3 and S1 exposed in sub-block VIIa are inferred to be detached above fault g6. Faults g5 and g6 are event 3c structures. Structures formed during earlier events are recognized in sub-block VIIa. A possible event 1 thrust (fault t1) is present; low-angle faults t2 and t3 which may be event 1 or event 3a structures are also recognized. The timing of the north-dipping normal(?) fault u is not known. Fault segment AA is believed to be a low-angle younger-over-older normal fault, and is overlapped by sub-block VIIb1 in the NE1/4 of Section 6. Fault AA, and the inferred low-angle normal fault at the base of sub-block VIIb1 are thought to be event 3c faults, and along with fault g6 are intruded by the breccia unit of the Sugarloaf Intrusive Complex. These faults are interpreted to have been truncated by an intruded fault zone at the base of overlying sub-block VIIc1. Fault f1 may be a segment of this fault zone. Rocks of block VIII appear to overlap the trace of this intruded fault, suggesting original cross-cutting fault relationships. The high-angle faults within block VIII, both exposed (x) and inferred from outcrop distribution, probably formed before its final emplacement. The original low-angle fault contact between block VIII and overlying block IX is locally present (fault segments Q). Elsewhere, later high-angle faults (labelled R) have downdropped block IX relative to block VIII. Here as in the Green Canyon area to the northeast, emplacement of the higher allochthons during event 3c involved a complex sequence of faulting. In this area, however, plutonic disruption owing to emplacement of the Sugarloaf Intrusive Complex has been more severe.

The source area for the allochthons VII, VIII and IX is not certain, as was mentioned above. These rocks probably lay in the upper plate of the Doble Thrust. Rocks of the upper Big Bear Group and overlying formations are missing in the lower allochthons. Tectonically denuded potential source areas are certainly available. Detachment fault geometry may provide some insight to the transport direction. The Green Canyon basal fault is the principal detachment surface for block VII. This basal fault has the geometry of a gently W plunging through. Trough-form, younger-over-older fault surfaces are common in the Cenozoic extensional terrane

studied by Proffett (1977). He concluded that transport directions were parallel to the long axes of the fault surface troughs (confirmed by offsets of unique, linear features and other directional indicators). By analogy, I suggest westward relative transport for block VII (movement down the plunge of the troughlike basal fault surface). Block VII may have sat on top of blocks VI or V (see Figs. 55 and 56). In this case, the complex event 3c faulting recognized above the Green Canyon basal fault in sub-blocks VIIa, VIIb1 and VIIb2 may involve significant strike-slip motion. After emplacement of block VII, north to northwestward translation of the sub-block VIIe-VId allochthon occurred. The transport direction for blocks VIII and IX remains uncertain.

There are faults which may be event 3c structures, but whose age cannot be demonstrated with certainty. The Balky Horse Fault cuts event 3a structures. Its sense of separation and outcrop geometry suggest it is a northwest-dipping normal fault. Its relation to intrusive rocks is not known.

The Woodlands Fault on the north side of Deadman's Ridge cuts the Erwin Fault (west segment) and presumably cuts the basal detachment for sub-block VId, an event 3c structure. This low-angle normal fault could be Mesozoic or Cenozoic in age. The exposed fault could be the tear-away for a gravity slide whose buried toe is in the valley to the north.

Event 3 structures are spatially associated with igneous rocks. In most cases final crystallization of the intrusive rocks at Sugarloaf postdates movement on intruded faults. However, evidence indicates some intrusive rocks were emplaced while event 3 faulting was in progress.

Structures formed during events 3b and 3c are only developed in the vicinity of the Sugarloaf Intrusive Complex. The Sugarloaf Quartz Diorite intrudes faults formed during event 3. It structurally underlies, and locally engulfs blocks VII, VIII and IX. The distribution of

associated dikes indicates it underlies sub-block VIc and parts of block Va in lower Green Canyon.

Evidence suggests that some of the earliest magmatic units in the complex were emplaced during event 3c faulting. In Chapter III, intrusive breccias of the Sugarloaf Complex were described which were injected along fault zones interpreted to have formed during event 3c. These faults cut rocks of sub-blocks VIIa, VIIb1 and VIIb2, and include segments of the Green Canyon basal fault, the main detachment surface along which block VII was emplaced. North of Sugarloaf Mountain, the igneous breccias locally grade into recrystallized fault gouge, thought to have formed along event 3c detachment faults. It was suggested in Chapter III that faulting occurred first, followed by injection of the shallow-level dioritic breccias. Apparent local gradation between meta-cataclastic and intrusive breccias, and the presence of tectonite fabrics elsewhere in the igneous breccia unit are interpreted to indicate faulting and magmatism were in part contemporaneous.

As discussed above, the Green Canyon basal fault and other faults within sub-blocks VIIa and VIIb2 along which the breccia unit is recognized are interpreted as early event 3c structures. Thus, contemporaneous magmatism and faulting is inferred during the initial stages of event 3c. Final emplacement of the higher allochthons including VIIc1, VIII and IX, probably occurred during later stages of event 3c. Their bounding faults are intruded by hornblende-bearing diorites, monzodiorites and monzonites. All these units may be younger than the breccia unit, as discussed in Chapter III. Local xenoliths of the breccia unit found in intrusives near blocks VIII and IX suggest the later stage faults may also have been intruded by injection breccias.

To the east of Green Canyon, dacite porphyries intrude several low-angle faults, including an event 3a structure, fault four, and suspected low-angle normal faults cutting basement gneisses in block III. Locally developed tectonite fabrics within the dike rocks (discussed in Chapter III) are interpreted to have formed during post-emplacement movement on the faults. Deformation occurred under metamorphic conditions,

and probably predated emplacement of nearby Sugarloaf Quartz Diorite. It cannot presently be resolved whether dike emplacement and deformation overlapped with events 3a or 3c, or took place later. It should be noted that syn- or postkinematic recrystallization of fault gouge along the event 3a Wildhorse Fault was recognized in a locality 400 m southwest of tectonized dacite dikes (discussed above). This metamorphism may also be related to magmatism.

Also unresolved is the subsurface extent of the Sugarloaf Intrusive Complex and the dacite porphyries. In the northwest part of the area, the allochthons bottom out atop Sugarloaf Quartz Diorite. It is unknown how far these rocks extend beneath the lower allochthons to the east and south. The Cretaceous batholith certainly extends beneath this terrane, but it is unknown if there are older Mesozoic igneous rocks above the granites. The presence of dacite dikes and sills and associated granitoid bodies further east in block III suggests there may be. In Chapter III it was hypothesized that the dacite porphyries may be early, shallow-level dikes related to the composite Sugarloaf Intrusive Complex. If so, the extent of dikes may indicate subsurface continuation of the intrusive complex beneath much of block III.

Event 4: Emplacement of the Sugarloaf Intrusive Complex. Intrusion of some early units of the Sugarloaf Intrusive Complex was apparently contemporaneous with the later phases of event 3 extensional tectonism. The bulk of the composite Sugarloaf Quartz Diorite, however, consolidated after fault movements had ended. To what extent the higher allochthons were rafted atop the diorite prior to its final consolidation is not certain. It is possible that after intrusion the allochthonous blocks continued to move with respect to one another, floating on unconsolidated magma or crystal mush (Hamilton and Myers, 1967, 1974, discuss other possible examples). Locally recognized igneous flow fabric may be related to rafting; however, the relative lack of protoclastic fabric in the diorite suggests that any rafting must have occurred before consolidation of the crystal mush was far progressed.

The fact that structural blocks can still be recognized within the roof rocks of the diorite, in spite of severe plutonic invasion, indicates the allochthons were not significantly disrupted by intrusion. Only minor jostling of the blocks could have occurred. Any major relative motion was between coherent plates; large-scale chaotic mixing of the country rocks is not recognized. The absence of chaotic structure argues against stoping as a major factor in pluton emplacement at this structural level. If stoping was important, significant vertical jumbling of country-rock blocks would be expected. The distribution of roof rocks instead outlines a stack of thin, locally overlapping sheets. Any relative motion between these blocks during intrusion was primarily horizontal, as it was in event 3, and not vertical.

There is evidence of limited country rock assimilation. Metasedimentary xenoliths are present in the diorite, although not abundantly. Limited metasomatism of the diorite is locally recognized over narrow zones adjacent to the marbles. Calcite-epidote-tremolite-plagioclase rocks grade into diorite and marble on either side.

The contact metamorphic effects of the diorite and related leucocratic bodies are often difficult to evaluate. Contact metamorphism was superposed on event 1 metamorphic and tectonite fabrics. In general, the effects were minimal. Narrow skarn zones are recognized at some marble-diorite contacts. Recrystallization of marbles within a few meters of the intrusive rocks is sometimes recognized. Distinctive contact metamorphic mineral assemblages are sometimes formed (discussed below), but local obliteration of S_1 or S_2 cleavage by recrystallization of the marbles is the most typical feature.

Veins of calc-silicate minerals are common in the marbles, extending several tens of meters above the contact. Typically these are tremolite veins, often in asbestiform habit. These veins are cut by small faults, but are not folded.

Contact metamorphic effects in pelitic rocks and quartzites are minor. Tectonite fabrics persist in pelitic rocks even within a few

meters of diorite outcrops. In the case of quartz-rich metapelites, it is difficult to establish if granoblastic fabrics recognized near the diorite reflect static recrystallization or the lack of development of any event 1 tectonite fabrics. Quartzites adjacent to the diorite are notable for their lack of recrystallization or recovery-related fabrics. These rocks are highly strained, suggesting little post-event 1 annealing has occurred. Alternatively, the quartzite fabrics may reflect continued intragranular deformation during pluton emplacement.

It was suggested above that intrusion of the dacite porphyries occurred prior to intrusion of the Sugarloaf Quartz Diorite. Their emplacement was synchronous with low-angle faulting during either event 3a or 3c, or during a later episode of fault reactivation. The emplacement of associated granitoid dikes occurred somewhat later. The granitoids may be part of the Sugarloaf Intrusive Complex, or alternatively they could be related to the younger granitic batholith.

Event 5: Emplacement of Cretaceous Granite - Quartz Monzonite. Intrusion of Cretaceous granite and quartz monzonite is the last major Mesozoic deformational event to affect the area. These rocks are part of the extensive granitic batholith complex that undoubtedly extends beneath the entire Big Bear area. Post-crystallization deformation and hydrothermal metamorphism of rocks of the Sugarloaf Intrusive Complex is attributed to emplacement of this batholith. Regional heating associated with the batholith disturbed the K/Ar isotopic systems of the older plutonic and metamorphic rocks (discussed below).

Granitic rocks are believed to be intruded along the trace of the inferred Onyx Summit Fault. They often crop out as small dikes and sills near Route 38. Southeastward along Route 38, blocks of Wildhourse Quartzite are engulfed by granite. Narrow chill zones were not recognized, nor was any appreciable textural variation observed in the granites near contacts. Locally developed flow foliation, defined by micas, was noted parallel to some intrusive contacts. The textural effects of contact metamorphism on the metamorphic country rocks usually appeared relatively minor.

In one locality, a granite dike may have been intruded parallel to

an earlier greenstone dike. In the south center of Section 27 (T2N, R2E), a granitic dike which dips gently south intrudes Precambrian gneisses. This dike has a crude flow foliation parallel to its margin. Locally, a massive greenstone dike, approximately one meter thick, is present along the contact. It is parallel to the granitic dike and intruded by it. Relict phenocrysts of feldspar are present in the greenstone. These rocks develop a foliation parallel to the dike margin as the overlying gneisses are approached. The banded gneisses also locally develop this new foliation, which cross cuts s_1. Where the new foliation is present, the gneisses are recrystallized, forming epidote-albite-quartz-biotite schists. The contact with the greenstone is gradational over a few cm. It is thought that metamorphism occurred during intrusion of the granitic dike. It is unclear if the foliation at the gneiss-greenstone contact mimics an earlier fabric, or if it developed during granitic intrusion. The age of the greenstone is unknown. It could be Mesozoic, and perhaps injected along an event 3 fault.

Delamar Mountain Area

Introduction. In the Delamar Mountain area, metamorphism and polyphase folding are the earliest Mesozoic events recognized. Superposed fold structures were cut by southeast dipping low-angle normal faults. The early formed folds and faults are intruded by the Fawnskin Monzonite, and younger Bertha Diorite. The Bertha Diorite and the intermediate composition dike complex in the northern part of the area are shallow-level intrusive rocks, in part sub-volcanic. Emplacement of Cretaceous batholithic rocks is the last major Mesozoic event to affect the area. The sequence of events is summarized in Fig. 58.

Event 1: Metamorphism and Polyphase Folding. Superposed, synmetamorphic folds are the earliest Mesozoic structures recognized in the Delamar Mountain area. Polyphase folding is considered to have occurred during a progressive deformational event. Major structures formed during event 1 include the Delamar Mountain Antiform and adjacent Holcomb Creek

Figure 58: Sequence of structural events at Delamar Mountain

1. Metamorphism and polyphase folding
   Metamorphism: low-P, intermediate-T facies
   F_{1a}(?): zonal tight to isoclinal folding causing transposition of bedding
   F.A. orientations not determined
   A.P. and S_{1a}(?) cleavage parallel or at low angle to bedding (S_0)
   F_1: tight folds
   F.A. trend NW-SE, plunge varies
   A.P. and S_1 cleavage dip steeply to NE or are vertical
   vergence is to SW(?)
   F_2: tight and open asymmetric folds
   F.A. tend E-W, plunge varies
   A.P. dips S or sub-vertical, S_2 cleavage is locally developed
   vergence is to N; tectonic transport is to NW, parallel to A.P. of F_1 folds
2. Low-angle(?) normal faulting
3. Emplacement of the Fawnskin Monzonite
4. High-angle faulting
5a. Emplacement of Bertha Diorite (and associated normal faulting)
5b. Emplacement of the Dike Complex
6. Emplacement of Cretaceous granite-quartz monzonite

F.A. = fold axes

A.P. = axial planes

Synform (largely covered by surficial deposits) to the northeast. These structures are truncated to the southeast by the Bertha Diorite and Fawnskin Monzonite, which intruded along an inferred event 2 fault zone. Cambrian marbles south of this fault zone also record event 1 folding. Evidence of ductile flow and recrystallization in the pre-Mesozoic rocks indicates folding and low P, intermediate T metamorphism were contemporaneous.

The presence of superposed folds is indicated by the geometry of the Delamar Mountain Antiform. This structure is actually a dome formed by interfering fold sets (Type 1 interference structure of Ramsay, 1967); its southeastward continuation is truncated by the Bertha Diorite. This geometry can be seen in cross sections AA', BB' and CC', and by tracing bedding orientations of the Zabriskie Quartzite, which outlines a folded surface with a mushroom-like configuration. Along much of its outcrop trace the Zabriskie is overturned, and dips toward the antiform's core. At its northwestward hinge, this structure is a synformal anticline. This dome-like geometry formed by superposition of E-W trending F_2 folds across NW trending F_1 folds. For the purpose of geometric analysis, rocks in the vicinity of the antiform have been divided into sub-areas (see Fig. 59).

Although F_1 folds are the earliest macroscopic structures recognized in the Delamar Mountain area, they appear to refold locally present mesoscopic structures that may be related to an even earlier fold phase, F_{1a}(?). Compositional layering in Bonanza King Formation marbles and Carrara Formation marbles locally resembles tectonically transposed bedding recognized in the Sugarloaf area. This is best developed in the Papoose Lake Member in Section 6 (T2N, R1E). Thin color bands here may have been formed by mesoscopic isoclinal folding with axial surfaces parallel to original bedding. This transposed bedding is refolded and again locally transposed by tight to isoclinal, mesoscopic F_1 folds. Similar pre-F_1 transposition is recognized in Cambrian marbles exposed southeast of the Bertha Diorite.

Figure 59.

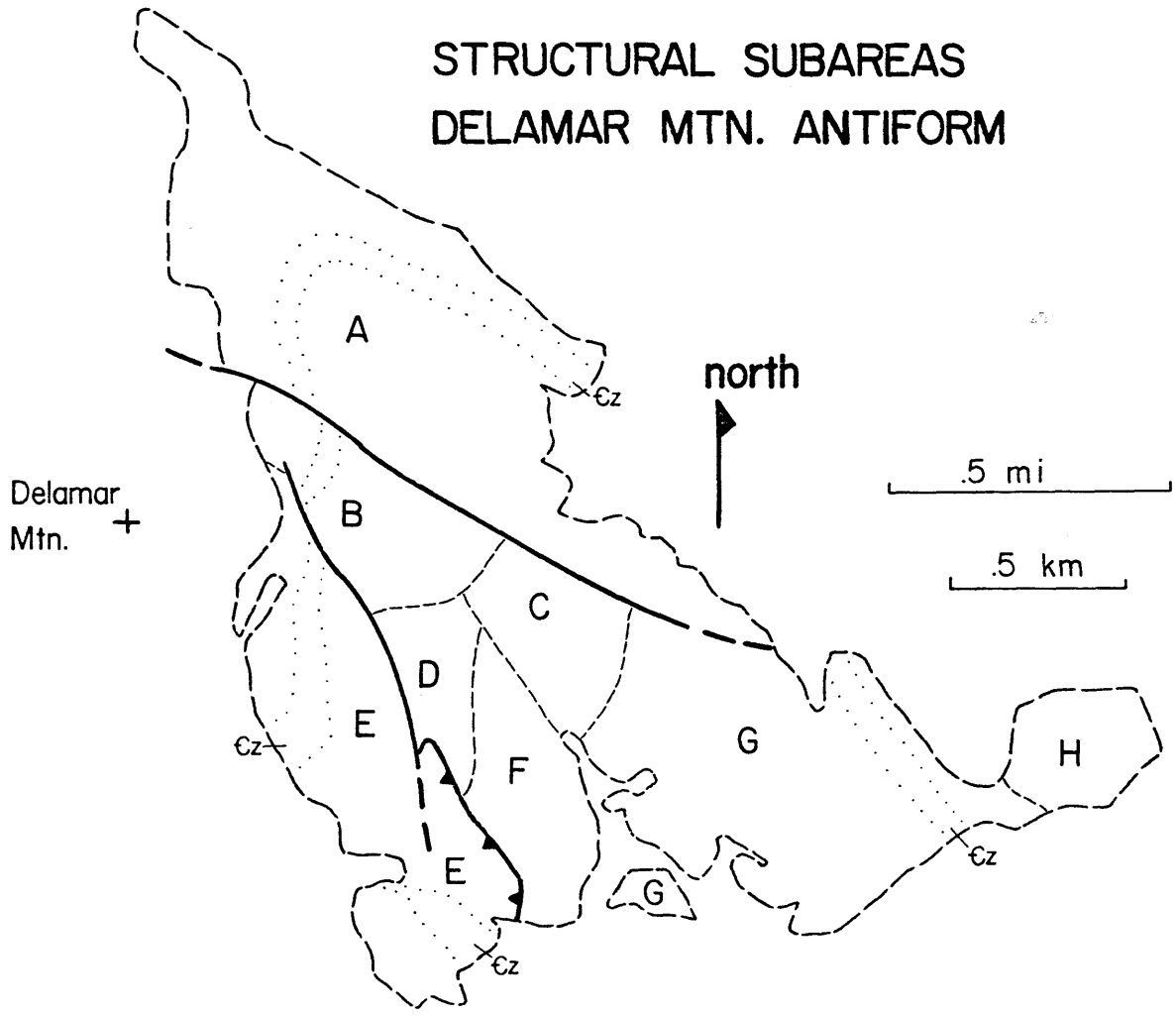
STRUCTURAL SUBAREAS
DELAMAR MTN. ANTIFORM
north
.5 mi
.5 km
Delamar
Mtn.
A
B
C
D
E
F
G
H
E
G
Cz
Cz
Cz
Cz

Pre-F_1(?) mesoscopic structures are locally present in the upper Wood Canyon Formation. In subarea E, possible Scolithus tubes in the upper Wood Canyon Formation are locally progressively rotated and flattened into parallelism with an "S_{1a}" cleavage. The orientation of this cleavage is not consistent with that of axial-planar cleavage (S_1) associated with macroscopic F_1 folds, which locally may crosscut S_{1a} cleavage. The S_{1a} cleavage appears to be locally developed, and may be related to the pre-F_1 mesoscopic folding event (F_{1a}?) which caused local transposition of bedding.

F_1 folds trend NW and control the structural grain in the Delamar Mountain area. The core of the Delamar Mountain Antiform is underlain by rocks of member D1 of the Delamar Mountain Formation. These rocks are exposed in the core of an F_1 anticline. Well-developed S_1 cleavage here is believed to be axial planar to the F_1 fold. This cleavage strikes NW and is subvertical or dips steeply NE. This F_1 fold may have been SW vergent; overturning of bedding on the SW limb of the antiform is probably a result of F_1 folding. Overturning on the NE limb and in the hinge area at the NW end of the antiform is the result of F_2 refolding.

F_1 folding was approximately cylindrical. The axis of the F_1 anticline at the SE end of the antiform (subareas F and G) is sub-horizontal, as are the plunges of minor F_1 folds and $S_0 \times S_1$ lineations. To the NW, a second, en echelon F_1 anticline is recognized in subarea C, formed in the quartzites of member D2. To the northwest, the plunge of the fold axes of these anticlines steepens in subareas C and BDF, as do the plunges of $S_0 \times S_1$ lineations. This progressive rotation of F_1 fold axes culminates in subarea A, where a synformal-anticlinal hinge is defined by Zabriskie Quartzite. This rotation of F_1 structures is the result of F_2 folding.

A younger-over-older thrust fault is recognized cutting the south-west limb of the antiform. In subarea D it overrides a tight, NW plunging syncline. This fold is coaxial with the F_1 anticline, and is probably an F_1 fold. The thrust may be an F_1 structure, and the syncline a locally developed drag fold.

NE of the Delamar Mountain Antiform, Banded Mountain Member marbles in the center of Section 6 (T2N, R1E) probably lie in the core of an F_1 syncline. A macroscopic S fold plunging 36°/N67W is an F_1 structure. This syncline may continue to the northwest where screens of Banded Mountain Member marbles occur within the dike complex. F_1 folds here also plunge moderately NW. Isolated exposures of the Wood Canyon, Zabriskie and Carrara formations north of Bertha Peak may lie in the northeast limb of this F_1 syncline.

F_2 folds trend approximately E-W and refold F_1 structures. The most spectacular example is the refolding of F_1 anticlines to form the dome-like Delamar Mountain Antiform. F_2 folds verge N; the northern limbs are often overturned. Mesoscopic F_2 folds are exposed in roadcuts of the Wood Canyon Formation on the southwest limb of the antiform (subarea E). In these exposures, bedding and S_{1a} cleavage (defined by flattening of burrow tubes) are folded about moderately W-plunging axes. Typically, F_2 folds are Z folds here, with short north limbs. Locally, poorly developed axial-planar cleavage is recognized which dips S. Larger-scale F_2 folds in subareas E, F, D and BDF (composite) are indicated by the presence of secondary girdles on $\perp S_0$ plots. These F_2 axes are summarized in Fig. 62. F_2 folds are responsible for the westward deflections of the outcrop pattern of the Zabriskie Quartzite in subareas B and E. On the northwest limb of the antiform, in subarea G, a mesoscopic F_2 S fold plunges 50°/N60E; its vergence is consistent with mesoscopic F_2 folds on the opposite limb.

F_2 folds refold macroscopic and mesoscopic F_1 structures. Mesoscopic F_1 fold axes and $S_0 \times S_1$ lineations (Fig. 60) and macroscopic F_1 fold axes determined for the different subareas (Fig. 61) lie along NW trending, near vertical planes. A visual fitting of these data indicates they lie along great circle girdles rather than small circle girdles. If all the F_1 linear element data are combined, they lie along a NW trending vertical plane, which could be interpreted as a great circle girdle or a small circle girdle. However, the NE trending, horizontal axis of the small circle girdle bears no relation to observed F_2 fold axes, which trend

Figure 60: Equal-area plot of mesoscopic F_1 linear elements from the Delamar Mountain Antiform.

Figure 61: Equal-area plot of macroscopic F_1 fold axes for each subarea of the Delamar Mountain Antiform.

F_1 axes obtained from contoured pole to S_0 plots for each subarea (data available from author on request). Great circle girdles are shown for reference.

Delamar Mtn. Antiform

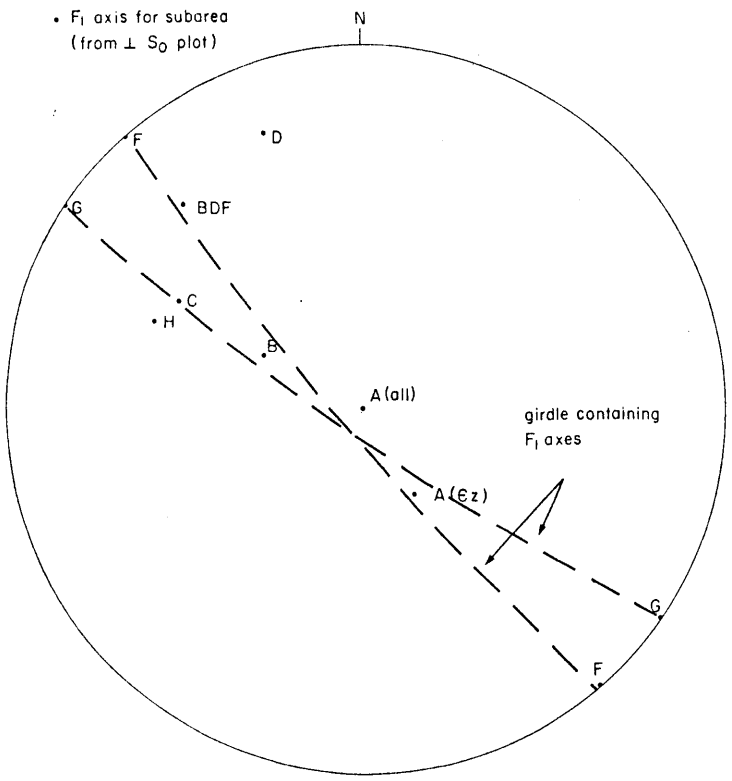

Delamar Mtn. Antiform

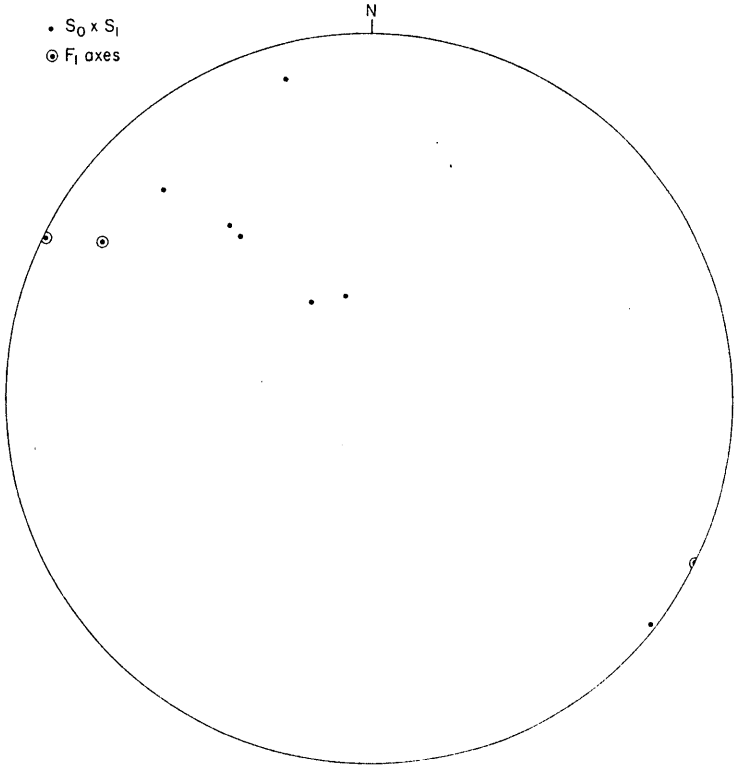

E-W. Therefore, F_1 linear elements are interpreted to lie along great circle girdles and to have been rotated during F_2 similar-type folding (Turner and Weiss, 1963). If F_2 folds are similar, the direction of material transport during F_2 folding lies within these girdles. The intersection of the F_2 slip plane with the composite girdle of F_1 linear elements yields the F_2 transport direction. Unfortunately, the F_2 slip plane is poorly defined. Axial-planar cleavage was recognized in one locality only. If F_2 folds are cylindrical, then the great circle containing the F_2 fold axes yields the slip plane (the axial plane in this case). The girdle obtained here is poorly defined, not surprisingly, as F_2 folds are disharmonic. Thus the slip plane determined from F_2 fold axes is approximate. Using these two potential slip planes it is possible to constrain the F_2 transport direction to a field outlined in Fig. 62. The F_2 transport direction is subvertical or slightly NW directed and lies within the plane of the F_1 axial surface. I suggest that F_1 and F_2 folds formed progressively during a single deformational event.

Since the F_2 transport direction was parallel with the axial surface of F_1 folds, the effects of F_2 folding are more difficult to recognize in the limbs of F_1 folds than in their hinges. I suggest that the dramatic overturning of the Zabriskie Quartzite and other units on the northeast limb of the antiform may reflect F_2 refolding. This oversteepening decreases southeast of Hill 7856'. The geometry of F_2 folding east of here is uncertain. Whether or not the rocks north of Bertha Peak were refolded during F_2 is unknown.

Metamorphism accompanied F_1 and probably F_2 folding as well. Quartzites and marbles show evidence of plastic flow during F_1 folding. Axial planar cleavage is frequently present in metapelitic rocks, and is defined by metamorphic biotite and muscovite. Evidence of metamorphic mineral growth prior to F_1 folding is present. Prekinematic biotite is common, and often forms elongate clots of randomly oriented grains. These elongate clots are rotated into parallelism with the S_1 axial planar

Figure 62: Equal-area plot summarizing structural data used to constrain F_2 tectonic transport direction.

All structural data for mesoscopic and macroscopic F_1 linear elements are plotted here. These F_1 elements are inferred to be reoriented along a vertical great circle girdle by F_2 similar-type folding. F_2 tectonic transport dirction is constrained to lie along the vertical great circle fitted to F_1 linear features, between its intersections with possible F_2 slip planes S_2 and $\sim S_2$. F_2 tectonic transport direction probably lies closer to former intersection, indicating northwestward transport.

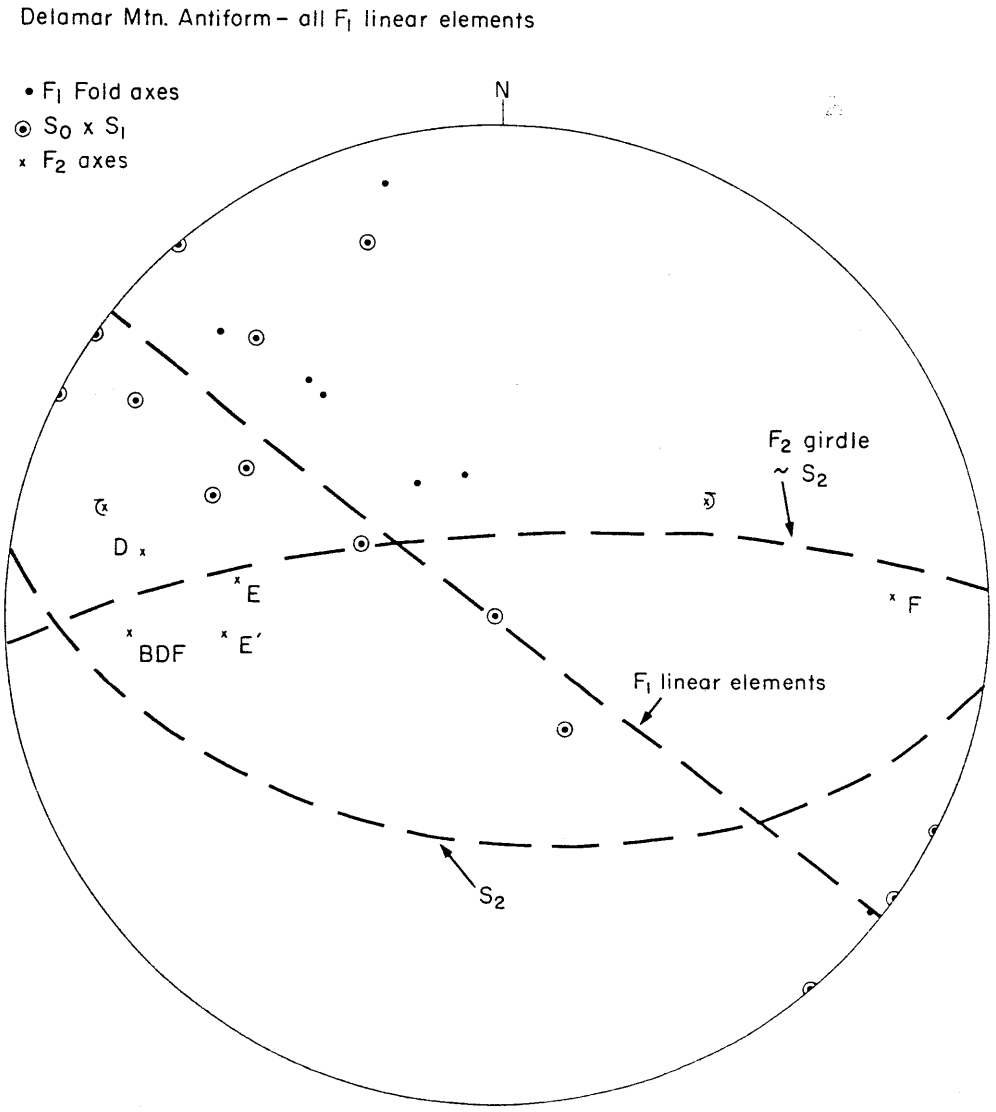

cleavage. Some prekinematic biotites deformed by kinking during rotation. Matrix micas wrap around these biotite clots, as well as irregular or lensoidal pseudoporphyroblasts composed of quartz-muscovite or biotite-muscovite-quartz. The pseudoporphyroblasts may be retrograde after prekinematic andalusite. Richmond (1960) locally observed the assemblage andalusite-biotite-muscovite-quartz in the map area, although andalusite was not observed here during this study. Apparent retrogression indicated by prekinematic pseudoporphyroblasts suggests a decrease in metamorphic grade as deformation progressed.

Flattening of matrix micas about pre- or early synkinematic porphyroblasts or "porpyro-clots" caused local warping and crinkling of the axial-planar cleavage (Fig. 63). In some cases the axes of these crinkle folds display a linear preferred orientation parallel to $S_0 \times S_1$ lineations and the axes of mesoscopic F_1 folds. The axial surfaces of these crinkle folds are discontinuous and irregularly oriented. Penetrative crenulation cleavage is seldom present in these folds. The crinkles described above formed during progressive development of the S_1 axial planar fabric.

Metamorphic mineral growth is recognized locally in association with F_2 folds. Weakly developed S_2 cleavage is defined by growth of biotite and muscovite. F_2 folding is believed to have occurred during the waning stages of the event 1 metamorphism.

Southeast of the Bertha Diorite, marbles assigned to Bonanza King and Nopah(?) formations are complexly folded but were not studied in detail. Bonanza King marbles west of Polique Canyon are folded in a NW plunging F_1(?) antiform. The limbs of this structure are warped by NE-SW trending folds which could be F_2 structures. F_1 folds fold transposed bedding here; this earlier fold phase (F_{1a}(?)) is characterized by small-scale isoclinal folding. East of Polique Canyon original bedding is also transposed, probably prior to F_1 . I did not map here in sufficient detail to separate F_1 and F_2 generation folds.

Event 2: Low-angle(?) Normal Faulting. Event 2 faults cut event 1 folds and are intruded by the Bertha Diorite and the Fawnskin Monzonite.

Figure 63: Photomicrograph of crinkled S_1 cleavage in the Delamar Mountain Formation (member D1). S_1 cleavage is parallel to photo width. Quartz schist grades up (to left) into micaceous quartzite. S_1 cleavage is crinkled around a prekinematic pseudo-porphyroblast consisting of biotite-muscovite-quartz. S_1 cleavage is also crinkled around prekinematic biotite porphyroblasts and elongate "porphyroclots" (dark grains). Length of photo equals 5 mm.

a) plane polarized light
b) crossed polars
Sample is from SW1/4 of Section 6 (T2N, R1E) in the Delamar Mountain area.

Figure 63a.

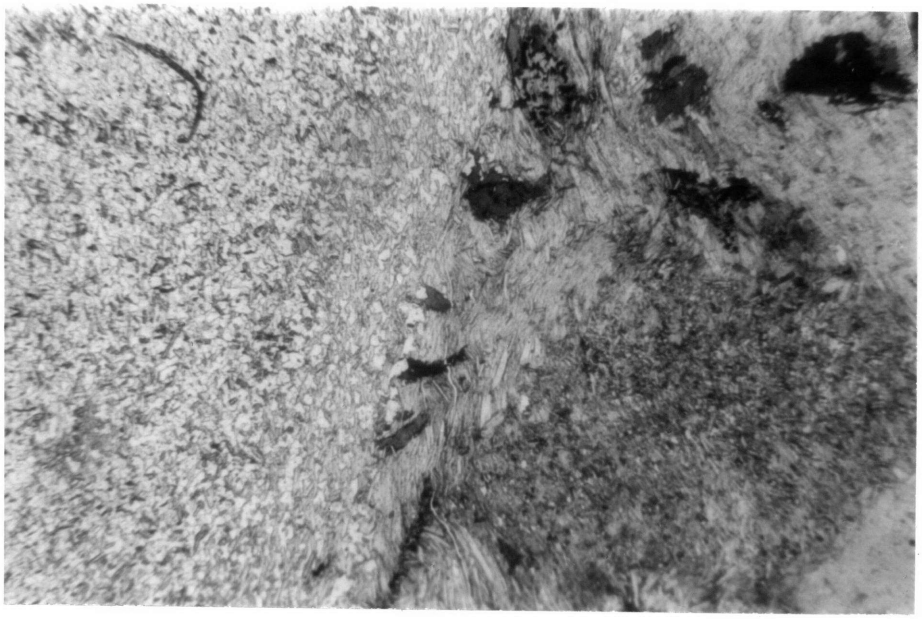

Figure 63b.

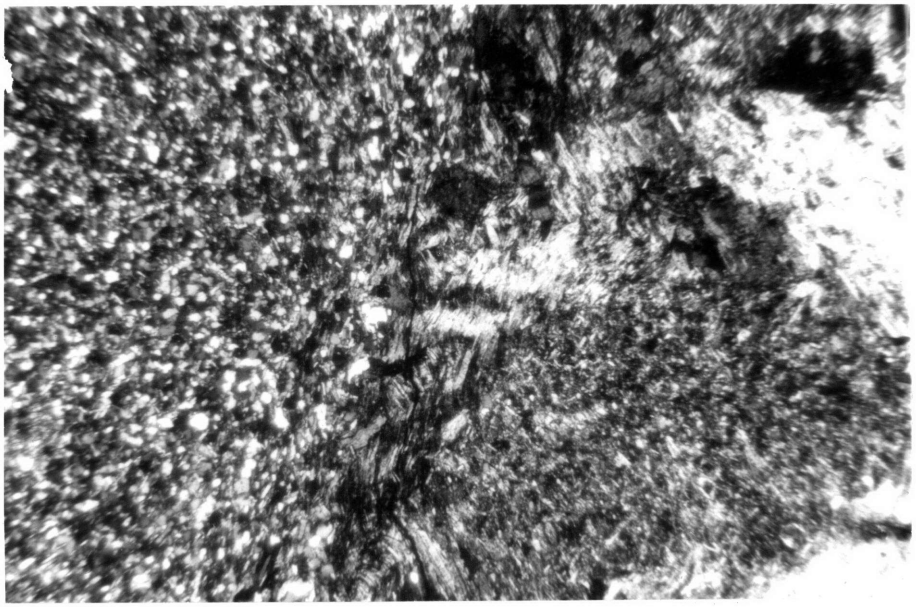

The Bertha Diorite in particular is localized along these faults. Intrusive activity has obliterated all but a few original fault contacts. Generally, event 2 faults must be inferred from outcrop distribution.

The southeastwardly truncation of the Delamar Mountain Antiform was first attributed to faulting by Richmond (1960). The adjacent synform to the northeast is likewise terminated. The fault zone which cuts these structures is now marked by outcrops of Bertha Diorite. Rocks to the south are relatively downdropped across this east-west trending fault.

Cambrian marbles south of the diorite are thought to be the intruded remnants of a major fault block. This block continues to the south and east of the map area (see plate I) and is interpreted here as a younger-over-older allochthon, similar to low-angle fault-bound plates in the Sugarloaf area. The basal fault zone was intruded by the Bertha Diorite, except north of Bertha Peak.

Formation of the fault zone predates emplacement of the Fawnskin Monzonite. The Fawnskin Monzonite is cut by the Bertha Diorite and intrudes rocks displaced along the fault zone. Small exposures of rocks of the Wood Canyon and Zabriskie formations are surrounded by intrusive rocks, and are thought to be remnants of tectonic slivers along the event 2 fault zone. The Fawnskin Monzonite locally intrudes these rocks and nearby exposures of Bonanza King marble of the downthrown block. The juxtaposition of these pre-Mesozoic rocks along the fault zone occurred before or during emplacement of the Fawnskin Monzonite. Later intrusion of the Bertha Diorite caused further spreading of pre-Mesozoic rocks across the fault zone.

The dip of the fault zone is poorly constrained. Analogy with the Sugarloaf area suggests the dips of intrusive contacts are similar to the dips of the intruded faults. If this is the case, gentle dips to the south on the fault are indicated. The contact between Bonanza King marbles and underlying Fawnskin Monzonite in the NW1/4 of Section 7 dips south at 25°. The intrusive lower contacts of Wood Canyon-Zabriskie outcrops along the fault zone dip gently south. Outcrop geometry suggests a pre-intrusive low-angle fault contact between these rocks in the NW1/4 of Section 7

and "underlying" rocks of the Delamar Mountain Formation. The orientation of faults downdropping small outcrops of Zabriskie Quartzite against member D2 of the Delamar Mountain Formation (SE1/4 of Section 1) and Wood Canyon Formation (SW1/4 of Section 6) are unknown.

Event 2 is interpreted as a low-angle faulting event, during which the younger-over-older allochthon comprised of Cambrian marbles was emplaced. Intruded faults juxtaposing Banded Member rocks and Nopah(?) marbles within this block may have formed at this time. The major event 2 structure is an east-west trending fault zone, believed to have dipped gently south. This is interpreted as a normal fault zone, which included slivers of Lower Cambrian units sandwiched between the overlying Middle-Upper Cambrian marbles and underlying Upper Precambrian-Cambrian rocks. As at Sugarloaf, an extensional origin is the most straightforward explanation.

Event 3: Emplacement of the Fawnskin Monzonite. The Fawnskin Monzonite is the earliest Mesoacoic igneous unit recognized in the Delamar Mountain area, and intrudes structures formed during events 1 and 2. The main body of the monzonite crosscuts the southwestern limb and hinge of the Delamar Mountain Antiform. The primary igneous foliation recognized in the Fawnskin Monzonite is grossly concordant with this contact. Mineral lineations in the monzonite indicate that material flow was sub-vertical during the later stages of pluton emplacement.

The contact is irregular in detail, and discordant to country rock structure. The contact dips both gently and steeply to the east and west. Whether this contact is fault controlled is uncertain. A small block of Zabriskie Quartzite in the SW1/4 of Section 1 may be a displaced fault zone sliver. The orientation of any pre-intrusive fault here is not constrained.

Emplacement of the smaller body of Fawnskin Monzonite along Holcomb Valley Road was structurally controlled along the major event 2 low-angle fault. The monzonite is only locally exposed along this fault. Whether it was originally more extensive is unknown. It was apparently emplaced as a thin sheet along the base of the detached Cambrian marbles. It is unknown if further displacement occurred along the fault after monzonite intrusion but prior to crystallization of the Bertha Diorite.

Contrary to Richmond's (1960) conclusions, it is here suggested that contact metamorphic effects of the Fawnskin Monzonite (and younger plutons as well) are minimal. Narrow skarn zones are present locally where the monzonite intruded Cambrian marbles. However, event 1 metamorphic and tectonite fabrics are preserved even in close proximity to the monzonite. The amount of deformation associated with monzonite emplacement is uncertain.

Event 4: High-angle Faulting. Two northwest trending high-angle faults which locally cut the Fawnskin Monzonite are included in this event. One of these faults cuts the younger-over-older thrust fault on the southwest limb of the Delamar Mountain Antiform. The faults are interpreted to predate emplacement of the Bertha Diorite, although this is not demonstrable. Rocks of the dike complex are locally injected along the northern event 4 fault. The principal outcrops of the dike complex may have been localized along faults of this generation.

Event 5a: Emplacement of Bertha Diorite. The Bertha Diorite intrudes the Fawnskin Monzonite, and was emplaced along the east-west trending event 2 fault zone. Injection of the diorite may have occurred contemporaneously with further movement on the fault zone, but this cannot be demonstrated. At the least, diorite emplacement caused a further spreading apart of pre-Mesozoic rocks here. Stoping is not considered to have been important at this structural level, as discussed in Chapter III.

Only minor contact metamorphic effects in pre-Mesozoic rocks can be attributed to intrusion of the Bertha Diorite. Narrow (0.5 m thick or less) skarn zones are locally developed in marbles adjacent to the diorite. Significant overprinting of event 1 fabrics was not recognized. Hydrothermal alteration and deformational features observed in the Fawnskin Monzonite outcrops nearby are attributed to the diorite's emplacement. The Bertha Diorite shows evidence of shallow level emplacement along pre-existing faults (see Chapter III).

Event 5b: Emplacement of the Dike Complex. The dike complex intrudes the Fawnskin Monzonite and folded Bonanza King marbles. The latite-andesite

dikes show features indicative of a sub-volcanic environment, as outlined in Chapter III. The marbles and the monzonite were spread apart by injection of these northwest trending, near vertical dikes.

The intermediate composition of these rocks and their shallow level of emplacement raise the possibility they are related to the Bertha Diorite. Both units cut the Fawnskin Monzonite and predate granitic rocks of the Cretaceous batholith. It is possible that these dikes are higher level volcanic feeders related to the Bertha Diorite. The subsurface extent of the Bertha Diorite is not known. Isolated dikes of its porphyritic facies occur in the S Center of Section 1. Similar rocks tentatively assigned to the dike complex intrude an event 4 fault in the NW1/4 of Section 1. These dikes may indicate that the Bertha Diorite extends beneath the pre-Mesozoic rocks comprising the Delamar Mountain Antiform. At present, correlation between the Bertha Diorite and the dike complex remains tentative.

Event 6: Emplacement of Cretaceous Granite-Quartz Monzonite.

Emplacement of Cretaceous granite, granite porphyry and quartz monzonite is the last major Mesozoic event recognized in the Delamar Mountain area. These rocks are correlative with granitic rocks in the Rose Mine and Sugarloaf areas, and represent a portion of an extensive batholith complex. These rocks are inferred to underlie the entire Delamar Mountain area some 100-300 m below the present level of exposure. The earlier Mesozoic igneous units, as well as the pre-Mesozoic metasedimentary rocks, are interpreted as a thin roof pendant above a generally flat-topped batholith. Internal rafting within the Delamar Mountain pendant during this event is not recognized.

Postcrystallization deformational features and hydrothermal alteration recognized in the older plutons are believed to be a result of Cretaceous batholith emplacement. Rocks particularly affected include the Bertha Diorite and the main body of the Fawnskin Monzonite.

Unresolved is the time of emplacement of the isolated bodies of hornblende-biotite-quartz diorite. They intrude the Bertha Diorite and are cut by the granitic rocks. Their lack of alteration or shallow-level textures suggests they may be related to the younger plutonic episode. Perhaps this diorite is an early unit in the Cretaceous batholithic sequence.

Summary

The study areas record a complex Mesozoic deformational history. A more detailed synthesis of Mesozoic deformation is presented in Chapter VI, which integrates geochronologic data from cross cutting plutonic rocks. Although the detailed sequence of events is not identical in each of the areas discussed, the general progression of events is similar.

Metamorphism and polyphase folding are the earliest events recognized in each area. The early fold phases are synmetamorphic; however the metamorphic peak is, locally at least, prekinematic. Although Precambrian gneisses are involved in folds and faults, only near the Doble Thrust do they display evidence of Mesozoic metamorphism or penetrative fabrics. Metamorphism, polyphase folding, and emplacement of the Doble Thrust are thought to have occurred during a progressive deformational episode.

This complexly folded terrane was disrupted by a complex sequence of faults, including high-angle and later low-angle normal faults. These may have developed over an extended time period. Younger-over-older allochthons are bound by the low-angle faults, and are present at Sugarloaf and Delamar Mountain. In the Sugarloaf area, at least, the later stages of this extensional faulting appear to have been contemporaneous with magmatism. At Delamar Mountain, the Fawnskin Monzonite and younger Bertha Diorite intrude along a low-angle younger-over-older fault zone. This tectonism appears to have largely ended after emplacement of the shallow-level, intermediate rocks including the Sugarloaf Intrusive Complex, the dacite porphyries, the Bertha Diorite and (?) the dike complex. All earlier

structures and older Mesozoic igneous rocks are intruded by the granite-quartz monzonite batholith which underlies the entire Big Bear area.

Conditions of Precambrian and Mesozoic Metamorphism

General Statement

Rocks in the Big Bear area record the effects of two dynamothermal metamorphic episodes. Precambrian deformation probably occurred at middle amphibolite facies conditions, although diagnostic mineral assemblages are lacking in the study areas. Unconformably overlying Upper Precambrian-Cambrian miogeoclinal rocks record the effects of Mesozoic dynamothermal metamorphism concurrent with major folding and thrusting. Richmond (1960) had previously ascribed most of the metamorphism to contact effects. Mineral assemblages indicate low pressures and temperatures indicative of the greenschist-amphibolite facies transition. These P, T conditions are typical of intra-arc metamorphic terranes (Miyashiro, 1973). The Precambrian metamorphic assemblages are stable at these conditions, so recrystallization and the development of tectonite fabrics in the basement gneisses during this Mesozoic event is limited. Recrystallization of Precambrian gneisses is principally restricted to rocks immediately above the Doble Thrust. This suggests that high strain and access to metamorphic fluids from underlying, devolatilizing cover rocks may have been important controls for localizing basement recrystallization.

Contact metamorphism related to Mesozoic plutonism is locally superimposed on the earlier events. Recrystallization or retrogression related to contact effects is quite limited, although K/Ar data (Chapter V) indicates significant reheating accompanied plutonism. Here again, pre-existing mineral assemblages typically remained stable except adjacent to intrusive contacts, or where favorable structures facilitated access to fluids necessary for reactions to proceed.

The conclusions drawn here are based on petrographic and field observations. Without mineral analyses, this treatment is necessarily of

a reconnaissance nature. The various general reactions suggested and discussed here are undoubtedly oversimplifications of the actual systems. In the absence of quantitative petrologic data, the application of experimental results for ideal systems to constrain metamorphic conditions of real rocks is but a crude first step.

Precambrian Metamorphism

Mineral assemblages recognized in the Precambrian gneiss complex formed primarily during Precambrian f_1 and f_2 folding. This metamorphic event is dated as Proterozoic by the presence of synkinematic granitic gneisses yielding a 1750 m.y. U/Pb zircon age (Silver, 1971). Unfortunately, the P, T conditions of this regional metamorphic event are not well constrained. Pelitic, mafic and carbonate rocks suitable for producing diagnostic metamorphic assemblages are lacking in the study area. Predominant rock types consist of quartzo-feldspathic paragneisses and quartz-rich schists, yielding high-variance assemblages. In the banded paragneisses, the assemblage biotite + muscovite + microcline + quartz + plagioclase is common, and according to Turner (1968) is typical of amphibolite facies quartzo-feldspathic rocks. Schists consist of biotite + muscovite + quartz $\pm$ microcline $\pm$ plagioclase. The absence of diagnostic index minerals probably reflects relatively Al-poor pelitic compositions rather than low-grade metamorphism. Chlorite and epidote are not present in non-retrograded basement rocks. An upper limit on Precambrian metamorphic conditions may be provided by the coexistence of muscovite + quartz + microcline which indicates P, T conditions below those required for muscovite dehydration by the reaction

$$\text{muscovite} = \text{K-feldspar} + \text{corundum} + H_2O \qquad (1)$$

at $P_{total} = P_{H_2O}$ (the univariant equilibrium curve for (1) is shown in Fig. 64; curve after Helgeson and others, 1978). The absence of an Al_2SiO_5 polymorph may be a function of the Al-poor bulk composition of these rocks rather than of T.

Figure 64: P, T grid summarizing constraints on conditions of Mesozoic dynamothermal metamorphism. Constraints provided by experimental and thermodynamic data concerning phase equilibria of key mineral assemblages. Stippled region represents allowed P, T conditions in the study areas at metamorphic peak. Numbers refer to univariant reaction curves discussed in text (source in parentheses).

(1) Muscovite = K-feldspar + corundum + H_2O (Helgeson and others, 1978)

(2) Pyrophyllite = andalusite + quartz + H_2O (Helgeson and others, 1978)

(3) Fe-chlorite + muscovite + quartz = cordierite + biotite + andalusite + H_2O (Winkler, 1979)

(4) Mg-chlorite + andalusite + quartz = cordierite + vapor (Helgeson and others, 1978)

(5) Mg-chlorite + muscovite + quartz = cordierite + phlogopite + H_2O (Helgeson and others, 1978)

(6) albite + epidote + chlorite + quartz = oligoclase + tschermakite + Fe_3O_4 + H_2O (Liou and others, 1974)

(7) chlorite + sphene + quartz = Al-amphibole + ilmenite + H_2O (Liou and others, 1974)

(8) tremolite + calcite + quartz = diopside + H_2O + CO_2 (curves represent range for maximum thermal stability of tremolite + calcite + quartz in T - X_{CO_2} space ($X_{CO_2} \sim 0.75$) as compliled from: Skippen, 1974; Slaughter and others, 1975; Winkler, 1976, 1979; Helgeson and others, 1978.)

(9) epidote + quartz = grossular + anorthite + magnetite + fluid (Liou, 1974)

(10) zoisite + quartz = grossular + anorthite + H_2O (Helgeson and others, 1978)

Note that greenschist facies lies left of curve (6) while amphibolite facies lies right of curve (7). Greenschist-amphibolite transition facies of Liou and others (1974) lies between (6) and (7). Al_2SiO_5 system is from Holdaway (1971).

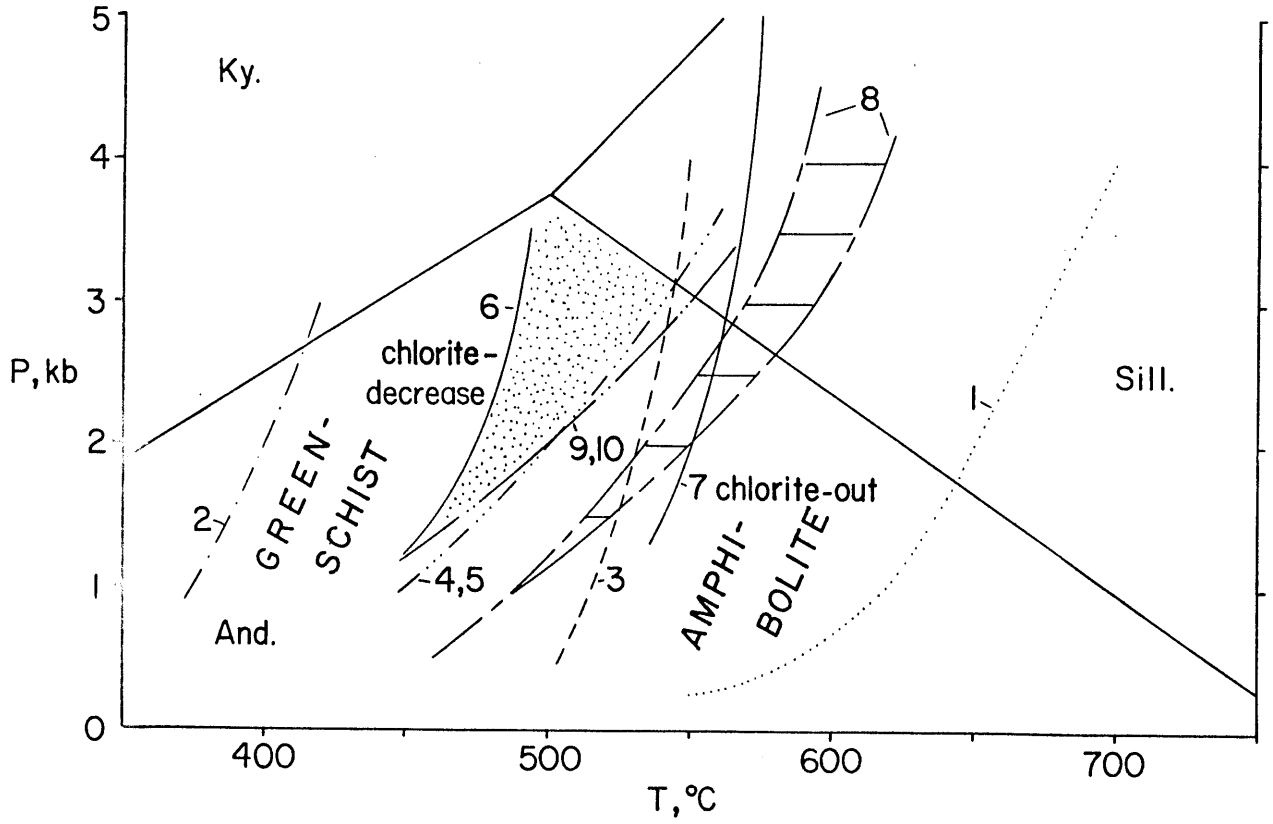
Ky.
And.
Sill.
P, kb
T, °C
5
4
3
2
1
0
400
500
600
700
8
6
chlorite-
decrease
9,10
7 chlorite-out
2
GREEN-
SCHIST
4,5
3
AMPHI-
BOLITE
1

At present, P_{total} of the Precambrian metamorphic event is also poorly constrained. The presence of muscovite in synkinematic granites and pegmatite dikes cannot be used to evaluate depth of emplacement as its P stability is compositionally controlled. Precambrian metamorphism in the Big Bear area was clearly associated in time and space with significant plutonism. Similar, multiply-deformed crystalline terranes have been described by Hamilton and Myers (1967, 1974) as the remobilized, often migmatized floor region beneath shallow-level batholiths. At present, however, the P, T conditions are too poorly constrained to warrant further speculation on the tectonic setting of Precambrian metamorphism at Big Bear.

Mesozoic Dynamothermal Metamorphism

Metamorphism of Miogeoclinal Rocks. The Upper Precambrian-Cambrian miogeoclinal sequence was thoroughly recrystallized during a dynamothermal metamorphic event which involved polyphase folding. In spite of wide variation in rock types, typical mineral assemblages encountered in the quartzites and marbles do little to constrain the P, T conditions of metamorphism. The mafic rocks of the Wildhorse Greenstone and the Al-rich pelitic rocks of the Lightning Gulch Formation provide the most useful information in this respect. These units are exposed only in the Sugarloaf area, so caution is required in generalizing about the Big Bear area as a whole. However, conclusions concerning P, T conditions at Sugarloaf are compatible with mineral assemblages recognized elsewhere.

Textural relations, discussed above, indicate that the highest grade assemblages recognized formed prior to the earliest penetrative deformation at Sugarloaf and probably at Delamar Mountain. Metamorphic conditions continued during the early fold phases, however, synkinematic growth of the higher grade "index" phases was not recognized. The frequent occurrence of prekinematic pseudoporphyroblasts indicates that retrogression locally predated penetrative deformation. Thus, the metamorphic peak was apparently prekinematic. This discussion focusses on the highest grade

assemblages recognized. The P, T conditions indicated by these assemblages apparently prevailed at the initiation of Mesozoic folding in the Big Bear area.

Metapelitic rocks and quartzites in the study areas typically contain high-variance mineral assemblages, which are not particularly useful for delimiting metamorphic conditions. Biotite + chlorite + muscovite + quartz $\pm$ K-feldspar $\pm$ plagioclase is a ubiquitous assemblage, but only indicates a minimum of middle greenschist facies conditions (low-grade metamorphism of Winkler, 1979) and a P, T maximum defined by the muscovite dehydration curve. The aluminous pelitic rocks of the Lightning Gulch Formation are an important exception. The assemblage andalusite + biotite + chlorite + muscovite + quartz is common in the lower and middle members of the Lightning Gulch Formation in the Sugarloaf area. This assemblage is prekinematic with respect to the earliest phase of Mesozoic folding. It was also reported from the Delamar Mountain area by Richmond (1960). Although in some cases chlorite is secondary after biotite, primary chlorite is present as well. The presence of andalusite rather than sillimanite or kyanite constrains P_{total} of metamorphism to less than 3.76 kb (Holdaway, 1971; Helgeson and others, 1978). The absence of pyrophyllite places a lower limit on T which is defined by the reaction

$$\text{pyrophyllite} = \text{andalusite} + \text{quartz} + H_2O \qquad (2)$$

The univariant equilibrium curve for the pyrophyllite breakdown reaction (after Helgeson and others, 1978) is shown in Fig. 64 and indicates a minimum T range of about 400 ± 20°C.

An approximate upper limit on T for these aluminous pelitic rocks may be provided by the absence of cordierite. Winkler (1979) has defined the low grade-medium grade transition by the first appearance of cordierite and/or staurolite in rocks of appropriate bulk compositions. The bulk rock Fe/Mg ratio for these rocks may be too low for the presence of staurolite, as evidenced by the absence of chloritoid. These rocks do appear compositionally suitable to record the presence of cordierite, however (see Fig. 65).

Figure 65: AFM diagram depicting mineral assemblages recognized in metapelitic rocks. Tie lines shown are schematic and not based on quantitative mineral analyses. Assemblages also contain quartz + muscovite.

Almd: almandine
And: andalusite
Chlrt: chlorite
Chltd: chloritoid
Cord: cordierite
St: staurolite

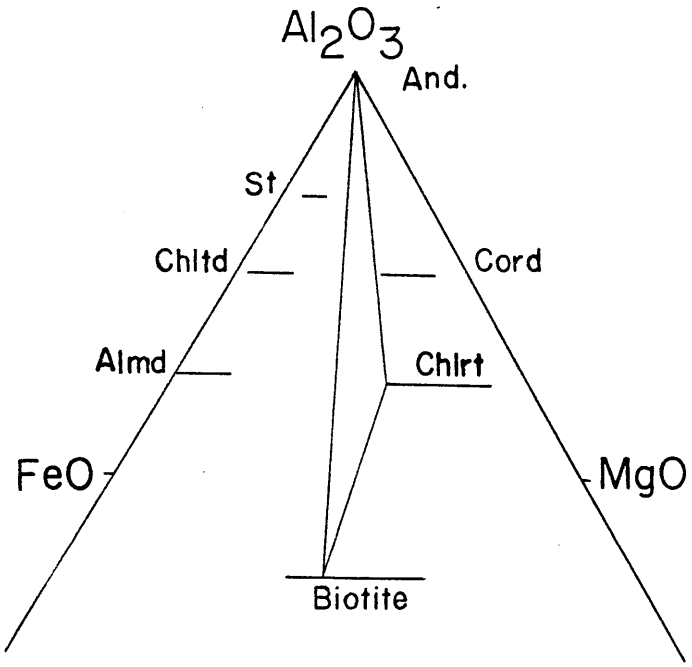

Appearance of cordierite is accompanied by breakdown of chlorite in the presence of muscovite and/or quartz. Possible reactions include:

$$\text{Fe-chlorite} + \text{muscovite} + \text{quartz} = \text{cordierite} + \text{biotite} + \text{andalusite} + H_2O \quad (3)$$

$$\text{Mg-chlorite} + \text{andalusite} + \text{quartz} = \text{cordierite} + \text{vapor} \quad (4)$$

and

$$\text{Mg-chlorite} + \text{muscovite} + \text{quartz} = \text{cordierite} + \text{phlogopite} + H_2O \quad (5)$$

As the composition of the chlorite involved here is not known, the stability field for both Fe- and Mg-rich varieties must be considered. Univariant equilibrium curves for reactions (4) and (5) (after Helgeson and others, 1978) are nearly coincident and are shown in Fig. 64, along with a curve fit to experimental data for reaction (3) reported by Winkler (1979). These data suggest first appearance of cordierite should occur between about 500-525°C at P_{H_2O} = 2 kb and between about 535-550°C at P_{H_2O} = 3 kb. Its absence in pelitic rocks in the Lightning Gulch Formation indicates these values are upper limits on T. Although cordierite was not recognized in thin section, pseudo-porphyroblasts consisting of quartz + muscovite + chlorite are present at Sugarloaf (Lightning Gulch Formation) and at Delamar Mountain (member D_1 of the Delamar Mountain Formation). In some cases this assemblage may be retrograde after cordierite. It may be that the stability field of cordierite was briefly reached in some areas prior to retrogression and the onset of penetrative deformation.

The Wildhorse Greenstone underlies the andalusite - bearing phyllites of the Lightning Gulch Formation, and contains assemblages typical of the greenschist-amphibolite transition zone described by Liou and others (1974). The greenstone usually includes actinolite-hornblende + epidote + chlorite + albite ($\pm$oligoclase) + opaques + quartz $\pm$ biotite. Actinolite and hornblende coexist as complex intergrowths, often in

optically continuous grains. Both albite and oligoclase are present in single thin sections, however albite predominates. Chlorite and epidote occur in variable proportions, as do biotite and quartz. Opaques are abundant, and include magnetite and ilmenite; sphene is also usually present.

Liou and others (1974) recognized a transition zone between mafic greenschists and amphibolites at low to intermediate pressures (2-5 kb). Chlorite begins to break down in actinolite + chlorite + epidote + albite + quartz greenschists at about 475°C at 2 kb. Chlorite disappears at approximately 550°C at that pressure, and at 575°C at 5 kb (see Fig. 64). Liou and others (1974) have suggested generalized reactions which may be important in this transition zone, including a "chlorite decreasing" reaction

$$\text{albite} + \text{epidote} + \text{chlorite} + \text{quartz} = \text{oligoclase} + \text{tschermakite} + Fe_3O_4 + H_2O \qquad (6)$$

and a "chlorite out" reaction

$$\text{chlorite} + \text{sphene} + \text{quartz} = \text{Al-amphibole} + \text{ilmenite} + H_2O\ . \qquad (7)$$

The stoichiometry of the complex reactions leading to the breakdown of actinolite + chlorite ± epidote + albite and the formation of hornblende + plagioclase remains unresolved. The persistence of chlorite in the Wildhorse Greenstone is diagnostic of the transitional facies of Liou and others (1974). The absence of garnet in these greenstones suggests, but does not require, P, T conditions below the garnet isograd (T = 500°C, F. Spear, personal comm., 1980)。 The stability of both chlorite and garnet is strongly dependent on Fe/Mg so the P, T limits cited above are approximate.

The assemblages recognized in marbles and calc-silicate rocks do not provide appreciably tighter P, T constraints, as the critical fluid phase compositions for these rocks were not determined. The general

proximity of the marbles to intrusive rocks in the Sugarloaf area causes further uncertainty in differentiating dynamothermal and superimposed contact metamorphic assemblages. In rocks clearly recording the earlier metamorphism alone, the assemblage tremolite + calcite + quartz is widespread, although more typically quartz is absent. The upper thermal stability of this assemblage is determined by the reaction

$$\text{tremolite} + \text{calcite} + \text{quartz} = \text{diopside} + CO_2 + H_2O. \qquad (8)$$

Experimental and thermodynamic data indicate the maximum thermal stability of this assemblage in $T\text{-}X_{CO_2}$ space occurs at approximately $X_{CO_2} = 0.75$ (Winkler, 1979; Helgeson and others, 1978). $T\text{-}X_{CO_2}$ curves generated by Helgeson and others (1978) agree reasonably well with the experimental data of Skippen (1974), Slaughter and others (1975), and that reported by Winkler (1976; 1979). These data are summarized in Fig. 64 and outline the maximum thermal stability field for tremolite + calcite + quartz. The assemblage diopside + tremolite + calcite was recognized in one locality (in member G1, Green Canyon Formation, in the Sugarloaf area: NE1/4 Section 6, T1N, R2E). The presence of diopside here may record local temperature variations or more likely variability in X_{CO_2}.

The persistence of epidote + quartz in many calc-silicate rocks at Sugarloaf may provide an additional constraint on metamorphic conditions. Liou (1973) has provided experimental data on the reaction

$$\text{epidote} + \text{quartz} = \text{grossular} + \text{anorthite} + \text{magnetite} + \text{fluid} \qquad (9)$$

at f_{O_2} of the QFM buffer (see Fig. 64). These data suggest an upper stability of epidote + quartz of ~500°C at P_{fluid} = 2 kb and 540°C at P_{fluid} = 3 kb.

In the Delamar Mountain area, calc-silicate rocks of the Carrara Formation contain the assemblages zoisite + grossular + anorthite + calcite and zoisite + quartz + anorthite + calcite. The isobaric invariant assemblage zoisite + grossular + quartz + anorthite + calcite may be present in these rocks but was not observed. The assemblages described may reflect the reaction

zoisite + quartz = grossular + anorthite + H_2O. (10)

The univariant equilibrium curve for this reaction for $P_{total} = P_{H_2O}$ (after Helgeson and others, 1978) is nearly coincident with that of the epidote + quartz breakdown reaction (8) and the equilibrium curve for the isobaric invariant assemblage zoisite + grossular + anorthite + quartz + calcite reported by Winkler (1979), which has $X_{CO_2} \simeq 0$. These curves are represented by the "epidote/zoisite + quartz out" curve in Fig. 64. These data suggest temperatures between 500-550°C, and fluid pressures of 2-3 kb for calc-silicate rocks at Delamar Mountain.

Pertinent reaction curves which constrain the conditions of dynamothermal metamorphism at Big Bear are summarized on a P, T grid in Fig. 64. The presence of andalusite, and the absence of cordierite in Al-rich pelitic rocks at Sugarloaf indicates low pressure, upper low-grade metamorphic conditions (Winkler, 1979). Temperature is constrained between 475-560°C by the presence of a transitional greenschist-amphibolite facies assemblage in the Wildhorse Greenstone. A further upper limit on T of approximately 500-550°C is indicated by experimental phase equilibria of calc-silicate assemblages recognized, and is compatible with the presence of the assemblage tremolite + calcite + quartz in marbles. The rare occurrence of diopside may be explained by variable X_{CO_2} of metamorphic fluids, rather than by significant local temperature fluctuations. Available data suggest the range of P, T conditions is T = 475-500°C at P_T = 2 kb and 500-540°C at P_T = 3 kb during the peak of the dynamothermal metamorphic event.

The lower limit on P and T is greatly dependent on the lower stability of the greenschist-amphibolite transition zone as constrained by the work of Liou and others (1974). The stability field of this facies at lower P and T conditions is presently unknown, so minimum P, T conditions may be slightly lower than that indicated above. Nevertheless, the presence of andalusite requires a minimum geothermal gradient of $\geq$ 38°C/km during metamorphism, as indicated by Holdaway (1971). Using intermediate values from the P, T range suggested here (T = 500°C, P_{total} = 2.5 kb) a

gradient of 58°C/km is determined. The range 38-58°C/km falls within the field of low pressure intra-arc metamorphic belts defined by Miyashiro (1973).

Recrystallization in Basement Gneisses. Although the miogeoclinal cover sequence was completely recrystallized during the early dynamothermal metamorphic event, the underlying basement gneisses generally show little or no evidence of Mesozoic metamorphism. The exception occurs in exposures of Precambrian gneisses immediately above the Doble Thrust near Rose Mine (structural petrography discussed above) where gneisses override the cover sequence. Here, a new generation of fine-grained muscovite and green-brown biotite is recognized in the quartzo-feldspathic banded geneisses. The assemblage present,

microcline + quartz + biotite + muscovite

is similar to that present in nearby Precambrian gneisses which show no evidence of Mesozoic fabric. In the latter rocks, however, the micas are medium to coarse-grained and red-brown biotite is present. In gneisses with the Mesozoic fabric, coarse microcline and quartz are highly strained and appear to be relict from the Precambrian mineral paragenesis. Finer grained strain-free quartz and K-feldspar apparently recrystallized during development of the Mesozoic foliation.

The metamorphic assemblage recognized in both the recrystallized and non-recrystallized gneisses is stable over a wide P, T range. The superficial similarity of these assemblages may reflect a high variance bulk composition, and not identical metamorphic conditions. Available data from the miogeoclinal rocks indicates low P, intermediate T conditions during the Mesozoic event, somewhat below the inferred amphibolite facies conditions of Precambrian metamorphism. Without mineral analyses, however, retrogression of the Precambrian gneisses during the Mesozoic dynamothermal event cannot presently be demonstrated. The reactions involved in the recrystallization of the basement gneisses are not clear. However, new mica growth almost certainly requires the presence of H_2O. Recrystalli-

zation and penetrative deformation of basement gneisses above the Doble Thrust may have been facilitated by the presence of H_2O derived from prograde metamorphism of the underlying miogeoclinal sequence. This is discussed further below.

Mesozoic Contact Metamorphism

As discussed in Chapter III and above, recrystallization owing to contact metamorphism appears to be limited to zones within a few tens of meters of intrusive rocks. Contact metamorphic assemblages were not examined in detail. In general, little evidence of recrystallization is recognized in quartz-rich rocks, particularly near the older plutons. The mineral assemblages formed during the dynamothermal metamorphic event remained stable during the emplacement of Fawnskin Monzonite, Bertha Diorite and Sugarloaf Intrusive Complex. Marbles were more reactive, and complex skarns are recognized in places. As mentioned above, transformations are often textural rather than mineralogical. However, both prograde and retrograde contact assemblages are recognized locally. Marbles of member G7, Green Canyon Formation, exposed north of Sugarloaf Mountain, are intruded by the Sugarloaf Quartz Diorite and contain

tremolite + calcite + spinel + phlogopite + chondrodite + (?)forsterite.

This assemblage is typical of high temperature, low pressure contact metamorphism (Winkler, 1979) and is compatible with the interpretation of the Sugarloaf Quartz Diorite as part of a shallow-level intrusive complex. Basement gneisses, on the other hand, display retrograde assemblages adjacent to Cretaceous granitic rocks. Banded paragneisses and schists are sometimes transformed into epidote + albite + biotite + quartz greenschists at intrusive contacts. Such retrogression involves hydration reactions. This requirement and the general localization of contact metamorphism along veins or near intruded fault zones suggests that access to fluid (magmatic, hydrothermal or meteoric) was critical for the presence or absence of contact metamorphism.

The older Mesozoic plutons record effects of hydrothermal and contact metamorphism owing to emplacement of younger intrusives. These effects include sericitization and saussuritization of feldspar, and chloritization of biotite. Temperatures were sufficient to disturb K/Ar isotopic systems, often drastically.

Late Cenozoic Events

The present range morphology of the San Bernandino Mountains is the result of uplift within one of the most tectonically active mountain systems in the world, the Transverse Ranges. The San Bernardino Mountains are being uplifted rapidly between the south branch of the San Andreas Fault and the Mojave Desert. The Big Bear area lies northeast of the San Andreas fault zone. Rocks in the northern San Bernardino Mountains are geologically part of the Mojave Desert geologic terrane and have been thrust south along the north dipping Santa Ana Thrust exposed south of the Sugarloaf map area. Miocene-Pliocene(?) strata are overridden by this thrust, which according to McJunkin (1976) is intruded by a 6 m.y. basalt. Along the north side of the mountains the Pre-Cenozoic rocks have been thrust northward during the Quaternary (Dibblee, 1975). The study areas lie within a structural block (Big Bear Lake block) that is bound on both the north and south by late Cenozoic thrust faults. Rapid Quaternary uplift of this block is documented in the Sugarloaf area by the presence of older fanglomerate deposits on top of ridge crests, which contain clasts that are not locally derived. The Sugarloaf fan was beheaded at its source by rapid erosion related to Quaternary uplift.

Above the bounding thrusts, the Big Bear Lake block contains relatively few structures demonstrably of Cenozoic age. McJunkin (1976) recognized a S vergent antiform, possibly of late Cenozoic age, south of the Sugarloaf map area (discussed above) which he considered to be breached by the Santa Ana Thrust. Numerous faults, including the Balky Horse and Woodlands faults, and the Baldwin, Shay and Ranch faults, for example, and folds (the F_4 synform at Rose Mine) could be of Cenozoic age, but share

similarities in structural style or orientation with Mesozoic structures exposed nearby. Many of the features have been provisionally assigned to various Mesozoic structural events, as discussed above. High-angle faults which cut Mesozoic plutonic rocks in the Sugarloaf area may be of Cenozoic age.

The NW trending Helendale Fault cuts Bonanza King marbles below the Doble Thrust and displays a youthful fault scarp. NW trending high-angle faults exposed to the northeast of the Helendale Fault may be en echelon faults related to the development of the Helendale. The Helendale fault zone has been traced for several tens of km northwest of the Rose Mine area (Jennings, 1977). Garfunkel (1974) suggested 10-15 km of right-lateral strike-slip offset across the Helendale fault zone, based largely on outcrop pattern offsets of Mesozoic volcanic rocks. Evidence for major strike-slip separation is lacking at Rose Mine, where relatively minor dip-slip separations can be postulated. Tyler (1975) and E. Miller (1977a) also concluded that offsets across segments of the Helendale Fault they studied are more consistent with dip-slip displacement, and not the major strike-slip motions suggested by Garfunkel (1974).

Late Cenozoic gravity slides and Quaternary landslide deposits are recognized in the Delamar Mountain and Sugarloaf areas. Gravity slide blocks typically moved as coherent rock sheets. McJunkin (1976) suggested that much of the Sugarloaf area consisted of overlapping Quaternary gravity slides (he used the term landslide). Many of these bear no spatial relation to the younger-over-older allochthons of Mesozoic age described herein. In several cases, I found no evidence for bedrock offsets indicated by the gravity slide interpretation. Some of the slides, like the Broom Flat Slide, may be of Mesozoic age. Although late Cenozoic gravity slides are present in the Sugarloaf area, I do not believe they are as widespread as McJunkin (1976) has indicated.

CHAPTER V: GEOCHRONOLOGY

Introduction

K/Ar and $^{40}Ar/^{39}Ar$ geochronologic studies of intrusive rocks were undertaken to better constrain the timing of Mesozoic magmatic and deformational events in the Big Bear area. Published radiometric age data from the region suggest that the younger granite-quartz monzonite batholith is of Late Cretaceous age. Armstrong and Suppe (1973) and C. Miller (1977) also recognized older plutons within the range, perhaps of Early Mesozoic age. Three intrusive units known or inferred to predate Cretaceous batholithic rocks on the basis of field relationships were selected for study. These include the Fawnskin Monzonite, Bertha Diorite and Sugarloaf Quartz Diorite. K/Ar ages were obtained from hornblende and biotite mineral pairs where possible. $^{40}Ar/^{39}Ar$ total-fusion dates and age spectra were obtained for hornblende separates. Hornblende and biotite dates are highly discordant indicating a disturbance of the K/Ar isotopic systems since initial intrusion and crystallization of these older plutons. Biotite K/Ar data indicate a total resetting of the K/Ar system by heating during intrusion of the Late Cretaceous batholith. Hornblendes yield older K/Ar and $^{40}Ar/^{39}Ar$ total fusion ages than biotite and their $^{40}Ar/^{39}Ar$ age spectra are disturbed. This disturbance is attributed to severe post-emplacement loss of ^{40}Ar related to the Late Cretaceous heating event, hence, only minimum ages of crystallization for these units can be reported. However, $^{40}Ar/^{39}Ar$ age spectra and other data suggest both Triassic and Late Jurassic intrusives are present at Big Bear. Some age spectra record the presence of significant excess ^{40}Ar in low temperature gas fractions, which has important implications for interpretation of K/Ar dates elsewhere in the batholith belt.

Previous Work

Only limited geochronologic data has been published for the Big Bear area, or the range as a whole. Silver (1971) reported a 1750 m.y.

age (U/Pb zircon) on granitic gneisses within the basement complex. Armstrong and Suppe (1973) presented K/Ar data for Mesozoic plutonic rocks in the San Bernardino Mountains. Biotite separates from younger granitic rocks and older plutonic rocks they intrude uniformly yield Late Cretaceous ages (70.2-83.3 m.y.; ages recalculated using correction factors suggested by Dalrymple (1979). Unpublished K/Ar biotite ages from Mesozoic plutons and Precambrian gneisses obtained by the U.S. Geological Survey also conform to this pattern (F. Miller, personal comm., 1979). Armstrong and Suppe (1973) reported ages for two hornblende-biotite mineral pairs, both discordant. The Cienga Seca Diorite yields slightly discordant mineral ages (hornblende: 79.7 $\pm$ 1.0 m.y.; biotite: 70.2 $\pm$ 1.0 m.y.). The mineral ages obtained for the Fawnskin Monzonite, however, are highly discordant (hornblende: 198.5 $\pm$ 3 m.y.; biotite 83.3 $\pm$ 1.2 m.y.). Armstrong and Suppe interpreted these data to indicate the monzonite is an Early Mesozoic pluton. They attributed the discordance of this pluton's mineral ages and the areal uniformity of K/Ar biotite ages to deep burial and/or regional heating during Late Cretaceous magmatism.

C. Miller (1977) suggested the Fawnskin Monzonite is part of a belt of Early Mesozoic alkalic plutons present in southern California. Based on geochemical and petrologic similarities, he correlated the Fawnskin Monzonite with the Granite Mountains Monzonite, exposed 20 km north of Delamar Mountain (Fig. 2). He traced these two units within 6 km of one another. Two zircon separtes from the Granite Mountains Monzonite yielded concordant U/Pb ages of 230 $\pm$ 10 m.y. (C. Miller, 1977). Miller's attempt to date the Fawnskin Monzonite was not successful. No isochron was obtained from five Rb/Sr whole-rock analyses. A single zircon separate yielded highly discordant ages ($^{206}Pb/^{238}U$: 496 $\pm$ 10 m.y.; $^{207}Pb/^{235}U$: 665 $\pm$ 20 m.y.). He interpreted this discordance as due to crustal contamination, and resulting from a mixture of 1600-1800 m.y. Pb from relict zircon of the Precambrian basement complex with 200-250 m.y. Pb associated with zircon of magmatic origin. The absence of an Rb/Sr isochron for the monzonite was similarly attributed to

incomplete isotopic homogenization after contamination with upper crustal materials. Major and trace element data, combined with isotopic results, led C. Miller to conclude that the Granite Mountains Monzonite and Fawnskin Monzonite were derived from the same parental monzonitic magma. However, the quartz-rich Fawnskin Monzonite incorporated somewhat greater volumes of upper crustal material, which did not achieve complete isotopic equilibration with the magma.

In the northwesternmost San Bernardino Mountains, at Juniper Flats, outcrops of monzonite are recognized by C. Miller (1977) which he correlated with the Fawnskin and Granite Mountains plutons. This monzonite is intruded by syenite which has yielded a discordant U/Pb zircon age of approximately 160 m.y. The reliability of this age is in question due to evidence of severe common Pb contamination in this sample ($^{206}Pb/^{204}Pb = 60$).

A small monzonite body at Black Mountain was also correlated by C. Miller with the Granite Mountains pluton, exposed 8 km to the south. E. Miller and Sutter (1979) obtained a $^{40}Ar/^{39}Ar$ hornblende age spectrum from the Black Mountain Monzonite. Although the spectrum indicates significant ^{40}Ar loss during thermal disturbance, the minimum age for the pluton indicated by the fusion step is 233 ± 13.7 m.y., and corresponds well with the zircon age for the Granite Mountains Monzonite. $^{40}Ar/^{39}Ar$ age spectrum studies were undertaken in the Big Bear area in hopes of recovering geologically meaningful ages for the older plutons there.

Sample Selection

The igneous units selected for geochronologic study are among the earliest plutons in the Mesozoic batholithic terrane of the Big Bear area. They are preserved as roof pendants overlying younger granitic rocks. All of these older plutons have experienced some degree of post-crystallization deformation, recrystallization and alteration. Three criteria were stressed during sample selection: 1) maximum distance from contacts with younger plutons; 2) obtain sample with least evidence of chemical alteration or mechanical deformation of

hornblende and biotite; 3) obtain sample from which high purity separates could be recovered while maintaining grain size greater than 100 microns. The objective of the last criterion was to minimize the effect of ^{39}Ar recoil during irradiation. All potential geochronology samples were examined in thin section. Samples containing significant amounts of chloritized biotite, pyroxene cores in hornblende, or obvious grain margin alteration of biotite or hornblende were rejected.

Three samples were selected from the Fawnskin Monzonite, and one each from the Bertha Diorite and Sugarloaf Quartz Diorite. Fawnskin Monzonite samples include SB 378 (SE1/4 of Section 2, T2N, R1W, see Plate III for location) and samples SB 368c and SB 370c collected northwest of the Delamar Mountain map area (Plate I). SB 378 is a quartz monzonite and contains the freshest hornblende recognized in any sample, but almost no biotite. These hornblendes contain no pyroxene cores. SB 368c is a quartz monzonite and was collected from the same locality (SC-69-22) sampled by Armstrong and Suppe (1973). SB 370c is a "mafic monzonite" (as described by C. Miller, 1977) exposed near SB 368c. Unfortunately, a pure hornblende separate could not be obtained from this sample owing to fine-grained biotite intergrowths.

SB 575 was collected from the Bertha Diorite near Holcomb Valley Road (S center of Section 6, T2N, R1E, see Plate III). This quartz diorite is medium grained and not of the porphyritic facies of this unit. Xenoliths were not observed in the diorite near this locality. Biotite was not present in sufficient quantity to obtain a pure separate. The hornblende separate from SB 575 was provided by the U.S. Geological Survey.

Sample SB 381 is a hornblende-biotite quartz diorite of the Sugarloaf Quartz Diorite composite pluton. This sample was collected from a narrow outcrop belt near Wildhorse Road (N center of Section 32, T2N, R2E, see Plate II), where the Sugarloaf Diorite intrudes along pre-existing faults. A post-crystallization fault and hydrothermal veins cut the diorite here, however, hornblende in SB 381 shows the least evidence of alteration of any hornblende-bearing diorite collected from this pluton.

Mineral Separation Techniques

All mineral separates, save SB 575, were prepared by the author at the Geochronology Lab, Branch of Isotope Geology, U.S. Geological Survey, Menlo Park, California. Mineral separation techniques used are described by Dalrymple and Lanphere (1969) among others. Samples were obtained from interior portions of outcrops. Weathered material was removed by repeated hammer blows. The samples were further reduced to pieces a few cm in longest dimension. Pieces with epidote or hydrothermal veinlets, xenoliths or obvious xenocrysts were discarded. Acceptable material was crushed and sieved into several size fractions (Tyler mesh sizes >45, 45 to 60, 60 to 100, <100 were typical splits). The optimum size fraction for further concentration of hornblende or biotite was washed with water and dried. Concentration of the desired mineral was achieved using magnetic, heavy liquid and mechanical separation techniques. Rough concentration was first obtained using a Carpco magnetic separator. Heavy liquids were used as necessary. A ceramic-ball mill and mica table were useful for biotite separation, while an ultrasonic probe and Frantz magnetic separator aided with concentration of hornblende. To minimize the effects of ^{39}Ar loss due to recoil, grain size was kept above 140 mesh size, making hornblende concentration laborious. High purity separates (>99%) were obtained. Hornblende separates, in particular, were carefully examined microscopically for evidence of fine-grained biotite intergrowths. Where present in final concentrates, the contaminant consists primarily of fine-grained quartz inclusions. The consistency of K_2O and Na_2O analyses on these separates indicates their homogeneity, and supports the contention of high purity.

SB 575 was crushed and sized by the author, but the final hornblende concentrate was provided by the Western Environmental Geology Branch, U.S. Geological Survey. This was a difficult sample from which to obtain a pure concentrate, and microscopic analysis of the final concentrate indicates the presence of minor micaceous contaminant (probably biotite) which is intricately intergrown with some hornblende grains. Time constraints did not permit further purification of this separate.

Analytical Techniques

K/Ar Procedures

Conventional K/Ar mineral age determinations were made to identify materials suitable for $^{40}Ar/^{39}Ar$ age spectra analysis, and as a check on the $^{40}Ar/^{39}Ar$ age data. Potassium concentrations were measured by the U.S. Geological Survey Analytical Lab at Menlo Park, using flame photometry with internal standards. Two splits were analyzed, and their average value was used in the age calculation. Ar analysis was by isotope dilution with ^{38}Ar, using techniques and equipment described by Dalrymple and Lanphere (1969). All Ar extractions were made at Menlo Park. Sample fusion was achieved by radio-frequency induction heating. The gas was extracted, purified and mixed with a bulb type ^{38}Ar tracer in a high vacuum extraction line. The purified Ar was collected at a take-off tube and isotopic analyses were made later on a Nier-type six inch radius, 60° sector mass spectrometer operated in the static mode. Because of machine breakdown at Menlo Park, all conventional analyses were made at the Branch of Isotope Geology, U.S. Geological Survey, Denver, Colorado. Corrections for instrumental discrimination were determined from atmospheric Ar analyses made prior to and after the samples were analyzed. Constants used for age calculation are those recommended by Steiger and Jager (1977).

$^{40}Ar/^{39}Ar$ Dating Method

The $^{40}Ar/^{39}Ar$ dating method has been described in detail by several authors (see Merrihue and Turner, 1966; Dalrymple and Lanphere, 1971, 1974; Lanphere and Dalrymple, 1971). In this technique a fraction of ^{39}K is converted to ^{39}Ar by irradiation with fast neutrons. After the sample is subsequently fused and Ar is released, the age of the material can be determined by measuring the ratio of $^{40}Ar^*$ (radiogenic ^{40}Ar produced by decay of ^{40}K) to $^{39}Ar_K$ (potassium-derived ^{39}Ar). The age equation is

$$t = 1/\lambda \ln (1 + J (^{40}Ar^*/^{39}Ar_K))$$

where λ is the total decay constant for ^{40}K ($= 5.543 \times 10^{-10}$ yr^{-1}). The quantity J is a function of the known age of a mineral standard (flux

monitor), irradiated with the sample of unknown age, and the integrated fast neutron flux. It is determined by the equation

$$J = (e^{\lambda t_s} - 1) \ (^{40}Ar^*/^{39}Ar_K)_s$$

where t_s is the known age of the flux monitor and $(^{40}Ar^*/^{39}Ar_K)_s$ is the isotopic ratio measured for the monitor used in the particular irradiation.

In the case where a sample of unknown age is fused in a single step, a total fusion age is obtained, analogous to a conventional K/Ar age determination. The great attraction of the $^{40}Ar/^{39}Ar$ method lies in the incremental heating technique. In this procedure, fractions of the total $^{39}Ar_K$ and $^{40}Ar^*$ are released by stepwise heating of the sample at successively higher temperatures until the sample is fused. The $^{40}Ar^*/^{39}Ar_K$ ratio for each step is measured and the apparent age of that gas fraction is determined. The ages of each step are plotted versus accumulative percent of ^{39}Ar released which yields an age spectrum.

An age spectrum can provide great insight into the K/Ar systematics of a sample and its thermal history. Samples which have experienced little or no diffusive Ar loss after crystallization yield undisturbed age spectra, with little or no deviation in the $^{40}Ar/^{39}Ar$ age obtained for each step (Turner, 1968; Dalrymple and Lanphere, 1974). Even where moderate Ar loss has occurred (less than 20%), a plateau of ages equalling or closely approaching the time of post-crystallization Ar-diffusion closure still persists for gas fractions released at high temperatures. In this case, the age obtained from the lowest temperature fractions approaches the age of the thermal disturbance (Turner, 1968). In cases of more severe Ar loss, more complex age spectra have been recognized. Lanphere and Dalrymple (1976) suggested that the shape of age spectra can also indicate the presence of excess ^{40}Ar, not derived by in situ decay of ^{40}K.

$^{40}Ar/^{39}Ar$ Procedures

All $^{40}Ar/^{39}Ar$ total fusion analyses and age spectra experiments for SB 378 and SB 368c were undertaken by the author at Menlo Park. Age spectra experiments for SB 575 and SB 381 were performed by J. Sutter at

the Ohio State University. Sample handling, irradiation, and experimental procedures are similar in both labs to those described by Lanphere and Dalrymple (1971). Samples ranging from 0.5 to 2.0 gm were sealed in air in fused silica vials and irradiated together with neutron flux monitors. Samples from Menlo Park were irradiated for 30 MW hours in the central thimble of the U.S. Geological Survey TRIGA reactor in Denver, and received a neutron dose of about 3×10^{18} nvt. The Menlo Park monitor is a 160 m.y. biotite described by Dalrymple and Lanphere (1971). Samples from Ohio State were irradiated at the Ford Reactor, Phoenix Memorial Lab, University of Michigan and also received an approximate neutron dose of 3×10^{18} nvt. The monitor used at Ohio State is a 520 m.y. hornblende described by Alexander and others (1978). Correction factors for undesirable Ca- and K-derived Ar isotopes produced during irradiation are the same in both cases (Dalrymple and Lanphere, 1971).

Ar extractions at Menlo Park were made in an off-line system. Heating steps were one-half hour intervals and temperatures were monitored by a thermocouple imbedded in the sample crucible. After Ar extraction and purification, the Ar released for each step was collected at a cut-off tube. After all gas fractions were collected, Ar isotopic analyses were made with a Nier-type rare-gas mass spectrometer of six-inch radius with 60° sector. The spectrometer was operated in the static mode. Corrections for instrumental discrimination were determined from atmospheric argon analyses made immediately before the gas fractions for each separate were analyzed. The amount of ^{39}Ar released during each step was calculated from the ion-beam intensity, calibrated using a known amount of ^{38}Ar measured immediately prior to analyses of gas fractions from each sample.

Ar extractions at Ohio State were made using a high-vacuum extraction system on-line with the mass spectrometer. Five heating steps were used, with heating intervals of about 40 minutes and temperatures calibrated with an optical pyrometer. Immediately after extraction and purification, each gas fraction was analyzed on a Nuclide mass spectrometer (SGA-6-60) of six-inch radius with 60° sector, operated

statically. Instrument discrimination corrections and calibration of ion beam intensity were determined as discussed above. Ar analyses of both interlaboratory and intralaboratory standards at both labs show analytical reproducibility of better than 1%, as reported by Fleck and others (1977). Constants used in all age calculations are those recommended by Steiger and Jager (1977).

Results

K/Ar and $^{40}Ar/^{39}Ar$ Total Fusion Ages

The results of conventional K/Ar analyses are presented in Table 1. The data for $^{40}Ar/^{39}Ar$ total fusion ages are presented in Table 2. Duplicate conventional Ar analyses are reported for most samples and the results are indistinguishable at the 95% confidence level (based on the critical value test, Dalrymple and Lanphere, 1969). Hornblende and biotite total-gas ages are strongly discordant for both the Fawnskin Monzonite and Sugarloaf Quartz Diorite. Biotite from the Sugarloaf Quartz Diorite yields an age of 70.2 - 70.3 $\pm$ 1.0 m.y. Biotite from the Fawnskin Monzonite yields ages ranging from 74.9 $\pm$ 1.2 to 83.5 $\pm$ 1.2 m.y. These Late Cretaceous biotite ages are in good agreement with the biotite ages reported by Armstrong and Suppe (1973) from the Big Bear region.

K/Ar ages from Fawnskin Monzonite hornblendes range from 164.1 $\pm$ 2.9 to 212.5 $\pm$ 3.8 m.y. Hornblendes from SB 378 yield identical K/Ar and $^{40}Ar/^{39}Ar$ total fusion ages (212.5 $\pm$ 3.8 m.y. and 212.8 $\pm$ 2.8 m.y. respectively). These data indicate that ^{39}Ar recoil effects are insignificant for this sample (see Fleck and others, 1977). The $^{40}Ar/^{39}Ar$ total fusion age for SB 368c is 20 m.y. older than the conventional ages. This discrepancy might be attributable to ^{39}Ar loss during irradiation-induced recoil but this is considered unlikely. The grain size of SB 368c is only slightly less than that of SB 378 which shows no recoil effects. Sutter (personal comm., 1980) has found little evidence for ^{39}Ar loss due to recoil from hornblendes considerably finer-grained than those studied here. The data of Alexander and others (1977) also

TABLE 1

Conventional K/Ar Ages

Sample	K_2O(wt.%)(1)	Weight (gm)	$^{40}Ar^*$/gm (x 10^{-10} moles)	Percent $^{40}Ar^*$	Age(2)(3) (x 10^6 yr)
Fawnskin Monzonite					
SB 378 hornblende	0.844,0.844	1.5186	2.74	82.7	212.5 ± 3.8
SB 368c hornblende	0.975,0.975	1.6014	2.411	86.7	164.1 ± 2.9
		1.6147	2.431	82.9	165.4 ± 3.0
SB 368c biotite	9.38, 9.37	0.1618	10.34	73.9	74.9 ± 1.2
		0.1460	10.39	61.5	75.3 ± 1.3
SB 370c biotite	9.28, 9.27	0.3692	11.10	86.0	81.3 ± 1.2
		0.3451	11.41	88.5	83.5 ± 1.2
Sugarloaf Quartz Diorite					
SB 381 hornblende(4)	0.701,0.696				
SB 381 biotite	9.00, 8.99	0.3421	9.274	91.1	70.2 ± 1.0
		0.3320	9.296	85.8	70.3 ± 1.0

---

* Radiogenic argon

(1) Average of duplicate analyses used for age calculation.

(2) Error estimate reflects analytical precision only, calculated in manner described by Cox and Dalrymple (1967).

(3) Constants used for age calculation are those recommended by Steiger and Jäger (1977).

(4) No conventional K/Ar analyses made.

TABLE 2: Analytical data for $^{40}Ar/^{39}Ar$ Incremental Heating and Total Fusion Experiments

Sample	Temp (°C)	$^{40}Ar/^{39}Ar$ (1)	$^{37}Ar/^{39}Ar$ (2)	$^{36}Ar/^{39}Ar$ (1)	$^{40}Ar^*/^{39}Ar_K$ (3)	^{39}Ar (% of total)	$^{39}Ar_K$ (4) (moles x10^{-12})	$^{40}Ar^*$ (%)	$^{36}Ar_{Ca}$ (5) (%)	Apparent K/Ca (6) (mole/mole)	AGE (7) (x10^6 yr)
SB 378											
hornblende, Fawnskin Monzonite, J = 0.00667, size = 149-250 microns, wt. = 0.5029 gm											
	750	2079	1.869	5.703	394.7	1.25	0.0810	18.96	0.009	0.278	2327 ± 185.9
	840	182.2	8.885	0.5447	22.09	2.13	0.138	12.056	0.444	0.0585	247.9 ± 30.1
	890	38.69	7.640	0.08582	14.00	8.92	0.577	36.021	2.422	0.0681	161.1 ± 4.6
	940	21.19	6.721	0.02493	14.41	31.55	2.04	67.75	7.333	0.0774	165.6 ± 2.5
	975	19.49	5.987	0.01341	16.06	26.71	1.73	82.097	12.141	0.0869	183.5 ± 2.5
	1000	25.55	6.059	0.02902	17.52	7.09	0.459	68.32	5.679	0.0858	199.4 ± 4.2
	1025	29.68	6.121	0.04405	17.22	4.37	0.283	57.783	3.78	0.0850	196.1 ± 5.2
	1050	30.32	6.540	0.04356	18.05	2.62	0.170	59.265	4.084	0.0795	205.0 ± 7.6
	Fuse	22.98	6.748	0.01591	18.89	15.36	0.993	81.877	4.538	0.0771	214.1 ± 2.9
Total Gas		--	--	--	21.39	100.	6.47	--	--	--	240.6
SB 378											
hornblende, Fawnskin Monzonite, J = 0.00667, size = 149-250 microns, wt. = 0.5091 gm											
	Total Fusion	23.79	6.623	0.01904	18.77	--	--	78.567	9.463	0.0785	212.8 ± 2.8
SB 368c											
hornblende, Fawnskin Monzonite, J = 0.00676, size = 125-177 microns, wt. = 0.5310 gm											
	750	128.5	0.6999	0.1325	89.46	1.86	0.158	69.578	0.144	0.743	853.5 ± 18.7
	890 (8)	--	--	--	--	18.64	1.59	--	--	--	--
	925	13.96	5.666	0.008240	12.02	35.88	3.04	85.776	18.704	0.0917	140.9 ± 2.0
	960	16.84	19.03	0.01101	15.30	8.73	0.733	89.734	47.023	0.0273	177.6 ± 2.6
	1000	18.84	5.732	0.01476	14.99	5.20	0.440	79.259	10.562	0.0907	174.1 ± 3.5
	1075	16.93	5.835	0.005918	15.71	14.73	1.25	92.408	26.822	0.0891	182.1 ± 2.5
	Fuse	17.81	5.469	0.008271	15.85	14.97	1.27	88.710	17.985	0.0951	183.7 ± 2.6
Total Gas		--	--	--	--	100.	8.48	--	--	--	--
SB 368c											
hornblende, Fawnskin Monzonite, J = 0.00676, size = 125-177 microns, wt. = 0.5648 gm											
	Total Fusion	20.10	5.442	0.01538	16.04	--	9.01	79.536	9.627	0.0955	185.8 ± 2.9

(Continued)

Sample	Temp (°C)	$^{40}Ar/^{39}Ar$ (1) meas.	$^{37}Ar/^{39}Ar$ (2) corr.	$^{36}Ar/^{39}Ar$ (1) meas.	$^{40}Ar^*/^{39}Ar_K$ (3)	^{39}Ar (% of total)	$^{39}Ar_K$ (4) (moles x10^{-12})	$^{40}Ar^*$ (%)	$^{36}Ar_{Ca}$ (5) (%)	Apparent K/Ca (6) (mole/mole)	AGE (7) (x10^6 yr.)
SB575											
hornblende, Bertha Diorite, J = 0.004966, size = 105.149 microns, wt. = 2.0 gm											
	850	11.565	0.451	0.009068	8.920	17.41	8.27	77.10	1.40	1.15	78.19 ± 1.38
	1025	12.537	2.549	0.009002	10.101	29.20	13.85	80.42	7.96	0.204	88.30 ± 1.21
	1075	13.445	4.283	0.010092	10.846	23.18	10.98	80.42	11.92	0.121	94.64 ± 1.31
	1125	13.672	4.319	0.008718	11.484	20.82	9.86	83.74	13.92	0.120	100.06 ± 1.41
	Fuse	34.123	8.261	0.068482	14.655	9.39	4.44	42.69	3.39	0.0629	126.73 ± 3.55
Total Gas		14.842	3.491	0.014793	10.782	100.	47.40	72.46	6.63	0.149	94.09
SB 381											
hornblende, Sugarloaf Quartz Diorite, J = 0.004966, size = 105-149 microns, wt. = 2.0 gm											
	850	104.795	0.965	0.251141	30.678	6.88	1.31	29.25	0.11	0.539	255.81 ± 11.64
	1025	120.033	3.500	0.370314	10.917	8.39	1.60	9.07	0.27	0.149	95.25 ± 13.18
	1075	63.733	7.635	0.169762	14.276	20.90	3.97	22.28	1.26	0.0681	123.56 ± 5.90
	1125	28.163	8.693	0.042378	16.459	23.57	4.48	58.08	5.76	0.0598	141.74 ± 3.00
	Fuse	36.988	9.246	0.069816	17.235	40.25	7.64	46.28	3.72	0.0562	148.15 ± 3.10
Total Gas		52.135	7.727	0.121938	16.832	100.	19.00	32.10	1.78	0.0673	144.82
SB 381											
hornblende, Sugarloaf Quartz Diorite, J = 0.00676, size = 105-149 microns, wt. = 0.5409 gm											
	Total Fusion	19.58	7.701	0.02734	12.17	--	4.40	61.87	7.66	0.0675	142.7 ± 2.7

(1) Measured value.

(2) Corrected for decay of ^{37}Ar.

(3) $^{40}Ar^*$ = radiogenic ^{40}Ar $^{39}Ar_K$ = K-derived ^{39}Ar.

(4) Calculated using sensitivity determined from ion-beam intensity.

(5) $^{36}Ar_{Ca}$ = Ca-derived ^{36}Ar.

(6) Apparent K/Ca = 0.52 ($^{39}Ar_K/^{37}Ar$) mol/mol (Fleck and others, 1977).

(7) Age calculated using method of Dalrymple and Lanphere (1971), using constants recommended by Steiger and Jager (1977); error is one σ and reflects analytical precision only, calculated as described by Cox and Dalrymple (1967).

(8) Gas fraction lost; moles ^{39}Ar and $^{39}Ar_K$ determined by difference between the sum of the remaining steps and values for total fusion experiment.

suggest recoil is not a likely explanation. The age discrepancy may reflect spurious K_2O analyses or may be due to inhomogeneous distribution of ^{40}Ar within individual separates (discussed below).

The $^{40}Ar/^{39}Ar$ total-fusion age for hornblende from the Sugarloaf Quartz Diorite is 142.7 ± 2.7 m.y. No conventional analysis was made for this sample since pure separate was in limited supply.

Age Spectrum Results

General Statement. The analytic data for the incremental heating experiments are presented in Table 2. Resultant ages are plotted as a function of accumulative percentage of ^{39}Ar released in Figs. 66-68. Recalculated total gas ages were determined by recombining data from individual heating steps. For undisturbed samples these total gas ages should be equivalent to $^{40}Ar/^{39}Ar$ total-fusion and conventional K/Ar ages. Amounts of ^{39}Ar released for each step (in moles) were calculated from the mass spectrometer ion-beam intensity. K/Ca ratios for each gas fraction were calculated from the measured value of $^{37}Ar_{Ca}/^{39}Ar_{K}$. The conversion expression appropriate for the reactors used here is K/Ca = 0.52 ($^{39}Ar_K/^{37}Ar_{Ca}$) mol/mol as defined by Fleck and others (1977).

SB 575-Bertha Diorite. The age spectrum for SB 575 is strongly disturbed. No plateau is present, rather a staircase pattern is recognized. Apparent ages increase progressively from lowest to highest temperature step, from 78.19 ± 1.38 m.y. to 126.73 ± 3.55 m.y. The calculated K/Ca ratio decreases progressively for each step, and only the high temperature fractions yield K/Ca values in the range typical of hornblende.

SB 381-Sugarloaf Quartz Diorite. Sample SB 381 displays a disturbed age spectrum. The lowest temperature fraction gives an apparent age of 255.81 ± 11.64 m.y., higher than any other step. Subsequent steps

Figure 66: $^{40}Ar/^{39}Ar$ age spectrum and K/Ca plot for hornblende from the Bertha Diorite (SB 575)

Figure 67: $^{40}Ar/^{39}Ar$ age spectrum and K/Ca plot for hornblende from the Sugarloaf Quartz Diorite (SB 381)

Figure 68: $^{40}Ar/^{39}Ar$ age spectra and K/Ca plots for hornblendes from the Fawnskin Monzonite
a) SB 368c
b) SB 378

Figure 66.

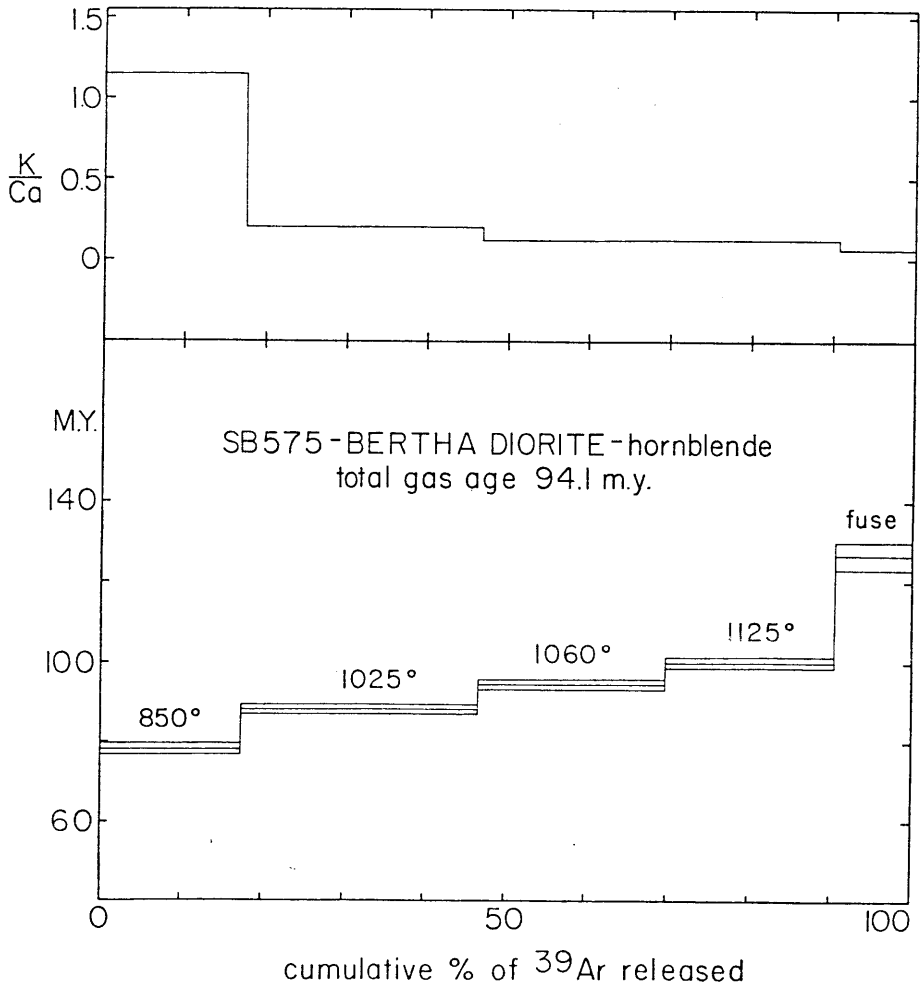
1.5
1.0
K/Ca 0.5
0
M.Y.
SB575 - BERTHA DIORITE - hornblende
total gas age 94.1 m.y.
140
100
60
fuse
1125°
1060°
1025°
850°
0
50
100
cumulative % of 39Ar released

Figure 67.

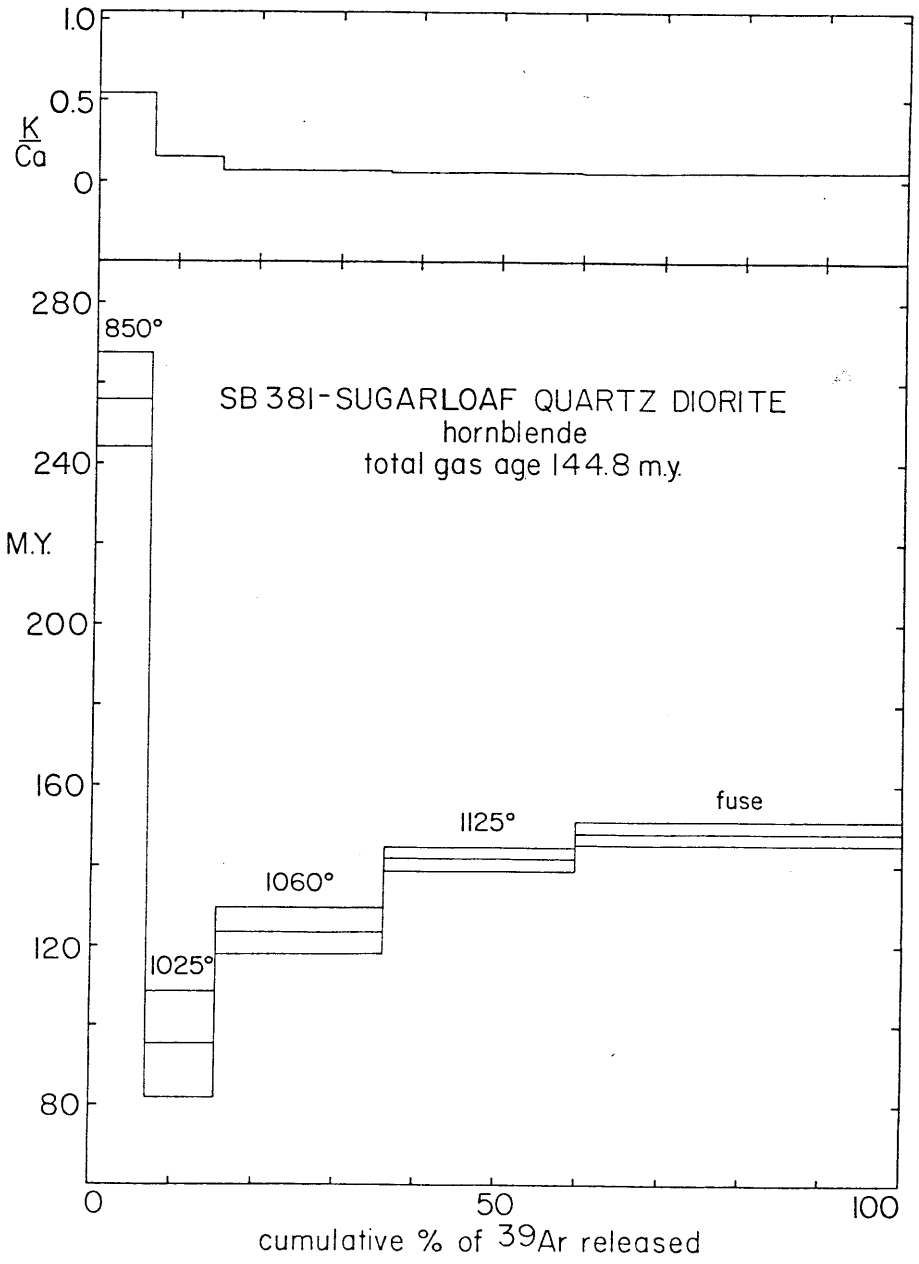
1.0
0.5
K/Ca
0
280
240
200
160
120
80
M.Y.
850°
1025°
1060°
1125°
fuse
SB 381-SUGARLOAF QUARTZ DIORITE
hornblende
total gas age 144.8 m.y.
0
50
100
cumulative % of 39Ar released

Figure 68a.

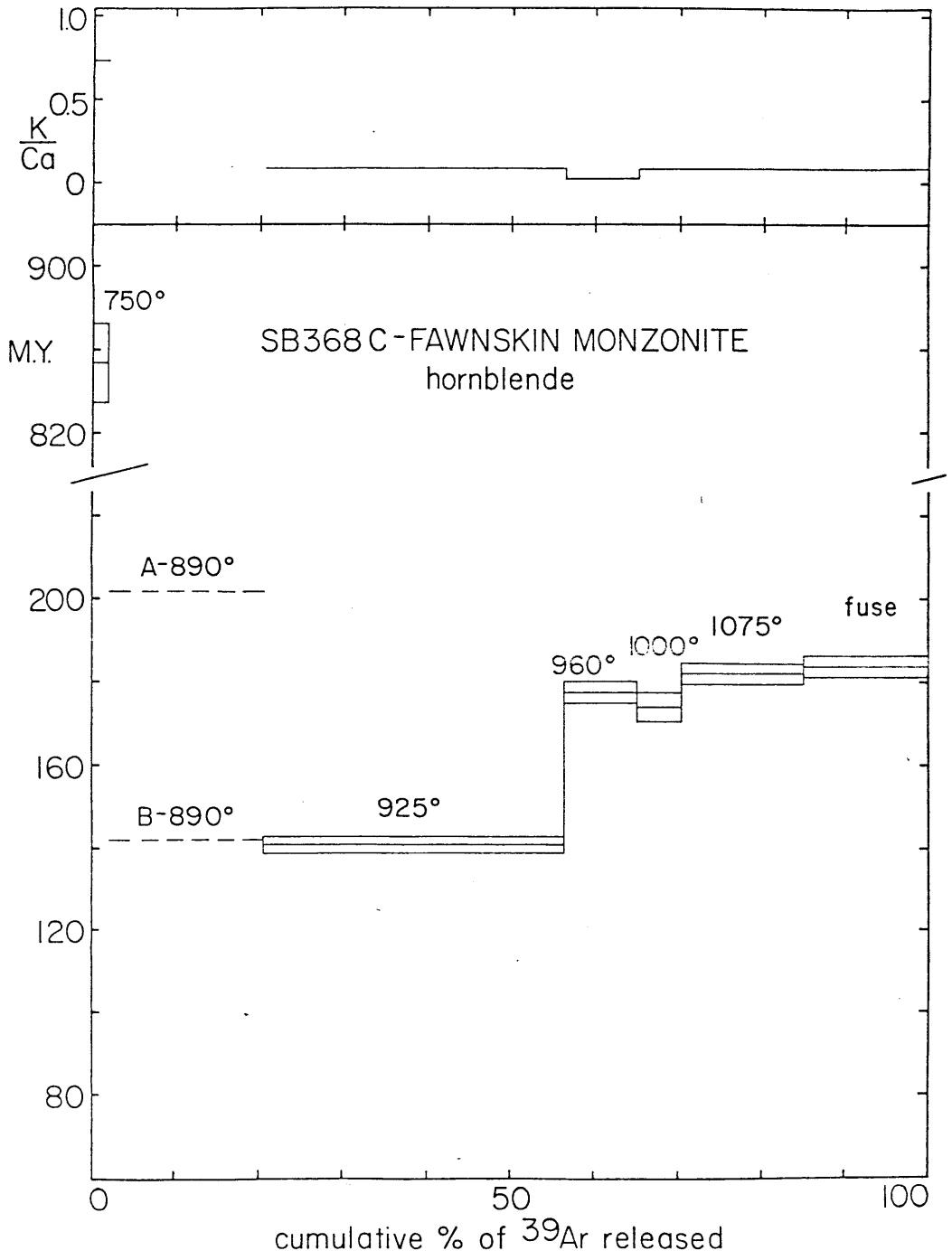
1.0
0.5
K/Ca
0
900
750°
M.Y.
820
SB368C-FAWNSKIN MONZONITE
hornblende
A-890°
200
fuse
1075°
1000°
960°
160
B-890°
925°
120
80
0
50
100
cumulative % of 39Ar released

Figure 68b.

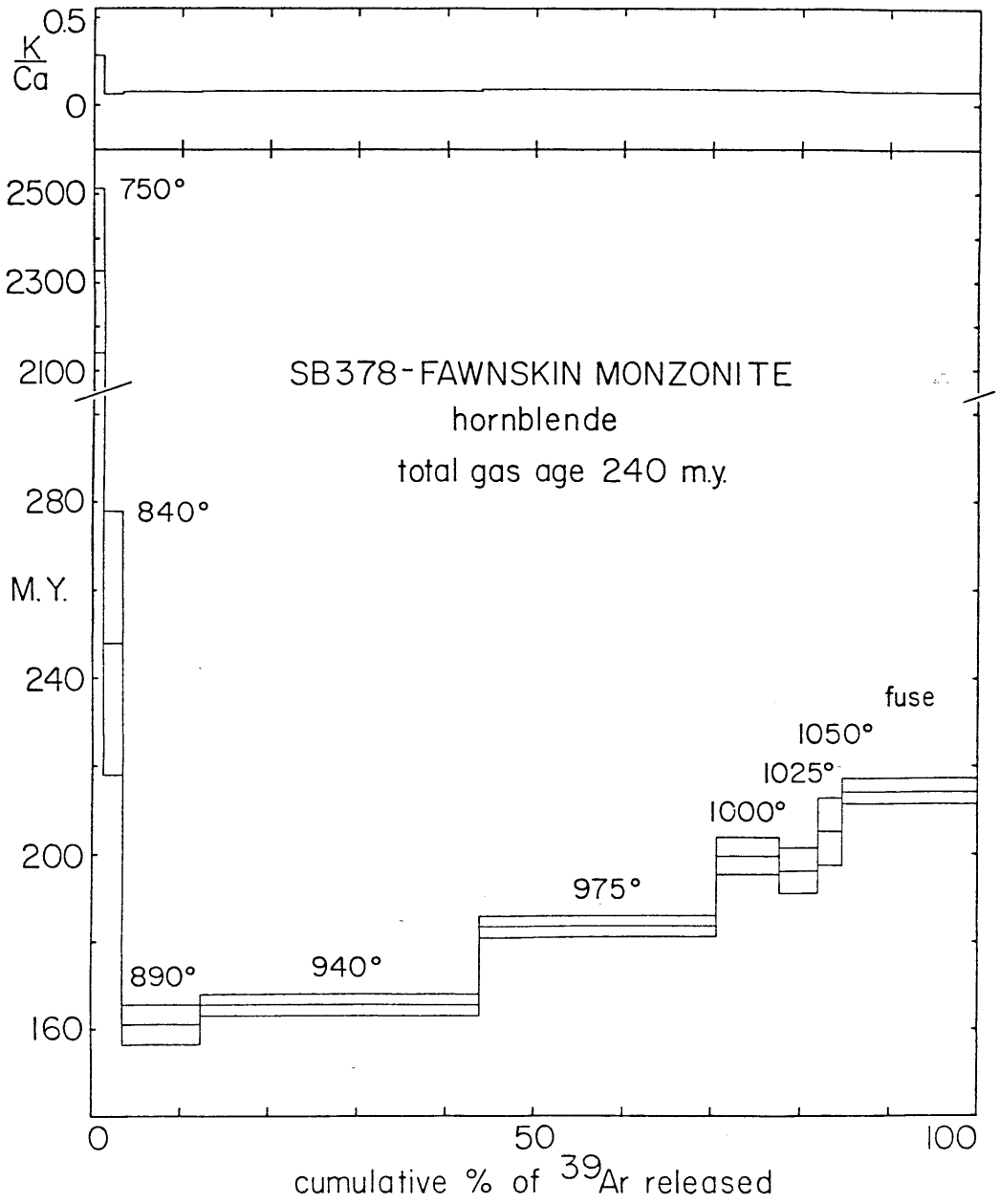
0.5
K/Ca
0
2500
2300
2100
750°
SB378-FAWNSKIN MONZONITE
hornblende
total gas age 240 m.y.
280
840°
M.Y.
240
fuse
1050°
1025°
1000°
200
975°
890°
940°
160
0
50
100
cumulative % of 39Ar released

yield a staircase spectrum with ages progressively increasing from 95.25 ± 13.18 m.y. to a maximum of 148.15 ± 3.10 m.y. The age of the 1025° step is poorly constrained because of the low yield (9%) of radiogenic ^{40}Ar. The 1125° and fusion steps account for over 60% of the total ^{39}Ar released, and the ages for these steps are indistinguishable at the 95% confidence level as evaluated by the critical value test (Fleck and others, 1977). The difference in apparent ages between these steps is less than the critical value, 8.5 m.y. in this case. These two steps define a high temperature plateau, as defined by Fleck and others (1977) with a weighted mean age of 145.8 m.y. Its significance is discussed below. The total fusion age (142.7 ± 2.7 m.y.) and recalculated total gas age (144.82 m.y.) are in good agreement, although the yield of radiogenic ^{40}Ar differs considerably. The K/Ca values increase progressively from the 750° step and are similar to values for typical plutonic hornblendes (Deer and others, 1966) for the 1075°-fusion steps.

SB 378-Fawnskin Monzonite. The hornblende separate from SB 378 yielded a highly disturbed 9-step age spectrum. The lowest temperature fractions yield very old ages of 2327 ± 185.9 m.y. (750° step) and 247.9 ± 30.1 m.y. (840° step). The uncertainties for these ages are high due to high percentages of atmospheric argon in these steps, and the small amounts of ^{39}Ar released. Although these steps account for less than 4% of the total ^{39}Ar released, they include much of the total ^{40}Ar in the sample. Subsequent steps yield a staircase-type spectrum, which increases progressively in apparent age from a minimum of 161.1 ± 4.6 m.y. to a maximum of 214.1 ± 2.9 m.y. for the fusion step. No high temperature plateau was formed. The recalculated total gas age of 240.6 m.y. for this sample contrasts sharply with the concordant K/Ar and total-fusion ages of 212.5 - 212.8 m.y. The K/Ca ratio of the 750° step is relatively high, but succeeding steps give consistent K/Ca ratios typical of plutonic hornblende.

SB 368c-Fawnskin Monzonite. Seven gas fractions were extracted from hornblende sample SB 368c; unfortunately, the second step (890°) was lost prior to isotopic analysis. The percent of ^{39}Ar contained in the 890° step was determined by subtracting the moles/gm of ^{39}Ar yielded by the remaining steps from the moles/gm of ^{39}Ar obtained during the total-fusion run. These samples occupied adjacent positions in the irradiation canister and their rate of ^{39}Ar production and possible loss due to recoil is assumed to have been identical. Unfortunately, the apparent age of the 890° step is ambiguous. The discrepancy between the $^{40}Ar/^{39}Ar$ total-fusion and K/Ar ages for this sample make it impossible to assign a reliable value for radiogenic ^{40}Ar. The extreme difference in the K/Ar and total-fusion ages and the recalculated total gas age for SB 378 suggest that homogeneous ^{40}Ar concentrations within individual hornblende separates from the Fawnskin Monzonite cannot be assumed. For reference purposes, however, two model ages for the 890° step were calculated. Model A assumes the incremental heating sample yields the same moles/gm of radiogenic ^{40}Ar as the total-fusion sample (2.583×10^{-10} moles/gm calculated from ion-beam intensity and millivolts of signal of ^{40}Ar) and results in an age of 202 m.y. for this step. The recalculated total-gas age equals the total-fusion age of approximately 186 m.y. in this case. Model A yields a saddle-shaped age spectrum for SB 368c. Model B assumes the total yield of radiogenic ^{40}Ar for the incremental heating experimental equals that of the K/Ar experiments (average value 2.421×10^{-10} moles/gm) and results in an apparent age of 142 m.y. for the 890° step. Model B yields a modified staircase-type age spectrum, similar to that of SB 378. The recalculated total gas age is 176 m.y. in this case and the $^{40}Ar^*/^{39}Ar_K$ ratio is 15.18.

The discrepancy between the total gas age for Model B and the K/Ar dates can be explained by about 6% ^{39}Ar loss owing to recoil (considered unlikely, see above) or may indicate that the K_2O values used in the K/Ar age calculation are too high and are incorrect. Error in K_2O could result from faulty analyses or the presence of contaminant not found in the total fusion sample. K_2O values for hornblendes from the Fawnskin Monzonite were determined by microprobe analysis by C. Miller (1977) and range from 0.82 to 1.32 wt.%, however, most samples ranged from 0.82 to 0.93 wt.%, similar to the range reported in this study.

If the K/Ar ages for SB 368c are recalculated using K_2O = 0.844 (value for SB 378) the dates obtained are 188.3 m.y. and 189.7 m.y. which are nearly identical to the $^{40}Ar/^{39}Ar$ total fusion age of 185.8 ± 2.9 m.y. This close correspondence causes me to question the accuracy of the measured K_2O values for SB 368c used in the K/Ar age calculation reported in Table 1. For this reason I favor Model A over Model B for the age of the 890° step. However, because homogeneous distribution of ^{40}Ar within the separate is not certain, this age should be regarded with caution.

The 750° step for SB 368c contains a much higher percentage of radiogenic ^{40}Ar than low-temperature steps in SB 378, and its age is more precisely defined. As in SB 378, the lowest temperature step contains a significant amount of the total ^{40}Ar in the sample. Steps 925° to fusion increase in age from 140.9 ± 2.0 m.y. to 183.7 ± 2.6 m.y. Although steps 960°-fusion are similar in age they do not define a plateau according to the criteria of Fleck and others (1977). The difference in apparent age between any two steps does not always satisfy the critical value test. As these four steps contain less than 50% of the total ^{39}Ar released, they would not constitute a well-defined plateau (Lanphere and Dalrymple, 1978) in any case. K/Ca ratios decrease from a maximum for the lowest temperature step. Higher temperature steps yield consistent K/Ca values of approximately 0.09, save the 925° step, which is unusually low.

Interpretation of Age Spectra

General Statement

The hornblende age spectra described here are disturbed. Even for disturbed spectra, however, meaningful geologic ages can frequently be obtained. Lanphere and Dalrymple (1978) have outlined the criteria for evaluating geologically meaningful ages from samples which have experienced partial diffusive argon loss. These include: 1) a well-defined high-temperature plateau for more than 50% of the ^{39}Ar released; 2) a well-defined isochron for the plateau steps; 3) concordant plateau

and isochron ages; and 4) $^{40}Ar/^{36}Ar$ intercept not significantly different from 295.5. Some geochronologists argue that in certain cases meaningful isochron ages can be obtained for samples with $^{40}Ar/^{36}Ar$ intercept values significantly different than 295.5 (Sutter and Smith, 1979; Ozima and others, 1978). $^{40}Ar_{R+A}/^{36}Ar_A$ vs. $^{39}Ar_K/^{36}Ar_A$ ratios are presented in Table 3 and isochron plots in Figs. 69 a-d.

More recently, Harrison and McDougall (1980) have presented examples of plutonic hornblendes which have experienced post-recrystallization heating and yield disturbed age spectra which are similar to theoretical release spectra modeling ^{40}Ar loss by volume diffusion (Turner, 1968; Huneke, 1976). They suggest that for age spectra which resemble theoretical diffusive loss spectra, it is possible to model both the age of thermal disturbance and the original K/Ar age of the sample (time of original closure to Ar diffusion) even in the absence of the criteria mentioned above. This was attempted here, using a visual fit of the data to model curves of Turner (1968) and Huneke (1976). The time of the heating event is assumed to be 80 m.y., based on the Late Cretaceous biotite ages and the K/Ar hornblende age for the Cienga Seca Diorite.

Bertha Diorite

The age spectrum for SB 575 is typical of samples which have experienced severe diffusive loss of ^{40}Ar during reheating. No plateau is recognized, so the original age of this sample could not be recovered. The $^{40}Ar_{R+A}/^{36}Ar_A$-$^{39}Ar_K/^{36}Ar_A$ plot for this sample does not yield an isochron. By analogy with Turner's (1968) model for diffusive Ar loss, the fusion step age, 126.73 $\pm$ 3.55 m.y., is a minimum age for these hornblendes. The lowest age obtained, 78.19 $\pm$ 1.38 m.y., would normally be interpreted as a reasonable estimate of the time of closure to Ar diffusion after thermal disturbance since it is consistent with K/Ar biotite ages obtained from rocks in the Big Bear area.

Apparent K/Ca ratios for the lower temperature gas fractions indicate caution must be exercised in interpreting the significance of

TABLE 3

Isochron Data

Sample	Temp (°C)	$^{40}Ar_{R+A}/^{36}Ar_A$	$^{39}Ar_K/^{36}Ar_A$
SB 378	750	364.6	0.1751
hornblende	840	336.0	1.834
	890	461.9	11.88
	940	916.8	43.10
	975	1653	84.53
	1000	933.2	36.39
	1025	700.1	23.50
	1050	725.6	23.83
	Fuse	1632	70.76
SB 368c	750	971.5	7.556
hornblende	890	——Gas fraction lost——	
	925	2083	148.7
	960	2887	169.4
	1000	1426	75.47
	1075	3909	230.1
	Fuse	2624	146.9
SB 381	850	417.7	3.983
hornblende	1025	325.0	2.701
	1060	380.2	5.933
	1125	705.2	24.88
	Fuse	550.3	14.78
SB 575	850	1293	111.8
hornblende	1025	1513	120.5
	1060	1513	112.1
	1125	1822	132.8
	Fuse	515.8	15.02

R: radiogenic argon

A: atmospheric argon

K: K-derived argon

Figure 69: $^{40}Ar_{R+A}/^{36}Ar_A$ vs. $^{39}Ar_K/^{36}Ar_A$ isochron plots for hornblendes

a) SB 575, Bertha Diorite
b) SB 381, Sugarloaf Quartz Diorite
c) SB 368c, Fawnskin Monzonite
d) SB 378, Fawnskin Monzonite

R: radiogenic argon
K: K-derived argon
A: atmospheric argon

Figure 69a.

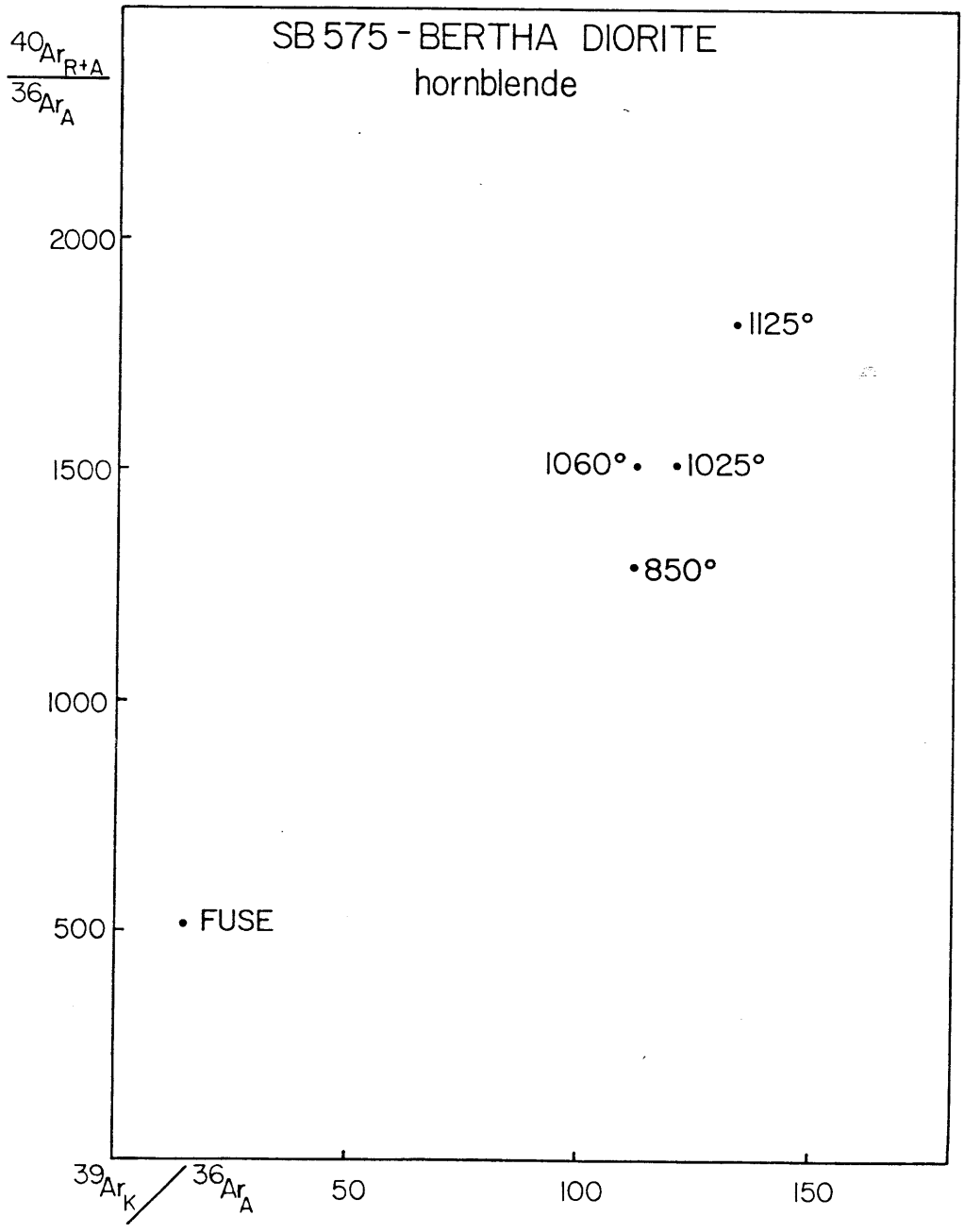
SB 575 - BERTHA DIORITE
hornblende
$\frac{40Ar_{R+A}}{36Ar_A}$
2000
1500
1000
500
1125°
1060°
1025°
850°
FUSE
$\frac{39Ar_K}{36Ar_A}$
50
100
150

Figure 69b.

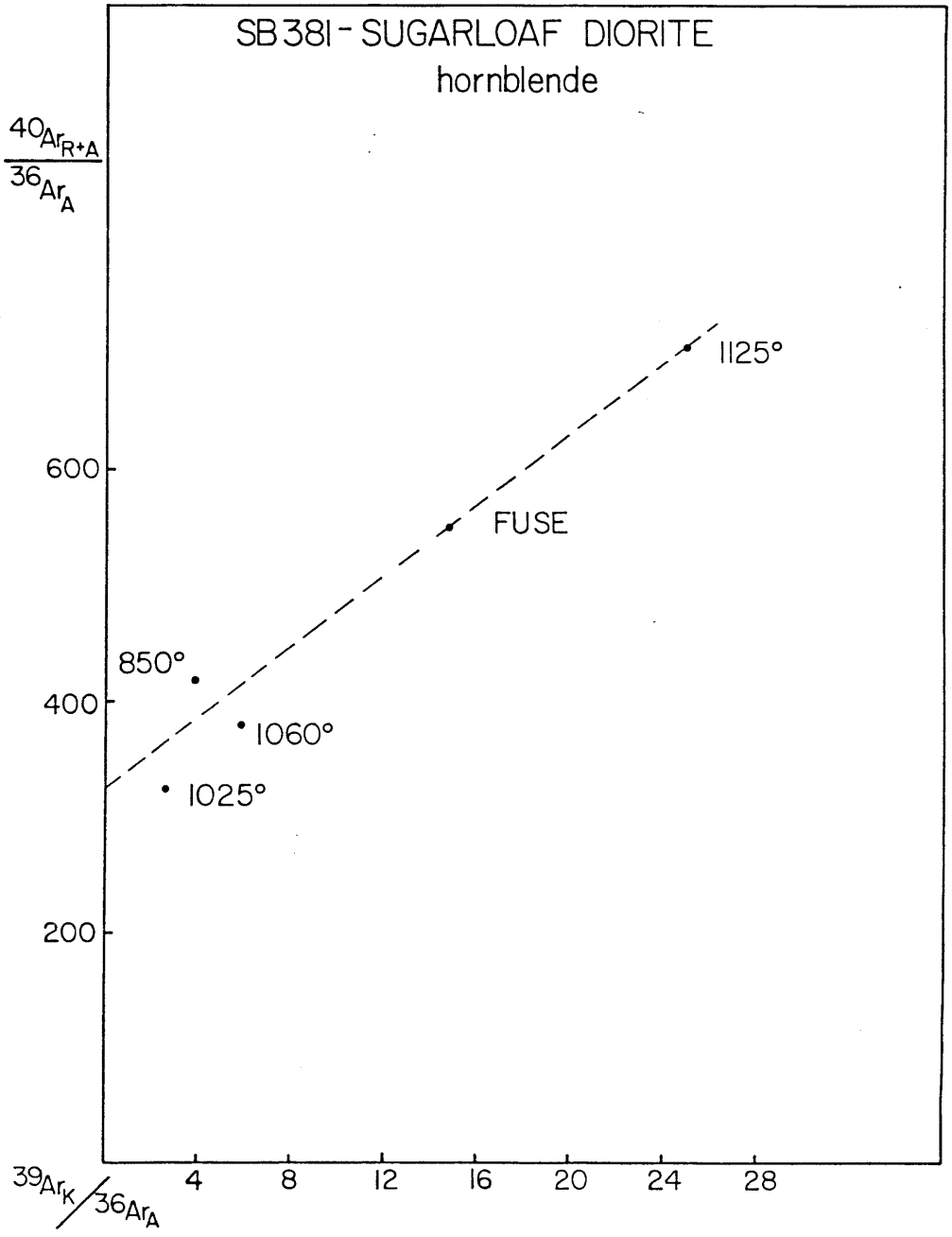
SB381 - SUGARLOAF DIORITE
hornblende
40Ar R+A / 36Ar A
600
400
200
1125°
FUSE
850°
1060°
1025°
4
8
12
16
20
24
28
39Ar K / 36Ar A

Figure 69c.

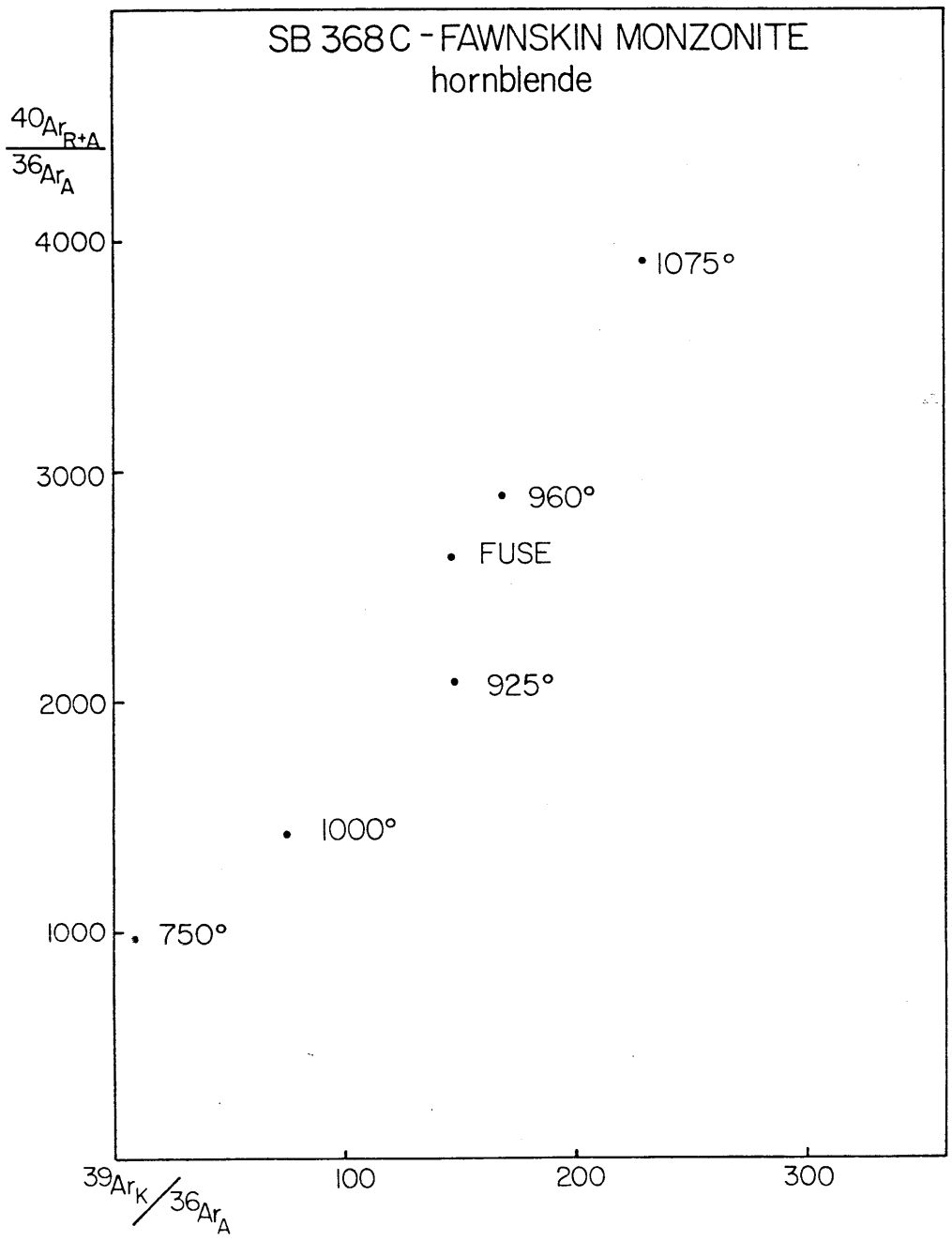
SB 368C - FAWNSKIN MONZONITE
hornblende
$\frac{40Ar_{R+A}}{36Ar_A}$
4000
3000
2000
1000
1075°
960°
FUSE
925°
1000°
750°
100
200
300
$39Ar_K / 36Ar_A$

Figure 69d.

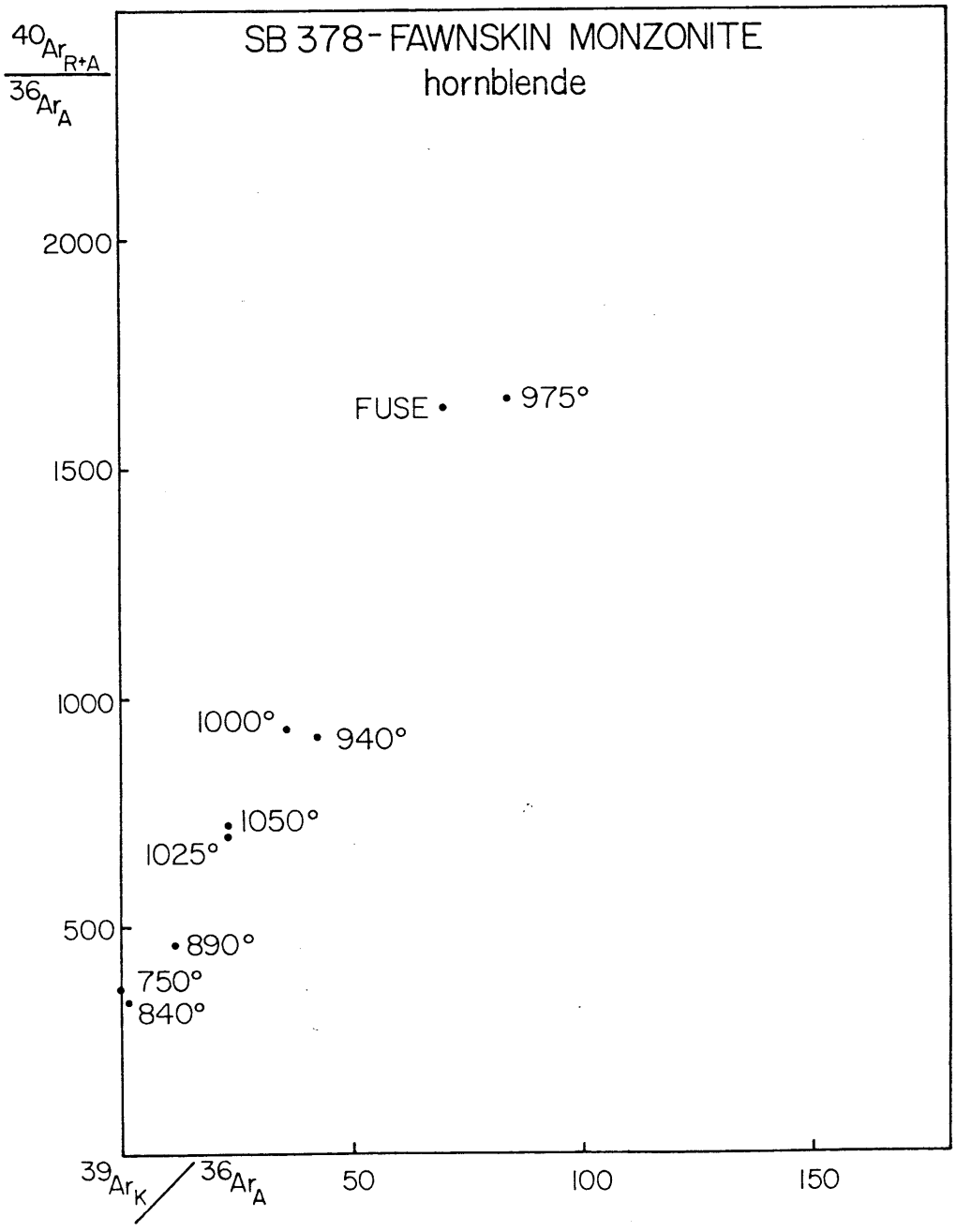
SB 378 - FAWNSKIN MONZONITE
hornblende
$^{40}Ar_{R+A}$ / $^{36}Ar_A$
2000
1500
1000
500
FUSE
975°
1000°
940°
1050°
1025°
890°
750°
840°
$^{39}Ar_K$ / $^{36}Ar_A$
50
100
150

these ages. The fusion step yielded an apparent K/Ca ratio typical of hornblende, and probably represents hornblende-derived Ar. Progressively higher apparent K/Ca ratios were calculated for the lower temperature steps. The 850° step yields a ratio of 1.15, much higher than typical magmatic or igneous hornblende. The presence of very fine-grained biotite intergrowths in this separate was noted above. The anomalous K/Ca ratio of the 850° step may reflect degassing of hornblende and trace amounts of biotite (typical K/Ca ratio of 4.75; Deer and others, 1966). Hence the age for this step is that of a hornblende-biotite mixture. Intermediate-temperature steps may also contain smaller traces of biotite-derived Ar, whose presence would decrease the apparent age obtained, if only slightly. This contaminant is likely gone by the 1075° step. Because of the biotite contaminant, it is not possible to clearly identify the time of quantitative retention of ^{40}Ar after thermal disturbance of the hornblende K/Ar system but a reasonable estimate would be 80 m.y.

A model for SB 575 was calculated by comparing this spectrum (without the 850° step) to the theoretical curve for a sample (consisting of log normal spheres, J = 0.33) experiencing 90% Ar loss at 80 m.y. (Turner, 1968). This yields a model K/Ar age of about 158 m.y. (this assumes the $^{40}Ar^*/^{39}Ar_K$ ratio for the fusion step is about 40% less than the undisturbed plateau value). The same age is calculated for 60% Ar loss from spheres of uniform size (after Huneke, 1976), although the model spectrum in this case is a poorer match.

Sugarloaf Quartz Diorite

The age spectrum for SB 381 is fairly typical of samples recording diffusive Ar loss, with the exception of the lowest temperature step. Steps 1025°-fusion show a pattern of progressive increase in ages similar to theoretical age spectra for thermally disturbed samples (represented by spheres of uniform size) calculated by Turner (1968). In spite of the apparent plateau for the two highest temperature steps, the age of original closure to Ar diffusion could not be recovered. When plotted on a $^{40}Ar_{R+A}/^{36}Ar_A$-$^{39}Ar_K/^{36}Ar_A$ plot, the plateau steps

yield a slope of 15.33 (slope equals model $^{40}Ar^*/^{39}Ar_K$ ratio) and an apparent age of 132.4 m.y. This age is not in agreement with the weighted-mean plateau age of 145.8 m.y. The $^{40}Ar/^{36}Ar$ intercept of this line is approximately 328, but the error in this value was not determined. The discrepancy between the plateau and isochron ages indicates disturbance of the age spectrum was too great to permit the age of initial Ar closure to be recovered, based on the criteria of Lanphere and Dalrymple (1978). If the disturbed nature of this spectrum is due to diffusive Ar loss, the fusion step age of 148 m.y. represents a minimum age for this sample.

A model K/Ar age of 156 m.y. for SB 381 was calculated using the theoretical curve of Huneke (1976) for a sample represented by uniform spheres which experienced 30% Ar loss at 80 m.y. The 850° step is disregarded in this comparison. The model predicts a 10% decrease in the $^{40}Ar^*/^{39}Ar_K$ value of the fusion step from the undisturbed plateau value.

Although an Ar loss model is favored for SB 381, an alternative interpretation is possible and requires discussion. The anomalously old age for the lowest temperature step causes the SB 381 spectrum to resemble saddle-shape spectra described by Lanphere and Dalrymple (1976). They suggest saddle-shaped spectra can be indicative of samples containing excess ^{40}Ar, not derived by <u>in situ</u> decay of ^{40}K. Such spectra yield anomalously high ages for their low and high temperature gas fractions, and a "saddle" of lower ages for intermediate steps. The minimum age obtained from saddle-type spectra examined by Lanphere and Dalrymple (1976) always exceeded the actual age of the minerals when independent age constraints were available. An excess argon interpretation for SB 381 would place its <u>maximum</u> cooling or retention age at 95.25 $\pm$ 13.18 m.y.

This interpretation is not thought likely for SB 381 for numerous reasons. Some samples believed to contain excess argon yield well-defined plateaus, not saddle-shaped release patterns (Roddick, 1978; J. Sutter, personal comm., 1980). Conversely, saddle-shaped spectra or spectra yielding anomalously old ages from the lowest temperature steps

are not exclusive to samples containing excess argon. Saddle-shaped spectra were obtained from hornblendes interpreted by Lanphere and Dalrymple (1971) as having experienced diffusive Ar loss. Thermally disturbed biotites studied by Dallmeyer (1975) sometimes yielded saddle-shaped spectra. Anomalously old ages from low temperature steps from otherwise "undisturbed" hornblende samples have been attributed to recoil effects or isotopic fractionation by Lanphere and Dalrymple (1976). Dallmeyer and Sutter (1976) have attributed similar anomalous ages from low-temperature steps of hornblendes from a variably retrograded terrane to the presence of small quantities of excess argon held in loosely bound sites (such as along grain boundaries or cleavage planes). Ar released over the remainder of these spectra appears to be derived from in situ decay of ^{40}K, and hence records useful information concerning the sample's age, and sometimes well-defined plateau ages. More recently, Harrison and McDougall (1980) have described disturbed age spectra from plutonic hornblendes which record the presence of excess ^{40}Ar in low temperature release fractions superimposed on patterns typical of diffusive Ar loss obtained from higher temperature steps. The degree of Ar loss is variable and is related to reheating during emplacement of a younger batholith. These disturbed spectra often yield well-defined plateau and isochron ages consistent with the independently determined age of the older pluton. The minimum ages agree well with the known age of the thermal disturbance event. Excess argon of high $^{40}Ar/^{36}Ar$ ratio was locally assimilated along the margins of some hornblende grains after major ^{40}Ar loss had occurred; its source is uncertain. The SB 381 age spectrum closely resembles spectra obtained by Harrison and McDougall, and may represent another example of excess argon contamination occurring after and/or during diffusive Ar loss.

Alternatively, the high age of the 850° step could reflect diffusive redistribution of ^{40}Ar to loosely bound sites within the sample during thermal disturbance. This would suggest that redistribution of ^{40}Ar occurred with relatively small overall ^{40}Ar loss from individual grains. Somewhat analogous ^{40}Ar redistribution has been reported from basalts studied by Fleck and others (1977), and from retrograded biotites studied by Dallmayer and Sutter (1976).

At the present time it is not possible to determine which model best explains the anomalously old age of the low temperature step, either excess ^{40}Ar contamination, ^{40}Ar redistribution, ^{39}Ar recoil, or some combination of these factors. It is suggested that the remaining steps yield meaningful data which include the minimum age of the Sugarloaf Quartz Diorite (148 m.y.) and the maximum age of Ar closure after thermal disturbance (95 m.y.).

Fawnskin Monzonite

Both age spectra from hornblendes of the Fawnskin Monzonite are disturbed, and yield anomalously high ages in the low-temperature steps. No plateaus are present for these spectra. $^{40}Ar_{R+A}/^{36}Ar_A$-$^{39}Ar_K/^{36}Ar_A$ plots yield crude linear arrays but no well-defined isochrons. The staircase nature of the intermediate to high-temperature steps in both cases is typical of samples recording severe Ar loss. In such an interpretation, the fusion step age represents a minimum cooling or retention age for the respective samples. The fusion step age is 214.1 $\pm$ 2.9 m.y. for SB 378, and approaches the $\sim$230 m.y. U/Pb zircon and $^{40}Ar/^{39}Ar$ hornblende ages obtained for the Granite Mountains Monzonite and Black Mountain Monzonite which may correlate with the Fawnskin Monzonite (C. Miller, 1977; E. Miller and Sutter, 1979). The Fawnskin Monzonite is clearly older than 126.73 $\pm$ 3.55 m.y., the minimum age of the Bertha Diorite which intrudes it.

As in the case of SB 381, the explanation for the extremely high ages in the lowest temperature steps is not certain. As the age for the 890° step of SB 368c is unknown, this discussion focusses on the age spectrum for SB 378. Unlike excess argon-bearing minerals studied by Lanphere and Dalrymple (1976), all gas fractions save the first yield consistent K/Ca ratios, and these values are typical for plutonic hornblendes. The saddle-shaped spectra Lanphere and Dalrymple described were obtained from rocks which apparently did not experience subsequent reheating. This is not the case with the Fawnskin Monzonite as it must have been reheated during emplacement of the Bertha Diorite, which in turn shows evidence of severe Ar loss from hornblende during an even later

heating, evidenced by Late Cretaceous biotite K/Ar cooling ages being recorded in the older plutons in the Big Bear area. What effect reheating would have on an originally saddle-shaped spectrum is unknown. In view of the other geochronologic evidence for significant reheating, and evidence of post-crystallization alteration and deformation of the Fawnskin Monzonite, it seems most reasonable to interpret the intermediate to high temperature staircase portion of these two spectra as the result of diffusive ^{40}Ar loss, and not as relicts of an original saddle-shaped spectrum.

Although the staircase geometry of intermediate to high temperature steps is thought to result from diffusive Ar loss, the low temperature release fractions may indeed record the presence of excess ^{40}Ar. Irreproducibility of total gas ages (K/Ar and $^{40}Ar/^{39}Ar$) of individual mineral separates is a typical feature of samples known to contain excess ^{40}Ar (Lanphere and Dalrymple, 1976). The significant discrepancy between the recalculated total gas age (240.6 m.y.) and the K/Ar and total fusion ages ($\sim$213 m.y.) of SB 378 may be owing to excess argon, inhomogeneously distributed in loosely bound sites. As in the examples described by Harrison and McDougall (1980), assimilation of excess argon may have occurred after diffusive argon loss. The discrepancy between yield of $^{40}Ar^*$ (moles/gm) obtained from the $^{40}Ar/^{39}Ar$ total fusion and conventional Ar analyses for SB 368c may similarly reflect effect of excess argon, distributed inhomogeneously within the sample in non-crystallographic sites. The total fusion sample of SB 368c contains 0.162×10^{-10} moles/gm more radiogenic ^{40}Ar than the average of the two K/Ar samples. The reason for reproducibility of the K/Ar ages for SB 368c, and the $^{40}Ar/^{39}Ar$ total fusion and K/Ar age for SB 378, is unknown. The high K/Ca ratios of the lowest temperature steps of SB 378 and SB 368c suggests that some excess ^{40}Ar may have preferentially accumulated in association with zones of micaceous alteration along grain margins.

Any model of the original Ar retention age of SB 378 is complicated by uncertainty concerning the magnitude of Ar loss during emplacement of the Bertha Diorite. If it is assumed that only the 80 m.y.

event is responsible for the Ar loss recorded here, and if the 750°, 840° and 890° steps (believed to contain excess ^{40}Ar) are omitted, then a reasonable visual fit may be made for a curve including the 940°-fusion steps. This part of the spectrum resembles model spectra for a sample (represented by log normal spheres, J = 0.33) which experienced 60-70% Ar loss. The model age for original Ar retention is 229 m.y. (this assumes a $^{40}Ar^*/^{39}Ar_K$ ratio for the fusion step is 10% less than the undisturbed plateau value). This model age is in good agreement with ages for the Granite Mountains Monzonite and Black Mountain Monzonite discussed above. The SB 378 age spectrum cannot easily be fit to a model Ar loss spectrum for spheres of uniform size. The spectrum for SB 368c reflects even greater Ar loss, but no attempt was made to fit this partial spectrum to model Ar loss curves.

Chronology of Mesozoic Magmatic and Thermal Events

In spite of the extreme disturbance of K/Ar mineral systems during the Late Cretaceous, some important constraints can now be placed on the timing of earlier Mesozoic magmatic events in the Big Bear region. The Fawnskin Monzonite is the oldest intrusive unit recognized in the Delamar Mountain area. Its two hornblende age spectra are believed to record the effects of diffusive loss of ^{40}Ar, and this unit is assigned a minimum age of 214.1 $\pm$ 2.9m.y. A model Ar retention age of 229 m.y. was calculated for this pluton. The minimum age is compatible with ages obtained for the Triassic monzonites near Victorville, and supports C. Miller's (1977) interpretation that the Fawnskin Monzonite is part of a widespread Early Mesozoic plutonic belt in southern California.

The Bertha Diorite yields a minimum age of 126.73 $\pm$ 3.55 m.y. and a model Ar retention age of 158 m.y. It intrudes the Fawnskin Monzonite. It is unknown if significant reheating of the monzonite occurred during emplacement of the diorite.

The Sugarloaf Quartz Diorite yields a minimum age of 148.15 $\pm$ 3.10 m.y. and a model Ar retention age of 156 m.y. The Sugarloaf Quartz Diorite

and the Bertha Diorite are believed to be of Late Jurassic age. Plutons of this age have not been widely recognized in the western Mojave region, though they are common further east (Armstrong and Suppe, 1973; Silver and Anderson, 1974; Powell and Silver, 1979). The thermal effects of Late Jurassic magmatism on older plutons such as the Fawnskin Monzonite are not known.

Regional reheating during emplacement of Cretaceous batholithic rocks caused resetting of all biotite K/Ar systems and variable Ar loss from hornblendes. Biotites from Precambrian gneisses were affected (F. Miller, personal comm., 1979) as well as biotites from earlier Mesozoic plutons. The biotite ages almost certainly represent cooling ages, and may be somewhat younger than crystallization ages for the Cretaceous granitic rocks, as is the case for the Cretaceous Peninsular Ranges batholith (Krummenacher and others, 1975) and Cretaceous batholithic rocks of the Salinian block (Armstrong and Suppe, 1973). The Cienga Seca Diorite shows none of the alteration and deformation characteristic of the older plutons. It is believed to be related to the Late Cretaceous batholith, and its slightly discordant hornblende and biotite ages (79.7 $\pm$ 1.0 m.y. and 70.2 $\pm$ 1.0 m.y. respectively) are believed to date times of closure to Ar diffusion. As discussed by Krummenacher and others (1975), K/Ar cooling ages for hornblende may also be somewhat younger than U/Pb zircon crystallization ages, so the time of emplacement of the Cretaceous batholithic rocks is still not closely defined.

The presence of excess Ar in hornblendes from the Fawnskin Monzonite and perhaps the Sugarloaf Quartz Diorite is of special interest. Most geochronologic data available for southern California consists of K/Ar ages. The presence of excess ^{40}Ar can greatly affect the resultant K/Ar mineral ages. Caution must be taken in interpreting the significance of single mineral ages, or discordant mineral pairs when only conventional K/Ar data is available. Evidence from the Big Bear area indicates that the frequent assumption that hornblende ages of a discordant mineral pair provide a reasonable minimum age for dated rocks may often be unjustified.

CHAPTER VI: INTERPRETATION OF MESOZOIC DEFORMATION AT BIG BEAR, ITS REGIONAL SETTING AND IMPLICATIONS

Interpretation and Correlation of Mesozoic Events

Introduction

In Fig. 70, the geochronological constraints discussed in Chapter V are integrated with the sequence of structural, igneous and metamorphic events reviewed in Chapter IV. These individual events are here grouped into area-wide deformational phases (D_1, D_2, etc.), based on similarities of structural style and timing. As some events can only be documented locally (i.e., emplacement of individual plutons) and as detailed mapping throughout the Big Bear area is incomplete, this synthesis is both speculative and provisional. Nevertheless, some important conclusions can be drawn although many significant questions are still unresolved.

D_1

Deformational phase D_1 is recognized throughout the study area and includes polyphase folding and thrust or reverse faulting. The locally variable sequence of D_1 events is here attributed to a progressive deformational episode which also involved pre- and synkinematic low P, intermediate T metamorphism typical of intra-arc terranes. Evidence indicates that locally, at least, the metamorphic peak was prekinematic. The D_1 deformation is rather arbitrarily divided into D_{1a} and D_{1b} subphases. This division is based on orientation of structures and their relation to metamorphism. D_{1a} structures are synmetamorphic; there is evidence these structures formed under P, T conditions permitting recrystallization and ductile flowage. Cleavage is typically associated with D_{1a} folds. D_{1b} structures typically lack associated cleavage, and may be largely post- or late synmetamorphic. It should be noted, however, that ductile deformation and new mineral growth (particularly in pelitic rocks) during later D_{1b} folding would be restricted by dehydration of these rocks during earlier D_{1a} metamorphism. Lack of synmetamorphic

Figure 70: Interpretive Correlation of Mesozoic Structural Events in the Big Bear Area

	Rose Mine Area	Sugarloaf Area	Delamar Mountain Area
D_{1a}	1) Synmetamorphic polyphase folding and thrusting Metamorphism: min. greenschist F_1: zonal isoclinal folds F_2: N-NW trending, NE vergent folds and thrusts	1) Metamorphism and polyphase folding Metamorphism: low P, intermediate T facies F_1: zonal tight-isoclinal folds F_2: N-NW trending, NE vergent folds and faults	1) Metamorphism and polyphase folding Metamorphism: low P, intermediate T facies F_{1a}(?): zonal folding and transposition F_1: NW trending, SW(?) vergent folding
Permo-Triassic (?)	2) High-angle faulting		
	3) Emplacement of Doble Thrust		
	4) Crenulation cleavage (F_3) NW trending		
D'_{1b}	5) ? Open folding (F_4) NE trending	F_3: NE trending open folds	F_2: E-W trending, N vergent folds
D'_{2a}			2) Low-angle (?) normal faulting
D'_{2b}			3) Emplacement of the Fawnskin Monzonite pre- 214.1±2.9 m.y.
		2) ?High-angle faulting	
		3) Low-angle, younger-over-older faulting a: lower allochthons emplaced b: high-angle faulting c: higher allochthons emplaced	4) ?High-angle faulting 5a) Emplacement of Bertha Diorite pre- 126.7±3.5 m.y. 5b) ?Emplacement of Dike Complex
D'_3 Late Jurassic		4) Emplacement of Sugarloaf Intrusive Complex, pre- 148.2±3.1 m.y. (may have occurred concurrently with event 3)	
D'_4 Late Cretaceous	6) Intrusion of Cretaceous granitic rocks	5) Emplacement of Cretaceous granite-quartz monzonite	6) Emplacement of Cretaceous granite-quartz monzonite

fabrics in later structures does not require a dramatic decrease in temperature or pressure, but rather may reflect changes in mechanical properties of rocks after metamorphic devolatilization (see Yardley, in press).

In the Sugarloaf-Rose Mine area, D_{1a} structures include F_1 and F_2 folds and the Doble Thrust. Mesoscopic and macroscopic F_1 folds are tight or isoclinal, with short overturned limbs (S or Z fold geometry). These folds are disharmonic, and best developed mesoscopically in pelitic rocks and marbles where they cause transposition of bedding. Some macroscopic F_1 folds are present in quartzite units (Wildhorse Road Syncline, syncline in sub-block VId) but major F_1 recumbent isoclinal folds are not present in the map area. F_1 folding could not be demonstrated to affect Precambrian gneisses in the map areas. Below the Doble Thrust, F_1 and F_2 folds are (at least locally) coaxial. Above the thrust, the orientation of F_1 folds appears to be variable. Locally, as in sub-block VIa, F_1 folds are approximately coaxial with NW trending F_2 folds. At higher stratigraphic-structural levels, F_1 folds in sub-block VId and blocks VII and VIII apparently trend SW-NE or E-W and are SE or S vergent.

Non-coaxial F_1 folding may have resulted from areally inhomogeneous, bedding-parallel slip. This would produce folds of variable axial orientations (tundra-slide model of Hansen, 1971). Unfortunately, my mesoscopic structural data is insufficient, and later structural complications are too severe to permit a further test of this model by evaluating F_1 fold separation angles (Hansen, 1971).

Alternatively, non-coaxial F_1 folding would also be expected if bedding was not strictly planar throughout the area prior to F_1. If bedding were gently warped prior to F_1, then the intersection between bedding (S_0) and the flattening plane of the finite strain ellipsoid associated with F_1 ($\sim S_1$) would vary in orientation, as would F_1 fold axes. Such warping might be unrelated to the deformational sequence described here. Alternatively, such warping could conceivably have been related to an early stage of F_2 folding, involving the Precambrian gneisses. It may be that the

formation of broad warps which were to serve as the nucleus of some later F_2 folds actually preceded the formation of F_1 folds in the miogeoclinal cover sequence.

F_2 folds are tight (locally isoclinal) or open, form major macroscopic structures and involve Precambrian gneisses. Overturned and upright F_2 folds are present. Cleavage is associated with overturned folds. Schistosity associated with S_2 axial-planar cleavage is not as penetrative as in S_1 cleavage; in quartz-rich phyllites, microscopic crenulation cleavage is sometimes present instead. F_2 folds trend N to NW and are E to NE vergent. Possible F_2 transport directions were obtained from two folds (a fold in sub-block VIc and the Green Canyon Synform) and are to the NE. WSW plunging pebble elongation lineations from the east limb of the Arrastre Creek Antiform may parallel the local F_2 transport direction and are consistent with the NE transport direction determined for other F_2 folds. The relation between F_1 and F_2 material transport directions is unknown.

Events 2-4 from the Rose Mine area, which include final emplacement of the Doble Thrust, are included in phase D_{1a}. The Doble Thrust cuts earlier event 1 folds and event 2 faults in the lower plate and the overturned east limb of the Arrastre Creek Antiform in its upper plate. S_2 cleavage in upper plate gneisses parallels axial-planar cleavage of second order folds in the Wildhorse Quartzite and may be axial-planar to the major fold. It is evident that the Doble Thrust is synmetamorphic and that recrystallization outlasted translation along the thrust contact. It was suggested above that the Arrastre Creek Antiform may be analogous to thrust ramp anticlines commonly recognized in foreland thrust belts (Dahlstrom, 1970). The magnitude of thrust displacement is uncertain. Both upper and lower plate folding may have initiated contemporaneously, however continued thrust plate movement eventually truncated the Rose Mine Synform and related lower plate structures.

Event 4 structures at Rose Mine, including F_3 crenulation cleavage and associated folds, are localized adjacent to the thrust contact. They

may have formed across this narrow zone in response to late stage relative movement between the upper and lower plates after thrust translation ceased.

The structural response of Precambrian gneisses to D_{1a} deformation in the Sugarloaf-Rose Mine area is of particular interest. These rocks were apparently not involved in F_1 folding which produced the most penetrative D_1 fabrics present in the miogeoclinal cover sequence. F_1 folding may have died out structurally downward. The hot, but dry Precambrian gneisses may not have been able to deform by mesoscopic ductile folding (Fig. 71). Precambrian gneisses were involved in F_2 (and F_3) folds; here too, however, they rarely display evidence of penetrative deformation in the cores of folds. It appears that the gneisses did not accommodate shortening by distributed shear but rather by flexure and brittle faulting on overturned fold limbs. Geometric considerations suggest that basement-cored F_2 folds may be of a décollement type at depth (Fig. 71). Only above the Doble Thrust, where basement gneisses override the rocks of the cover sequence, are well developed penetrative F_2 fabrics recognized. It was previously suggested that access to fluids was the key factor in limiting Mesozoic recrystallization in the Precambrian gneisses. The Precambrian gneisses were clearly hot during D_1 metamorphism, but as long as they remained dry they deformed brittlely if at all. They remained dry as long as they structurally underlay the wet cover rocks. It is suggested that F_2 faults which breached the overturned limbs of folds provided conduits for fluids and carried basement gneisses over the cover rocks. Once structural overriding had begun, access to fluids would have been enhanced. The faults could have quickly developed into ductile zones of high strain. These ductile faults may have served as the locus for further shortening. The Doble Thrust may have evolved in such a manner and may represent a major décollement. The thrust may have initiated as a reverse fault breaching the east limb of the Arrastre Creek Antiform. The S_2 cleavage in the gneisses, although parallel to axial-planar cleavage of the F_2 folds, may be fundamentally related to thrusting.

Figure 71: Interpretive model for involvement of Precambrian gneisses in D_{1a} structures.

F_2 thrusts and reverse faults: heavy lines
S_2 cleavage developed in Precambrian gneisses: short dashes
Older Precambrian fabrics: wavy lines

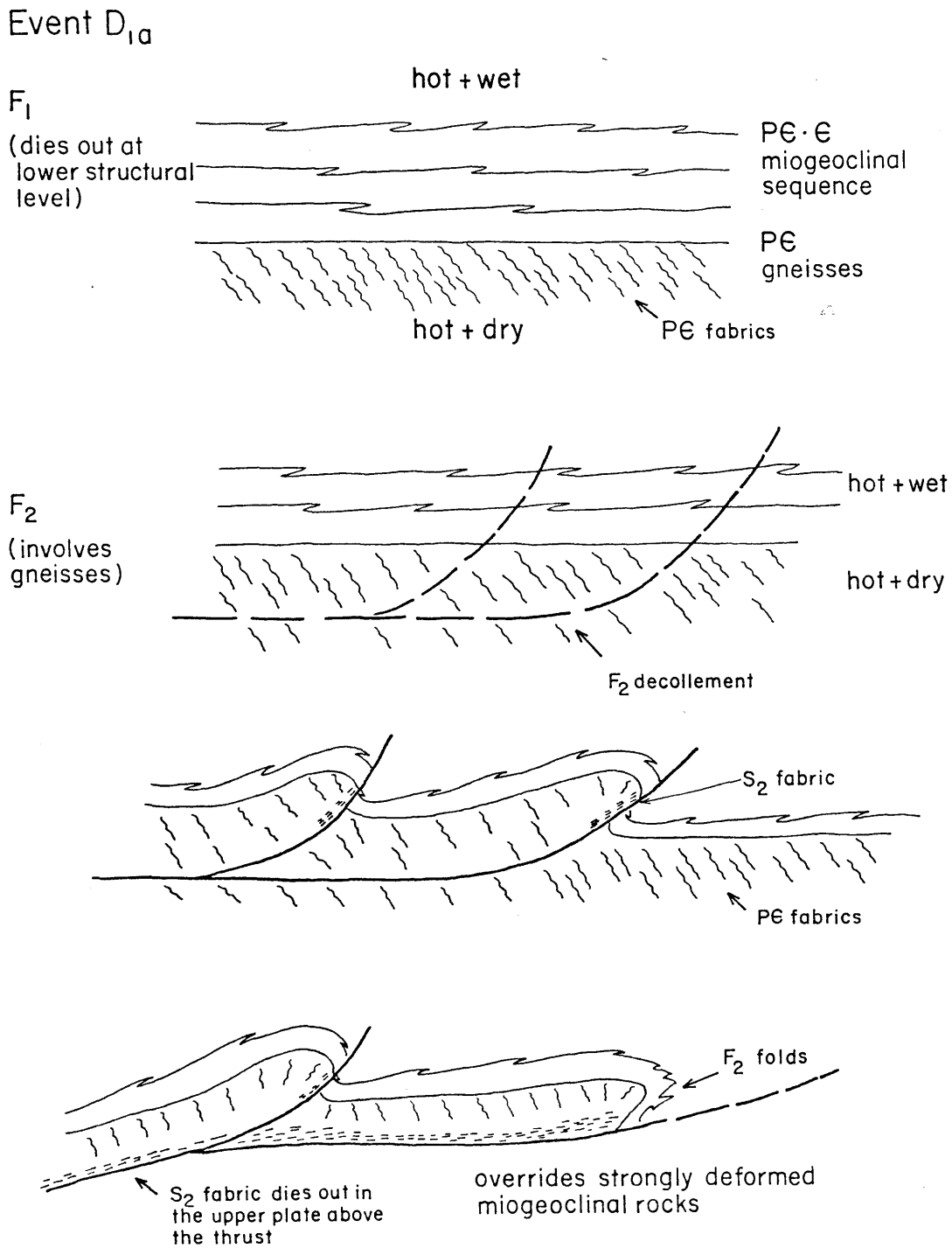

D_{1b} structures in the Sugarloaf-Rose Mine area include F_3/F_4 folds which refold F_1 and F_2 folds and the Doble Thrust. These generally NE-SW trending folds are transverse to the F_2 structural grain. Cleavage is only rarely associated with F_3 folds (F_3(?) folds in sub-block VIa). However, this local occurrence of mica growth associated with S_3 suggests that these folds, at least, may have formed during the later stages of D_1 metamorphism. Age constraints in the Sugarloaf-Rose Mine area permit the interpretation that F_3/F_4 folds may be significantly younger than D_{1a} structures; locally however, F_3 folds predate the Late Jurassic Sugarloaf Quartz Diorite.

Rocks in the Delamar Mountain area provide the upper age limit on D_1 deformation, as structures of this generation are cut by the Fawnskin Monzonite, which yields a minimum $^{40}Ar/^{39}Ar$ fusion-step age of 214.1 $\pm$ 2.9 m.y. NW trending F_1 folds are the earliest macroscopic D_{1a} structures recognized in the map area, but refold transposed bedding which is locally present in Bonanza King and Carrara marbles and possibly in the upper Wood Canyon Formation (associated with S_{1a} cleavage). This local transposition may have occurred during an earlier mesoscopic folding event (F_{1a}?). In the Cambrian marbles these folds are isoclinal and resemble F_1 folds recognized in the Sugarloaf-Rose Mine area. These two transposition folding events may be correlative. If so, the D_{1a} folding sequence at Delamar Mountain is quite similar to that in the Sugarloaf-Rose Mine area. F_1 folds at Delamar Mountain may correlate with F_2 folds in the latter area. Although the axial orientations of these two fold sets are similar, their vergence is not. The axial surface of F_1 folds at Delamar Mountain may have dipped steeply NE before F_2 refolding. This would indicate SW vergence as opposed to the E to NE vergence of correlative folds at Sugarloaf-Rose Mine. I cannot presently explain this discrepancy.

E-W trending, N vergent F_2 folds refold D_{1a} structures at Delamar Mountain. The F_2 transport direction is subvertical or to the NW. Axial-planar cleavage is locally associated with F_2 folds. Like D_{1b} structures at Sugarloaf-Rose Mine, F_2 folds at Delamar Mountain are transverse to

earlier D_{1a} folds. The transport direction of F_2 folds at Delamar Mountain lies within the axial surface of F_1 folds, and suggests to me these fold sets formed progressively during a single deformational event predating emplacement of the Fawnskin Monzonite. I infer that F_3/F_4 folding at Sugarloaf-Rose Mine also predated emplacement of the Fawnskin Monzonite during the D_2 event, but this cannot presently be demonstrated.

D_2

Events related to episodes D_{2a} and D_{2b} are only known with certainty from the Delamar Mountain area. Event 2 low-angle, younger-over-older faulting (D_{2a}) is believed to predate emplacement of the Fawnskin Monzonite during event 3 (D_{2b}). The Fawnskin Monzonite has yielded a minimum $^{40}Ar/^{39}Ar$ fusion-step age of 214.1±2.9 m.y. and is the oldest Mesozoic intrusive unit presently recognized in the Big Bear area. The monzonite may be correlative with Permo-Triassic plutons recently recognized elsewhere in the western Mojave Desert (Chapter V). Although the Fawnskin Monzonite discordantly cuts D_1 folds it is possible that this episode of magmatism was broadly coeval with the low P, intermediate T metamorphism that accompanied D_1 deformation. If D_1 metamorphism was the result of conductive heating in an intra-arc plutonic terrane, it may be that elevated temperatures persisted after the D_1 metamorphic peak. The general transition from more to less ductile fold styles observed during D_1 may reflect a change in mechanical behavior from wet to dry rocks, and not a reflection of significant cooling prior to emplacement of the Fawnskin Monzonite. Regional heating, polyphase deformation and plutonism probably represent an intra-arc orogenic continuum.

The inferred event 2 younger-over-older fault along which the Fawnskin Monzonite locally intrudes near Polique Canyon may be analogous to low-angle faults associated with emplacement of the Sugarloaf Intrusive Complex. This D_{2a} structure may have formed during extensional faulting related to emplacement of the Fawnskin Monzonite. This fault zone may have had recurrent movement.

In the Sugarloaf area, possible D_{2a} structures may be present, but their age cannot be confirmed. Event 2 high-angle faults and event 3a low-angle younger-over-older faults cut structures assigned to D_1. This sequence of faulting, which is at least in part extensional, may be correlative to D_{2a} events in the Delamar Mountain area. At present, however, no intrusive rocks correlative in age with the Fawnskin Monzonite are known at Sugarloaf. Emplacement of the dacite porphyry dikes was in part contemporaneous with movement on event 3a faults, but the age of the dikes is not known. Kinematic data, summarized below, suggest to me that all event 3 faulting may have been related in time, and was perhaps associated with emplacement of the Late Jurassic Sugarloaf Intrusive Complex during D_3.

D_3

The D_3 deformational episode includes tectonic and magmatic events inferred to be associated with emplacement of shallow-level intermediate intrusive rocks of Late Jurassic age. In the Sugarloaf area, event 3b high-angle faults and event 3c low-angle younger-over-older faults are spatially and at least in part temporally associated with emplacement of the Sugarloaf Intrusive Complex, one unit of which has yielded a $^{40}Ar/^{39}Ar$ fusion-step age of 148.2 ± 3.1 m.y., a minimum age for the pluton. Low-angle normal faulting and detachment of the higher allochthons is interpreted to have occurred as the roof rocks extended to accommodate emplacement of this intrusive complex. Event 3a faulting and emplacement of the lower allochthons may have occurred at this time or earlier as discussed above. However, the similarity of structural style between events 3a and 3c suggests a similar origin. Movement along some suspected event 3a faults occurred contemporaneously with emplacement of dacite porphyry dikes. It was suggested above that these dikes may be related to the Sugarloaf Intrusive Complex. At the least, this suggests some reactivation of event 3a structures during D_3. The match-up of D_1 fold structures offset across event 3a faults indicates principally east to west displacement for the

lower allochthons. Significant east-west extension occurred during event 3a. Principal displacement of the higher allochthons during event 3c is interpreted to have been to the west also, down the plunge of the trough-like Green Canyon basal fault surface. The similar geometry and transport direction for event 3a and main-stage event 3c faulting, and the local occurrence of tectonized dacite porphyry dikes along event 3a faults suggests to me that all event 3 faulting at Sugarloaf represents a continuum of east-west extensional tectonism, probably related to the emplacement of the Sugarloaf Intrusive Complex and associated rocks. I tentatively assign structural events 3 and 4 to the D_3 deformational episode.

In Chapter IV, event 3 faulting in the Sugarloaf area was described as extensional in nature. The geometry of D_3 faulting in the Sugarloaf area places important constraints on the relationship between low-angle normal faulting and plutonism. Field relationships are not compatible, for example, with a model relating low-angle, younger-over-older faulting to plutonic doming and associated gravity sliding from the resulting uplift (Fig. 72). As discussed in Chapter IV, the younger-over-older allochthons do not show internal structures typical of Quaternary gravity slides or landslides known from well-exposed desert ranges (Burchfiel and Davis, 1971; in prep.). A gravity slide interpretation requires that toe relationships (faults juxtaposing older rocks over younger ones) should be equally developed in this terrane. Toe relationships are conspicuous in their absence. Most major event 3 faults dip toward exposures of the Sugarloaf Intrusive Complex; transport of fault blocks is toward the intrusive rocks. The opposite relationship is predicted by a doming-sliding model, in which a tectonically denuded area of older rocks should surround exposures of the plutonic rocks. Instead, the highest allochthons and the youngest rocks in the study area are found to overlie the Sugarloaf Intrusive Complex. For these reasons, I find a plutonic doming-gravity sliding model untenable.

Figure 72: Models to explain younger-over-older faulting associated with plutonism.

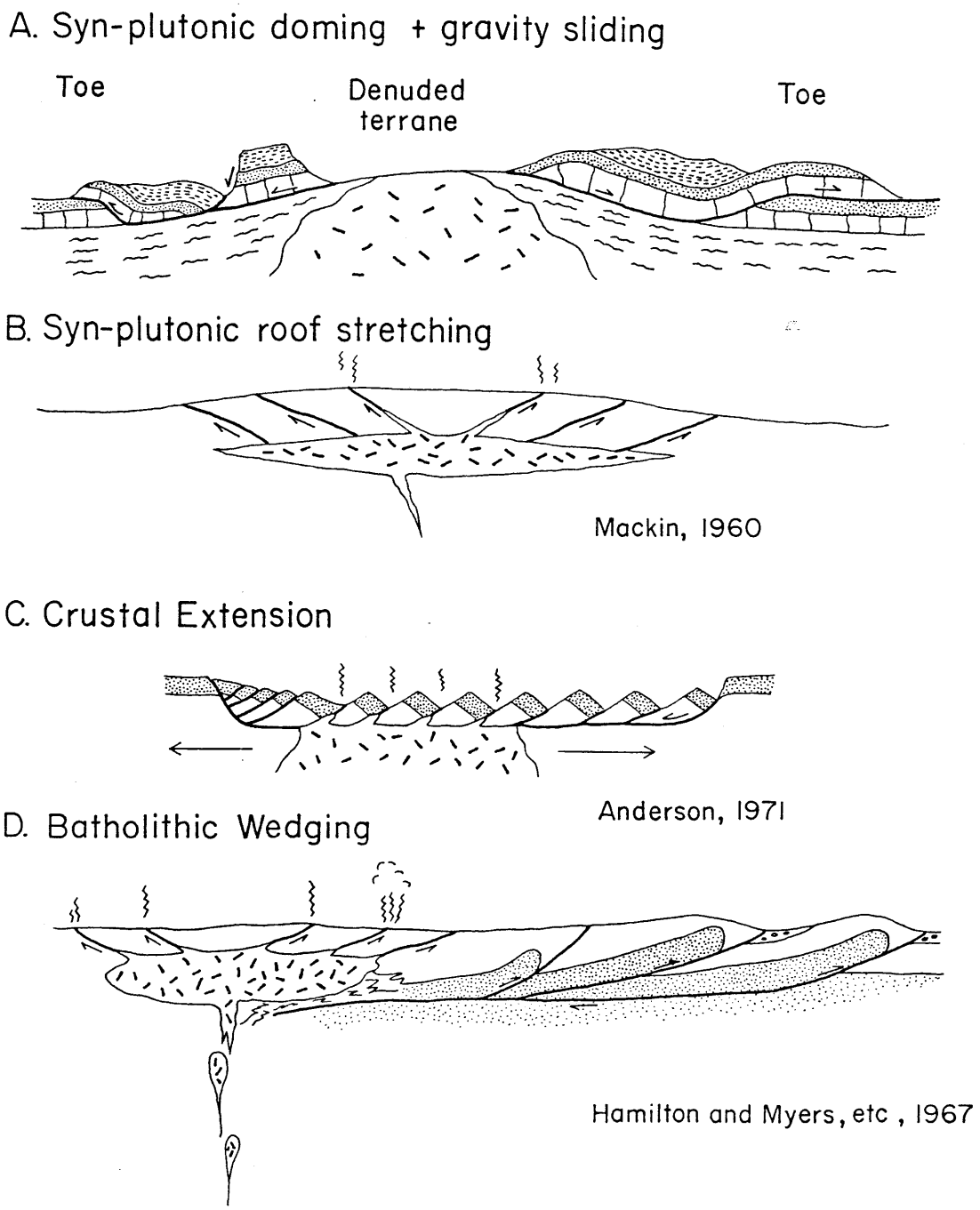

Event 3 younger-over-older faulting is the result of extension. The spatial and temporal association of Late Jurassic magmatism with event 3c and perhaps event 3a faulting suggests these events are connected. Tectonic extension of roof rocks occurring during the emplacement of plutons has been suggested by several authors. In general, these geologists view such extensional faulting as the result of tectonic stretching of the roof terrane to make room for material added to the upper crust by magmatism. Mackin (1960) presented examples from the Basin-Range province of southwestern Utah where late Cenozoic extensional faulting may have resulted as the roof rocks failed by normal faulting to accommodate broad arching or doming associated with the emplacement of shallow plutons (Fig. 72). Mackin was referring to plutons of a specific geometry, plutons of "low structural relief" (sill-like, concordant intrusions). In the case of such thin plutonic bodies, upper crustal extension to accommodate the additional volume of magmatic material may be confined to roof stretching only. General upper crustal extension is not a requirement. In an extreme case (a convex upward, half-cylinder shaped body for example) roof extension would approach ~50% in excess of original width, however, for more realistic intrusive geometries the amount of roof extension would be much less.

Other models have suggested that extension related to plutonism need not be confined to the roof rocks, but may involve spreading or wedging of wall rocks as well. Along this line, Anderson (1971) suggested that an extensive late Cenozoic low-angle normal fault terrane in southern Nevada might have formed above a coeval plutonic terrane. In Anderson's model, general upper crustal extension at depth is accommodated by plutonism, while the overlying roof rocks extend by low-angle normal faulting (Fig. 72; in the case described by Anderson, the contact between the underlying plutonic terrane and overlying normal fault terrane is not directly exposed). No claim is implicit whether plutonism triggers upper crustal extension, or whether the sites of plutonism are localized where upper crustal extension occurs. Hamilton and Myers (1967, 1974), Hamilton (1978)

and Gastil (1979) have related the emplacement of batholiths to extensional and contractional tectonics in volcano-plutonic arcs. They suggest that arc magmatism adds material to the upper crust. The thermo-gravitationally driven ascent and spreading of magma bodies at upper crustal levels is attended by compression of batholithic wall rocks and extensional rafting of roof rocks (Fig. 72). These geologists envision the roof rocks as consisting primarily of arc volcanics, in part coeval with the plutons; however, their general model is applicable to a non-volcanic roof as well. Intruded faults serve as magma conduits from sub-volcanic plutonic to the overlying volcanic edifice.

I suggest that D_3 low-angle normal faulting in the Sugarloaf area occurred as roof rocks extended to make room for Late Jurassic plutons. It is uncertain whether extension was confined to the roof rocks (a la Mackin), or whether plutonism was attended by more general upper crustal extension (a la Anderson, Hamilton and Myers, and Gastil). A key unknown is the original, 3 dimensional geometry of the Late Jurassic plutons, without which, neither model can be rigorously tested. The magnitude of observed roof extension (60-100%, see Chapter IV), in the Sugarloaf area, and the possible extent of this extensional terrane in the Big Bear area (discussed below) are suggestive that some component of general upper crustal extension is involved. Discussion of the relationships between roof-rock extension and back-arc fold and thrust belts is deferred for the moment.

In the Delamar Mountain area, emplacement of the Bertha Diorite and the dike complex are included in the D_3 event. The Bertha Diorite has yielded a minimum age of 126.7±3.6 m.y., based on a hornblende $^{40}Ar/^{39}Ar$ fusion-step age. The model $^{40}Ar/^{39}Ar$ age calculated for hornblende from the Bertha Diorite is 158 m.y., similar to the 156 m.y. model age for hornblende from the Sugarloaf Quartz Diorite. It is suggested that the Sugarloaf Intrusive Complex, the dacite porphyries, Bertha Diorite and the dike complex north of Delamar Mountain may all be part of an intermediate composition, shallow-level batholith of Late Jurassic age. Structures

possibly associated with D_3 magmatism in the Delamar Mountain area include NW trending faults of event 4. The Bertha Diorite intruded along low- and moderate-angle normal faults. In particular, the diorite intruded along the low-angle fault zone inferred to underlie the Cambrian marbles on Bertha Ridge. At least part of the displacement along this fault zone occurred during D_2. However, renewed movement and/or fault propagation is believed to have taken place during D_3. Here again, extensional spreading of the pre-existing roof and wall rocks by low-angle normal faulting and diking occurred in response to shallow-level intrusion.

Geologic reconnaissance suggests that several of the younger-over-older allochthons described here extend beyond the limits of the map areas. Block IX, the highest allochthon in the Sugarloaf area, may extend west to the Gold Mine Ski Area to include rocks correlated with the Zabriskie Quartzite and Carrara and Bonanza King Formations. An undated diorite pluton intrudes these rocks and Precambrian gneisses exposed west of them near Snow Summit (Dibblee, 1964a; see Plate I). This diorite may intrude along a large displacement, E dipping(?) normal fault zone which separated the Precambrian gneisses and younger rocks to the east. Based on Dibblee's (1964a) and McJunkin's (1976) maps of this area, it is tentatively suggested that younger-over-older allochthons (possibly blocks VI and IX) recognized near Sugarloaf Mountain may have extended west to this area where they are truncated by the intruded normal fault zone. This fault may have been a bounding structure for the extensional terrane in the Sugarloaf area. Southwest of Sugarloaf Mountain Dibblee (1964a) has mapped as depositional a N dipping contact along which quartzites (of sub-block VIb ?) overlie Precambrian gneisses. McJunkin (1976) apparently did not recognize basal conglomerate here, although he also considered this as a depositional contact. Alternatively, this contact may also be a low-angle normal fault, at the base of block VI. If these speculations are even partially correct, the magnitude of extension in the area west of Sugarloaf Mountain may be as great or greater than in the Sugarloaf map

area and all totalled perhaps 100% extension occurred between the Doble Thrust and the Precambrian gneisses at Snow Summit. Conceivably, all of this extensional tectonism may be related to plutonism as was suggested for the Sugarloaf area.

Northward, across Bear Valley, the inferred younger-over-older allochthon of Bonanza King marbles recognized southeast of Delamar Mountain may extend eastward the length of Bertha Ridge to the Van Dusen Canyon area (Plate I). There, granitic rocks of Cretaceous(?) age intrude a SW dipping fault zone (dip angle is unknown) separating complexly folded marbles to the southwest (tentatively assigned to the Bonanza King Formation) from undifferentiated quartzites assigned to the Big Bear Group. Like the largely intruded fault zone bounding the Bertha Ridge marble terrane further east, this is inferred to be an intruded moderate- or low-angle normal fault.

The underlying quartzites on Gold Mountain may be detached as well. Guillou (1953) mapped the lower contact of these quartzites on the north side of Gold Mountain as a low-angle fault, the "Saragossa Thrust", juxtaposing quartzite over Precambrian gneisses. Tyler (1975) reassigned the "gneisses" (calc-silicate rocks according to Tyler) exposed beneath this fault to the Carrara Formation, and suggested the low-angle fault beneath the quartzites on Gold Mountain was the continuation of the Doble Thrust. He inferred the presence of a depositional contact (concealed by alluvium) between the upper plate quartzites and isolated exposures of Precambrian gneisses north of Baldwin Lake (Plate I). In Tyler's interpretation, the Gold Hill quartzites might lie within an F_2 synform west of the Arrastre Creek Antiform, and the Doble Thrust would cut across these F_2 folds from southeast to northwest along the fault's trace. B.C. Burchfiel (personal comm., 1980) has suggested the Gold Mountain quartzite section may correlate with the Sugarloaf Quartzite, rather than the lowermost Wildhorse Quartzite. A possible interpretation is that the exposed fault at the base of these quartzites is a low-angle normal fault. Similar structures are recognized cutting rocks of the lower Big Bear Group on Gold Hill, south of

Baldwin Lake. These structures may continue northwestward to the Gold Mountain area. It is suggested that northwest of Baldwin Lake, the Doble Thrust may be overlapped by a post-D_1, younger-over-older allochthon. Its emplacement predates final emplacement of Cretaceous batholithic rocks.

D_4

Mesozoic magmatism in the Big Bear area culminated with emplacement of the Late Cretaceous batholithic rocks, above which the older Mesozoic and pre-Mesozoic rocks are preserved as roof pendants. Late Cretaceous plutonic rocks are present throughout the Big Bear area. Although granite and quartz monzonite predominate, small diorite bodies are locally present and represent early plutons within the batholith. The hornblende biotite quartz diorite unit recognized at Delamar Mountain is probably one of these, as is the Cienga Seca Diorite south of the Sugarloaf area. The 79 m.y. K/Ar hornblende age for Cienga Seca Diorite (from Armstrong and Suppe, 1973) probably represents a cooling or uplift age. Although contact metamorphism associated with Cretaceous plutonism is only locally developed, areal reheating and disturbance of K/Ar isotopic systems occurred. The nearly complete resetting of K/Ar systems in biotites of older plutons as well as the Precambrian gneisses in the Big Bear area (F. Miller, personal comm., 1979; this study) indicates the country rocks were buried beneath several km of cover (presumably intra-arc deposits) at the time of batholith emplacement. The narrow age range of K/Ar biotite ages, and the small discordancy between the hornblende and biotite ages of the Cienga Seca Diorite reported by Armstrong and Suppe (1973) suggests uniform, rapid uplift and/or cooling (discussed below).

Cretaceous granitic rocks locally intruded along pre-existing faults. Granitic rocks were emplaced along the inferred Onyx Summit fault zone, probably a D_3 structure, and may have caused further spreading of the country rocks there. It is tempting to speculate that extensional spreading of roof rocks occurred during Cretaceous magmatism as well as during the Late Jurassic event. C. Miller (1977) has suggested that presently isolated exposures of

the Fawnskin Monzonite north and west of the map area were spread apart by later (Cretaceous) plutonism. Another possible example might be the Bertha Diorite and Sugarloaf Intrusive Complex. Could these be remnants of a shallow-level, Late Jurassic batholith that was rafted apart during Cretaceous plutonism? Could the Bonanza King marbles on Bertha Ridge and those of block IX north of Sugarloaf Mountain have originally been part of a single younger-over-older allochthon atop the Late Jurassic batholith? Any significant amount of Late Cretaceous synplutonic extension across Bear Valley would almost certainly require accommodation in the Baldwin Lake-Gold Hill-Deadman's Ridge area. The ages of several low-angle and high-angle faults here are poorly constrained at present (such as the Woodlands Fault, and faults on the west end of Gold Hill). These could conceivably include D_4 structures.

Regional Setting of Mesozoic Deformation

Inception of Arc Tectonism

Upper Precambrian Paleozoic rocks in the Big Bear-Victorville region record deposition in shallow marine, continental shelf or platform environments along the ancient Cordilleran continental margin (Stewart and Poole, 1975; Tyler, 1975; E. Miller, 1977; Cameron, 1980). From Permo-Triassic to Late Cretaceous time, these areas lay within the Mesozoic batholith terrane of the southern Cordillera. Hamilton (1969) was the first to suggest that Mesozoic California was the site of a long-lived Andean-type arc, which developed in response to plate interactions along the western margin of North America. The batholith appears to crosscut earlier Palezoic paleogeographic and tectonic trends in California (Hamilton and Myers, 1966). More recently, Davis and others (1978) and Burchfiel and Davis (1981) have suggested this truncation of the older margin occurred by complex left-lateral transform faulting during Permo-Triassic time. Recent data indicates the initiation of arc tectonism closely followed or perhaps overlapped somewhat with this strike-slip faulting.

Burchfiel and others (1980) have noted that apparent continental margin truncation and the inception of arc magmatism in southern California overlaps in time with Sonoman orogenic events in northwestern Nevada. Speed (1979) suggested that the Permo-Triassic Sonoman orogeny records the collision between North America and an east-facing(?) island arc terrane (exposed in northwestern Nevada, northern Sierra Nevada, and eastern Klamath Mountains (Fig. 1)). This collision may have been diachronous, occurring first in southern California and later in Nevada. Thus, while final closure of the intervening later Paleozoic oceanic terrane continued to the north, post-collisional strike-slip faulting and a flip in arc polarity may have occurred in southern California (Fig. 73). A possible analog is the Neogene arc-continent collision between the northern New Guinea-Banda arc complex and the northern Australian continental shelf. Collision there occurred first in New Guinea, followed by a reversal in arc polarity and complex strike-slip faulting while subduction of the Australian plate seafloor beneath the Banda arc continued further to the west (Hamilton, 1979).

In the western Mojave Desert region the Mesozoic arc developed on top of two pre-Mesozoic terranes: Precambrian basement and Upper Precambrian-Paleozoic cover rocks of the Cordilleran miogeocline and craton to the east and south (including the Big Bear-Victorville area); and out-of-place Paleozoic eugeoclinal rocks of the western Mojave terrane to the northwest (Miller and others, 1979). Although basement rocks for the latter terrane are not known, Sr isotopic characteristics of Mesozoic plutonic rocks here suggest this area was underlain by Precambrian continental crust during the Mesozoic (Kistler and Peterman, 1978). Davis and others (1978) and Burchfiel and Davis (1981) have suggested that the western Mojave terrane represents a tectonic sliver, displaced southward during Permo-Triassic strike-slip faulting (Fig. 73).

Permo-Triassic Events

In the western Mojave Desert region, arc-related teconism probably began as early as Permo-Triassic time; rocks

Figure 73: Interpretive tectonic model of Permo-Triassic (Sonoman) events in the southern Cordillera.

Sonomia arc of Speed (1979) is presently exposed in northwestern Nevada, northern Sierra Nevada and eastern Klamath Mountains.

Locus of Andean arc activity is denoted by v's.
SB: San Bernardino Mountains

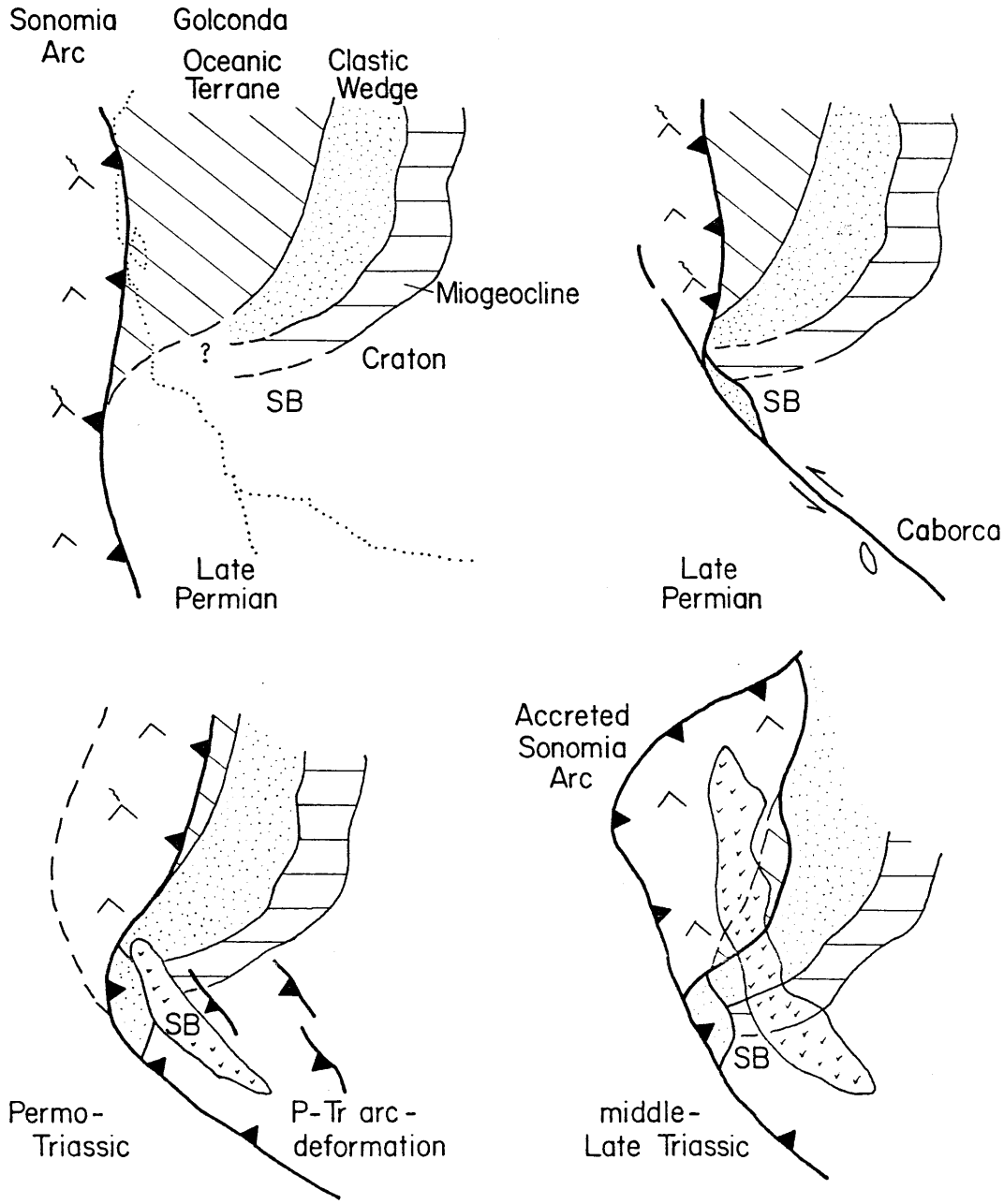

in the Big Bear area record this regional event. Evidence of Permo-Triassic deformation is presently known from both the miogeoclinal terrane at Victorville and the western Mojave terrane in the El Paso Mountains.

In the El Paso Mountains, Lower Paleozoic eugeoclinal rocks (perhaps equivalent to and offset from rocks of the Roberts Mountain allochthon in central Nevada) and Upper Paleozoic rocks (perhaps equivalent to the Antler belt overlap or foredeep sequence) are present and constitute the Garlock Series (Poole and Sandberg, 1977; Poole and Christiansen, 1980). These eugeoclinal Paleozoic rocks were complexly deformed by W vergent folding synchronous with greenschist facies metamorphism (Christiansen, 1961). Christiansen suggested that plutonism occurred synchronously with the later stages of folding of the Garlock Series rocks, as evidenced by a progressive increase in metamorphic grade approaching a protoclastically deformed pluton. Rocks adjacent to the pluton contain metamorphic assemblages which include andalusite, cordierite and garnet, and are indicative of low P, intermediate T conditions. The apparently syntectonic pluton has yielded a K/Ar hornblende age of 248 m.y. (J. Morton, personal comm., 1980) and is intruded by an undeformed pluton yielding concordant K/Ar ages of 239$\pm$7 m.y. from hornblende and 230$\pm$7 m.y. from biotite (Cox and Morton, 1980). Rocks as young as Permian are involved in the synmetamorphic folding event (Christiansen, 1961).

In the Victorville area, Upper Precambrian-Paleozoic rocks of the miogeocline-craton terrane are exposed in several roof pendants (E. Miller, 1977). These rocks record polyphase folding, thrusting and synkinematic metamorphism at upper greenschist facies. Locally, the Black Mountain Monzonite (minimum age 233$\pm$13.7 m.y., E. Miller and Sutter, 1978) intrudes these deformed rocks. Undated clastic and carbonate rocks of the Fairview Valley Formation unconformably overlie this pluton and the deformed pre-Mesozoic rocks. The Fairview Valley Formation contains clasts of the monzonite, of locally derived metamorphic rocks, and of gneissic

rocks and Early Permian carbonates not presently exposed in the Victorville area. E. Miller (1978) has suggested the postkinematic Black Mountain Monzonite is related in time and space to folding and metamorphism of the pre-Mesozoic rocks. She has related this complex deformational event to the initiation of Mesozoic arc activity in this region. This deformed belt was deeply eroded prior to deposition of the Fairview Valley Formation.

I suggest that the belt of Permo-Triassic deformation and plutonism recognized in the El Paso Mountains and at Victorville continues southeastward into the Big Bear area. The complex sequence of events included here in episodes D_1 and D_2 probably correlates with the events discussed above. The Fawnskin Monzonite has been described by C. Miller (1977) as part of a belt of early Mesozoic arc-related plutons. The minimum age for this pluton, 214 m.y., and its model age, 229 m.y., are certainly compatible with C. Miller's suggestion ($^{40}Ar/^{39}Ar$ age data are discussed above). As in the Victorville area, this pluton crosscuts structures formed during an episode of progressive deformation involving metamorphism, folding and thrusting. This deformation is of areal extent (D_1). Low P, intermediate T metamorphism, folding, faulting and plutonism (D_2) are believed to have been broadly contemporaneous in the Big Bear area, as was the case in the El Paso Mountains and perhaps at Victorville (diagnostic low P, intermediate T metamorphic assemblages have not been reported at Victorville, however). The P, T constraints on D_1 metamorphism at Big Bear, discussed above, are certainly suggestive of an intra-arc setting. Widespread plutonism during the Permo-Triassic may have been responsible for regional heating of the upper crust and widespread low P, intermediate T metamorphism. Conclusive evidence of an earlier episode of deformation, perhaps related to Latest Paleozoic arc-continent collision, is not present at Big Bear nor probably at Victorville.

In the study areas, the youngest rocks involved in inferred Permo-Triassic deformation are of suspected Late Cambrian age. However, marbles underlying the Cushenbury Thrust on the north slope of the range record a

similar structural history (Cameron, unpublished data). This sequence has yielded Carboniferous fossils (Hollenbaugh, 1968) and probably includes rocks of Permian age as well (equivalent to the Bird Spring Formation). Folding and metamorphism of these rocks and the emplacement of the Cushenbury Thrust are inferred to have occurred during D_1. Near Victorville, the youngest rocks involved in the Permo-Triassic deformation are of inferred Mississippian age (E. Miller, 1977). However, clasts of Wolfcampian limestones found in the Fairview Valley Formation may have been derived from the Permo-Triassic deformed belt. These, along with clasts of Precambrian(?) gneisses, may have had a source area near the San Bernardino Mountains.

Burchfiel and others (1980) have suggested that this Permo-Triassic deformed belt may extend well east of the El Paso Mountains-Victorville-Big Bear area. They have suggested that widespread occurrences of shallow marine rocks, including locally-derived conglomerate, limey clastic rocks, carbonates and quartz sandstones, may represent remnants of an early Mesozoic (Early Triassic?) post-orogenic overlap assemblage. These sections, including the Fairview Valley Formation, locally overlie highly deformed Paleozoic rocks with angular unconformity. Some sections have yielded Early Triassic fossils, thus providing an upper limit on the age of deformation even in areas where Permo-Triassic plutons have not been recognized. This deformed belt extends at least to the vicinity of Baker, California, and could conceivably extend to the Clark Mountains-New York Mountains area, where folds and thrusts involving Precambrian basement are cut by plutons yielding K/Ar minimum ages as old as 200 m.y. (Burchfiel and Davis, 1981; Burchfiel and Davis, 1977). Rocks included in the overlap assemblage are found within both the miogeoclinal terrane and the western Mojave terrane. The distribution of the overlap assemblage provides additional evidence that the juxtaposition of these pre-Mesozoic terranes occurred by earliest Mesozoic time.

Although Permo-Triassic deformation in the western Mojave Desert is temporally and spatially associated with arc plutonism and low P, intermediate T metamorphism, the kinematic relationship between this extensive deformed belt and arc plutonism and metamorphism is not clear. Burchfiel and Davis (1972; 1975; 1981) have suggested that most Mesozoic folding and thrusting recognized further east in the Mojave Desert-Death Valley-southern Nevada region occurred within a back-arc thrust belt along the eastern margin of the active arc. They suggested that crustal shortening occurred here in response to intraplate compressional stresses transmitted across the arc (see Stauder, 1975; Burchfiel and Davis, 1976). Burchfiel and Davis (1981) note that major periods of deformation in the back-arc thrust belt coincided with times of most conspicuous arc magmatism and metamorphism. In their view, the locus of intraplate shortening at any time is restricted to the eastern margin of the coeval volcanic-plutonic terrane. Along the margin of the batholith, steep thermal gradients may cause a sharp mechanical contrast between more ductile rocks in the vicinity of the arc and more rigid lithosphere toward the craton. Intraplate shortening is accommodated here by underthrusting of the rigid, cratonal lithosphere beneath the eastern margin of the arc. Hamilton (1978) has also related back-arc fold and thrust belts of the Cordillera to arc tectonism; however, he suggests that foreland belt deformation results from the wedging effect of batholiths which rise and spread gravitationally in the upper crust. No crustal shortening is required in Hamilton's model. In addition, polyphase deformation can occur within batholithic terranes, according to Hamilton (1978), as wall rocks caught between rising or spreading plutons are squeezed.

The areas of known or suspected Permo-Triassic deformation in the western Mojave Desert locally display characteristics more typical of the back-arc fold and thrust belt in the eastern Mojave Desert described by Burchfiel and Davis (1981). The sequence of polyphase folding events recognized by E. Miller (1977) at Quartzite Mountain is strikingly similar to that in the Big Bear area. F_1 isoclinal folds transpose bedding but stratigraphic sequence is preserved; F_2 folds trend NW and are NE

vergent; F_1 and F_2 folds may have been coaxial. As is generally true at Big Bear, the early folds apparently trend parallel to the trend of the batholith belt, and are vergent toward the craton (antithetic to the inferred dip of the subduction zone and consistent with a back-arc thrust belt model). However, the suspected vergence of F_1 folds at Delamar Mountain is to the SW, away from the craton. In the El Paso Mountains also, fold vergence is away from the craton, to the west, however the axial orientation of folds (N-S) parallels the local orogenic trend. These folds are vergent towards the syntectonic Permo-Triassic pluton. Regional and local variations in fold orientations may reflect later tectonic rotations. Alternatively, variable fold vergence and complex polyphase deformation might be expected if, in part, this terrane represents wall rocks caught between Permo-Triassic plutons (see Hamilton, 1978, discussion of wall rock deformation in the Sierra Nevada; and Hamilton and Myers, 1967). It may be that Permo-Triassic deformation recorded in the western Mojave Desert occurred along the margins of the coeval batholith terrane (back-arc setting) and in an intra-batholith setting.

Later-stage cross folds, of EW or NE-SW trend at Big Bear (D_{1b} structures) are distinctive in their discordance to the general NW or N orogenic trend. A possible explanation for these folds is to relate them to Permo-Triassic wrench tectonics (Wilcox and others, 1973) perhaps associated with recurrent strike-slip faulting parallel to the margin. If this is the case, the inferred left-lateral strike-slip faulting which caused apparent continental margin truncation may have continued episodically after arc magmatism had begun. This may also indicate that Permo-Triassic plate convergence was oblique to the continental margin (Fitch, 1972).

It is uncertain if the Permo-Triassic deformed belt extends southeast of the Big Bear area. The Mt. Lowe "granodiorite" (actually a monzodiorite) is extensive in the San Gabriel Mountains and has yielded

a U/Pb zircon age of 220 m.y. (Silver, 1971). Correlative plutons are exposed in desert ranges east of the San Andreas Fault and southeast of the San Bernardino Mountains. These plutons intrude Precambrian crystalline rocks of the San Gabriel terrane (Silver, 1971), which are now offset across the San Andreas Fault zone. C. Miller (1978) suggested the Mt. Lowe suite may correlate with the alkalic Permo-Triassic plutons in the Victorville-Big Bear area. Powell and Silver (1979) have reported that rocks of the San Gabriel terrane structurally overlie miogeoclinal metasedimentary rocks exposed in the Pinto Mountains and nearby ranges. Deformation associated with the juxtaposition of these terranes involved complex thrusting, folding and metamorphism of variable grade (R. Powell, personal comm., 1980). This deformed belt is cut by areally extensive rocks of the Late Jurassic (165 m.y. U/Pb zircon age) batholith belt to the east. What is uncertain is the relationship between this deformed belt and the Mt. Lowe plutonic suite. Was Mt. Lowe magmatism contemporaneous with orogenic events described by Powell and Silver (1979)? In Chapter II it was suggested that the miogeoclinal rocks in the Pinto Mountains may be correlative with the Big Bear Group and are paleogeographically tied to the Cordilleran miogeocline. It is possible that the deformed belt described by Powell and Silver (1979) and the Mt. Lowe plutonic suite correlate with the Permo-Triassic intra-arc deformed belt in the Mojave Desert region. Alternatively, Powell (personal comm., 1980) has suggested the San Gabriel terrane and underlying Pinto Mountains terrane may be far-travelled with respect to miogeoclinal rocks in the Mojave Desert. These disparate terranes may be juxtaposed along a strike-slip fault zone, whose trace was intruded by the Jurassic batholith and further obscured by subsequent Mesozoic-Cenozoic tectonics. In this case, the Pre-Late Jurassic deformed belt of Powell and Silver (1979) and the Permo-Triassic deformed belt in the Mojave Desert need not be related.

Triassic-Jurassic Events

Deposition of the Fairview Valley Formation and related strata attest to deep erosion in the western-central

Mojave after Permo-Triassic deformation and magmatism. Overlying the Fairview Valley Formation near Victorville is the Sidewinder Group, a thick and stratigraphically complex intermediate volcanic sequence. The undated Sidewinder Group probably records at least two episodes of magmatism, separated by folding and faulting (E. Miller, 1977). Neither the Fairview Valley Formation nor the Sidewinder Volcanics are recognized in the Big Bear area, where late Cenozoic erosion exposed a deeper structural level than at Victorville. It is suggested the Late Jurassic magmatism and tectonism (phase D_3) in the Big Bear area may have been in part coeval with Sidewinder volcanism. The shallow-level diorite plutons and intermediate composition dikes in this area may represent a subvolcanic edifice for volcanic rocks (now eroded) correlative with the Sidewinder Group. Richmond (1960) was the first to suggest such a connection, speculating that the dike complex north of Delamar Mountain might represent feeders for the Sidewinder Group. I suggest that the Sidewinder Group might be in part Late Jurassic in age. Late Jurassic plutons have not been previously recognized in the western Mojave Desert region. Late Jurassic plutons are recognized further east, in the central Mojave Desert. Although few dates are available in the central Mojave, that region lies astride the trend of a major Jurassic batholith belt extending from Sonora (Silver and Anderson, 1974) into the western Death Valley-Sierra Nevada region (Dunne and others, 1978). The results of this study, and recent recognition of Late Jurassic plutons in the Goldstone area of the western Mojave terrane (E. Miller and J. Sutter, personal comm., 1980) indicate an even wider extent for the Late Jurassic batholith complex. In the Big Bear area, extensional faulting is associated with phase D_3 magmatism. It may be that faulting recognized by E. Miller (1977) which predates and interrupts deposition of portions of the Sidewinder Group is related to similar extensional tectonism at depth. Burchfiel and Davis (1981) noted that Late Jurassic magmatism in the Mojave Desert-Death Valley region apparently coincided with a major episode of back-arc thrusting east of the active arc (in the Death Valley-southern Nevada-eastern Mojave Desert region).

Cretaceous Events

Late Cretaceous plutonism recognized in the Big Bear area is widespread in the western Mojave Desert region. The Cretaceous batholith is comprised largely of granite and quartz monzonite (Armstrong and Suppe, 1973; E. Miller, 1977; F. Miller, personal comm., 1979), similar to Late Cretaceous plutonic rocks in the San Bernardino Mountains. Where dated, these rocks yield Late Cretaceous (70-80 m.y.) K/Ar biotite and hornblende ages which are almost certainly cooling or uplift ages (and are somewhat younger than the age of emplacement). Regional reheating of country rocks during this time caused variable Ar loss; biotite ages from pre-Cretaceous rocks were reset and hornblende isotopic systems were disturbed in the San Bernardino Mountains-Victorville region (Armstrong and Suppe, 1973; F. Miller, personal comm., 1979; this study). The effects of Late Cretaceous reheating decrease to the north (El Paso Mountains, Cox and Morton, 1980) and to the east (Armstrong and Suppe, 1973) where known and suspected pre-Cretaceous rocks yield older K/Ar biotite ages. Cretaceous plutons are present in the eastern Mojave Desert, but may not be as areally extensive as in the western Mojave Desert (Burchfiel and Davis, 1981). Mid to late Cretaceous plutonism in the eastern Mojave Desert appears to have been approximately concurrent with back-arc thrusting there. Available geologic and geochronologic data suggest the San Bernardino Mountains-Victorville region lay in the axial portion of the Late Cretaceous batholith, which continues northward into the southern Sierra Nevada. Granitic rocks in the Salinian block may represent the offset western portion of the Cretaceous batholith exposed in the western Mojave Desert (Armstrong and Suppe, 1973).

A contributing factor to the severe Cretaceous reheating recorded in pre-Cretaceous rocks in this part of the Mojave Desert was their relative depth of burial during Cretaceous magmatism. The younger granitic rocks in the study areas do not show textures indicative of shallow-level emplacement, in marked contrast to the Late Jurassic plutons. As speculated above, the volcanic equivalents of the Late

Jurassic intrusives may have covered the Big Bear area. These, and their possible correlatives in the Sidewinder Group, may have constituted a thick volcanic pile now largely stripped away. Missing too are any volcanic rocks associated with the Cretaceous batholith. Northward, evidence of a coeval volcanic edifice above the Cretaceous batholith of the Sierra Nevada is found in roof pendants (Fiske and Tobisch, 1978) and in the Cretaceous sedimentary rocks of the Great Valley Sequence which record progressive unroofing of the batholith (Dickinson, 1970). It is suggested that Mesozoic sedimentary and volcanic rocks, including perhaps units equivalent to the Fairview Valley Formation, the Sidewinder Group, and Cretaceous volcanics, probably overlay the Big Bear area during emplacement of the Cretaceous batholith. Pre-Cretaceous rocks presently exposed in the Big Bear area were probably buried to several km depth during the Late Cretaceous plutonism.

The absence of Mesozoic sedimentary and volcanic rocks in the Big Bear region indicates this area was deeply eroded after emplacement of the Cretaceous batholith. The presence of early-middle Mesozoic metasedimentary and volcanic rocks in the Victorville area (E. Miller, 1977) and in the Rodman Mountains (E. Miller and Carr, 1978) and their absence in the Big Bear area may in part reflect differential uplift of the San Bernardino Mountains during the latest Cenozoic (Dibblee, 1975). However, an earlier period of regional uplift affecting this terrane during the Late Cretaceous may be recorded by the K/Ar biotite ages. Both Cretaceous plutons and older country rocks yield similar K/Ar biotite ages indicating this terrane was heated above the closure temperature for Ar diffusion in biotite. There is no field or textural evidence for a regional metamorphic event affecting these rocks <u>after</u> emplacement of the Cretaceous plutons. Thus the concordance or near-concordance of K/Ar biotite ages from this plutonic terrane reflects either 1) rapid, regional uplift or 2) regional cooling (rapid decay of the geothermal gradient and decrease in areal heat flow ; see Armstrong and Suppe, 1973 and Krummenacher and others, 1975, for discussions of concordance

of K/Ar ages). Decrease in regional conductive heat flow would result if arc magmatic processes were interrupted.

Both rapid uplift and regional cooling may have occurred in the western Mojave Desert region in response to shallow-dipping subduction during the Late Cretaceous. During this period of shallow-dipping subduction, upper crustal rocks of the arc terrane may have overridden rocks of the Franciscan Complex accretionary wedge along the Vincent Thrust and related structures. Burchfiel and Davis (1981) have suggested such an event, and following Yeats (1968), argue that the Pelona-Orocopia-Rand schists which are exposed in thrust windows beneath Mesozoic plutonic and older crystalline rocks are correlative with Jurassic-Cretaceous Franciscan Complex rocks exposed further west.

The Pelona and Orocopia schists are exposed in thrust windows that lay southeast of the San Bernardino Mountains prior to San Andreas faulting; the Rand-Garlock schists and possibly correlative Schist de Sierra Salinas lay to the northwest (Fig. 74). Correlative rocks presumably extended beneath the San Bernardino Mountains-Victorville region as well. Shallow-dip underthrusting of Pelona-type rocks may have occurred during more than one episode. K/Ar whole rock and Rb/Sr mineral ages from metamorphic rocks formed during underthrusting of the Pelona and Orocopia schists range from 50-60 m.y. (data cited by Haxel and Dillon, 1978), but these are minimum ages. Underthrusting of the lithologically similar Rand Schist and Schist de Sierra Salinas may have occurred somewhat earlier, as these rocks are cut by 80 m.y. plutons (data cited by Burchfiel and Davis, 1981). Late Cretaceous uplift in the San Bernardino Mountains might be related to either episode.

Shallow-dipping subduction interrupted Cretaceous arc magmatism in the upper plate. No post-Late Cretaceous batholiths are exposed in the western Mojave region. The locus of latest Cretaceous-early Tertiary magmatism shifted far to the east (into Arizona, New Mexico and Colorado); this perhaps was a result of a change from steep to shallow-dipping subduction (Burchfiel and Davis, 1975). The end of arc activity in the

Figure 74: Distribution of Pelona Schist and equivalent rocks plotted on a pre-Miocene palinspastic base (after Burchfiel and Davis, 1981; same base as in Figure 29).

Plutonic rocks of the Sierra Nevada, Salinian block and Peninsular Ranges: v's
Paleozoic rocks of the western Mojave terrane displaced during Permo-Triassic truncation: black
Pelona-Orocopia-Rand Schist and correlatives: vertical lines
Schist of Sierra de Salinas (SS): cross-hatched
Terranes accreted during Triassic-Jurassic: shaded
Great Valley sequence and correlatives: dots
Franciscan rocks: dashes
WLSB: western limit of Sierran basement
S87: $^{87}Sr/^{86}Sr = 0.706$
PTTB: Permo-Triassic truncation boundary
ELPTS: Eastern limit of Permo-Triassic sliver (western Mojave terrane)
C: Chocolate Mountains
M: McCoy Mountains
O: Orocopia Mountains
P: Palen Mountains
R: Rand Mountains
SB: San Bernardino Mountains

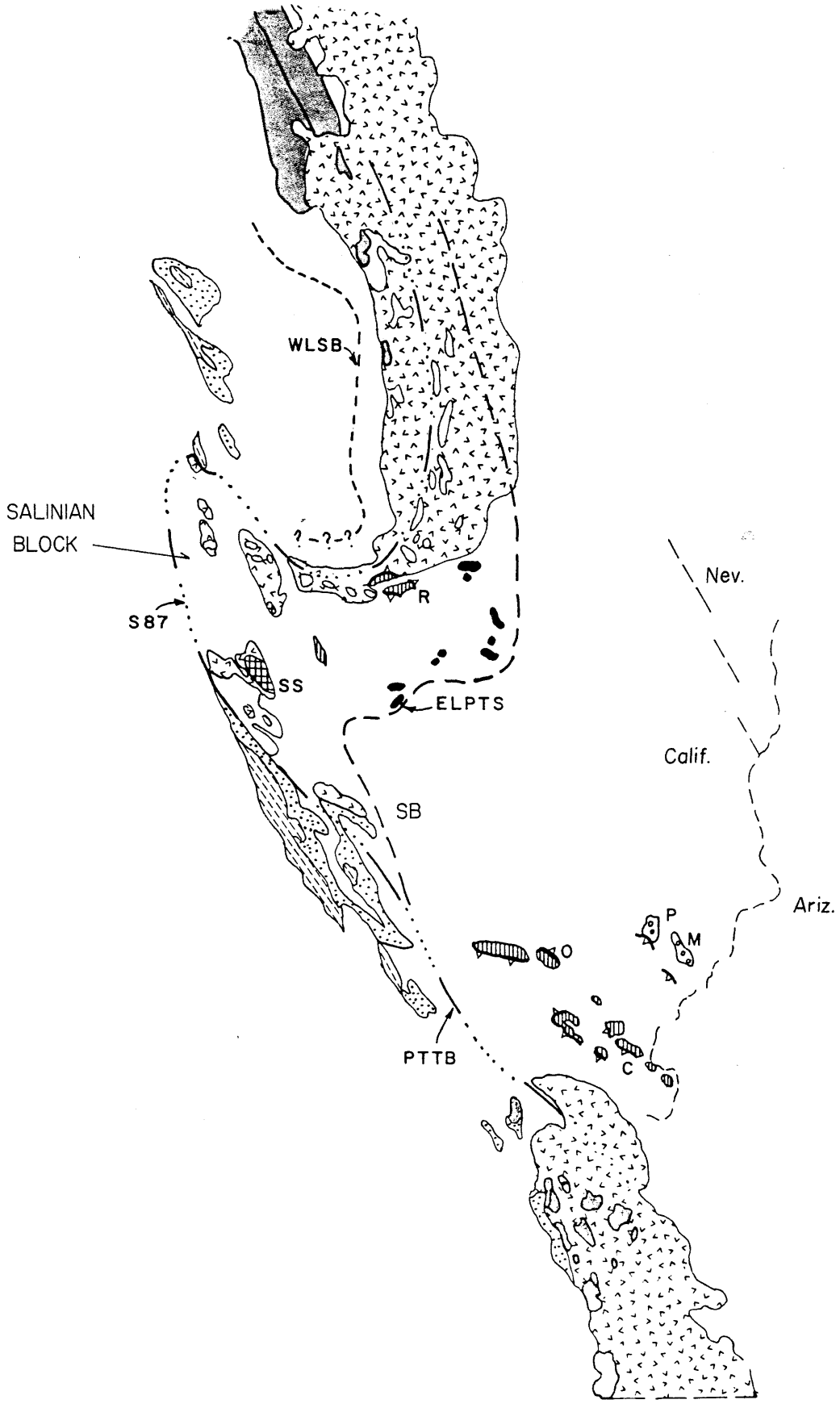
WLSB
SALINIAN
BLOCK
? - ? - ?
S87
R
SS
ELPTS
SB
PTTB
Nev.
Calif.
Ariz.
P
M
O
C

western Mojave Desert may have also been associated with rapid cooling as heat flow diminished. Thus K/Ar biotite ages from the western Mojave Desert may reflect both rapid uplift and cooling during the Late Cretaceous, as changes in the geometry of subduction brought the long history of arc activity here to an end.

Implications for Intra-arc Tectonism

Structural Style and Wet vs. Dry Basement

The San Bernardino Mountains occupy a rather unique geologic position within the Mesozoic batholithic terrane of southern California. The three major episodes of Mesozoic plutonism presently recognized in the Mojave region are superposed here, so in a sense this area records the transition from a youthful to a mature intra-arc setting. A striking feature of the tectonic history of this terrane is the lack of penetrative deformation and metamorphism associated with the Jurassic and Cretaceous plutonic episodes, in contrast to regional metamorphism and complex polyphase deformation associated with Permo-Triassic arc activity. To some extent this variation in structural style reflects contrasting structural levels and tectonic settings between the Permo-Triassic and Jurassic-Cretaceous deformational events. An additional factor, however, may have been the evolving mechanical characteristics of the country rocks through time, a variation that may be a function of their earlier metamorphic history.

The pre-Mesozoic structural basement upon which the Permo-Triassic arc developed consisted of a thick section of previously unmetamorphosed shallow marine sedimentary rocks, and underlying amphibolite facies(?) Precambrian gneisses. Thorough recrystallization of the cover rocks occurred during D_{1a} metamorphism and folding; metamorphic assemblages suggest peak temperatures of about 500°C at pressures of about 2-3 kb. During this same event the underlying gneisses were essentially non-reactive and display little textural evidence of the regional metamorphic

event that affected the terrane. It was suggested above that recrystallization and penetrative deformation in the Precambrian gneisses was restricted by the availability of fluids to facilitate recrystallization (retrograde metamorphism?) and ductile deformation (small amounts of water can significantly reduce the strength of silicate minerals in the ductile regime, as Griggs and Blacic, 1965, first demonstrated; see Tullis, 1979, for a summary of recent work in this field). While the hot, fluid-rich miogeoclinal cover rocks were able to deform ductilely during the early phases of the D_1 event, the underlying, hot, dry gneisses generally deformed more brittlely, if at all. During the later stages of D_1 folding, and during D_2 events, structural behavior of the miogeoclinal cover rocks evolved from a ductile to a more brittle style, perhaps in response to earlier metamorphism. D_{1b} folds exhibit only rare examples of associated penetrative fabrics. The emplacement of the Fawnskin Monzonite was apparently associated with brittle faulting of the roof rocks. Contact metamorphic effects associated with the monzonite are minimal, and pre-existing mineral assemblages generally remained stable except adjacent to the pluton or along fractures where fluids were available. $P_{lithostatic}$ and T conditions may have remained relatively stable during the D_1 and D_2 events; however, a drop in P_{fluid} relative to $P_{lithostatic}$ following the early D_{1a} metamorphism may have caused a dramatic change in rock mechanical properties (see Yardley, in press).

The metamorphic terrane formed during Permo-Triassic events constituted the structural basement into which the younger Jurassic and Cretaceous batholiths were emplaced. There was no thick, wet section of sedimentary rocks at structural levels now exposed at Big Bear during Jurassic and Cretaceous plutonism. The absence of such wet rocks, capable of providing large volumes of water by prograde metamorphic devolatilization, may have controlled the extent of contact metamorphism and of ductile deformation associated with Jurassic and Cretaceous plutonism. Late Jurassic extension associated with magmatism involved

rigid fault block displacements. Coeval penetrative deformation within the fault blocks is not present, although metamorphic recrystallization may have occurred syntectonically along narrow fault zones (where access to fluids was presumably greater). Contact metamorphic effects were limited to the immediate margins of plutons or along fractures where fluids could migrate. Unfortunately, the K/Ar isotopic record of Late Jurassic thermal events was thoroughly overprinted by Cretaceous events. However, local evidence of metamorphism associated with Late Jurassic events suggests that this terrane was heated, but remained relatively non-reactive except where brittle faulting provided access to fluid reservoirs.

Major reheating of rocks exposed in the Big Bear area occurred during emplacement of the Late Cretaceous batholith, a thermal event documented by resetting of K/Ar biotite ages from pre-Cretaceous rocks. The roof of the Cretaceous batholith presently exposed at Big Bear is interpreted to have been more deeply buried than the roof of the Late Jurassic batholith. Nevertheless, although elevated temperatures are indicated during the Late Cretaceous, evidence of metamorphism of the pre-Mesozoic rocks is again minimal. The earlier Mesozoic plutons display the most conspicuous evidence of intracrystalline deformation and metamorphism associated with Cretaceous plutonism. Here again, penetrative deformation and metamorphic recrystallization or hydrothermal alteration was best developed adjacent to pluton margins, and especially along fractures and faults which provided avenues for fluid circulation. Extensional tectonism possibly associated with Late Cretaceous plutonism (discussed above) was apparently similar in style to normal faulting related to the emplacement of the earlier plutons.

In a general way, the structural response of all pre-Mesozoic metamorphic rocks and earlier Mesozoic plutons during the Jurassic and Cretaceous plutonic events (D_3 and D_4) was analogous to the brittle, non-reactive character of the Precambrian gneisses during the early phases of Permo-Triassic deformation (D_1 events). After Permo-Triassic

metamorphism drove off the *in situ* volatile components from the Upper Precambrian-Palezoic miogeoclinal sequence, the rocks deformed in a predominantly brittle mode during later Mesozoic events. During Permo-Triassic orogenesis, the contrast in development of metamorphic and tectonite fabrics was rather striking between the underlying, dry Precambrian gneisses and overlying, wet miogeoclinal sequence. During later episodes of plutonism, both the Precambrian gneisses and the overlying miogeoclinal sequence were dry and deformed similarly. For example, the major Late Jurassic normal faults in the Sugarloaf area (D_3 structures) cut across the Precambrian gneiss-Wildhorse Quartzite basal contact and in general ignore stratigraphic control; the Precambrian gneiss-Wildhorse Quartzite contact was not a major décollement zone. Older plutons were apparently involved in later Mesozoic extensional tectonism related to the emplacement of the younger batholiths along with pre-Mesozoic metamorphic rocks. Evidence from the Big Bear area suggests that elevated temperature and pressure alone are not sufficient to result in widespread metamorphism and ductile deformation of a batholith's roof terrane. During Jurassic and Cretaceous plutonism at Big Bear, rock type and previous deformational history of the country rocks played a critical role in controlling structural style. The previously metamorphosed sedimentary rocks and relatively dry crystalline rocks whose mineral assemblages were stable at P, T conditions imposed by later heating events did not, apparently, experience widespread retrogression or ductile deformation in the absence of a sufficiently high P_{fluid}. At Big Bear, regional low $P_{lithostatic}$, intermediate T metamorphism associated with arc plutonism did occur during the Permo-Triassic when country rocks suitable to record prograde metamorphism were present.

These observations concerning the important role of fluids in limiting the extent of metamorphism and the style of deformation associated with arc magmatism at Big Bear may have more general applicability to Andean-type orogenic belts. In a general way, it may be possible

to characterize the structural style of deformation and extent of metamorphism associated with arc orogenesis at a particular crustal level as typical of either (1) wet basement or (2) dry basement (basement here refers to "structural basement", the pre-existing rocks within which the arc develops). In case (1) (wet basement), the arc develops within a supracrust consisting of a sequence of relatively wet unmetamorphosed or low-grade rocks. Upon regional heating, this wet terrane readily undergoes prograde metamorphism and devolatilization. The availability of fluids (especially water) facilitates deformation (either contractional or extensional) by ductile processes. In case (2) (dry basement), the arc develops within a relatively dry, crystalline terrane, consisting of previously metamorphosed sedimentary rocks or pre-existing plutonic rocks. Penetrative ductile deformation within this dry terrane during arc orogenesis may be greatly inhibited by the scarcity of water to permit metamorphic reactions to proceed and the absence of interconnected pore space to allow migration of fluids. Contractional and extensional deformation occur primarily by brittle failure of hot, dry rocks. Faulting may provide access to fluids which would permit the zonal development of penetrative deformation and retrograde metamorphism. During the Permo-Triassic deformational event at Big Bear for example, the arc developed within a terrane that was wet at high structural levels and dry at deeper levels. During Jurassic-Cretaceous arc activity, the structural basement was dry.

Presently available data are suggestive that the Mesozoic history of the western and central Mojave Desert region as a whole may illustrate the importance of wet vs. dry basement in controlling the extent of regional metamorphism associated with a particular orogenic episode, and as a result, the structural style of attendant deformation. During the Permo-Triassic, the structural basement for the nascent Andean arc in the northern Mojave Desert consisted of wet sedimentary rocks at the highest crustal levels, and dry, Precambrian gneisses at lower structural levels. The wet, supracrustal rocks included the previously unmetamor-

phosed Upper Precambrian-Paleozoic rocks of the Cordilleran miogeocline and Paleozoic rocks of the western Mojave terrane. Regional heating and resultant metamorphism (locally, at least, of low P facies) of the wet supracrustal rock was presumably associated with Permo-Triassic plutonism, although plutons of this generation are only known presently in the western Mojave Desert. Nevertheless, metamorphism and polyphase ductile deformation of the wet, supracrustal rocks apparently occurred in both the western and central Mojave Desert regions, and extended eastward to the vicinity of Baker, California. It is possible that this Permo-Triassic deformed belt extends southward into portions of the eastern Transverse Ranges studied by Powell and Silver (1979), as discussed above.

The wide extent of the Permo-Triassic deformed belt and especially of associated metamorphism is striking considering the limited distribution of known Permo-Triassic plutons. There is no compelling reason to presume that regional heating associated with the Permo-Triassic arc was greater or more extensive than heating associated with later Mesozoic magmatic episodes. Instead, it may be that the wide extent of the Permo-Triassic deformed belt and in particular of associated metamorphism may be the result of its development within a wet supracrustal terrane. The unmetamorphosed sedimentary rocks at high structural levels readily underwent prograde metamorphism when heated during initial arc magmatism; fluids, particularly water, produced by metamorphic devolatilization facilitated widespread ductile deformation. To some extent, however, the Permo-Triassic metamorphic terrane may have been thin-skinned. At least locally the dry, older Precambrian crystalline rocks which underlay the wet supracrustal cover experienced only limited recrystallization and retrogression associated with the Permo-Triassic metamorphic event (this was the case at Big Bear). Shortening of these hot but dry basement rocks may have occurred by relatively rigid block thrusting, with ductile deformation localized near narrow fault zones where water was available (the Doble Thrust may be an example).

Major arc activity resumed in the western-central Mojave Desert during the Middle to Late Jurassic, when the region was the site of extensive plutonism (the record of associated arc volcanism is far less complete). The structural basement for Jurassic arc development in the northern Mojave Desert was far more complex than that of the Permo-Triassic arc. Over much of the western and central portions of the northern Mojave Desert, the Jurassic arc was superposed atop the Permo-Triassic deformed belt. Thus, the structural basement here included dry pre-Mesozoic metasedimentary rocks (which lost their volatile components during Permo-Triassic metamorphism), dry older Precambrian gneisses, early Mesozoic plutonic rocks, and wet Triassic and Jurassic sedimentary and volcanic rocks which unconformably overlay the variably eroded Permo-Triassic deformed belt. The distribution of the latter rocks is incompletely understood, but may have been quite localized (Miller and Carr, 1978; Burchfiel and others, 1980). In contrast to Permo-Triassic time, no regionally continuous sheet of wet miogeoclinal rocks was present at supracrustal levels in this portion of the northern Mojave. Instead, the wet, Mesozoic intra-arc deposits, best suited for recording metamorphism associated with plutonism, were present at the highest structural levels, were irregularly distributed, and of variable thickness. It is not surprising that evidence of extensive Jurassic-Cretaceous regional metamorphism in the western and central Mojave Desert is lacking. Jurassic metamorphism and penetrative deformation of the wet Mesozoic rocks is recognized, but it is often localized and rather feeble.

In the Victorville region for example, lower Mesozoic sedimentary and volcanic rocks (Fairview Valley Formation and lower portions of the Sidewinder Group) which unconformably overlie rocks deformed in the Permo-Triassic event are variably metamorphosed and are locally penetratively deformed (E. Miller, 1977). This deformation predates deposition of upper Sidewinder Group rocks (pre-Latest Jurassic(?), discussed above).

In contrast, evidence of post Permo-Triassic metamorphism is only sporadically recognized in structurally underlying, previously deformed miogeoclinal rocks in the Victorville-Big Bear region. For example, extension of the dry pre-Mesozoic roof rocks during Late Jurassic plutonism at Big Bear was accommodated by brittle failure, with the only evidence of associated recrystallization localized along fault zones.

In the central Mojave Desert, west of Baker, California, pre-Mesozoic rocks which record the Permo-Triassic deformational event apparently do not record a later Mesozoic regional metamorphic event. Triassic-Jurassic sedimentary and volcanic rocks known or inferred to have overlain the Permo-Triassic deformed belt are in general feebly metamorphosed, although local zones of high grade metamorphism and intense penetrative deformation of Mesozoic rocks are recognized (Burchfiel and Davis, 1981). Pre-Mesozoic and Mesozoic rocks are structurally interleaved by thrusting of Jurassic or Cretaceous(?) age at Cave Mountain (Cameron and others, 1979) and at Old Dad Mountain (Dunne, 1977). Evidence of ductile flowage is recognized along these thrusts, however penetrative deformation does not extend more than a few meters above or below the fault zones (Dunne, 1977; Cameron and others, unpublished data). Penetrative deformation may have been limited to the vicinity of the fault zones where fluids were available. In general, metamorphism and penetrative deformation within the Jurassic plutonic terrane in the central and western Mojave Desert appears to have been locally or zonally developed, and is often absent in the dry pre-Mesozoic rocks which were previously deformed during the Permo-Triassic.

Late Jurassic regional metamorphism of pre-Mesozoic rocks is recognized in areas adjacent to the western and central Mojave Desert region which apparently did not experience the Permo-Triassic metamorphic event. These terranes lie east of the Permo-Triassic deformed belt, and extend along a northwest trending belt from the Death Valley

region to the southeastern Mojave Desert. The Death Valley region metamorphic terranes of Late Jurassic age are located on the eastern margin of the arc, between the Late Jurassic batholith belt and coeval foreland thrust belt further east (Dewitt and others, 1979). The structural position of the Late Jurassic metamorphic terranes in the southeastern Mojave Desert is more analogous to the western and central Mojave region discussed above. Both regions lay within the Middle-Late Jurassic batholithic terrane, however, associated amphibolite grade regional metamorphism is extensive in the southeastern Mojave terrane, which apparently did not experience the Permo-Triassic metamorphic event, and hence constituted a wet basement for the Jurassic arc. In the southeastern Mojave, the previously undeformed section of Paleozoic and lower Mesozoic rocks, and locally the underlying Precambrian gneisses as well, are involved in fold and thrust nappes which formed synchronously with amphibolite facies metamorphism (Hamilton, 1971; Howard and others, 1980; Burchfiel and Davis, 1981). This highly ductile style of deformation is believed to have been associated with the emplacement of the Middle-Late Jurassic batholithic rocks (Hamilton, 1971; Burchfiel and Davis, 1981). To some degree, the difference in the style of deformation and extent of metamorphism associated with Late Jurassic magmatism between the western and central Mojave region and the southeastern Mojave region, may represent contrasting levels of exposure. (For example, Late Jurassic tectonism in the Big Bear area represents roof level deformation, as opposed to deeper level wall rock deformation exposed in the Big Maria Mountains studied by Hamilton, 1981). Compared on a regional scale, however, the contrast in deformational styles and extent of regional metamorphism during Jurassic orogenesis between the western and central Mojave region and southeastern Mojave region may fundamentally reflect contrasting dry and wet structural basement.

The emplacement of Cretaceous batholithic rocks which underlie much of the western and central Mojave Desert was attended by a regional

heating event which resulted in disturbance and often complete resetting of K/Ar isotopic systems in rocks of the pre-Cretaceous structural basement. In spite of the significant reheating indicated by these data, (discussed in detail above) Cretaceous regional metamorphic terranes comparable in extent to the Permo-Triassic and Jurassic terranes discussed above are not known from the western and central Mojave.

The apparent absence of Cretaceous regional metamorphism may in part reflect level of exposure. At present exposure levels over most of the Mojave region, the Cretaceous arc developed within a dry basement complex that had evolved during long history of earlier Mesozoic deformation. Wet supracrustal crustal sedimentary and volcanic rocks of upper Mesozoic age which are inferred to have overlain the batholith at higher structural levels may have recorded Cretaceous prograde metamorphism, but these rocks have been largely stripped away. Localized dynamothermal metamorphism occurs along some suspected Cretaceous thrusts in the eastern Mojave (Burchfiel and Davis, 1981), and the zonal distribution of such metamorphism may have been in part controlled by access to fluids along faults. It is noteworthy that even though no Cretaceous metamorphic core complexes are known in the northeastern Mojave, Cretaceous thrusting nevertheless continued in the foreland belt. Zonal syntectonic metamorphism and mylonitization are recognized within dry Precambrian and Mesozoic crystalline rocks which overrode Pelona Schist-type rocks during the Late Cretaceous along the synthetic Vicent Thrust and related structures. This deformation disappears at higher structural levels (Haxel and Dillon, 1978; Burchfiel and Davis, 1981). The zonal development of these Cretaceous metamorphic terranes may have resulted as hot but dry arc basement rocks overrode relatively wet Pelona type rocks along shallow dipping synthetic thrusts. Similarly deformed Precambrian and Mesozoic crystalline rocks are also present further north in the eastern Mojave region adjacent to the Colorado River (Davis and others, 1980). What underlies these metamorphic terranes is not known. These rocks may be allochthonous, detached along synthetic thrusts

(related to shallow-dip subduction) or antithetic thrusts (related to back-arc shortening). The implication is that these hot dry rocks may have overridden a wet section of sedimentary rocks, and that Mesozoic metamorphism of these dry rocks may have been facilitated by access to fluids from below.

The data base upon which the preceding discussion is based is limited; nevertheless available data from the west-central Mojave are consistent with the hypothesis that the style of deformation and extent of metamorphism associated with a magmatic episode may depend significantly on the presence or absence of wet basement. It is my impression that most models concerning the dynamics of Andean-type orogenesis tacitly assume a wet basement is present. This seems particularly true for models of back-arc thrusting. Many geologists consider back-arc thrust belts to be a salient feature of Andean-type orogens. Some geologists attribute back-arc thrust belts to intraplate crustal shortening (Burchfiel and Davis, 1972), while others relate the thrust belts to batholithic wedging (Hamilton, 1978) or upwelling and spreading at upper crustal levels of metamorphic core complexes (Price and Mountjoy, 1970). Whatever the mechanism, there appears to be consensus that a change in structural style occurs between the foreland region, where brittle décollement folding and thrusting occur, and the arc, where deformation becomes progressively more penetrative and is associated with widespread metamorphism. The crustal shortening hypothesis receives special attention in the following discussion because Burchfiel and Davis (1981) have suggested that Mesozoic tectonism in the Mojave region was dominated by east-directed, back-arc thrusting resulting in intraplate crustal shortening. In their view, plate convergence causes compressional stresses to be transmitted through the overriding continental lithosphere; intraplate crustal shortening is the result (Burchfiel and Davis, 1976). Arc magmatism causes regional heating of the crust along the cratonward margin back-arc of batholithic terrane. As a result, the upper crust of the back-arc region is presumed

to be more ductile than the cooler cratonic lithosphere to the east. Underthrusting of the cratonic lithosphere is localized along this back-arc zone of high ductility contrast. The result is brittle shortening by thrusting at shallow levels further east, and penetrative ductile shortening at deeper crustal levels marginal to the arc (Armstrong and Dick, 1974; Burchfiel and Davis, 1975).

The ductility contrast model assumes that ductile behavior follows if rocks in proximity to the magmatic arc are heated. As discussed above, this may be a reasonable assumption if the arc develops within a wet basement (as during the Permo-Triassic in the western and central Mojave, or during the Late Jurassic in the southeastern Mojave). If, however, the arc develops in a dry basement terrane, then brittle shortening may extend far back toward the arc hinterland, and even to fairly deep crustal levels proximal to the arc (as during the Jurassic and Cretaceous in the northern Mojave?). More typically, the basement terrane will probably consist of a wet supracrustal cover of variable thickness and areal extent overlying a dry crystalline terrane. Regional heating may produce a thin-skinned metamorphic terrane at higher crustal levels, with metamorphism and penetrative deformation largely confined to the overlying wet rocks. In general, the structural style at this level may be analogous to thin-skinned collisional metamorphic terranes, such as that described by Bartley (1981). Unlike collisional terranes, where metamorphism occurs because of tectonic burial beneath allochthonous rock sheets, Andean-type metamorphic terranes are a result of regional heating associated with magmatism. Rigid behavior of dry rocks cannot necessarily be assumed to persist at deeper crustal levels beneath the arc. The high geothermal gradient and expulsion of volatile components carried from depth by rising magmas may combine to cause extensive basement remobilization at middle crustal levels (Hamilton and Myers, 1967; Hamilton, 1978). At somewhat higher(?) structural levels, hydrothermal systems associated with arc magmatism may provide avenues for fluid migration into dry crystalline rocks and hence facilitate ductile deformation. In view of the complex variables

involved, it is probable that the structural level at which hot but relatively dry rocks deform penetratively might vary considerably. It is conceivable that the vertical spatial configuration of dynamothermal metamorphism and related penetrative deformation associated with Andean-type, back-arc crustal shortening could be very complex. A thin-skinned metamorphic terrane might develop at high crustal levels in the back-arc region (where a wet cover sequence overlies a dry crystalline basement), while at deeper crustal levels, in closer proximity to the arc, the dry basement rocks may deform penetratively. If penetrative deformation was not pervasive but confined to relatively narrow shear zones, the underthrust cratonic basement might persist as internally rigid blocks to considerable depths beneath the arc. In this framework, most Andean-type metamorphic terranes are considered as allochthonous, and not as part of a rooted infrastructure.

Extensional Tectonism and Plutonism

Extension by low-angle normal faulting of roof rocks may have occurred during all three plutonic episodes at Big Bear, although these structures are best developed in association with Late Jurassic plutonism at Sugarloaf. To my knowledge, similar structures have not been documented previously in the Mesozoic Cordilleran batholith belt, although their existence has been inferred (Hamilton and Myers, 1967; Gastil, 1979). Analogous structures of Cenozoic age may be present in the Basin and Range Province (Mackin, 1960; Anderson, 1971). The existence of such structures bears on several problems, among them the mechanism of batholith emplacement. Arc magmatism results in transfer of material to the upper crust (Hamilton and Myers, 1967; Pitcher, 1978; Gastil, 1979). Accommodation of upper crustal magmatic batholiths requires removal or displacement of pre-existing rocks. Frequently, stoping and/or uplift of large crustal blocks has been hypothesized to resolve this room problem (Pitcher, 1978). All too often, field evidence for stoping on a massive scale is absent or ambiguous; the down-dropped crustal

blocks mysteriously lie below the present erosion level in many cross sections (see Pitcher, 1978, p. 175). Uplift models cannot explain the common presence of relatively young rocks as roof pendants, and the frequent scarcity of older rocks overlying the batholith (the Sierra Nevada synclinorium is a classic example).

These difficulties are resolved, however, if upper crustal extension accompanies the emplacement of batholiths (Hamilton and Myers, 1967; Gastil, 1979). Lateral displacement of wall rocks may result in folding and thrusting marginal to the batholith (batholithic wedging, see Hamilton, 1978). A corollary to this model is the extension of pre-existing roof rocks. In the case of thinner "sill-like" batholiths "instrusions of low structural relief, Mackin, 1960), upper crustal extension might be entirely confined to stretching of the roof rocks, and compression of wall rocks might not occur. As discussed above, however, the magnitude of roof extension associated with emplacement of the Late Jurassic Sugarloaf Intrusive Complex appears to be too great to be explained by roof doming and stretching alone. I suggest that emplacement of the Late Jurassic plutonic rocks (at least) was accommodated by upper crustal extension involving both roof and wall rocks (i.e. the wall rocks were spread apart).

The recognition of extensional faulting associated with batholith emplacement has important implications for models of back-arc thrusting. Models which do not require crustal shortening, such as gravity sliding (Mudge, 1970), mobile infrastructure spreading (Price and Mountjoy, 1970) or batholithic wedging (Hamilton, 1978) postulate that tectonic shortening in the thrust belt must be matched by extension in the hinterland. Lack of evidence of such extension, or absence of extension of sufficient magnitude, has caused many geologists (Misch, 1960; Armstrong, 1968; Fleck, 1970; Burchfiel and Davis, 1972) to reject these models in favor of the crustal shortening hypothesis. Palinspastic reconstructions of thrust belts (Bally and others, 1966, for example), document cases where total shortening exceeds the maximum postulated extension and are the most

conclusive evidence that crustal shortening occurs both in back-arc and collisional thrust belts. In the case of back-arc thrust belts, this implies that intraplate compressive stresses are transmitted across the arc region.

Burchfiel and Davis (1981) present evidence that back-arc folding and thrusting and arc magmatism appear to be broadly contemporaneous in the Mojave Desert region. The occurrence of upper crustal extension associated with batholith emplacement in the hinterland at Big Bear is evidence that thrust belt telescoping may represent the combined effects of crustal shortening and batholithic wedging. The relative importance of crustal shortening vs. batholithic wedging in back-arc fold and thrust belts is uncertain, although I strongly suspect that most of the tectonic overlap in the thrust belt is attributable to intraplate crustal shortening. A critical unknown in evaluating the importance of wedging effects is the regional extent of roof extension in the Mojave batholithic terrane. One might argue that isolated roof pendants, widely separated by Mesozoic plutons, may be the intruded remnants of low-angle normal fault-bound allochthons (analogous to the intruded higher allochthons at Sugarloaf). Of particular interest are batholithic terranes, such as the Cretaceous Sierra Nevada batholith to the north, where younger Mesozoic rocks are found as roof pendants and screens in the axial portion, and pre-Mesozoic rocks are generally restricted to the batholith's flanks. Could this reflect extensional downfaulting of the younger rocks to accommodate emplacement of the batholith (see Gastil, 1979)? The possibility exists that roof rock extension may be widespread above Cordilleran batholiths. Such faulting would be difficult, if not impossible, to recognize where the basement rocks for younger batholiths consist of structurally and stratigraphically complex accreted oceanic terranes (dismembered ophiolites, flysch, or melange, for example) or intra-arc deposits. Recognition of such structures requires the presence of well-ordered stratigraphy in the pre-batholithic roof rocks, so that younger-over-older faults can be identified even in the absence of

paleontologic control. The miogeoclinal basement rocks of the Mojave Desert region meet this requirement, and this terrane may be best suited for evaluating the extent of roof rock extension.

Available data from the northern Mojave Desert suggests that during at least the Late Jurassic, both intra-arc extension and back-arc crustal shortening occurred simultaneously. If true, this implies the regional tectonic stresses varied with crustal level. For example, if net crustal shortening in the back-arc is assumed during the Late Jurassic, then intra-plate compressional stresses were transmitted through the overriding North American plate. In detail, the situation was probably far more complex, however. Within the arc region, extension in the roof terrane passed at deeper levels into intraplate compression, while in the back-arc terrane compressional structures formed in the upper crustal thrust belt (Fig. 75). Seen in this light, the complex superposition of contractional and extensional structures present in the Big Bear area is to be expected. During the Permo-Triassic, for example, the progression of deformational events at Big Bear may record the evolution from a back-arc fold and thrust belt (D_1 events) to an intra-arc plutonic belt (D_2 events).

Evidence from the Big Bear area indicates some interesting twists in the role of arc magmatism in Andean-type orogenesis. The addition of new material to the upper crust during arc-plutonism at least locally is attended by significant extension of roof rocks. This apparently can occur even if the major plate motions result in concurrent upper plate crustal shortening. Regional heating associated with magmatism has a variable effect on the style of intra-plate deformation, depending on country-rock type. Following the megasuture concept of Bally (1975), the arc along with its flanking forearc/accretionary prism terrane and back-arc fold and thrust belt may be envisioned as a lithospheric wedge, detached from underthrust oceanic lithosphere and underthrust cratonic lithosphere respectively. Bally (1975), Armstrong and Dick (1974),

Figure 75: Comparison of the crustal shortening and batholithic wedging models for Andean-type orogenic belts.

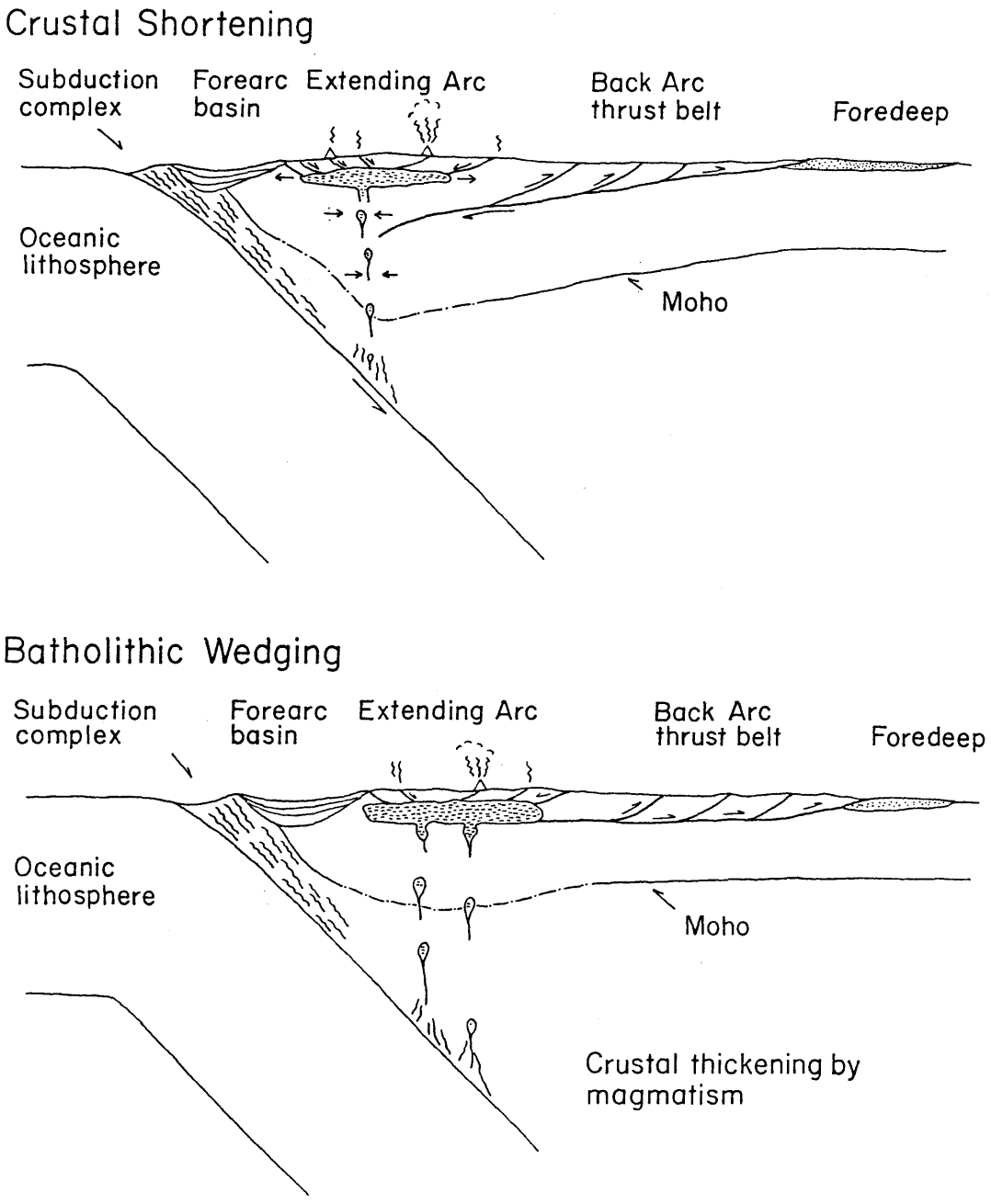

and numerous others have suggested that telescoping in back-arc thrust belts is matched by penetrative ductile shortening beneath the arc occurring in a thoroughly remobilized infrastructure. Though this may occur in some cases, I do not believe it is required. In cases where the arc's basement consists of relatively dry crystalline rocks, shortening may occur by relatively rigid block thrusting. Even when back-arc, synmetamorphic fold and thrust belts are developed, they may be thin-skinned, and decoupled from hot, but rigid cratonic lithosphere below.

REFERENCES

Aitken, J. D., 1966, Middle Cambrian to middle Ordovician cyclic sedimentation, southern Rocky Mountains of Alberta: Bull. of Canadian Petroleum Geology, v. 14, p. 405-441.

Aitken, J. D., 1978, Revised models for depositional grand cycles, Cambrian of the southern Rocky Mountains, Canada: Bull. of Canadian Petroleum Geology, v. 26, p. 515-542.

Alexander, E. C., Jr., Coscio, M. R., Jr., Dragon, J. C., Pepin, R. O., and Saito, K., 1977, K/Ar dating of lunar soils III: Comparison of ^{39}Ar-^{40}Ar and conventional techniques; 12032 and the age of Copernicus: Proc. Lunar Sci. Conf. 8th, p. 2725-2740.

Alexander, E. C., Jr., Mickelson, G. M., and Lanphere, M. A., 1978, MMhb-1: A new ^{40}Ar-^{39}Ar dating standard, in Zartman, R. E., ed., Short Papers of the Fourth International Conference, Geochronology, Cosmochronology, Isotope Geology: U. S. Geol. Survey Open-File Report 78-701, p. 6-8.

Anderson, R. E., 1971, Thin-skinned distension in Tertiary rocks of southeastern Nevada: Geol. Soc. America Bull., v. 82, p. 43-58.

Anderson, T. H., and Silver, L.T., 1977, Geochronometric and stratigraphic outlines of the Precambrian rocks of northwestern Mexico [abstract]: Geol. Soc. America Abstr. with Prog., v. 9, p. 880.

Anderson, T. H., and Silver, L. T., 1979, The role of the Mojave-Sonora megashear in the tectonic evolution of northern Sonora, in Anderson, T. H., and Rodan-Quintana, J., eds., Geology of Northern Sonora, Guidebook -- Fieldtrip #27: Pittsburgh, Pennsylvania, The University of Pittsburgh, p. 59-68.

Anderson, T. H., Eells, J. H., and Silver, L. T., 1979, Precambrian and Paleozoic rocks of the Caborca Region, Sonora, Mexico, in Anderson, T. H., and Rodan-Quintana, J., eds., Geology of Northern Sonora, Guidebook -- Fieldtrip #27: Pittsburgh, Pennsylvania, The University of Pittsburgh, p. 1-22.

Armstrong, R. L., 1968, Sevier orogenic belt in Nevada and Utah: Geol. Soc. America Bull., v. 79, p. 429-458.

Armstrong, R. L., 1972, Low-angle (denudation) faults, hinterland of the Sevier orogenic belt, eastern Nevada and western Utah: Geol. Soc. America Bull., v. 83, p. 1729-1754.

Armstrong, R. L., 1975, Precambrian (1500 m.y. old) rocks of central Idaho -- the Salmon River Arch and its role in Cordilleran sedimentation and tectonics: Am. Jour. Sci., v. 275A, p. 437-467.

Armstrong, R. L., and Dick, H. J., 1974, A model for the development of thin overthrust sheets of crystalline rock: Geology, v. 2, p. 35-40.

Bally, A. W., 1975, A geodynamic scenario for hydrocarbon occurrences: Proc. 9th World Petroleum Congress, Tokyo, 1975, Vol. 2 -- Geology: Applied Science Publishers Ltd., Ripple Road, Barking, Essex, England, p. 33-44.

Bally, A. W., Gordy, P. L., and Stewart, G. A., 1966, Structure, seismic data, and orogenic evolution of southern Canadian Rocky Mountains: Bull. of Canadian Petroleum Geology, v. 14, p. 337-381.

Barnes, I., and Palmer, A. R., 1961, Revision of stratigraphic nomenclature of Cambrian rocks, Nevada Test Site and vicinity, Nevada: U. S. Geol. Survey Prof. Paper 424-C, p. C100-C103.

Bartley, J. M., 1981, Structural geology, metamorphism, and Rb/Sr geochronology of East Hinnøy, North Norway: Unpub. Ph. D. dissert., M. I. T., 263 p.

Blake, M. C., Jr., Morton, D. M., and Jayko, A., 1979, Tectono-stratigraphic terrane map of western Baja California, western California, and southwest Oregon [abstract]: Geol. Soc. America Abs. with Prog., v. 11, p. 389.

Burchfiel, B. C., and Davis, G. A., 1971, Clark Mountain thrust complex in the cordillera of southeastern California, geologic summary and field trip guide: Univ. Calif. Riverside Mus. Contr., v. 1, p. 1-28.

Burchfiel, B. C., and Davis, G. A., 1972, Structural framework and evolution of the southern part of the Cordilleran orogen, western United States: Am. Jour. Sci., v. 272, p. 97-118.

Burchfiel, B. C., and Davis, G. A., 1975, Nature and controls of Cordilleran orogenesis, western United States: Am. Jour. Sci., v. 275A, p. 363-396.

Burchfiel, B. C., and Davis, G. A., 1976, Compression and crustal shortening in Andean-type orogenesis: Nature, v. 260, p. 693-694.

Burchfiel, B. C., and Davis, G. A., 1977, Geology of the Sagamore Canyon-Slaughterhouse Spring Area, New York Mountains, California: Geol. Soc. America Bull., v. 88, p. 1623-1640.

Burchfiel, B. C., and Davis, G. A., 1981, Mojave Desert and environs, in Ernst, W. G., ed., The Geotectonic Development of California (Rubey Vol. 1): Englewood Cliffs, New Jersey, Prentice-Hall, Inc., p. 217-252.

Burchfiel, B. C., and Davis, G. A., in prep., Geology of the Clark Mountain thrust complex, California.

Burchfiel, B. C., Cameron, C. S., Guth, P. L., Spencer, J. E., Carr, M. D., Miller, E. L., McCulloh, T. H., 1980, A triassic overlap assemblage in northern Mojave/Death Valley region, California: an interpretation[abstract]: Geol. Soc. Amer. Abstr. with Prog., v. 12, p. 395.

Cameron, C. S., 1980, Late Precambrian strata of the San Bernardino Mountains, California: Their relation to the Cordilleran miogeocline [abstract]: Geol. Soc. America Abstr. with Prog., v. 12, p. 100.

Cameron, S., Guth, P. L., and Burchfiel, B. C., 1979, The Early Mesozoic Cave Mountain sequence: Its implications for Mesozoic tectonics [abstract]: Geol. Soc. America Abst. with Prog., v. 11, p. 397.

Christiansen, R. L., 1961, Structure, metamorphism, and plutonism in the El Paso Mountains, Mojave Desert, California: Unpub. Ph. D. dissert., Stanford University, 180 p.

Compton, R. R., 1966, Granitic and metamorphic rocks of the Salinian block, California Coast Ranges, in Geology of Northern California: Calif. Div. Mines and Geology Bull. 190, p. 277-287.

Cooper, G. A., Arellano, A. R. V., Johnson, J. H., Okulitch, V. J., Stoyanow, A., and Lochman, C., 1952, Cambrian stratigraphy and paleontology near Caborca, northwestern Sonora, Mexico: Smithsonian Misc. Colln., v. 119, 183 p.

Cornwall, H. R., and Kleinhampl, F. J., 1961, Geology of the Bare Mountain quadrangle, Nevada: U. S. Geol. Survey Geol. Quad. Map GQ-157, scale 1:62,500.

Cox, B. F., and Morton, J. L., 1980, Late Permian plutonism, El Paso Mountains, California [abstract]: Geol. Soc. America Abst. with Prog., v. 12, p. 103.

Dahlstrom, C. D., 1970, Structural geology in the eastern margin of the Canadian Rocky Mountains: Bull. Canadian Petroleum Geol., v. 18, p. 332-406.

Dallmeyer, R. D., 1975, $^{40}Ar/^{39}Ar$ ages of biotite and hornblende from a progressively re-metamorphosed basement terrain: Their bearing on interpretation of release spectra: Geochim. et. Cosmochim. Acta, v. 39, p. 1655-1669.

Dallmeyer, R. D., and Sutter, J. F., 1976, $^{40}Ar/^{39}Ar$ incremental-release ages of biotite and hornblende from variably retrograded basement gneisses of the northeasternmost Reading Prong, New York: Their bearing on Early Paleozoic metamorphic history: Am. Jour. Sci., v. 276, p. 731-747.

Dalrymple, G. B., 1979, Critical tables for conversion of K-Ar ages from old to new constants: Geology, v. 7, p. 558-560.

Dalrymple, G. B., and Lanphere, M. A., 1969, Potassium-Argon Dating: Principles, Techniques and Applications to Geochronology: San Francisco, Freeman, 258 p.

Dalrymple, G. B., and Lanphere, M. A., 1971, $^{40}Ar/^{39}Ar$ technique of K-Ar dating: A comparison with the conventional technique: Earth and Plan. Sci. Letters, v. 12, p. 300-308.

Dalrymple, G. B., and Lanphere, M. A., 1974, $^{40}Ar/^{39}Ar$ age spectra of some undisturbed terrestrial samples: Geochim. et Cosmochim. Acta, v. 38, p. 715-738.

Davis, G. A., Monger, J. W. H., and Burchfiel, B. C., 1978, Mesozoic construction of the Cordilleran "collage", central British Columbia to central California, in Howell, D. G., and McDougall, K. A., eds., Mesozoic Paleogeography of the Western United States: Los Angeles, Pacific Section, Soc. Econ. Paleontologists and Mineralogists, p. 1-32.

Davis, G. A., Anderson, J. L., Frost, E. G., and Shackelford, T. J., 1980, Mylonitization and detachment faulting in the Whipple-Buckskin-Rawhide Mountains terrane, southeastern California and western Arizona, in Crittenden, M. D., Jr., Coney, P. J., and Davis, G. H., eds., Cordilleran Metamorphic Core Complexes: Geol. Soc. America Memoir 153, p. 79-130.

Deer, W. A., Howie, R. A., and Zussman, J., 1966, An Introduction to the Rock-Forming Minerals: New York, John Wiley and Sons, Inc., 528 p.

Dewitt, E., Wright, L. A., and Troxel, B. W., 1979, Mesozoic metamorphic terrains in the Death Valley area, southern California [abstract]: Geol. Soc. America Abst. with Prog., v. 11, p. 413.

Dibblee, T. W., Jr., 1964a, Geologic map of the San Gorgonio Mountain quadrangle, San Bernardino and Riverside Counties, California: U. S. Geol. Survey Misc. Geol. Invest. Map I-431, scale 1:62,500.

Dibblee, T. W., Jr., 1964b, Geologic map of the Lucerne Valley quadrangle, San Bernardino County, California: U. S. Geol. Survey Misc. Geol. Invest. Map I-426, scale 1:62,500.

Dibblee, T. W., Jr., 1967a, Geologic map of the Morongo Valley quadrangle, San Bernardino and Riverside Counties, California: U. S. Geol. Survey Misc. Geol. Invest. Map I-517, scale 1:62,500.

Dibblee, T. W., Jr., 1967b, Geologic map of the Old Woman Springs quadrangle, San Bernardino County, California: U. S. Geol. Survey Misc. Geol. Invest. Map I-518, scale 1:62,500.

Dibblee, T. W., Jr., 1975, Late Quaternary uplift of the San Bernardino Mountains on the San Andreas and related faults, in Crowell, J. C., ed., San Andreas Fault in Southern California: Calif. Div. of Mines and Geol. Spec. Rep. 118, p. 127-135.

Dickinson, W. R., 1970, Relations of andesite, granites, and derivative sandstones to arc-trench tectonics: Rev. Geophys. Space Phys., v. 8, p. 813-860.

Dickinson, W. R., 1981, Plate tectonics and the continental margin of California, in Ernst, W. G., ed., The Geotectonic Development of California (Rubey Vol. 1): New Jersey, Prentice-Hall, Inc., p. 1-28.

Diehl, P., 1974, Stratigraphy and sedimentology of the Wood Canyon Formation, Death Valley area, California, in Guidebook: Death Valley Region, California and Nevada, Geol. Soc. America Cordilleran section meeting field trip no. 1: Shoshone, California, Death Valley Publishing Co., p. 37-48.

Dunne, G. C., 1972, Geology of the Devil's Playground area, eastern Mojave Desert, California: unpubl. Ph. D. dissert., Rice University, Houston, Texas, 79 p.

Dunne, G. C., 1977, Geology and structural evolution of Old Dad Mountain, Mojave Desert, California: Geol. Soc. America Bull., v. 88, p. 737-748.

Dunne, G. C., Gulliver, R. M., and Sylvester, A. G., 1978, Mesozoic evolution of rocks of the White, Inyo, Argus and Slate ranges, eastern California, in Howell, D. G., and McDougall, K. A., eds., Mesozoic Paleogeography of the Western United States: Pacific Section, Soc. Econ. Paleontologists and Mineralogists, p. 189-208.

Eells, J. L., 1972, The geology of the Sierra de la Berruga, northwestern Sonora, Mexico: Unpubl. M. S. thesis, San Diego State College, 86 p.

Elliott, T., 1978, Clastic shorelines, in Reading, H. G., ed., Sedimentary Environments and Facies: New York, Elsevier, p. 143-177.

Fiske, R. S., and Tobisch, O. T., 1978, Paleogeographic significance of volcanic rocks of the Ritter Range pendant, central Sierra Nevada, Calif., in Howell, D. G., and McDougall, K. A., eds., Mesozoic Paleogeography of the western United States: Los Angeles, Pacific Section, Soc. of Econ. Paleontologists and Mineralogists, p. 209-222.

Fitch, T. J., 1972, Plate convergence, transcurrent faults, and internal deformation adjacent to southeast Asia and the western Pacific: Jour. Geophys. Res., v. 77, p. 4432-4460.

Fleck, R. J., 1970, Tectonic style, magnitude, and age of deformation in the Sevier orogenic belts in southern Nevada and eastern California: Geol. Soc. America Bull., v. 81, p. 1705-1720.

Fleck, R. J., Sutter, J. F., and Elliott, D. H., 1977, Interpretation of discordant $^{40}Ar/^{39}Ar$ age-spectra of Mesozoic tholeiites from Antarctica: Geochim. et Cosmochim. Acta, v. 41, p. 15-32.

Gans, W. T., 1974, Correlation and redefinition of the Goodsprings Dolomite, southern Nevada and eastern California: Geol. Soc. America Bull., v. 85, p. 189-200.

Garfunkel, Z., 1974, Model for the late Cenozoic tectonic history of the Mojave Desert, California, and for its relation to adjacent regions: Geol. Soc. America Bull., v. 85, p. 1931-1944.

Gastil, R. G., 1979, A conceptual hypothesis for the relation of differing tectonic terranes to plutonic emplacement: Geology, v. 7, p. 542-544.

Griggs, D. T., and Blacic, J. B., 1965, Quartz: Anomalous weakness of synthetic crystals: Science, V. 147, p. 292-295.

Guillou, R. B., 1953, Geology of the Johnston Grade area, San Bernardino County, California: Calif. Div. Mines and Geol. Spec. Rep. 31, 18p.

Halley, R. B., 1975, Peritidal lithologies of Cambrian carbonate islands, Carrara Formation, southern Great Basin, in Ginsburg, R. N., ed., Tidal Deposits: New York, Springer-Verlag, p. 279-288.

Hamilton, W., 1969, The volcanic central Andes -- a modern model for the Cretaceous batholiths and tectonics of western North America, in McBirney, A. R., ed., Proceedings of the Andesite Conference (Int'l. Upper Mantle Project, Sci. Report 16): Oregon Dept. of Geology and Mineral Industries, Bull. 65, p. 175-184.

Hamilton, W., 1969, Mesozoic California and the underflow of Pacific mantle: Geol. Soc. America Bull., v. 80, p. 2409-2430.

Hamilton, W., 1971, Tectonic framework of southeastern California [abstract]: Geol. Soc. America Abst. with Prog., v. 3, p. 130-131.

Hamilton, W., 1978, Mesozoic tectonics of the western United States, in Howell, D. G., and McDougall, K. A., eds., Mesozoic Paleogeography of the Western United States: Los Angeles, Pacific Section, Soc. Econ. Paleontologists and Mineralogists, p. 33-70.

Hamilton, W., 1979, Tectonics of the Indonesian region: U. S. Geol. Survey Prof. Paper 1078, 345 p.

Hamilton, W., and Myers, W. B., 1966, Cenozoic tectonics of the western United States: Rev. of Geophys., v. 4, p. 509-549.

Hamilton, W., and Myers, W. B., 1967, The nature of batholiths: U. S. Geol. Survey Prof. Paper 554-C, 30 p.

Hamilton, W., and Myers, W. B., 1974, Nature of the Boulder Batholith of Montana: Geol. Soc. America Bull., v. 85, p. 365-378.

Hansen, E., 1971, Strain Facies: New York, Springer-Verlag, 207 p.

Harrison, T. M., and McDougall, I., 1980, Investigations of an intrusive contact, northwest Nelson, New Zealand II: Diffusion of radiogenic and excess ^{40}Ar in hornblende revealed by $^{40}Ar/^{39}Ar$ age spectrum analysis: Geochim. et Cosmochim. Acta, v. 44, p. 2005-2021.

Haxel, G., and Dillon, J., 1978, The Pelona-Orocopia Schist and Vincent-Chocolate Mountain thrust system, southern California, in Howell, D. G., and McDougall, K. A., eds., Mesozoic Paleogeography of the Western United States: Los Angeles, Pacific Section, Soc. Econ. Paleontologists and Mineralogists, p. 453-469.

Hazzard, J. C., 1937, Paleozoic section in the Nopah and Resting Springs mountains, Inyo County, California: Calif. Jour. of Mines and Geology, v. 33, p. 272-339.

Hazzard, J. C., and Mason, J. F., 1936, Middle Cambrian formations of the Providence and Marble Mountains, California: Geol. Soc. America Bull., v. 47, p. 229-240.

Heckel, P. H., 1972, Recognition of ancient shallow marine environments, in Rigby, J. K., and Hamblin, W. K., eds., Recognition of Ancient Sedimentary Environments: Soc. Econ. Paleontologists and Mineralogists Spec. Publ., v. 16, p. 226-296.

Heckel, P. H., 1974, Carbonate buildups in the geological record: A review, in Laporte, L. F., ed., Reefs in Time and Space: Soc. Econ. Paleontologists and Mineralogists Spec. Publ., v. 18, p. 90-154.

Helgeson, H. C., Delany, J. M., Nesbitt, H. W., and Bird, D. K., 1978, Summary and critique of the thermodynamic properties of rock-forming minerals: Am. Jour. Sci., v. 278-A, 229 p.

Hewett, D. F., 1931, Geology and ore deposits of the Goodsprings quadrangle, Nevada: U. S. Geol. Survey Prof. Paper 162, 72 p.

Hobbs, B. E., Means, W.D., Williams, P.F., 1976, An Outline of Structural Geology: New York, John Wiley & Sons, Inc., 571 p.

Hoffman, P., 1974, Shallow and deepwater stromatolites in Lower Proterozoic platform-basin facies change, Great Slave Lake, Canada: Bull. Am. Assoc. Petroleum Geologists, v. 58, p. 856-867.

Holdaway, M. J., 1971, Stability of andalusite and the aluminum silicate phase diagram: Am. Jour. Sci., v. 271, p. 97-131.

Hollenbaugh, K.L., 1968, Geology of a portion of the north flank of the San Bernardino Mountains, Calif.: Unpubl. Ph.D. dissert., Univ. Idaho, 109p.

Howard, K. A., Miller, C. F., and Stone, P., 1980, Mesozoic thrusting in the eastern Mojave Desert, California [abstract]: Geol. Soc. America Abst. with Prog., v. 12, p. 112.

Huneke, J. C., 1976, Diffusion artifacts in dating by stepwise thermal release of rare gases: Earth and Plan. Sci. Letters, v. 28, p. 407-417.

Hyndman, D. W., 1972, Petrology of Igneous and Metamorphic Rocks: New York, McGraw-Hill Book Co., 533 p.

Jennings, C. W., 1977, Geologic map of California: Calif. Div. Mines and Geology, scale 1:750,000.

Kay, M., 1951, North American geosynclines: Geol. Soc. America Mem. 48, 143 p.

King, P. B., 1959, The Evolution of North America: Princeton, New Jersey, Princeton University Press, 189 p.

King, P. B., 1969, Tectonic map of North America: U. S. Geol. Survey, scale 1:5,000,000.

Kinsman, D. J. J., 1975, Rift valley basins and sedimentary history of trailing continental margins, in Fischer, A. G., and Judson, S., eds., Petroleum and Global Tectonics: Princeton, New Jersey, Princeton University Press, p. 83-127.

Kistler, R. W., and Peterman, Z. E., 1978, Reconstruction of crustal blocks of California on the basis of initial strontium isotopic compositions of Mesozoic plutons: U. S. Geol. Survey Prof. Paper 1071.

Kistler, R. W., Peterman, Z. E., Ross, D. C., and Gottfried, D., 1973, Strontium isotopes and the San Andreas fault, in Kovach, R. L., and Nur, A., eds., Proceedings of the Conference on Tectonic Problems of the San Andreas Fault System: Stanford, California, Stanford Univ. Pubs. Geol. Sci., v. 13, p. 339-347.

Klein, G. deV., 1971, A sedimentary model for determining paleotidal range: Geol. Soc. America Bull., v. 82, p. 2585-2592.

Klein, G. deV., 1977, Clastic Tidal Facies: Champaign, Illinois, Cepco (Univ. Illinois), 149 p.

Krummenacher, D., Gastil, R. G., Bushee, J., and Doupont, J., 1975, K-Ar apparent ages, Peninsular Ranges Batholith, southern California and Baja California: Geol. Soc. America Bull., v. 86, p. 760-768.

Kupfer, D. H., 1960, Thrust faulting and chaos structures in the Silurian Hills, San Bernardino County, California: Geol. Soc. America Bull., v. 71, p. 181-214.

Labotka, T. C., 1980, Petrology of a medium-pressure regional metamorphic terrane, Funeral Mountains, California: Am. Min., v. 65, p. 670-689.

Labotka, T. C., Albee, A. L., Lanphere, M. A., McDowell, S. D., 1980, Stratigraphy, structure, and metamorphism in the central Panamint Mountains (Telescope Peak quadrangle), Death Valley area, California: Summary: Geol. Soc. America Bull., v. 91, p. 125-129.

Lanphere, M. A., 1964, Geochronologic studies in the eastern Mojave Desert, California: Jour. Geol., v. 72, p. 381-399.

Lanphere, M. A., and Dalrymple, G. B., 1971, A test of the $^{40}Ar/^{39}Ar$ age spectrum technique on some terrestrial materials: Earth and Plan. Sci. Letters, v. 12, p. 359-372.

Lanphere, M. A., and Dalrymple, G. B., 1976, Identification of excess ^{40}Ar by the $^{40}Ar/^{39}Ar$ age spectrum technique: Earth and Plan. Sci. Letters, v. 32, p. 141-148.

Lanphere, M. A., and Dalrymple, G. B., 1978, The use of $^{40}Ar/^{39}Ar$ data in evaluation of disturbed k-Ar systems, in Zartman, R. E., ed., Short Papers of the Fourth International Conference, Geochronology, Cosmochronology, Isotope Geology: U. S. Geol. Survey Open-File Report 78-701, p. 241-243.

Lanphere, M. A., Wasserburg, G. J. F., and Albee, A. L., 1963, Redistribution of strontium and rubidium isotopes during metamorphism, World Beater Complex, Panamint Range, California, in Craig, H., Miller, S. L., and Wasserburg, G. J., eds., Isotopic and Cosmic Chemistry: Amsterdam, North-Holland, p. 269-320.

Liou, J. G., 1973, Synthesis and stability relations of epidote, $Ca_2Al_2Fe\ Si_3O_{12}(OH)$: Jour. Petr., v. 14, p. 381-413.

Liou, J. G., Kuniyoshi, S., and Ito, K., 1974, Experimental studies of the phase relations between greenschist and amphibolite in a basaltic system: Am. Jour. Sci., v. 274, p. 613-632.

Lobo, C. F., and Osborne, R. H., 1976, Petrology of Late Precambrian-Cambrian quartzose sandstones in the eastern Mojave Desert, southeastern California: Jour. Sed. Pet., v. 46, p. 829-846.

Lowell, J. D., Genick, G. J., Nelson, T. H., and Tucker, P. M., 1975, Petroleum and plate tectonics of the southern Red Sea, in Fischer, A. G., and Judson, S., eds., Petroleum and Global Tectonics: Princeton, New Jersey, Princeton Univ. Press, p. 129-156.

Mackin, J. H., 1960, Structural significance of Tertiary volcanic rocks in southwestern Utah: Am. Jour. Sci., v. 258, p. 81-131.

McJunkin, R. D., 1976, Geology of the central San Bernardino Mountains, San Bernardino County, California: Unpub. M. S. thesis, California State University, Los Angeles, 102 p.

Merrihue, C., and Turner, G., 1966, Potassium-argon dating by activation with fast neutrons: J. Geophys. Res., v. 71, p. 2852-2857.

Miller, C. F., 1977, Early alkalic plutonism in the calc-alkalic batholithic belt of California: Geology, v. 5, p. 685-688.

Miller, C. F., 1977, Alkali-rich monzonites, California: Origin of near silica-saturated alkaline rocks and their significance in a calc-alkaline batholithic belt: Unpub. Ph. D. dissert., Univ. of California, Los Angeles, 283 p.

Miller, C. F., 1978, An early Mesozoic alkalic magmatic belt in western North America, in Howell, D. G., and McDougall, K. A., eds., Mesozoic Paleogeography of the Western United States: Los Angeles, Pacific Section, Soc. Econ. Paleontologists and Mineralogists, p. 163-187.

Miller, E. L., 1977, Geology of the Victorville region, California: Unpubl. Ph. D. dissert., Rice University, Houston, Texas, 226 p.

Miller, E. L., 1978, The Fairview Valley Formation: A Mesozoic intra-orogenic deposit in the southwestern Mojave Desert, in Howell, D. G., and McDougall, K. A., eds., Mesozoic Paleogeography of the Western United States: Los Angeles, Pacific Section, Soc. Econ. Paleontologists and Mineralogists, p. 277-282.

Miller, E. L., and Carr, M. D., 1978, Recognition of possible Aztec-equivalent sandstones and associated mid-Mesozoic metasedimentary deposits within the Mesozoic magmatic arc in the southwestern Mojave Desert, California, in Howell, D. G., and McDougall, K. A., eds., Mesozoic Paleogeography of the Western United States: Los Angeles, Pacific Section, Soc. Econ. Paleontologists and Mineralogists, p. 283-290.

Miller, E. L., and Sutter, J., 1979, $^{40}Ar/^{39}Ar$ incremental release ages on plutonic rocks from the Victorville region, California [abstract]: Geol. Soc. America Abs. with Prog., v. 11, p. 92.

Miller, E. L., Burchfiel, B. C., and Carr, M. D., 1979, Enigmatic metasedimentary rocks of the western Mojave Desert, California and their relationship to Corfilleran miogeocline/platform rocks [abstract]: Geol. Soc. America Abs. with Prog., v. 11, p. 92.

Misch, P., 1960, Regional structural reconnaissance in central-northeast Nevada and some adjacent areas: Observations and interpretations: Intermountain Association of Petroleum Geologists 11th Annual Field Conference Guidebook, p. 17-42.

Miyashiro, A., 1973, Metamorphism and Metamorphic Belts: Boston, George Allen and Unwin, 492 p.

Mount, J. F., and Rowland, S. M., 1979, Anatomy of a grand cycle [abstract]: Geol. Soc. Amer. Abs. with Prog., v. 11, p. 484.

Mudge, M. R., 1970, Origin of the disturbed belt in northwestern Montana: Geol. Soc. America Bull., v. 81, p. 377-392.

Nolan, T. B., 1929, Notes on the stratigraphy and structure of the northwest portion of Spring Mountain, Nevada: Am. Jour. Sci., 5th Ser., v. 17, p. 461-472.

Novitsky, J. M., and Burchfiel, B. C., 1973, Pre-Aztec (Upper Triassic(?)-Lower Jurassic) thrusting, Cowhole Mountains, southeastern California [abstract]: Geol. Soc. America Abs. with Prog., v. 5, p. 755.

Ozima, M., Kaneoka, I., and Yanagisawa, M., 1978, Effects of pressure and thermal disturbances on ^{40}Ar-^{39}Ar systematics, in Zartman, R. E., ed., Short Papers of the Fourth International Conference, Geochronology, Cosmochronology, Isotope Geology: U. S. Geol. Survey Open-File Report 78-701, p. 321-322.

Palmer, A. R., and Hazzard, J. C., 1956, Age and correlation of Cornfield Springs and Bonanza King formations in southeastern California and southern Nevada: Am. Assoc. Petroleum Geol. Bull., v. 46, p. 2494-2499.

Pitcher, W. S., 1978, The anatomy of a batholith: Jour. Geol. Soc. London, v. 135, p. 157-182.

Poole, F. G., 1974, Flysch deposits of the Antler foreland basin, western United States, in Dickinson, W. R., ed., Tectonics and Sedimentation: Soc. Econ. Paleontologists and Mineralogists Spec. Pub. no. 22, p. 58-82.

Poole, F. G., and Christiansen, R. L., 1980, Allochthonous lower and middle Paleozoic eugeosynclinal rocks in El Paso Mountains, northwestern Mojave Desert, California [abstract]: Geol. Soc. America Abs. with Prog., v. 12, p. 147.

Poole, F. G., and Hayes, P. T., 1971, Depositional framework of some Paleozoic strata in northwestern Mexico and southwestern United States [abstract]: Geol. Soc. America Abs. with Prog., v. 3, p. 179.

Poole, F. G., and Sandberg, C. A., 1977, Mississippian paleogeography and tectonics of the western United States, in Stewart, J. H., Stevens, C. H., and Fritsche, A. E., eds., Paleozoic Paleogeography of the Western United States: Los Angeles, Pacific Section, Soc. Econ. Paleontologists and Mineralogists, p. 67-86.

Powell, R. E., and Silver, L. T., 1979, Tectonic superposition of crystalline terranes in the Chuckwalla to Pinto Mountains region, eastern Transverse Ranges, southern California [abstract]: Geol. Soc. America Abs. with Prog., v. 11, p. 498.

Price, R. A., and Mountjoy, E. W., 1970, Geologic structure of the Canadian Rocky Mountains between Bow and Athabasca Rivers -- a progress report, in Structure of the southern Canadian Cordillera, Geol. Assoc. Canada, Spec. Pap. 6, p. 7-25.

Proffett, J. M., 1977, Cenozoic geology of the Yerington district, Nevada, and implications for the nature and origin of basin and range faulting: Geol. Soc. America Bull., v. 88, p. 247-266.

Ramsay, J. G., 1967, Folding and Fracturing of Rocks: New York, McGraw-Hill Book Co., 568 p.

Reineck, H.-E., and Singh, I. B., 1975, Depositional Sedimentary Environments: New York, Springer-Verlag, 439 p.

Richmond, J. F., 1960, Geology of the San Bernardino Mountains north of Big Bear Lake, California: Calif. Div. Mines and Geol. Spec. Rep. 65, 68 p.

Roddick, J. C., 1978, ^{40}Ar-^{39}Ar data on the distribution of argon in biotites with excess argon, in Zartman, R. E., ed., Short Papers of the Fourth International Conference, Geochronology, Cosmochronology, Isotope Geology: U. S. Geol. Survey Open-File Report 78-701, p. 356-359.

Ross, D. C., 1977, Pre-intrusive metasedimentary rocks of the Salinian block, California -- a paleotectonic dilemma, in Stewart, J. H., Stevens, C. H., Fritsche, A. E., eds., Paleozoic Paleogeography of the Western United States: Los Angeles, Pacific Section, Soc. Econ. Paleontologists and Mineralogists, p. 19-38.

Schuepbach, M. A., and Vail, P. R., 1980, Evolution of outer highs on divergent continental margins, in Continental Tectonics: Washington, D. C., National Academy of Sciences, p. 50-62.

Sellwood, B. W., 1978, Shallow-water carbonate environments, in Reading, H. G., ed., Sedimentary Environments and Facies: New York, Elsevier, p. 259-313.

Silver, L. T., 1971, Problems of crystalline rocks of the Transverse Ranges [abstract]: Geol. Soc. America Abs. with Prog., v. 3, p. 193-194.

Silver, L. T., and Anderson, T. H., 1974, Possible left-lateral early to middle Mesozoic disruption of the southwestern North American craton margin [abstract]: Geol. Soc. America Abs. with Prog., v. 6, p. 955-956.

Silver, L. T., McKinney, C. R., and Wright, L. A., 1961, Some Precambrian ages in the Panamint Range, Death Valley, California [abstract]: Geol. Soc. America Spec. Paper 68, p. 55.

Silver, L. T., Anderson, C. A., Crittenden, M., and Robertson, J. M., 1977a, Chronostratigraphic elements of the Precambrian rocks of the southwestern and far western United States [abstract]: Geol. Soc. America Abs. with Prog., v. 9, p. 1176.

Silver, L. T., Bickford, M. E., Van Schmus, W. R., Anderson, J. L., Anderson, T. H., and Medaris, L. G., Jr., 1977b, The 1.4-1.5 b.y. transcontinental anorogenic plutonic perforation of North America [abstract]: Geol. Soc. America Abs. with Prog., v. 9, p. 1176.

Skippen, G. B., 1974, An experimental model for low pressure metamorphism of siliceous dolomitic marble: Am. Jour. Sci., v. 274, p. 487-509.

Slaughter, J., Kerrick, D. M., and Wall, V. J., 1975, Experimental and thermodynamic study of equilibria in the system $CaO-MgO-SiO_2-H_2O-CO_2$: Am. Jour. Sci., v. 275, p. 143-162.

Sleep, N. H., 1971, Thermal effects of the formation of Atlantic continental margins by continental break up: Geophys. Jour. Royal Astron. Soc., v. 24, p. 325-350.

Sleep, N. H., and Snell, N. S., 1976, Thermal contraction and flexure of mid-continent and Atlantic marginal basins: Geophys. Jour. Royal Astron. Soc., v. 45, p. 125-154.

Speed, R. C., 1979, Collided Paleozoic platelet in the western United States: Jour. Geol., v. 87, p. 279-292.

Stauder, W., 1975, Subduction of the Nazca plate under Peru as evidenced by focal mechanisms and by seismicity: Jour. Geophys. Res., v. 80, p. 1053-1064.

Steiger, R. H., and Jäger, E., 1977, Subcommission on geochronology: convention on the use of decay constants in geo- and cosmochronology: Earth and Plan. Sci. Letters, v. 36, p. 359-362.

Stewart, J. H., 1970, Upper Precambrian and Lower Cambrian Strata in the southern Great Basin, California and Nevada: U. S. Geol. Survey Prof. Paper 620, 206 p.

Stewart, J. H., 1972, Initial deposits in the Cordilleran geosyncline: Evidence of a late Precambrian (<850 m.y.) continental separation: Geol. Soc. Amer. Bull., v. 83, p. 1345-1360.

Stewart, J. H., and Poole, F. G., 1975, Extension of the Cordilleran miogeosynclinal belt to the San Andreas FAult, southern California: Geol. Soc. America Bull., v. 86, p. 205-212.

Stewart, J.H., and Suczek, C. A., 1977, Cambrian and latest Precambrian paleogeography and tectonics in the western United States, in Stewart, J. H., Stevens, C. H., and Fritsche, A. E., eds., Paleozoic Paleogeography of the Western United States: Los Angeles, Pacific Section, Soc. Econ. Paleontologists and Mineralogists, p. 1-18.

Stone, P., and Howard, K. A., 1979, Paleozoic metasedimentary rocks in the eastern Mojave Desert, California [abstract]: Geol. Soc. America Abs. with Prog., v. 11, p. 130.

Streckeisen, A. L., 1979, Classification and nomenclature of volcanic rocks, lamprophyres, carbonatites, and melilitic rocks: Recommendations and suggestions of the I.U.G.S. Subcommission on the Systematics of Igneous Rocks: Geology, v. 7, p. 331-335.

Streckeisen, A. L., and many others, 1973, Plutonic rocks -- classification and nomenclature: Geotimes, v. 18, p. 26-30.

Sutter, J. F., and Smith, T. E., 1979, $^{40}Ar/^{39}Ar$ ages of diabase intrusions from Newark trend basins in Connecticut and Maryland; initiation of central Atlantic rifting: Amer. Jour. Sci., v. 279, p. 808-831.

Till, R., 1978, Arid shorelines and evaporites, in Reading, H. G., ed., Sedimentary Environments and Facies: New York, Elsevier, p. 178-206.

Tullis, J. A., 1979, High temperature deformation of rocks and minerals: Rev. of Geophys. and Space Physics, v. 17, p. 1137-1154.

Turner, F. J., 1968, Metamorphic Petrology: New York, McGraw-Hill Book Co., 403 p.

Turner, F. J., and Weiss, L. E., 1963, Structural analysis of metamorphic tectonites: New York, McGraw-Hill Book Co., 545 p.

Turner, G., 1968, The distribution of potassium and argon in chondrites, in Ahrens, L. H., ed., Origin and Distribution of the Elements: New York, Pergamon, p. 387-398.

Tyler, D. L., 1975, Stratigraphy and Structure of the Late Precambrian-Early Cambrian clastic metasedimentary rocks of the Baldwin Lake area, San Bernardino Mountains, California: Unpub. M. A. thesis, Rice University, Houston, Texas, 42 p.

Tyler, D. L., 1979, The Cordilleran miogeosyncline and Sevier(?) orogeny in southern California, in Newman, G. W., and Goode, H. D., eds., Basin and Range Symposium and Great Basin Field Conference: Denver, Colorado, Rocky Mountain Assoc. of Geologists, p. 75-80.

Vaughan, F. E., 1922, Geology of the San Bernardino Mountains north of San Gorgonio Pass: Univ. of Calif. Public. Geol. Sci., v. 13, p. 319-411.

Wasserburg, G. J. F., Wetherill, G. W., and Wright, L. A., 1959, Ages in the Precambrian terrane of Death Valley, California: Jour. Geol., v. 67, p. 702.

Weibe, R. A., 1970, Pre-Cenozoic tectonic history of the Salinian block, western California: Geol. Soc. Amer. Bull., v. 81, p. 1837-1842.

Wilcox, R. E., Harding, T. P., and Seeley, D. R., 1973, Basic wrench tectonics: Am. Assoc. Petroleum Geologists Bull., v. 47, p. 74-96.

Wilson, J. L., 1975, Carbonate Facies in Geologic History: New York, Springer-Verlag, 471 p.

Winkler, H. G. F., 1976, Petrogenesis of Metamorphic Rocks, Fourth Edition: New York, Springer-Verlag, 334 p.

Winkler, H. G. F., 1979, Petrogenesis of Metamorphic Rocks, Fifth Edition: New York, Springer-Verlag, 348 p.

Woodford, A. O., and Harris, T. F., 1928, Geology of Blackhawk Canyon, San Bernardino Mountains, California: Univ. California Dept. Geol. Sci. Bull., v. 17, p. 265-304.

Wright, L. A., Troxel, B. W., Williams, E. G., Roberts, M. T., and Diehl, P. E., 1974, Precambrian sedimentary environments of the Death Valley region, eastern California, in Guidebook: Death Valley Region, California and Nevada, Field Trip No. 1: Shoshone, California, Death Valley Publishing Co., p. 27-35.

Wunderlich, F., 1970, Genesis and environment of the "Nellenkopfschen-schichten" (Lower Emsian, Rheinian Devonian) at locus typicus in comparison with modern coastal environments of the German Bay: Jour. Sed. Petrol., v. 40, p. 102-130.

Yardley, B. W. D., in press, The effect of cooling on the water content and mechanical behaviour of metamorphosed rocks: submitted to Geology.

Yeats, R. S., 1968, Rifting and rafting in the southern California borderland, in Dickinson, W. R., and Grantz, A., eds., Proceedings of Conference on Geologic Problems of San Andreas Fault System: Stanford University Publications, v. XI, p. 307-322.

PLATE 1

GENERALIZED GEOLOGIC MAP OF THE BIG BEAR AREA

Compiled from many sources discussed in text

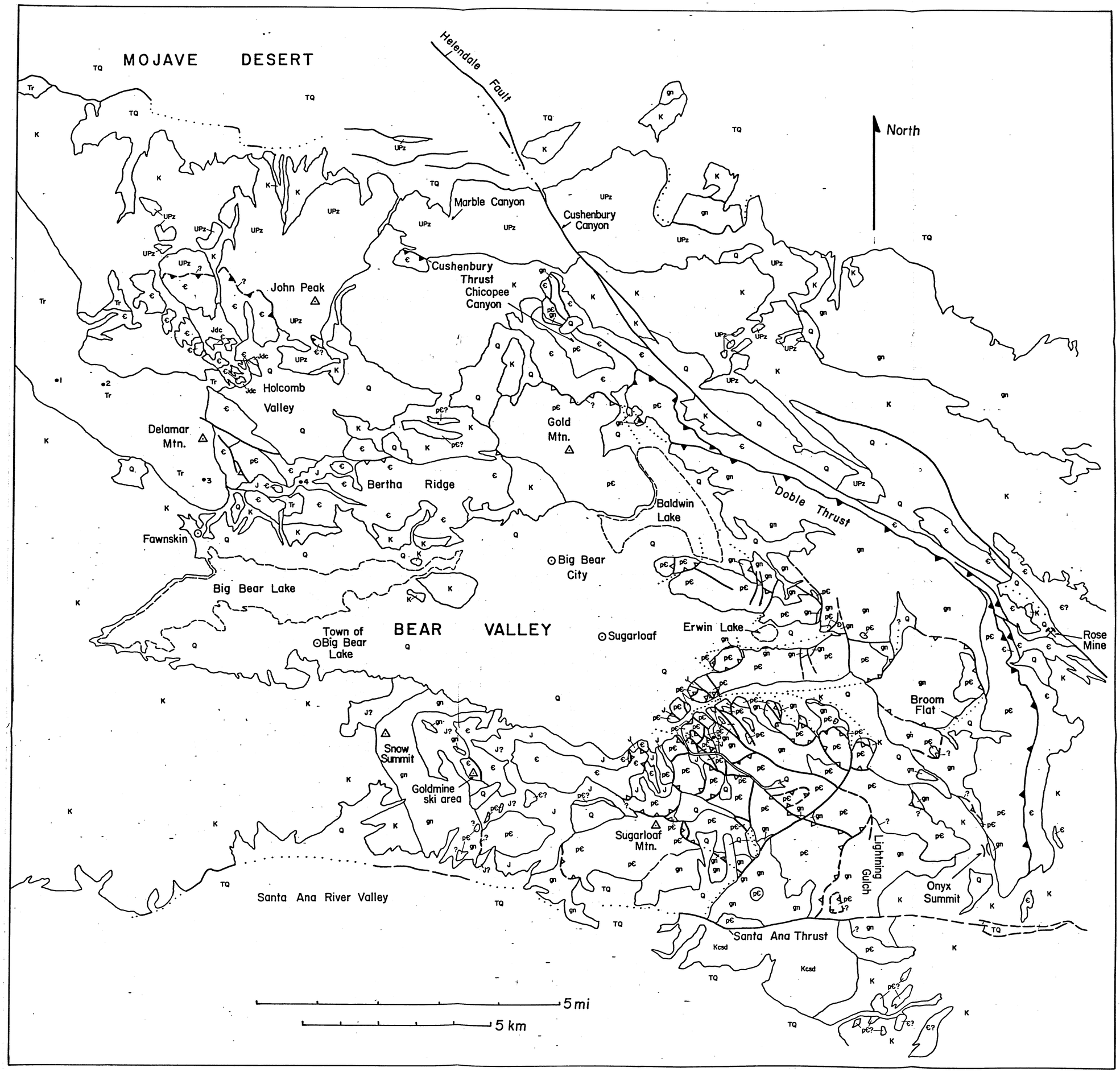

- Contacts
- High-angle faults
- Thrust faults
- Low-angle normal faults

Cenozoic

- Q / TQ — Tertiary rocks and/or Quaternary deposits

unconformity

Mesozoic

- K — Cretaceous granitic rocks
- Kcsd — Cretaceous Cienga Seca Diorite
- Jdc — Jurassic(?) dike complex
- J — Jurassic dioritic rocks
- Tr — Permo(?)-Triassic monzonite

Paleozoic

- UPz — Devonian-Permian(?) metasedimentary rocks

fault

- € — Upper Precambrian-Cambrian metasedimentary rocks

Precambrian

- p€ — Upper Precambrian Big Bear Group metasedimentary rocks

unconformity

- gn — Precambrian gneiss complex

- Geochronology samples (SB series)
  - 1: 370C
  - 2: 368C
  - 3: 378
  - 4: 575
  - 5: 381

PLATE II
GEOLOGIC MAP OF THE SUGARLOAF AREA

Structure Symbols

Contacts
- definite, approximate, concealed

Faults
- high angle, arrow indicates dip
- thrust, barbs on upper plate
- moderate or low angle normal fault
- base of gravity slides

Attitudes
- pε s_1 foliation
- pε s_2 foliation
- inclined, overturned, vertical, and horizontal bedding
- inclined or vertical bedding: transposed or facing unknown
- Mesozoic cleavage: S_1, S_2, S_3, unknown
- inclined, vertical igneous flow foliation

Mesoscopic Folds
- pε f_2 folds
- Mesozoic F_1 Folds
- " F_2
- " F_3
- Fold axial surface

(S, Z indicates assymetry otherwise not determined)

Lineations
- pε
- Mesozoic L_1
- " L_2
- " L_3

(i: intersection; m: mineral; p: pebble elongation)

ch structural chaos

geology by
C.S. Cameron
1978 - 1979

North

California

1 mile

1 km

contour interval 40 ft.

U.S.G.S. topographic base; includes Moonridge, Big Bear City, Rattlesnake Canyon, and Onyx Peak 7.5' Quads.

Stratigraphic Column

Surficial Deposits

Quaternary

- Qa Qt Qls — Qa: alluvium and undifferentiated surficial deposits; Qt: talus deposits; Qls: landslide deposits
- Qof — older fanglomerates

Mesozoic Igneous Rocks

Cretaceous Batholithic Rocks:
- g qm — g: granite + qtz. monzonite; qm: quartz monzonite
- mg — mg: muscovite granite

Jurassic
Sugarloaf Intrusive Complex
- sqm — sqm: quartz monzonite and monzodiorite; sqmd: quartz monzodiorite
- sb sqd sqmd — sqd: quartz diorite, etc.; sb: breccia unit

Wildhorse Road Sequence (age unknown)
- gu — gu: undifferentiated granitoids
- dp — dp: dacite porphyry
- ? du — du: undifferentiated diorite

Pre-Mesozoic Metamorphic Rocks

Cambrian
- €bb — Bonanza King Formation; €bb: Banded Mountain Member; €bp: Papoose Lake Member
- €bp
- €c — Carrara Formation
- €z — Zabriskie Quartzite
- €wc — Wood Canyon Formation
- d2 d1 — Delamar Mountain Formation
- g9 g8 g7 g6 g5 g4 — Green Canyon Formation (g8m)

fault or intrusive contact

Precambrian
- g3 g2 g1 — Green Canyon Formation
- s5 s4 s3 s2 s1 — Sugarloaf Quartzite
- L3 L2 L1 — Lightning Gulch Formation
- wgs — Wildhorse Greenstone
- w2 w1 — Wildhorse Quartzite (m) marker beds

Big Bear Group

unconformity
- pε grgn — granite orthogneiss
- pεgn — undifferentiated gneisses

Plate III: Geologic map of the Delamar Mtn. area

Symbols

Contacts
definite, approximate, concealed

Faults
high-angle fault
thrust
moderate or low-angle normal fault
barbs on upper plate
base of gravity slide

Attitudes
inclined, overturned, vertical and horizontal bedding
inclined or vertical bedding: transposed or facing unknown

Attitudes (cont.)
cleavage: S_{1a}(?), S_1, S_2
inclined or vertical igneous flow foliation

Folds
F_1 S,Z indicates assymetry otherwise not determined
F_2
axial surface

Lineations
L_1 I intersection
L_2 m mineral
igneous flow lineation

Macroscopic Folds
Axial trace of F_1 folds

Stratigraphic Column

Surficial Deposits

Quaternary
- Qa — alluvium
- Qof — older fanglomerate

Mesozoic Igneous Rocks

Cretaceous
- g — granite
- gp — granite porphyry
- hbqd — horn. biot. qtz. diorite
- bd — Bertha Diorite
- ? dc — dike complex

Jurassic Triassic
- fm — Fawnskin Monzonite

Pre-Mesozoic Metamorphic Rocks

Cambrian
- €ng / €n — Nopah (?) Formation; €ng: grey dolom. marble
- fault or intrusive contact
- €bb — Bonanza King Formation; €bb: Banded Mtn. Member
- €bp — €bp: Papoose Lake Member
- €c — Carrara Formation
- €z — Zabriskie Quartzite
- €wc — Wood Canyon Formation

Precambrian
- d2
- d1 — Delamar Mountain Formation
- base intruded

geology by C.S. Cameron, 1979

north

1 mile

1 km

California

contour interval 40 ft.
U.S.G.S. topographic base
Fawnskin 7.5' Quadrangle

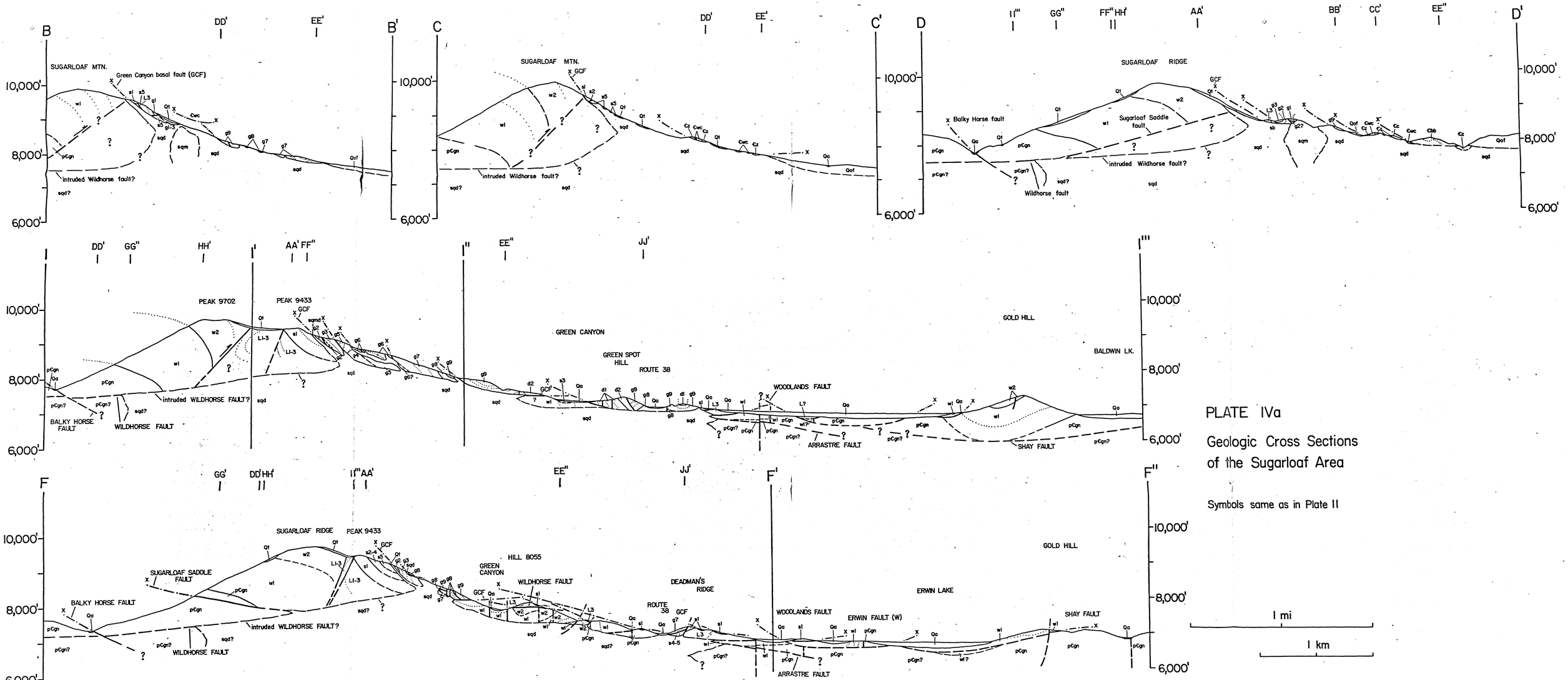

PLATE IVa

Geologic Cross Sections of the Sugarloaf Area

Symbols same as in Plate II

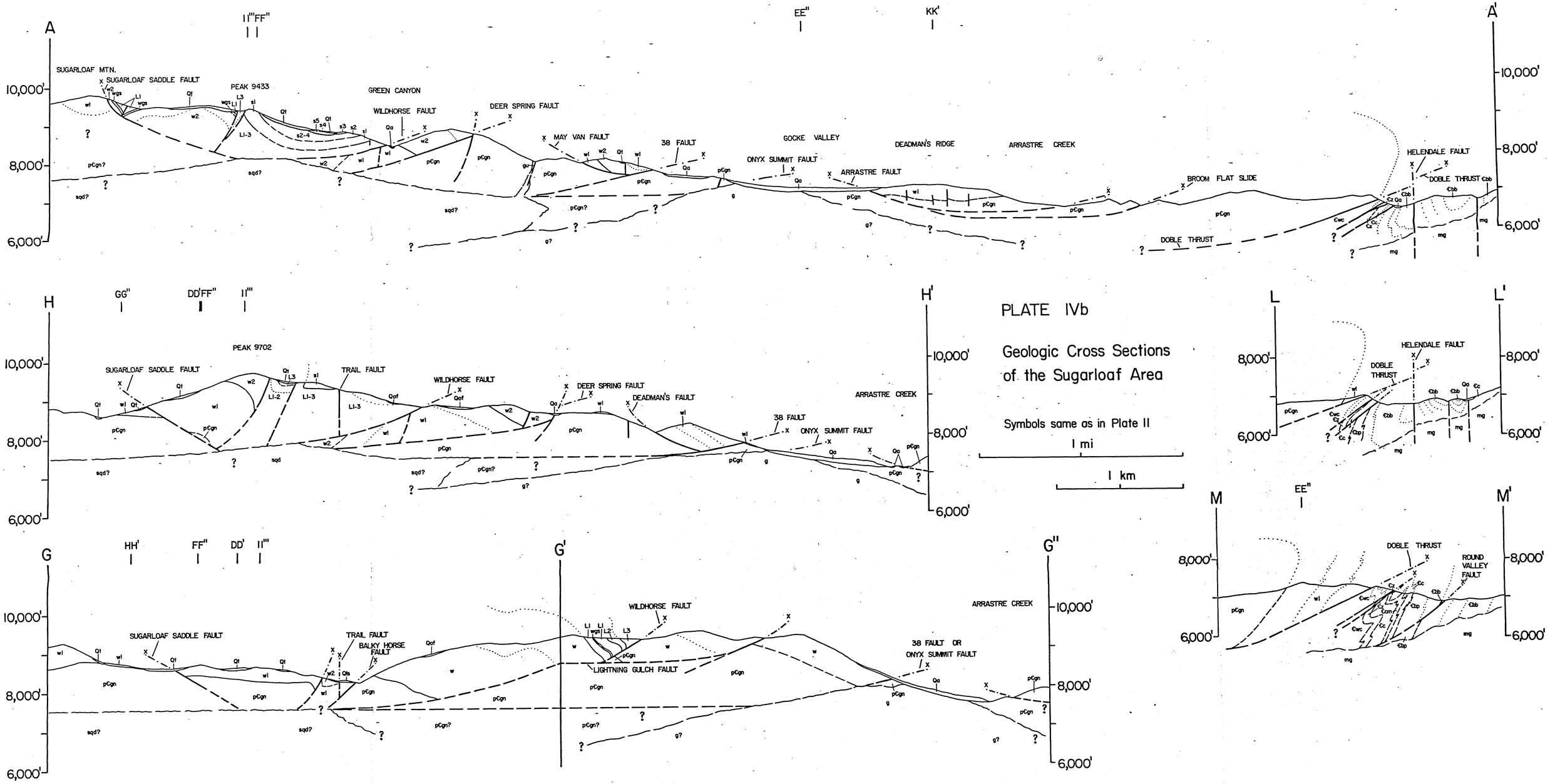
A
II'''FF''
EE''
KK'
A'
10,000'
8,000'
6,000'
SUGARLOAF MTN.
SUGARLOAF SADDLE FAULT
PEAK 9433
GREEN CANYON
WILDHORSE FAULT
DEER SPRING FAULT
MAY VAN FAULT
38 FAULT
GOCKE VALLEY
DEADMAN'S RIDGE
ARRASTRE CREEK
ONYX SUMMIT FAULT
ARRASTRE FAULT
BROOM FLAT SLIDE
HELENDALE FAULT
DOBLE THRUST
DOBLE THRUST
H
GG''
DD'FF''
II'''
H'
PEAK 9702
SUGARLOAF SADDLE FAULT
TRAIL FAULT
WILDHORSE FAULT
DEER SPRING FAULT
DEADMAN'S FAULT
38 FAULT
ONYX SUMMIT FAULT
ARRASTRE CREEK
G
HH'
FF''
DD'
II'''
G'
G''
SUGARLOAF SADDLE FAULT
TRAIL FAULT
BALKY HORSE FAULT
WILDHORSE FAULT
LIGHTNING GULCH FAULT
38 FAULT OR
ONYX SUMMIT FAULT
ARRASTRE CREEK
PLATE IVb
Geologic Cross Sections
of the Sugarloaf Area
Symbols same as in Plate II
1 mi
1 km
L
L'
HELENDALE FAULT
DOBLE THRUST
M
EE''
M'
DOBLE THRUST
ROUND VALLEY FAULT

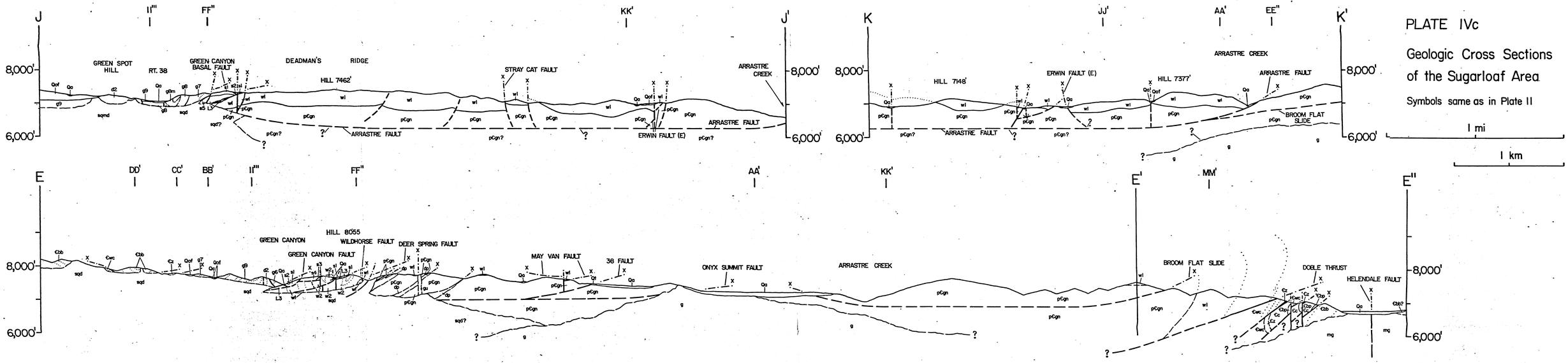
J
II'''
FF''
KK'
J'
8,000'
6,000'
GREEN SPOT HILL
RT. 38
GREEN CANYON BASAL FAULT
DEADMAN'S RIDGE
HILL 7462'
STRAY CAT FAULT
ARRASTRE CREEK
ARRASTRE FAULT
ERWIN FAULT (E)
K
JJ'
AA'
EE''
K'
HILL 7148'
ARRASTRE CREEK
HILL 7377'
BROOM FLAT SLIDE
E
DD'
CC'
BB'
HILL 8055
GREEN CANYON
GREEN CANYON FAULT
WILDHORSE FAULT
DEER SPRING FAULT
MAY VAN FAULT
38 FAULT
ONYX SUMMIT FAULT
E'
MM'
E''
DOBLE THRUST
HELENDALE FAULT
PLATE IVc
Geologic Cross Sections of the Sugarloaf Area
Symbols same as in Plate II
1 mi
1 km

PLATE V

Geologic Cross Sections of the Delamar Mtn. Area

Symbols same as in Plate III

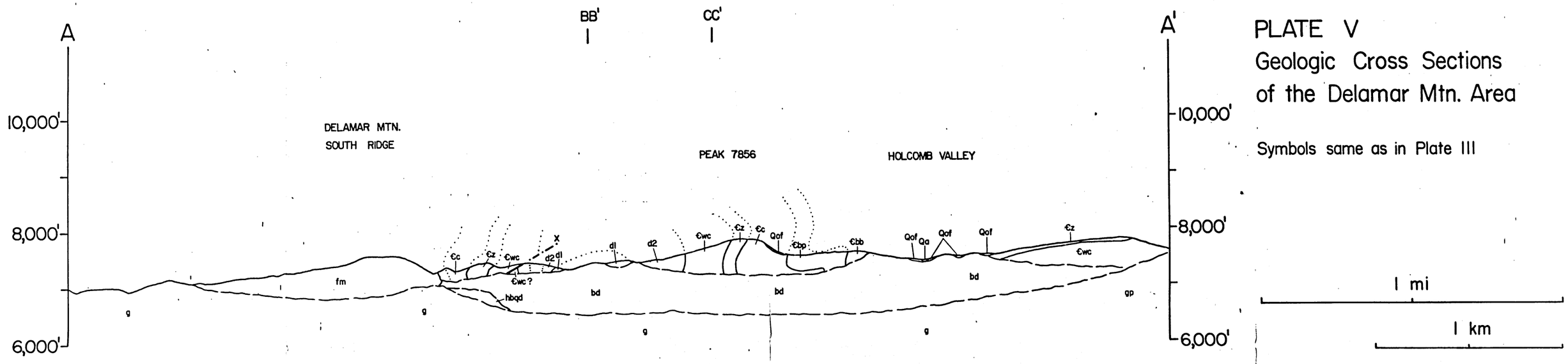

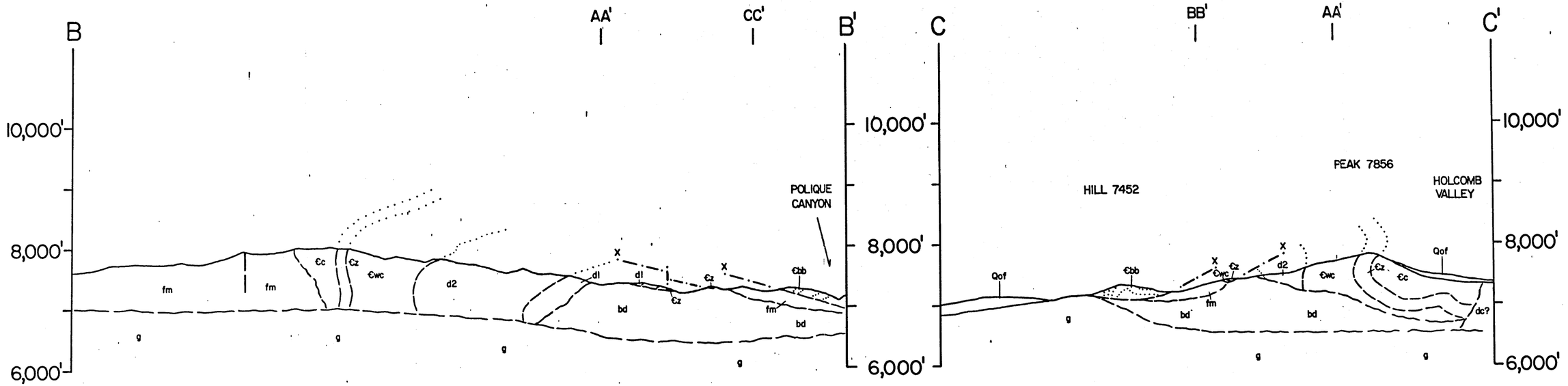

Plate VI
TECTONIC MAP OF THE SUGARLOAF AREA

STRUCTURES

FOLDS (post p€)

F_1 upright, overturned, concealed, plunging

F_2 upright, overturned antiform

upright, overturned synform

F_3,

F_4 upright, overturned antiform

upright, overturned synform

FAULTS

High-angle (or dip unknown) — approx., concealed

Thrust (barbs on upper plate)

Moderate- or Low-angle normal fault

Gravity slide

TECTONIC UNITS

IGNEOUS ROCKS

kg Cretaceous granitic rocks

jd Jurassic diorite complex

dp Dacite porphyry

METAMORPHIC ROCKS

p€-€ Miogeoclinal rocks

basal contact

gn p€ gneiss complex

1-9, etc., denote structural blocks bound by low-angle normal faults. a1, a2, b1, b2, etc., refer to fault segments discussed in text.

Baldwin Lake

BALDWIN FAULT

Gold Hill Synform

SHAY FAULT

SHAY FAULT

RANCH FAULT

Erwin Lake

Erwin Antiform

ERWIN FAULT (W)

ERWIN FAULT (W)

WOODLANDS FAULT

Deadman's Synform

STRAY CAT FAULT

Gocke Synform

Gocke Antiform

ERWIN FAULT (E)

ARRASTRE FAULT

Gocke Valley

38 FAULT

ONYX SUMMIT FAULT

MAY VAN FAULT

38 FAULT

May Van Antiform

DEADMAN'S FAULT

Green Canyon

DEER SPRING FAULT

Green Spring Antiform

Green Canyon Synf.

Sugarloaf Synform

BALKY HORSE FAULT

TRAIL FAULT

Sugarloaf Antiform

Sugarloaf Saddle Synform

SUGARLOAF SADDLE FLT.

Sugarloaf Mountain

Meadows Antiform

Lightning Antiform

WILDHORSE FAULT

LIGHTNING GULCH FAULT

Lightning Gulch

Arrastre Creek Antiform

HELENDALE FAULT

Rose Mine Synform

DOBLE THRUST

ROUND VALLEY FAULT

BROOM FLAT SLIDE

fault contact from McJunkin (1976)

Broom Flat

Onyx Summit

N

1 mi

1 km